

MSc Thesis Report



Corrosion in Submerged Offshore Slip Joints

Corrosion in Submerged Offshore Slip Joints

by
K.M. de Bruin

in partial fulfillment for the degree of **Master of Science** at the Technical University of Delft.
Defended on Friday August 30, 2019 at 10:00 AM.

Student number:	4142365		
Committee of thesis:	Prof. dr. M. Veljkovic	Chairman	TU Delft
	Ir. J.S. Hoving	Daily Supervisor	TU Delft
	Dr. Y. Gonzalez Garcia	Daily Supervisor	TU Delft
	S. Suur MSEng	Daily Supervisor	Van Oord

Preface

This report covers the work of the investigation towards crevice corrosion behavior in offshore underwater Slip joints by the development of a test and the execution of this test. It has been an excellent learning experience with a stimulating combination of theoretical and experimental work. Designing a test method and bringing the test into practice has been a great adventure. It learned me to deal with ups and downs and showed me that persistence is a great part of success.

The project would not have been advanced so well without help and support, for which I am very grateful. Firstly, the project would have never existed without Sander Suur providing guidance and encouragement, for which I am very thankful. Secondly, I would like to thank Yaiza Gonzalez Garcia and Nils Verkleij for sharing their knowledge and for their support, and Jeroen Hoving for his comforting guidance and feedback. I wish to express my gratitude to Milan Veljkovic for his constructive feedback and questions that helped to focus the direction of the project.

My girlfriend, Anouk, has been loving, patient and supportive throughout my whole MSc degree. For this I am very grateful. I would like to thank my parents for their kind support during my study. Finally, to my friends, thanks for the great time. The coffee and lunch breaks made long days of studying bearable.

K.M. de Bruin
Delft, August 2019

Abstract

In order to connect a monopile to a transition piece of an offshore wind turbine efficiently, a new connection method called the Slip Joint is being developed. The Slip Joint is made out of a conical section at the top of the monopile foundation and a conical section at the bottom of the transition piece which are slid over each other to form a connection. Van Oord is currently having the Slip Joint connection certified by DNVGL, requiring that the structural integrity must suffice during the total lifetime. Offshore with harsh salty conditions, corrosion is important to be aware of. The interface between the cones of the Slip Joint creates a local environment with crevices that has a unknown corrosion behavior. Because it is necessary to know the corrosion behavior within the Slip Joint, the following research question has been formulated: What corrosion behavior can be expected in offshore submerged Slip Joint crevices?

Because research towards steel crevices of large geometries was not carried out before, a test method had to be developed. This required multiple innovative methods, and thus trial tests to confirm the feasibility of the test method. Multiple crevice geometries had to be tested during a 60 days during immersion test. In total 260 steel plates and 37 different crevice geometries have been studied on their corrosion behavior. To monitor the corrosion behavior during the test period, open circuit potentials have been measured. After the test period the specimens were cleaned and weight losses have been measured. With the weight loss measurement, the corrosion rate of each specimen has been calculated. Additionally, the usability of Impressed Cathodic Corrosion Protection on a crevice is tested by applying a current on the specimens using a potentiostat.

Results of the test showed that local corrosion in the Slip Joint will occur. The potential data indicated local corrosion attack and indicated more stabilized local corrosion for smaller and longer crevices. Observed corrosion products on the steel plates also suggest a differential in oxygen content in the crevice. The corrosion rates of the specimens showed that especially the length influence the corrosion rate, but also the crevice height is of influence. Crevice geometries with a void did not indicate a significant difference to regular crevices, but this is expected to be caused by the chosen geometries in the test. Applied ICCP on a regular crevice suggested that it can be successfully applied to crevices and that isolated steel plates will still be influenced by a ICCP system.

For design purposes a model has been formulated that provides an estimation for the corrosion rate in a given crevice. The estimation is limited by the parameters of the test. An offshore underwater Slip Joint will be exposed to environmental conditions that are not found in the test. To further investigate the behavior of corrosion in the Slip Joint and improve estimations of corrosion rates, follow up research will be required.

Contents

Preface	i
Abstract	ii
Contents	iii
1 Introduction to corrosion in offshore Slip Joints	1
1.1 General thesis introduction	1
1.2 Introduction to the Slip Joint concept and the design tolerances	3
1.2.1 The Slip Joint concept	3
1.2.2 The interface of the Slip Joint	3
1.2.3 Steel properties of the Slip Joint	5
1.2.4 Tolerances for fabrication	6
1.2.5 Van Oord in-house FE-model for Slip Joint connections	11
1.2.6 Expected gap in the Slip Joint	13
1.3 Research question	13
1.4 Report structure	14
2 Fundamentals of offshore corrosion	15
2.1 Definition of corrosion	15
2.2 Parameters influencing corrosion	16
2.2.1 Effect of the pH	16
2.2.2 Effect of salinity	17
2.2.3 Influence of oxygen	17
2.2.4 Effect of temperature	18
2.2.5 Influence biological activity on corrosion	19
2.2.6 Passivity of a metal surface	20
2.3 Corrosion phenomena	21
2.3.1 Uniform corrosion	21
2.3.2 Pitting corrosion	22
2.3.3 Crevice corrosion	24
2.3.4 Fretting corrosion	25
2.4 Corrosion measurement techniques	25
2.4.1 Potential measurements	26
2.4.2 Experimental electrochemical set-ups	27
2.4.3 Weight loss measurements	29
2.5 Corrosion protection techniques in the offshore environment	29
2.6 Conclusion	33
3 Research to offshore corrosion in crevices	35
3.1 Geometry effect	35
3.2 Corrosion of structural steel in seawater	37
3.3 Methods for crevice corrosion experiments	39
3.3.1 Specimen size, composition and preparation	39
3.3.2 Test environment	41
3.3.3 Potentiostatic tests versus open circuit tests	41
3.3.4 Examination and measurements	42

3.4	Conclusion	42
4	Designed experiment to study corrosion in the Slip Joint	43
4.1	Specimen material, preparation and geometry	43
4.1.1	Specimen material	43
4.1.2	Specimen preparation	48
4.1.3	Specimen geometry	50
4.2	Test environment	51
4.2.1	Salt water solution	51
4.2.2	Temperature	52
4.2.3	Controlling the environment	52
4.3	Immersion of the samples	53
4.3.1	Immersing of specimens in the tub	53
4.3.2	Activities during immersion	54
4.4	Pull out of specimen and cleaning	55
4.4.1	Potentials	55
4.5	Trial test to check test parameters	56
4.6	Immersion of crevices ending in a void	57
4.7	ICCP test	58
5	Results of the experiments	61
5.1	Open circuit potential measurements and visual inspection	61
5.1.1	Open circuit potential measurements and analysis	61
5.1.2	Visual inspection analysis on potentials	70
5.2	Weight losses and corrosion rates	77
5.2.1	Weight losses	77
5.2.2	Corrosion rates	78
5.3	Results of crevices ending in a void	84
5.3.1	Open circuit potential measurements and visual inspection	84
5.3.2	Weight losses and corrosion rates	86
5.4	ICCP on crevices	90
5.5	Conclusion	93
6	Discussion of the test and the results	94
6.1	Interpretation of the results	94
6.1.1	Corrosion behavior and geometry effect	94
6.1.2	Corrosion rates and geometry effect	96
6.1.3	The influence of a void to crevice corrosion	98
6.1.4	The influence of ICCP on crevice corrosion	98
6.2	Practical appliance of results	99
6.2.1	Laboratory corrosion versus offshore corrosion	99
6.2.2	Emprical model to estimate offshore crevice corrosion rates	100
6.2.3	Implications of the results to the Slip Joint design	105
6.3	Improvements and further research	106
6.3.1	Additional tests	106
6.3.2	Improvements on the test set-up	107
7	Research conclusion and recommendations	109

7.1	Conclusion of the test design	109
7.2	Conclusion of the results	109
7.3	Crevice corrosion research recommendations	110
7.4	Slip Joint design recommendations	111
8	Bibliography	112
9	Appendices	115
9.1	APPENDIX 1: Work Method Statement	115
9.2	APPENDIX 2: Tafel plots S355J2 and S355ML	147
9.3	APPENDIX 3: Specimen codes and set codes	151
	List of Figures	156
	List of Tables	160

1 Introduction to corrosion in offshore Slip Joints

1.1 General thesis introduction

Compared to conventional energy sources, offshore wind energy is a new technical field, although a trend can be observed: most foundations for offshore wind turbines are monopiles and the wind turbines are typically connected to the monopiles by a transition piece, see Figure 1.1. At the moment there are two standard methods for assembling the monopile to the transition piece, either by bolting or by grouting. Both methods have had their issues and there still are issues to resolve. For example bolting has high maintenance because the bolts have to be checked at a regular basis and grouting connections have shown to be unreliable because settlements of these connections are not uncommon. New methods for connecting the monopile and the transition piece are being developed, such as the wedge method and the underwater Slip Joint connection for example.

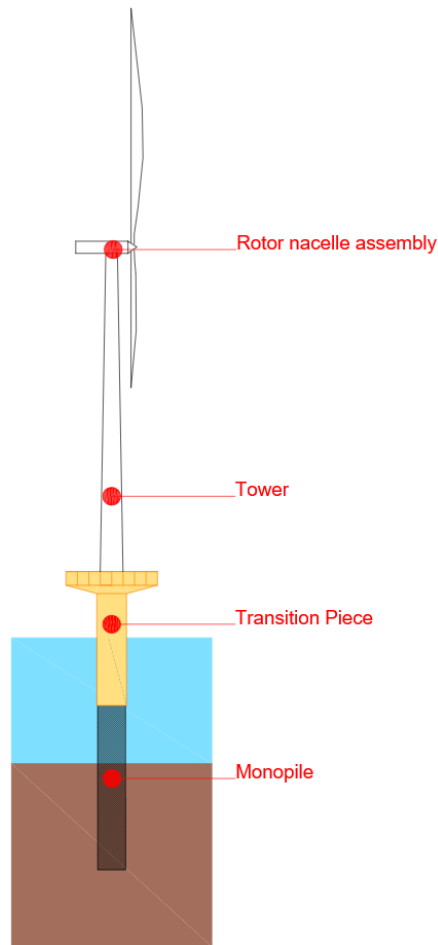


Figure 1.1: Components of an offshore wind turbine

The Slip Joint is an alternative connection between the transition piece and monopile that has promising beneficial properties. One of the benefits of the connection is that it can be made above and below sea level. Using a Slip Joint below sea level provides the opportunity for a better weight distribution between the monopile and the transition piece. Longer monopiles are not necessarily required for deeper waters if Slip Joint connections are used, while an increased length of the

transition piece can compensate for the water depth, see Figure 1.2, the connection is made below water level. (For grouted and bolted transition pieces the connection has to be around the water level) It is especially beneficial for logistical reasons. As the lifting capacity of vessels does not have to increase for deeper waters, due to the improved weight distribution between the monopile and transition piece. Another benefit of the Slip Joint is the relative short installation time and easy decommissioning method. The Slip Joint is therefore very promising to the Offshore Wind industry.

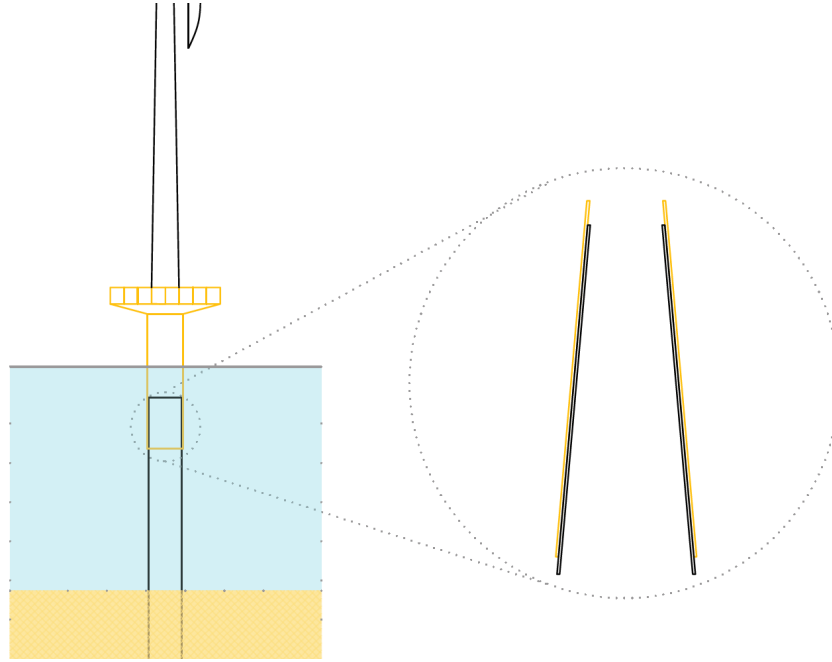


Figure 1.2: Slip Joint overview

Van Oord is currently having the Slip Joint connection certified by DNVGL. Certification requires in-depth investigation into the characteristics and offshore behavior of the Slip Joint. The structural integrity of the Slip Joint must be maintained during its total lifetime. A wind turbine is designed to survive the harsh offshore environment for at least 25 years. More insight into the lifetime reliability of the structure is therefore a critical part to consider. Especially offshore, with harsh salty conditions, corrosion is one of the things to be aware of.

Placing a steel structure in this environment is not without risk, therefore corrosion protection is part of offshore structure designs. The interface of the Slip Joint creates a local environment that has a currently unknown corrosion behavior. This thesis will form the basis into researching the corrosion behavior inside lap joints like the Slip Joint. Insight into the corrosion behavior and its characteristics is vital in optimizing the design and the corrosion protection of the Slip Joint, as the corrosion behavior inside the Slip Joint is not well understood.

External surfaces of primary steel (S355ML in most cases) in the submerged zone are recommended to have cathodic protection according to DNVGL-RP-0416 [1]. More protection by coating on the external surface is optional, but not required. The internal surface in the submerged zone can have cathodic protection and should at least have a corrosion allowance (increased wall thickness which

is allowed to corrode). Extra protection with coating is again optional. In practice, the internal surfaces are most often protected via a corrosion allowance according to DNVGL-RP-0416.

There is no additional corrosion protection prescribed for the interface of the monopile and transition piece. Because the joint is never going to be a perfect fit, water will find its way between the two conical sections and corrosion is likely to occur.

According to Hilbert et al. in [2] localized attacks and increased corrosion could occur in these areas. The seawater and oxygen content as well as microbial activity can possibly cause local corrosion problems. For this reason the corrosion of the inner surface should be taken into account for the risk of losing structural strength and risk of corrosion fatigue.

Mitigating measures, then, will be necessary to reduce corrosion. A solution can possibly be found in either design optimization, a local cathodic protection system, a coating, a watertight sealing of the interface or applying thicker steel parts to account for more corrosion allowance. However, first the severity of the corrosion has to be investigated.

1.2 Introduction to the Slip Joint concept and the design tolerances

In this section the Slip Joint concept is discussed in further detail. In section 1.2.1 the concept of the Slip Joint is explained in order to understand the concept and the implications. In section 1.2.2 the interface between the monopile and the transition piece is discussed, because this is the location of interest in this research. The steel composition of the Slip Joint is relevant to corrosion, because each metal shows different corrosion behavior, and will therefore be discussed in section 1.2.3. This results in determining the local environment that can be expected at the interface of the Slip Joint and will be used to formulate the research questions and the research goal.

1.2.1 The Slip Joint concept

The Slip Joint is made out of a conical section at the top of the monopile foundation and a conical section at the bottom of the transition piece which are slid over each other to form a connection, see Figure 1.2. Forces and moments from the wind turbine are passed through the Slip Joint by friction and radial pressure between the two conical sections. The forces are transferred further through the monopile foundation to the seabed. [3]

By lowering the transition piece on the monopile the connection is formed. The transition piece will settle until the slip is sufficient to counteract the gravitational forces. Installation of the tower and turbine on the transition piece will cause the Slip Joint to settle further. A simplified overview of this procedure is given in Figure 1.3.

1.2.2 The interface of the Slip Joint

The internal contact surface of the Slip Joint transfers the loads by friction and radial pressure. In order to have a solid connection, the cones should fit as precise as possible. A proper fitting Slip Joint will have a large connected surface. Friction stresses will be distributed and local stress concentrations are averted.

A perfect Slip Joint will not have a crevice between the two cones. This is not only positive structurally, without voids or crevices the interface will not be exposed to seawater during its operational lifetime and thus corrosion is prevented at the interface. Due to the limits of manufacturing, a perfect Slip Joint is never going to be manufactured, so voids or crevices will exist at the interface.

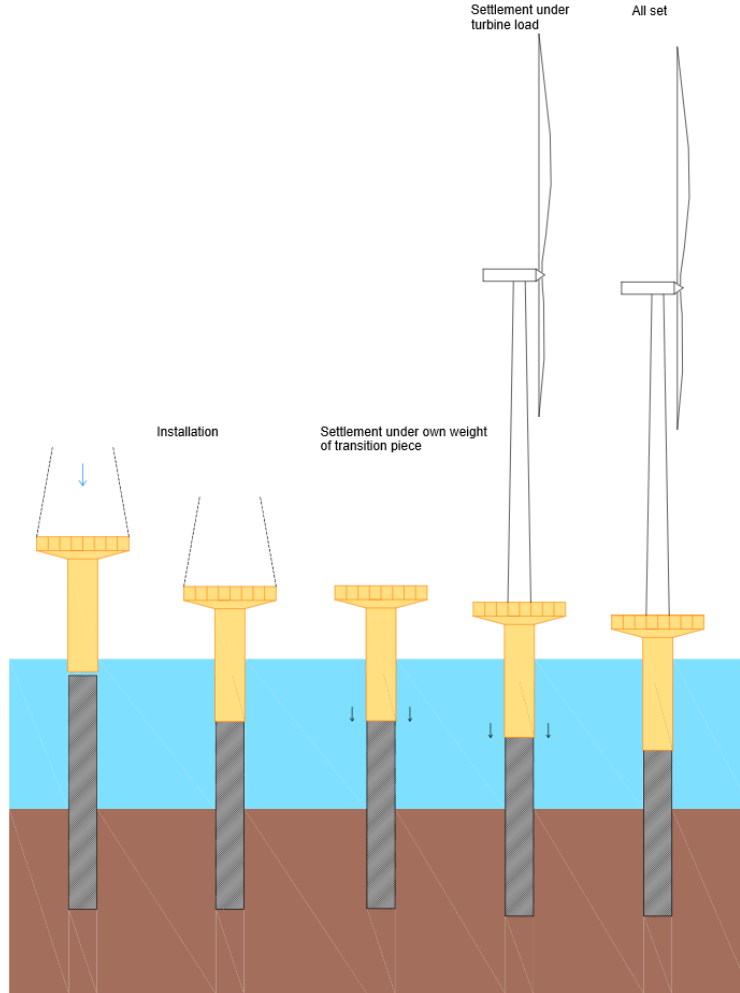


Figure 1.3: Installation procedure

The corrosion behavior of any material is determined by its environment. Environmental conditions, like voids and crevices, will influence the local corrosion behavior. [4] At the interface of the Slip Joint such environment can be found. See Figure 1.4.

During fabrication of the cones, for the monopile and transition piece, defects will occur. Manufacturing tolerances, applicable to the Slip Joint, cause imperfect cones. Mismatching cones will result in crevices between the two cones. These crevices are filled with seawater and are prone to local corrosion. Crevice corrosion, a local corrosion phenomenon, is very likely to occur. This will be explained in more detail in section 2.3.3.

The sizes of the crevices that can be found in a Slip Joint will be defined in section 1.2.4. The geometry will influence the corrosion behavior and is thus an important aspect to know for determining the corrosion behavior inside the Slip Joint. DNVGL, a global quality assurance agency, prescribes maximum manufacturing tolerances in Offshore Standard C401. [5] Van Oord requires manufacturers to work according to these tolerances and, if required, Van Oord obligates manufacturers to work with stricter tolerances. Since, at least, the DNVGL tolerances should be met, these are used in the next paragraph to calculate the worst case scenario resulting in the biggest

crevices between the monopile and transition piece.

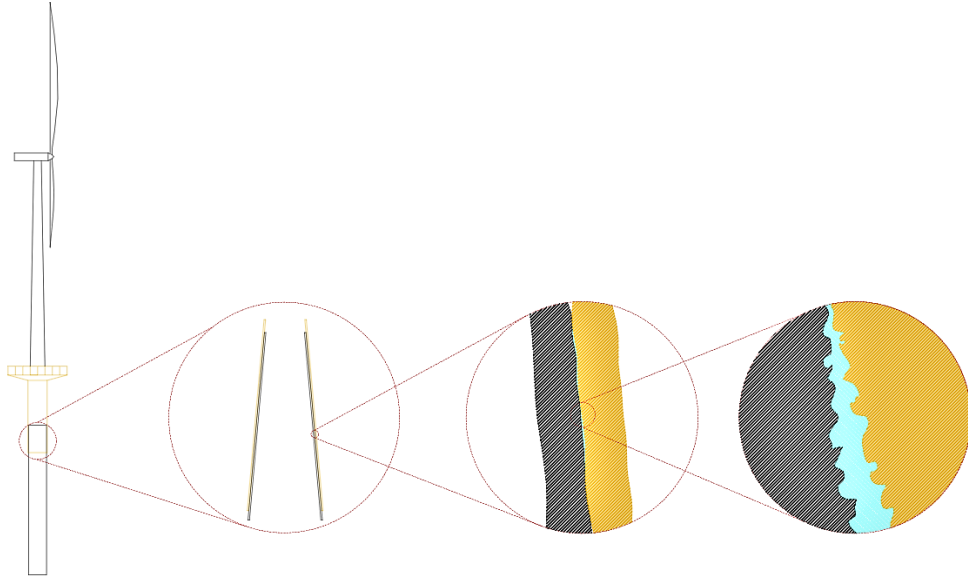


Figure 1.4: Local environment in the Slip Joint

1.2.3 Steel properties of the Slip Joint

Because of the fact that each metal reacts different with a corrosive environment, the properties of the steel that is used for a Slip Joint is discussed here. The primary steel of offshore wind turbine structures is required to have a steel strength S355. The transition piece and the monopile are both characterized as 'primary structural members'. (Primary structural members are components that are necessary to support the loads.) The primary steel is of great importance for the structural integrity, a high quality is expected from the steel manufacturers.

The preferred steel grade for the Slip Joint is S355ML. This means that the steel is thermomechanically rolled and has a specified notch toughness given by the Charpy V-notch impacts at $-50\text{ }^{\circ}\text{C}$. This steel is fine grained. S355J2-K is a similar steel composition which is often used in offshore constructions. S355J2-K has similar toughness as S355ML, however given by a temperature of $-20\text{ }^{\circ}\text{C}$ and it is hot rolled. Both steel grades are High Strength Low Alloy steels (HSLA). These type of steels have similar chemical compositions, but the steel grade ML has finer grains. [6]

The corrosion behavior of any structural steel will be very comparable. [7] Most studies towards structural steels (or mild steels) do not distinguish between any of these properties. Nevertheless, the chemical composition can have an affect on the corrosion behavior. Certain alloys form a metal oxide layer on the surface of the material that have the properties of a passive layer. A passive layer is a thin oxide film that is formed on the surface, which can act as a barrier that protects the metal. The stability of such layer determine the efficiency of protective nature. Aluminum alloys and stainless steels have efficient passivity and therefore high resistance to corrosion.

Structural steels do not form such chemical stable passive layer, due to the low alloy content the oxide layer is mainly composed of iron oxides that are normally porous and chemical unstable. This results in a poor passive behavior. [8]

In conclusion, the corrosion behavior is dependent on the kind of metal. Studies of corrosion to other metals therefore can not be adopted to these structural steels. The structural steels will show comparable results if the chemical composition is comparable.

1.2.4 Tolerances for fabrication

As mentioned in section 1.2.2, DNVGL prescribes tolerances for the fabrication of offshore structures. The tolerances of interest for the Slip Joint are, the maximum out of roundness, the tolerance to the nominal radius and the maximum deviation of the cone angle. In this paragraph, these tolerances have been calculated for a Slip Joint design as provided by Van Oord. In Figure 1.5 the dimensions of the provided Slip Joint can be found. The calculations in this paragraph resulted in the maximum tolerances on the Slip Joint that are allowed. These are used to find the maximum possible gap height in the Slip Joint. The crevices that can be expected in a Slip Joint are obtained in this way and thus the local environment is known. In section 2 and section 3 it becomes clear that the geometry of the crevice is rather important to the corrosion behavior.

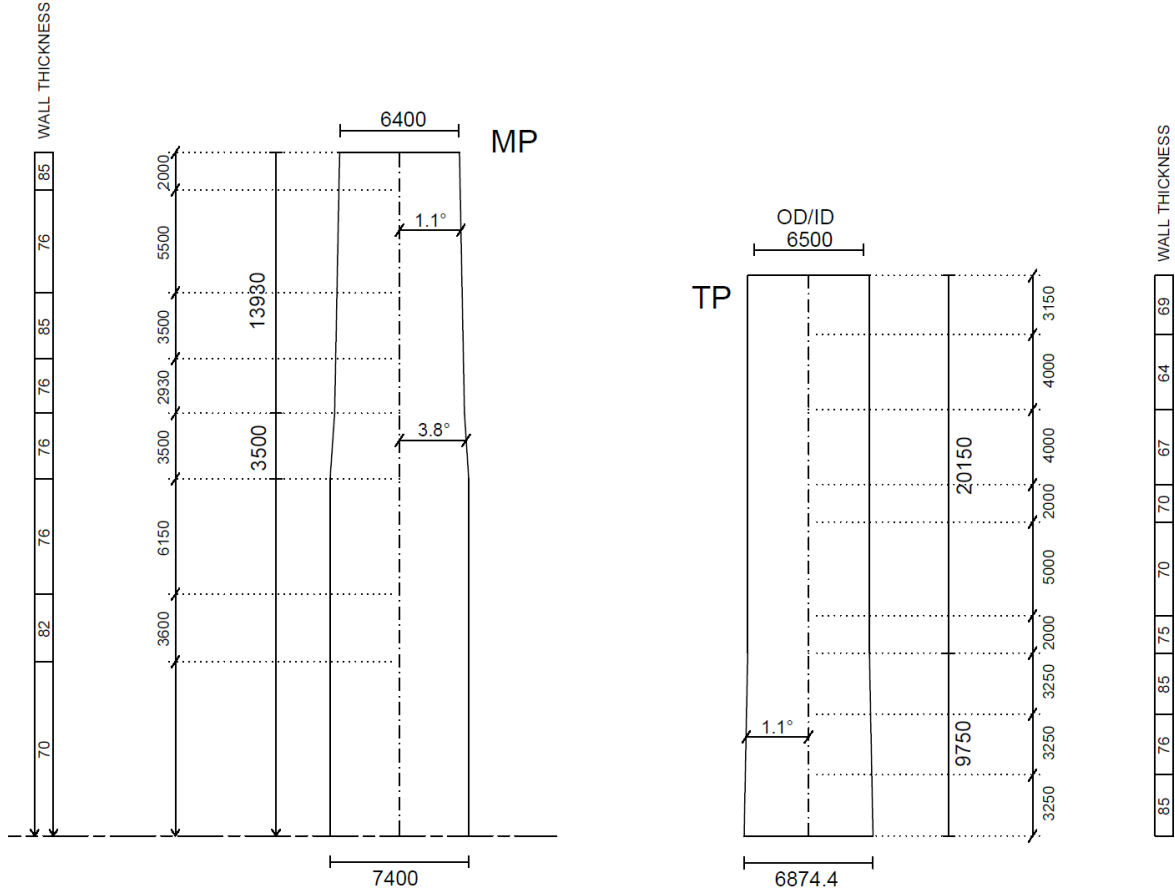


Figure 1.5: Dimensions monopile and transition piece

To get the worst case scenario, the tolerances are combined. The result is inserted in an Ansys model, made by the Van Oord structural engineering department as part of the certification of the Slip Joint. This model provides the resulting gap after installation of the transition piece on top of the monopile. Note that the tower and turbine are not included, because it is assumed that a

year is required before the tower is installed on top of the monopile-transition piece assembly. The transition piece will settle further after installment of the tower and turbine, which will narrow the gap between the monopile and transition piece. So in order to be conservative in this research, only the transition piece is included in the calculations for the maximum gap. This approach makes it possible to research the corrosion behavior of the offshore Slip Joint in its first year.

Maximum out of roundness

The maximum imperfection, or local out of roundness, is given in [5] by the equation:

$$\delta = \frac{0.01 \times g}{1 + g/r} \quad (1.1)$$

in which g is the length of the template and r the radius of the cone (see Figure 1.6). Out of roundness results in oval shapes, introducing gaps between the two cones. The maximum gap height with this tolerance, as shown in Figure 1.6, occurs when both the transition piece and monopile are shaped with the maximum allowable local out of roundness.

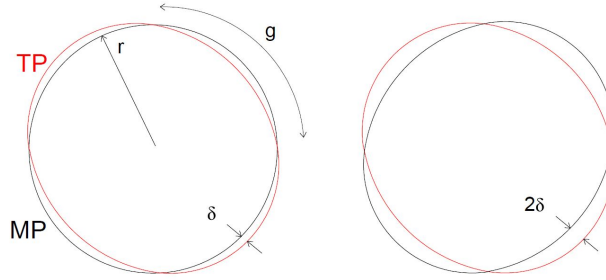


Figure 1.6: Combined local out of roundness for the transition piece and the monopile

The local out of roundness, δ , is maximum at the bottom of the Slip Joint (for the maximum diameter of the monopile and the transition piece). The maximum diameter of the transition piece is $D_{TP,Bottom} = 6874.4$ mm. Therefore,

$$g = \pi \times \frac{6874.4/2}{2} = 5399.14\text{mm}. \quad (1.2)$$

This gives:

$$\delta_{TP,Bottom} = \frac{0.01 \times 5399.14}{1 + \frac{5399.14}{3437.2}} \approx 21\text{mm} \quad (1.3)$$

In the same manner, the out of roundness is calculated for the monopile and the top of the transition piece. In table 1.1 the results are shown.

Maximum deviation of the cone angle

In order to make sure that sufficient contact is possible in the Slip Joint connection, the deviation from the cone angle is limited. The limits are, as shown in Figure 1.7, a maximum deviation of -0.05° for the transition piece and $+0.05^\circ$ for the monopile. The given tolerance guarantees contact at the bottom of the Slip Joint.

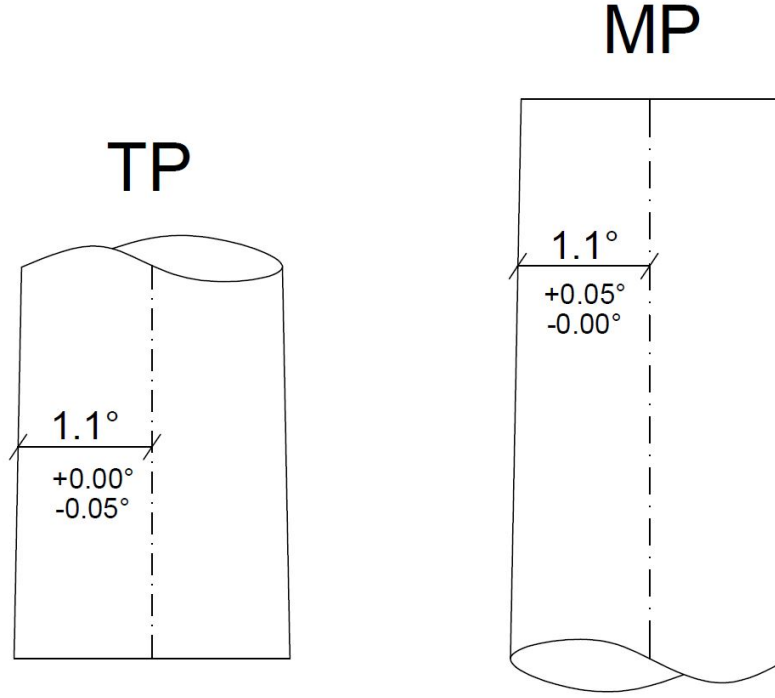


Figure 1.7: Cone angle tolerances for the transition piece and monopile.

In the most unfortunate situation, the transition piece will have a cone angle of 1.05° . The diameter of the transition piece changes only at the bottom and will become smaller. The minimum diameter within the tolerance is:

$$D_{TP,bottom,Min} = \tan 1.05^\circ \times 9750 \times 2 + 6500 = 6857.4mm \quad (1.4)$$

Decreasing the bottom radius by:

$$\epsilon_{TP,bottom} = (6874.4 - 6857.4)/2 = 8.5mm \quad (1.5)$$

A bigger cone angle at the monopile results in a smaller top diameter. A smaller top diameter introduces a gap between the monopile and the transition piece at the top, see Figure 1.8. With a cone angle of 1.15° the diameter of the monopile at the top becomes:

$$D_{MP,top,Min} = 6935 - \tan 1.15^\circ \times 2 \times 13930 = 6375.7mm \quad (1.6)$$

The radius is decreased by:

$$\epsilon_{MP,top} = (6400 - 6375.7)/2 = 12.2mm \quad (1.7)$$

The transition piece and monopile will touch at the bottom, which is at the maximum diameter of the transition piece. Using the inner diameter of the transition piece, the length of the overlapping part can be calculated. The wall thickness of $85mm$ is subtracted from the outer diameter:

$$L_{SJ,overlap} = \frac{(6857.4 - 2 \times 85) - 6375.7}{2} / \tan 1.15^\circ = 7764mm \quad (1.8)$$

The diameter of the transition piece at the top of the lap joint can be calculated:

$$D_{TP,topoverlap} = (6857.4 - 2 \times 85) - 2 \times \tan 1.05^\circ \times 7764 = 6403mm \quad (1.9)$$

Hence the gap is: $(6403 - 6375.7)/2 = 13.7mm$

Note that this is the maximum gap prior to installation. During installation the cones will settle and deform. The gap will be smaller after installation.

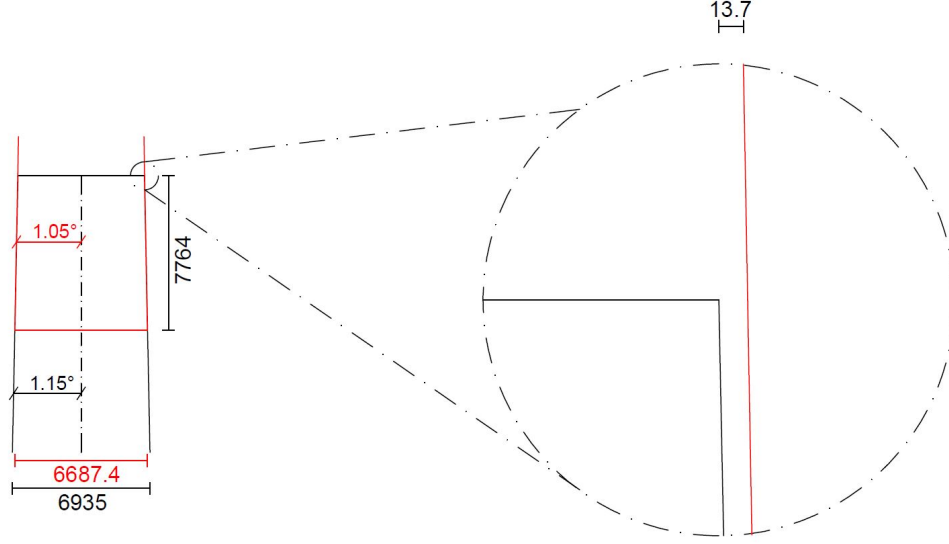


Figure 1.8: Gap between the transition piece (in red) and monopile (in black) for the maximum deviation of the cone angle.

Maximum deviation from nominal radius

The previous calculated tolerances have to comply with the tolerance for the nominal radius. A deviation from the nominal radius will not contribute to a gap between the transition piece and monopile directly. If the deviation is constant over the height of the cone, it will only cause a shift in the location of the connection. The maximum tolerance to the nominal radius can be calculated by the equation:

$$\sigma = (r_a - r) = 0.005 \times r \quad (1.10)$$

in which r_a is the actual distance from the cylinder axis to the shell wall and r is the nominal radius of the shell.

The maximum deviation from the nominal radius for the bottom of the transition piece is:

$$\sigma_{TP, Bottom} = 0.005 * \frac{6874}{2} = 17.2mm \quad (1.11)$$

The cone angle will change in the case that only the bottom of the transition piece deviates from its nominal radius. The angle is calculated with the difference between the diameter of the bottom and top of the cone equal to 6874.4 and 6500 respectively. The maximum deviation of 17.2 from the nominal radius is subtracted from the diameter at the bottom. The angle becomes:

$$\tan^{-1} \left(\frac{(6874.4 - 2 \times 17.2) - 6500}{2} / 9750 \right) = 1.0^\circ \quad (1.12)$$

The change of the cone angle is bigger than 0.05° , which is the tolerance on this angle as stated earlier. The angle limit is the limiting factor in this case. This can be found in table 1.1.

Combining the tolerances

An overview of the tolerances is given in table 1.1. The results show that the tolerance to the nominal radius is limiting for the out of roundness.

Tolerance	Location	Corresponding \emptyset [mm]	Max [mm]	Min [mm]
Out of roundness	TP cone top	6500	19.9	-19.9
	TP cone bottom	6874.4	21	-21
	MP cone top	6400	19.6	-19.6
	MP cone bottom	6935	21.2	-21.2
Nominal radius	TP cone top	6500	16.3	-16.3
	TP cone bottom	6874.4	17.2	-17.2
	MP cone top	6400	16.0	-16.0
	MP cone bottom	6935	17.3	-17.3
Cone angle	TP cone top	6500	0	0
	TP cone bottom	6874.4	0	-8.5
	MP cone top	6400	0	-12.2
	MP cone bottom	6935	0	0

Table 1.1: Tolerances of the transition piece and monopile radius

Within the limits of all tolerances, any combination of the tolerances is possible. The following combination is used in order to find the potential maximum gap. The scenario, as shown in Figure 1.9, is a combination of all three tolerances. σ is the tolerance of the nominal radius and δ is the maximum out of roundness. In this scenario the radius is adjusted with β such that two sections around the circumference are at the maximum out of roundness.

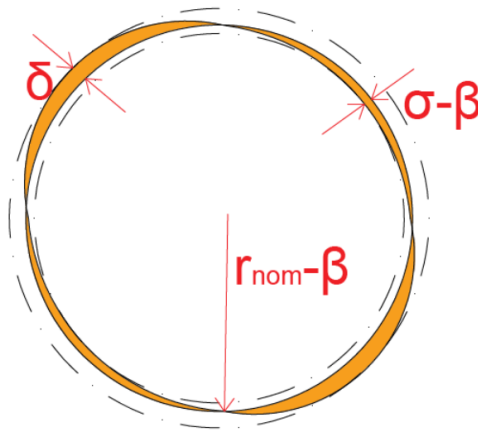


Figure 1.9: Combined tolerances

To clarify the tolerance combination, table 1.2 summarizes the used tolerances. The maximum tolerances calculated for the transition piece and monopile is taken and used over the whole transition piece and monopile respectively.

Tolerance	Location	Initial Ø[mm]	Max [mm]	Min [mm]
Out of roundness	TP cone top	6500	21	-13.4
	TP cone bottom	6874.4	21	-13.4
	MP cone top	6400	13.5	-21.2
	MP cone bottom	6935	13.5	-21.2
Nominal radius	TP cone top	6500	0	-3.8
	TP cone bottom	6874.4	0	-3.8
	MP cone top	6400	3.8	0
	MP cone bottom	6935	3.8	0
Cone angle	TP cone top	6500	0	0
	TP cone bottom	6874.4	0	-8.5
	MP cone top	6400	0	-12.2
	MP cone bottom	6935	0	0

Table 1.2: Tolerance combination

The maximum gap, resulting from this combination, is not a simple sum of the tolerances. During installation the cones will settle and deform. Therefore the above geometry is inserted in a finite element model, which calculates the gap after installation.

1.2.5 Van Oord in-house FE-model for Slip Joint connections

At Van Oord a finite element ANSYS model has been developed for the Slip Joint, by the engineering department. The purpose of the model is to design the Slip Joint. With this model deformations are calculated. The model is used to find the expected maximum gap between the two cones after installation. This model is only used to get an indicative maximum gap size in order to be able to investigate the corrosion in these gaps. This section therefore does not provide a full review of the model. The Slip Joint design, as shown Figure 1.5 with the given tolerances from paragraph 1.2.4, is put into the FE-model.

Table 1.3 presents the parameters that are used for the model. The parameters are related to the steel material of the monopile and transition piece.

Elasticity modulus	210 [GPa]
Poisson's ratio	0.3
Mass density	7850 [kg/m ³]
Gravity	9.81 [m/s ²]
Friction coefficient	0.2

Table 1.3: Parameters used in the FE-model

The modeled monopile is fully constrained at the bottom. Gravity is added to the system. The connection is loaded with the weight of the transition piece. In 100 steps the load is applied to the system. Under this load, the transition piece will slide over the monopile. Both, the transition piece and monopile will deform. The transition piece will slip until the situation is stable.

The resulting maximum gap is taken after the deformation of the monopile and transition piece. Although the resulting maximum crevice dimensions corresponds specifically to this case, the values are applicable for a broader use. It gives an indication of the order of magnitude of the crevice that can be expected in an offshore applied Slip Joint.

The maximum gap that is observed using the FE-model, is for the case that the transition piece and monopile have a cone angle of 1.05 degrees and 1.15 degrees respectively. The gap after installation is found to be 12 millimeter.

In Figure 1.10 a plot is made of the upper part of the Slip Joint, where the maximum gap is found. The model has also been run for the case that only the maximum out of roundness is applied to the monopile and transition piece. These calculations showed that the oval shaped monopile and transition piece will deform to a more perfect round shape. The gap that existed before settling of the transition piece is closed after applying the load.

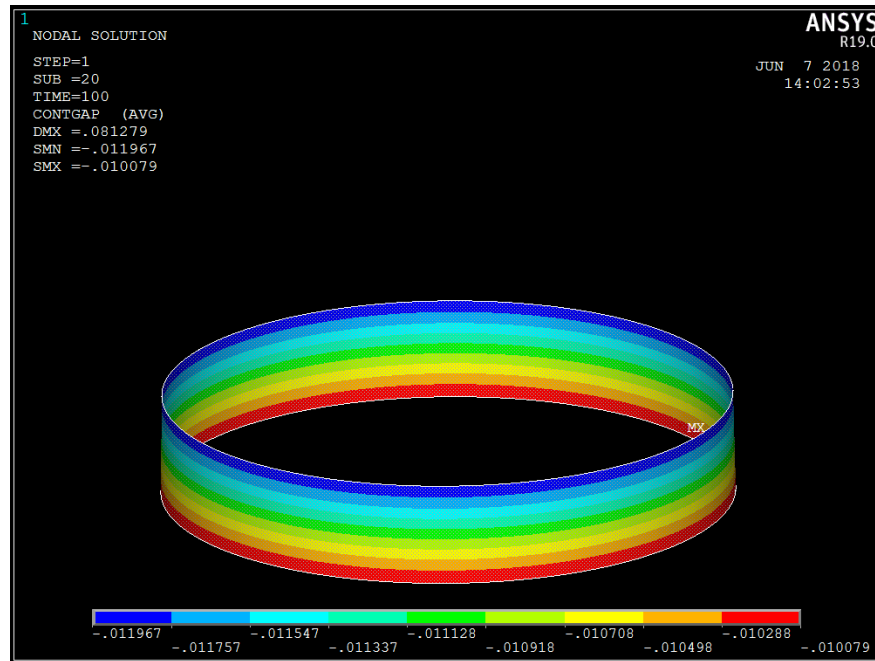


Figure 1.10: Maximum gap in slip joint for cone angle tolerance

Not only the cone angle tolerance is relevant for a possible gap after installation, also the tolerance on the roundness of the cone is an important factor. The maximum cone angle only due to this out of roundness has been put to the test.

The results of these tests show that the maximum allowed out of roundness will not result in a significant gap between the interface of the monopile and transition piece. The cone is forced to match between the transition piece and monopile. In comparison to the model with the cone angle

tolerance, this model finds contact at a higher position and thus this long slip distance is expected. In conclusion the expected maximum gap in the Slip Joint provided by Van Oord is expected to be approximately 12mm.

1.2.6 Expected gap in the Slip Joint

The maximum gap is expected to be approximately 12mm for the Slip Joint provided by Van Oord. The cone is flexible enough to be able to deform the out of roundness back to a circle. A deviation of the cone angle will give bigger gaps.

The given scenario is assumed to be sufficiently representing possible offshore gaps. The result is conservative to Van Oord, because Van Oord uses stricter tolerances for their designs and therefore smaller gaps would be expected. A more detailed study could be carried out in which the influence of parameters, like the friction coefficient, is investigated. This is outside the scope of this research.

To be on the conservative side and to be able to use the result for other slip joint designs, a maximum gap of 14mm in a Slip Joint is assumed to be sufficient to check for its corrosion behavior.

The material that should be used in the experiments is best to be the same or at least resemble the properties of S355ML or S355J2. The corrosion rate of the selected material will be checked, to establish possible differences with the alloy normally used in the Slip Joint.

1.3 Research question

In order to predict what will happen in the predicted gap of the Slip Joint connection, this investigation will study the corrosion behavior of crevices of S355 steel that is found in a typical offshore used foundation. Crevices like the crevice at the interface of the Slip Joint are possibly also found in different structures. Therefore, this research is not only relevant to the Slip Joint, but also gives a more general insight into corrosion of constructional steel in similar crevices. The parameters for this study, like crevice sizes and material properties, are taken from the Van Oord Slip Joint design. The main question of this research is:

- What corrosion behavior can be expected in offshore submerged Slip Joint crevices?

In order to answer the main question, the sub-questions are to be answered. The following questions will be answered based on literature.

1. What type of corrosion behaviour can be expected in the Slip Joint?
2. What are typical offshore corrosion rates for steel?
3. What is an appropriate experiment set-up to simulate corrosion in the Slip Joint?

The research further will have to give an answer to:

4. What corrosion rates can be observed experimentally in the local environment of the Slip Joint?
5. What corrosion type is observed experimentally in the local environment of the Slip Joint?
6. What research is further required?

The research is focused on understanding the behavior of corrosion at the interface of the Slip Joint. Corrosion on the outside surfaces of the monopile and transition piece is not of any interest for this research while especially the crevice is unknown for its corrosion behavior. Even though they are of relevance, the following objectives are excluded from the scope as they do not fit within the frame of the thesis:

- Development of a method to prevent corrosion in the Slip Joint, because first we must understand the corrosion behavior in the Slip Joint.
- Development of a numerical or theoretical model for corrosion prediction in the Slip Joint. Non the less, this will be shortly discussed in the thesis.
- Full scale testing. This is not possible in the time frame of a master thesis.

To answer the research questions adequately, the following approach is utilized. First, a literature study has been carried out, to analyze offshore corrosion in crevices and assess applicable experiment methods. This resulted in the conclusion that tests were necessary. An experiment method is developed, because corrosion tests with large specimen sizes, as required for this research, have not been carried out until now. Concepts of other crevice corrosion experiments have been used but had to be up scaled for larger specimen sizes. The methods for making specimens and creating a set up for the experiment required some preliminary tests. The final experiment method has been selected and the experiment was carried out. Following the experiment, the obtained data is analyzed and discussed. This resulted in a conclusion with recommendations.

1.4 Report structure

This report discusses the investigation towards corrosion in the crevice between the monopile and transition piece when using a Slip Joint. As the local environment is known, in chapter 2 the fundamentals of offshore corrosion are discussed to research what corrosion phenomena can occur in this local environment. In chapter 3 the relevant research for the corrosion inside the Slip Joint is discussed. In this chapter is found that there is a gap in research towards crevice corrosion. There is no knowledge of crevice corrosion in structural steel crevices of relative large geometries. Chapter 4 therefore discusses the tests, based on the knowledge from chapter 2 and 3, that had to be carried out to research the corrosion in these crevices. Additionally a corrosion prevention technique called Impressed Current Cathodic Protection is tested for its effectiveness on crevices. The results of the tests are given in chapter 5 and are discussed in chapter 6. In the final chapter, chapter 7, the research conclusion is discussed and recommendations are given.

2 Fundamentals of offshore corrosion

In order to get knowledge on typically offshore corrosion, this chapter will discuss offshore corrosion and different corrosion phenomena that are relevant to the Slip Joint. In section 2.4 electrochemical measurement techniques that are frequently used nowadays will be discussed, in order to get knowledge of possible experimental techniques that can be used in corrosion experiments. Finally, corrosion prevention techniques are discussed and the prevention technique of Impressed Cathodic Protection is introduced, because Impressed Current Cathodic Protection is tested for its effectiveness to prevent crevice corrosion as described in section 4.7.

2.1 Definition of corrosion

Corrosion is the degradation of metals and alloys by electrochemical reactions with the environment. During the corrosion process, metals are converted to a chemical more stable condition. [9]

Metals or alloys are unrepairably damaged via corrosion due to its reaction with the environment. During degradation, the alloy breaks down into oxides, hydroxides, salts or carbonates. Corrosion of iron results in iron-oxides which form a rust layer on the metal. [10]

There are several processes that result in corrosion, the aqueous corrosion process always goes according to the same principles. Corrosion is caused by a redox reaction, reduction and oxidation reactions are coupled. The two half-reactions together form a whole reaction. In a reduction reaction an atom will gain electrons, in an oxidation reaction atoms will lose electrons. The metal at which the oxidation occurs for corrosion is called the anode. The reaction causing the reduction for corrosion is called the cathodic reaction and thus the compound at which this reaction occurs is called the cathode. The most common corrosion reaction is with water, oxygen and iron. The corresponding redox reactions are given in the next equations.

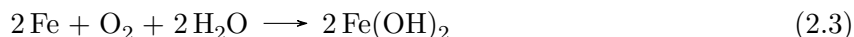
Reduction:



Oxidation:

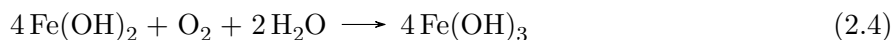


Overall reaction:



In Figure 2.1 an abstract representation is shown. The location of the cathodic and anodic reactions are not fixed. They alternate over the surface of the metal.

The product of the redox reaction shown in equation 2.3 is unstable and will turn into the more stable $\text{Fe}(\text{OH})_3$, which is a brown salt mostly known as rust:



Depending on environmental factors such as oxygen concentrations, acidity and the availability of water, other corrosion products can be formed during a corrosion process. For example, magnetite (Fe_3O_4) is a corrosion product of iron that occurs in anaerobic environments.

The corrosion process, as described above, only occurs if an electrolyte is present. The electrolyte is the corrosive medium, in this case seawater. The corroding metal dissolves in the electrolyte as positively charged ions (cations) by releasing electrons which are take part in the cathodic reaction. The current from the corrosion reactions, between the anode and cathode consists of electrons in the metals, from the dissolved metal, and ions flowing in the electrolyte.

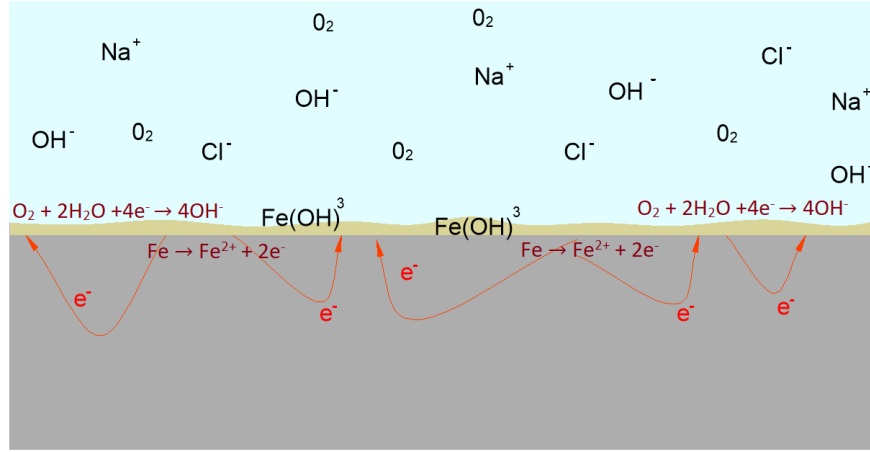


Figure 2.1: Uniform corrosion reactions

2.2 Parameters influencing corrosion

Oxygen and water are considered as the main components in the environment that are involved in aqueous corrosion on metals, shown by the redox reaction in the previous paragraph. Other components like nitrogen oxide or sodium chloride can accelerate the corrosion process. The factors discussed in this section are related to structural steels and marine environments. There are multiple other factors which influence corrosion, but these are considered irrelevant to the Slip Joint.

2.2.1 Effect of the pH

An acid is a substance which, when dissolved, dissociates in H^+ ions. Acidity is quantified using the pH value. The concentration of H^+ , in mole per liter, in a negative logarithm gives the pH. Acidity is a parameter that influence the corrosion rate. In Figure 2.2 the relation between pH-level and corrosion rate, in grams per squared meter per day, for steel is shown.

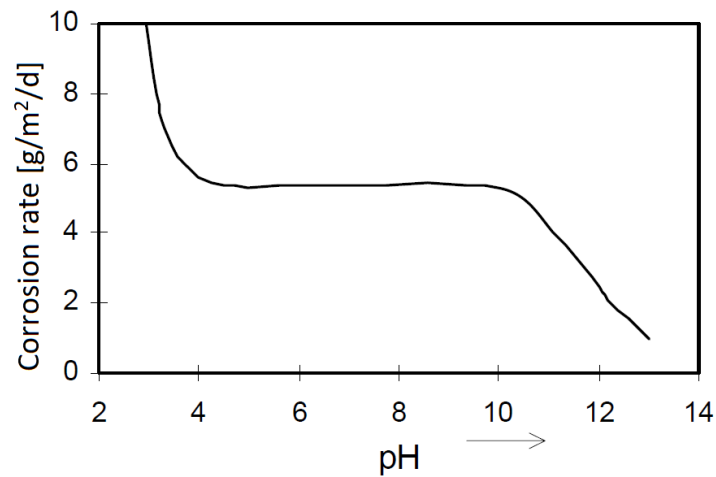


Figure 2.2: Corrosion rate as function of pH for low alloy steel in aerated aqueous solution [9]

In an acidic environment ($\text{pH} < 4$), impurities on the metal surface and the micro structure of the surface have a major influence on the corrosion rate, corrosion rates can increase up to more than 50 percent. In most cases hydrogen is formed around impurities. This increases the corrosion rates around these impurities. The cathodic reaction involved here, in an unaerated environment, is:



In medium acidity conditions containing O_2 cathodic reaction is:



For pH between 4 and 10.5 the corrosion is practically independent of the pH. Above $\text{pH} \approx 10.5$ the corrosion rate will decline when the pH gets higher. [9]

The given reduction in equation 2.6 is very possible to occur synchronous with reaction 2.1. The sum of the both reactions will give the total corrosion.

2.2.2 Effect of salinity

Electrolyte resistance is decreased by adding salt (NaCl) into water. This results in a change in the protective nature of the rust barrier. The conductivity of a sodium chloride solution is greater, anodes and cathodes are able to operate further apart from each other. According to Revie and Uhlig, at the anodes FeCl_2 can be formed in sodium chloride solutions. The FeCl_2 diffuses into the solution and reacts with NaOH to form $\text{Fe}(\text{OH})_2$ in the solution. [7]

In solutions with no NaCl or low NaCl concentrations below 3%, the rate of corrosion will increase very much by increased concentrations. Seawater has a NaCl concentration around 3.5% (0.5 mol/l). Oxygen becomes less soluble for higher concentrations of sodium chloride. Above a concentration of approximately 3.5% in water, the solubility of oxygen drops such that it will decrease the corrosion rate. This relation is shown by Revie and Uhlig in [7] as visualized in Figure 2.3.

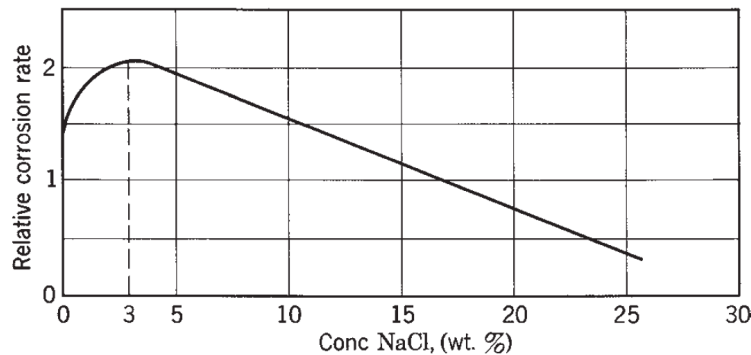


Figure 2.3: Corrosion rate of iron as function of sodium chloride concentration [7]

2.2.3 Influence of oxygen

For significant corrosion to occur at ambient temperatures, oxygen is necessary. The corrosion of steel is influenced by the oxygen content. In areas with stagnant water, oxygen will not be replenished and thus creates deaerated environments. Water flow will increase transport of the oxygen and thus increases corrosion rates. [10]

Differential aeration cells can be formed when transport of oxygen to an area is blocked or low. This can result into localized corrosion. The concept of a differential aeration cell will be explained in more detail in section 2.3.3.

2.2.4 Effect of temperature

Generally corrosion rates increase with temperature. Higher temperatures of the electrolyte will increase the diffusion rates through the electrolyte and increases the mass transfer. [11] The resistivity of seawater will drop as a function of temperature, see Figure 2.4. The corrosion current is directly influenced by this resistivity, for a lower resistivity the current will increase. However, the corrosion rate increase is mainly caused by the enhancement of diffusion of corrosive species, the increase of H^+ concentration and the increase of reaction rate.

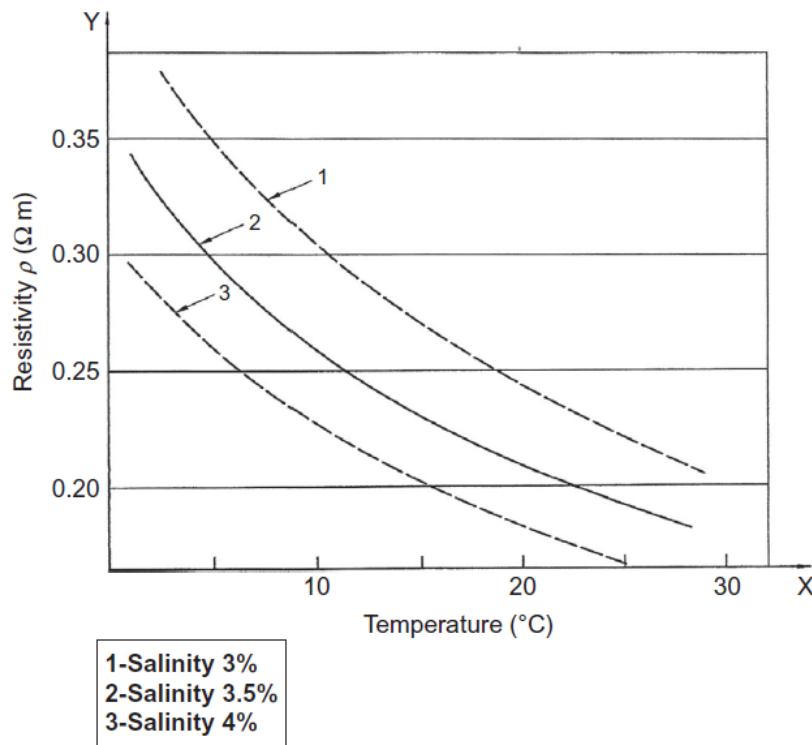


Figure 2.4: Seawater resistivity as a function of temperature [4]

In an open system, where oxygen can escape the solution, the corrosion rate increases with temperature only up to 80°C and then drops. (This solution temperature is not relevant to the marine environment.) The oxygen concentration drops with increasing water temperatures. From a temperature of 80°C the concentration of oxygen becomes limiting to the corrosion rate and thus the corrosion rate drops for higher temperatures. The influence of the oxygen concentration becomes more prominent than the increase in corrosion rate caused by the temperature. In a closed system the oxygen cannot escape, thus the corrosion rate will keep rising with temperature. (Although in the closed system over time oxygen can be depleted by the corrosion and then the corrosion rate will drop again.) In Figure 2.5 this effect is shown.

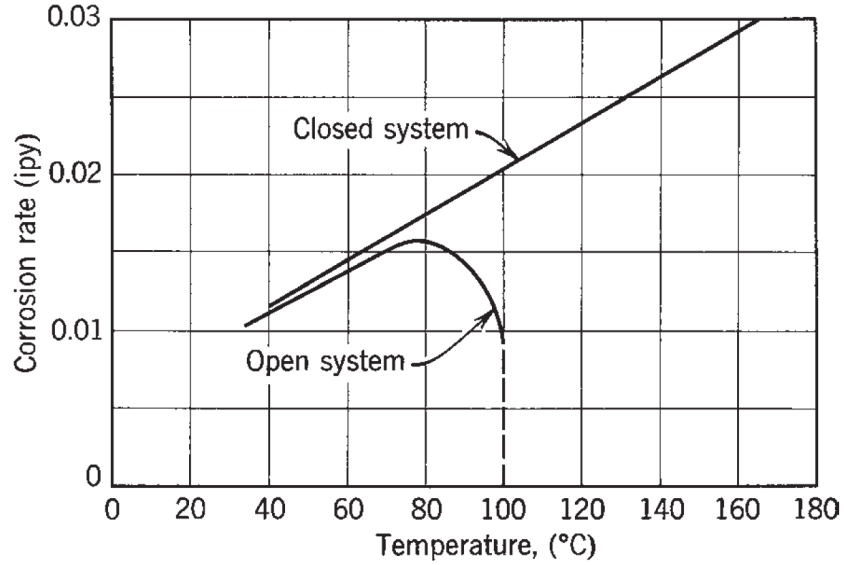


Figure 2.5: Temperature effect the corrosion rate of steel in water [7]

2.2.5 Influence biological activity on corrosion

In seawater living organisms are present. Biological activity can form a layer on metal objects submerged in seawater. Biofouling, as it is called, can result in crevice conditions and therefore effect the corrosivity of the environment. (Crevice conditions are conditions in which partly confined spaces result in differential aeration and thus local corrosion attack can occur.) [10] In Figure 2.6 an example of offshore equipment with a layer of biological activity, called biofouling, is shown.

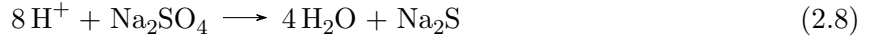
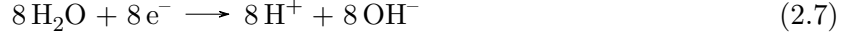


Figure 2.6: Example of biofouling in marine environment [12]

Not only do shellfish, or other visible fouling influence the corrosive environment. Microorganisms like microalgae, bacteria and fungi can cause various forms of corrosion. This is called microbi-

ologically influenced corrosion (MIC) which takes place in seawater and anaerobic environments. Iron does not corrode significantly in deaerated water, but in some cases high corrosion rates are measured due to sulfate-reducing bacteria. These bacteria can reduce SO_4 and use hydrogen to do so. This reduction forms a cathodic reaction that makes the oxidation of iron possible. [7]

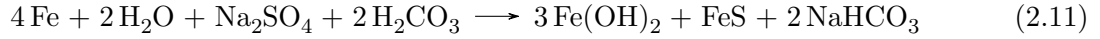
Given by [7] is a possible reaction sequence in which the cathodic reaction, reduced by the bacteria, is given as:



The anodic reaction of iron:



In summary the total reaction:



In this situation iron sulfide and iron hydroxide is formed. Other cathodic reactions are possible.

2.2.6 Passivity of a metal surface

Alloys are used in steels to improve their mechanical properties but can also be added to improve corrosion resistance. Certain metals are corrosion resistant in specific corrosive environments. Metals that passivate by interaction with the oxidizing environment or by anodic polarization are defined as active-passive. The formation of surface films through oxidation creating corrosion resistance is called passivity. [8]

In the passive region a metal is covered with an oxide or hydroxide layer preventing all direct contact between the metal itself and the environment. The layer will be porous for certain metals, which only partly protects the material. [13]

Due to the environment or the local conditions the passive layer can break down, for example in an acidic environment, which can result in localized corrosion mechanisms. Once initiated the corrosive activity starts rapidly and the corrosion rate is severe. Nevertheless, the structural steel which is used for monopiles and transition pieces, does not establish a passive layer in a marine environment and therefore corrodes uniformly over its surface. Structural steel does not have high chromium contents that would form a chromium oxide skin. Although iron oxides can be formed on structural steels, these are bulky and hygroscopic (the ability to attract and hold water) and do not adhere to the steel surface.[7]

In the section about crevice corrosion, section 2.3.3 it becomes clear that there are situations that structural steel will not corrode uniform.

2.3 Corrosion phenomena

There are multiple corrosion phenomena. In this section, the mechanisms which are relevant and applicable to the Slip Joint are being discussed. Most types of corrosion occur by electrochemical reactions, but appearance and damage are different for different conditions.

First of all, a distinction can be made between local corrosion and uniform corrosion. Uniform corrosion occurs over the total surface of the object. [9] Uniform corrosion occurs at the bare steel surfaces of the monopile which are unprotected by coatings or other means of protection and are fully exposed to the marine environment. (Biofouling can disrupt uniform corrosion, see 2.2.5)

Local corrosion cause more severe problems. Local corrosion rates are less predictable and localized attacks can be very aggressive, leading to pits in the material. [9] For the interface of the Slip Joint, crevice corrosion is of particular importance. A simplification of the Slip Joint foundation can be described by two contacting steel plates. It has been found that corrosion in the crevice itself and fretting corrosion are the most influencing occurrences within such lap joints. [14]

2.3.1 Uniform corrosion

Uniform corrosion, visualized in Figure 2.1, causes even degradation due to the fact that the location of the anodic and cathodic reactions continuously alternate. By the formation of rust on the steel surface, the oxygen transport towards the metal surface gets blocked. The barrier decreases the corrosion rate until a steady state is reached with a constant corrosion rate. [9]

In Figure 2.7 a monopile is shown. This steel pile is corroded due atmospheric corrosion. The monopile is corroded uniform over its surface.



Figure 2.7: Uniform corrosion on a monopile at the Aeolus

For uniform corrosion to occur, the metal surface must be unvarying accessible to the environment. The metal must be metallurgically uniform. According to Denny A. Jones this is not prevalent in

operating equipment and thus some degree of nonuniformity is tolerated within the definition of uniform corrosion. [10]

Uniform corrosion rates generally are in the range of 0.08 millimeter per year and 0.18 millimeter per year. Corrosion rates will decrease with increasing time of exposure. Data from a test of Reinhart shows a major decrease in corrosion rate in tests lasting approximately three years, see Figure 2.8. [15]

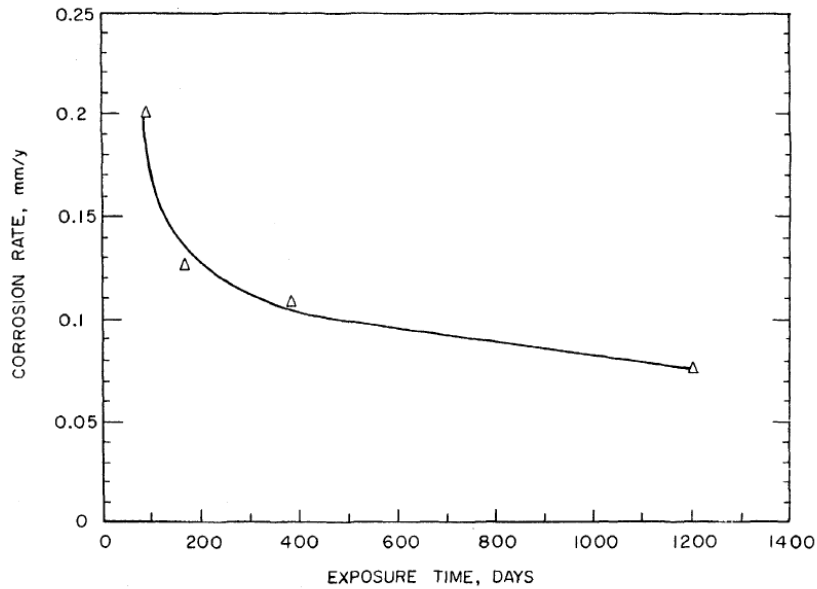


Figure 2.8: Development of corrosion rate over time of low-alloy steels [15]

The first year the corrosion rate decreases rapidly from 0.2 millimeter per year to 0.11 millimeter per year. The corrosion rate after three years was in this test 0.08 millimeters per year.

2.3.2 Pitting corrosion

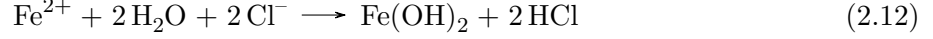
To help explaining crevice corrosion, first the local corrosion phenomenon pitting is discussed. There are several conditions that can lead to pitting corrosion. A few, which are relevant to this thesis, are discussed here. Apart from the fact that it is less predictable, it also is more difficult to check the severity.

On certain metals, a passive layer is present as being discussed in 2.2.6. The passive layer can be broken or scratched. Pitting could be caused by a local breach of the layer. This can create a passive-active local environment. Between the small anode, that is formed, and the big passive cathode of the surrounding area a high potential difference arises. Consequently, high corrosion rates will be observed locally. Under specific conditions, the passive layer will restore and the local attack is terminated. This is called repassivation. [9]

After breaking of the passive layer a passive-active element is formed in which a high potential difference can be found between the small anodic and big cathodic part. The concentration of chloride ions in the pit increases as a result of the contribution to the current transport through

the electrolyte. As a result of the hydrolysis of the dissolved metal, the acidity in the pit will drop. Due to the acidity repassivation will become impossible. [9]

Local pH reductions are formed by the reaction:



Lower pH levels will further accelerate the anodic reaction, see section 2.2.1, which in turn will further increase the chloride concentration, the H^+ ions attract Cl^- ion). However the anodic reaction is important, pit growth will stop when the electrons are not consumed by the cathodic reaction. [10]

In Figure 2.9 a drawing of the pit is shown and all the reactions are shown schematically. The pit is corroding and the rust deposit forms outside of this pit. Also visible is that the internal environment of the pit is low on oxygen, this is due to the depletion of oxygen and the insufficient aeration. Oxygen diffusion to the small pit is hindered due to the geometry.

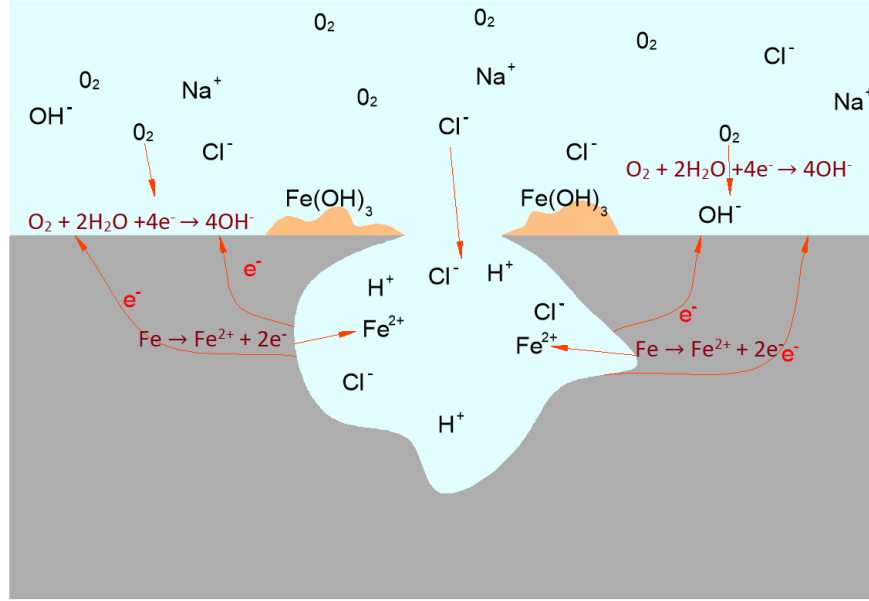


Figure 2.9: Schematic drawing of reactions occurring with pitting corrosion

The pit depth is found to be Gaussian distributed around the average. Pits on experimental test plates are therefore not directly related to practical pit forming, while test plates are much smaller than a construction would be. The maximum pit depth, therefore, will be different in each case. [9]

Structural steels do not form a passive layer in seawater, so pitting due to the breakdown of such a layer will not occur on structural steels. Pitting can occur on structural steels, for example caused by local damages to protective coatings or biological activity.

2.3.3 Crevice corrosion

The most interesting type of local corrosion for the Slip Joint is crevice corrosion. Small crevices can be found at connections like bolts, between two sheets, under paint blisters, biofilms formed and by micro organism which form semi-enclosed environments in which water is more or less stagnant.

There are multiple theories described that induce crevice corrosion. The most common and accepted are; the IR drop, the critical crevice solution (CCS) and the coupled environment theory. Although the approach of each theory is different, they are related. This will be explained further in this section.

In narrow spaces the oxygen concentration will drop due to the consumption of oxygen by corrosion. [9] Due to differential aeration and diffusion limitations this oxygen is not sufficiently resupplied. While the outside surface has access to oxygen it becomes cathodic and the area inside the crevice becomes anodic. The geometry of the crevice is very influential to the initiation of crevice corrosion. The height and length of the crevice control the access of oxygen into the crevice and influence the concentration gradient of oxygen. As with pitting corrosion, hydrolysis occurs: metal cations form metal hydroxides which lowers the pH value by the release of H^+ . The differential in aeration between the internal and external environment of the crevice forms local increased chloride concentrations. Oxygen is consumed by corrosion in the crevice, hence the concentration of the metal cations will be increased. The metal cations are positively charged ions and thus will attract negatively charged anions, chloride, from the external environment. Part of the process, when the mass transfer to the crevice becomes more difficult, is that the solution in the crevice becomes more aggressive. [16] [10]

The crevice has to be sufficiently narrow to make an aeration differential possible and wide enough to allow the electrolyte (seawater) in. Very narrow crevices may result in restrained propagation, deeper areas will stay unaffected. The geometry of the crevice has a major influence on the sensitivity to crevice corrosion. The geometry limits mass transport inside the crevice and permits a potential drop to occur. The influence of the potential drop is explained in further detail in the following parts of this section. [10]

A drop in potential will start by the separation of anodic and cathodic areas, caused by the differential in aeration. After this separation a net current will flow through the crevice. The anodic current flows from the crevice and the electrical resistive electrolyte causes a potential difference between the crevice and the cathodic areas, sometimes referred to as Ohmic drop or IR drop. Studies have shown that the potential drop should not be left disregarded, the effect of the potential drop alone can already induce crevice corrosion and increase the corrosion rate locally. The drop is caused by the resistance of the electrolyte inside the crevice:

$$\Delta E_{ohmic} = i \times R \quad (2.13)$$

i indicates the current within the crevice electrolyte and R the resistance of the electrolyte. The electrical resistance R is composed of:

$$R = \rho \times \frac{l}{A} \quad (2.14)$$

in which ρ is the electrical resistivity, l is the length of the electrical resistive path and A is the cross-sectional area of this path. The resistance will change as the crevice geometry changes, as can be seen in formula 2.14, a smaller gap will result in a smaller cross-sectional area and bigger resistance. The resistance increases linearly, for a constant resistivity, going deeper into the crevice.

There are multiple regions in the crevice that can be described. The region in the area of the mouth of the crevice, where the oxygen concentration is highest will act as the cathode. The active anodic area, which is working on a lower potential. Further into the crevice the potential drop can become so big that these deeper parts become passive. [17]

A similarity with pitting corrosion can be found, crevice corrosion continuously grows after initiation. Increased chloride concentration and acid hydrolysis enhances the localized anode which again is coupled with a larger external surface area acting as the cathode. By the corrosion process, more chloride will migrate into the crevice environment. Thus, the process is self catalytic. [10]

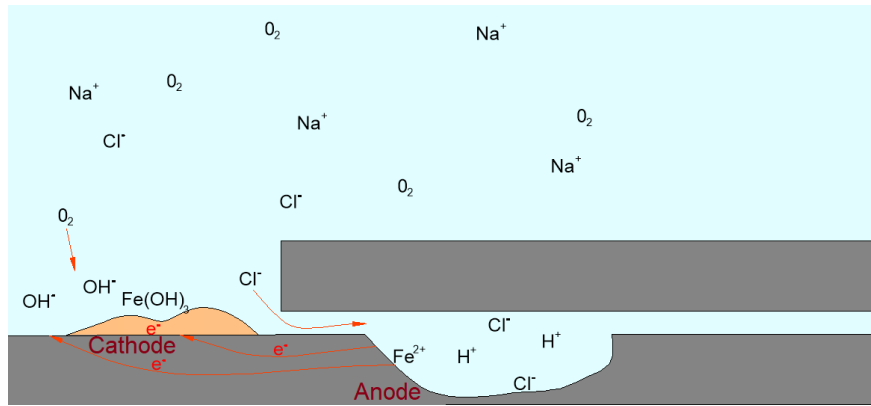


Figure 2.10: Schematic drawing of reactions with crevice corrosion

More about crevice corrosion and research towards this phenomenon is discussed in the next chapter, chapter 3.

2.3.4 Fretting corrosion

Another phenomenon that could occur in the slip joint, due to its dynamic behavior, is fretting corrosion. The loads on the turbine and monopile will cause movements and bending of the structure. By movement of the sheets contact surface can be scraped off. The product from the wear in combination with a corrosive environment can form reaction products. These reaction products can be oxides originated by a reaction with the oxygen from the environment. While oxides are mostly harder than the metal itself, the wear can be accelerated. Due to the deep sharp pits, cracks in the metal can appear. Therefore, fretting can be seen as a wear process which is enhanced by corrosion. [9]

2.4 Corrosion measurement techniques

Corrosion is an electrochemical process of which the released electrons by the oxidation and the collection of electrons by the reduction cause a current that can be measured. Electrochemical experiments and measurement techniques in combination with the properties of metals in an electrolyte can be characterized to each particular metal and electrolyte. This is helpful in determining corrosion rates and corrosion behavior of a metal. The measurement techniques that are described in this section, have been used during the experiments as described in chapter 4.

2.4.1 Potential measurements

A potential can be measured by checking the voltage difference between a reference electrode and a corroding metal. The sign of the measurement indicates whether the metal is negative or positive with regard to the reference electrode and the magnitude indicates the electromotive force. [13] The measured corrosion potential is a mixed potential of both the anodic and cathodic reactions. The corrosion potential is determined by the kinetics of the half-cell reactions. [10] Less noble metals show more negative corrosion potentials and more noble will show less negative corrosion potentials. [7]

Potential measurements are often used to monitor metals in operating situations and for corrosion studies. The potentials for certain materials in an electrolyte are determined. Especially for seawater most corrosion potentials for metals are known. The so called "Galvanic Series" help in finding the driving force for corrosion. In Figure 2.11 these "Galvanic Series" are shown. A less noble metal dissolves because it gives electrons to the more noble metal when these two metals are electrically connected. [8]

<u>Galvanic Series of Metals in Seawater</u>			
<u>Metals and Alloys</u>	<u>Corrosion Potential</u> (volts DC ref. Ag/AgCl)		
Magnesium and Magnesium Alloys	-1.60	to -1.63	anodic - active
Aluminum - Anode	-1.10		
Zinc	-0.98	to -1.03	
Aluminum Alloys	-0.76	to -1.00	
Mild Steel (clean & shiny)	-0.60	to -0.71	
Mild Steel (rusted)	-0.20	to -0.50	
Cast Iron (not graphitized)	-0.60	to -0.71	
Stainless steels	-0.46	to -0.58	
Stainless Steel, Type 316 (active in saltwater)	-0.43	to -0.54	
Aluminum Bronze (92% Cu, 8% Al)	-0.31	to -0.42	
Copper	-0.30	to -0.57	
Naval Brass (60% Cu, 39% Zn)	-0.30	to -0.40	
Yellow Brass (65% Cu, 35% Zn)	-0.30	to -0.40	
Red Brass (85% Cu, 15% Zn)	-0.30	to -0.40	
Muntz Metal (60% Cu, 40% Zn)	-0.30	to -0.40	
Admiralty Brass (71% Cu, 28% Zn, 1% Sn)	-0.28	to -0.36	
Aluminum Brass (76% Cu, 22% Zn, 2% Al)	-0.28	to -0.36	
Silicone Bronze (96% Cu max, 0.80% Fe, 1.5% Zn, 2.00% Si, 0.75% MN, 1.60% Sn)	-0.26	to -0.29	
90% Cu, 10% Ni	-0.21	to -0.28	
75% Cu, 20% Ni, 5% Zn	-0.19	to -0.25	
Lead	-0.19	to -0.25	
70% Cu, 30% Ni	-0.18	to -0.23	
Stainless steel, Type 304 (passive)	-0.05	to -0.10	
Stainless steel, Type 316 (passive)	-0.00	to -0.10	
Titanium	+0.06	to -0.05	
Platinum	+0.25	to +0.19	
Carbon, Graphite, Coke	+0.30	to +0.20	cathodic - noble

Figure 2.11: Galvanic Series of metals in seawater versus a saturated Ag/AgCl reference electrode [8]

With the corrosion of a metal, for example steel in a seawater solution, both the anodic and cathodic half-cell reactions occur simultaneously on the surface, see section 2.1. Both the anodic and cathodic reactions have their own potential. But, these two reactions will not occur separately on the metal surface. These reactions will change potential to a common intermediate value, which is the potential that is measured during an open circuit measurement. It is a mixed potential of the half-cell reactions and is also called the corrosion potential. A corrosion process can and will exist of multiple different half-cell reactions. In seawater there are multiple oxidizers that are involved in the corrosion process. Experiments have shown that adding an oxidizer will shift the corrosion

potential to more positive values and will increase corrosion rates. [10]

According to table 2.11 mild steel in seawater has a corrosion potential between -0.60 to -0.71 Volts. This will be the potential if the steel is corroding uniformly, as described in 2.3.1. If the corrosion potential is monitored over time, changes in the corrosion behavior can be measured. A change of the potential indicates that the reactions at the surface of the specimen are changing.

This technique is used in the experiments, described in chapter 4, to monitor differences in corrosion behavior between specimens, as described in section 4.4.1.

2.4.2 Experimental electrochemical set-ups

A polarization cell consists of an electrolyte solution, a reference electrode, a counter electrode and a metal sample which are connected to a potentiostat. The metal sample (called the working electrode), counter electrode and reference electrode are all immersed in the electrolyte. The potential is measured between the working electrode and the reference electrode by the connected potentiostat. A schematic representation of this type of setup is shown in Figure 2.12. [13]

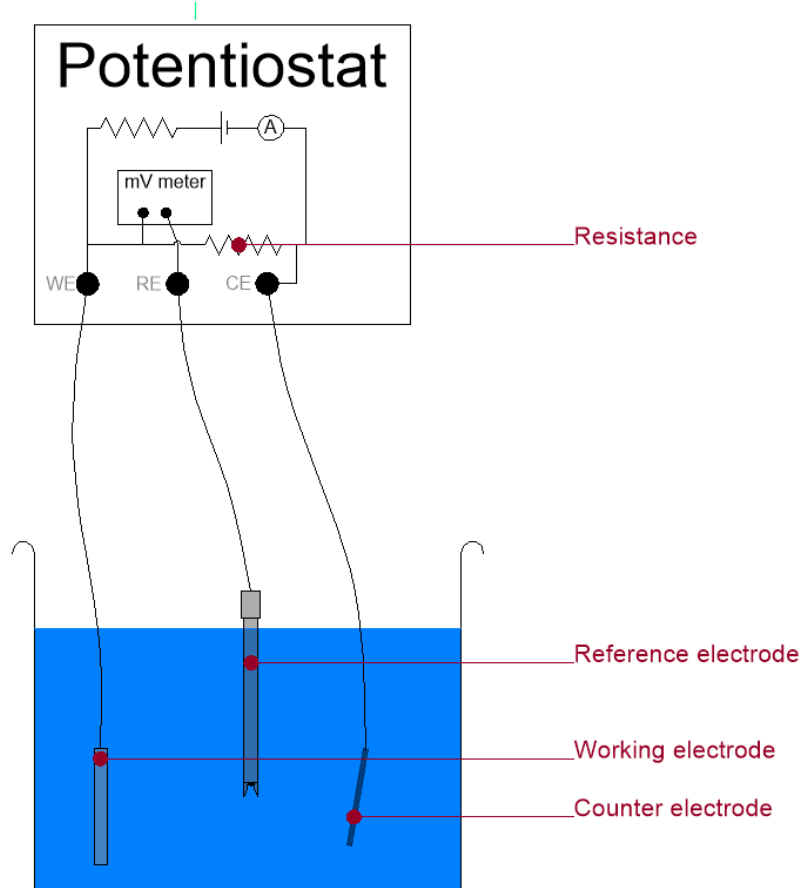


Figure 2.12: Standard polarization cell

The potentiostat can impose a specified potential on the working electrode by applying a current between the working electrode and the counter electrode. This setup allows for different experiments to be conducted. In a potentiostatic experiment for example, the potentiostat forces a constant

potential on the working electrode. The current can be monitored. The potential can also be changed over time, while the current is still being monitored. The applied potential is then plotted versus the resulting current. It is also possible to control the current and measure the resulting potential. These types of tests are called galvanostatic or galvanodynamic, depending on whether a variation in the current is applied. These tests are used to measure corrosion rates, electrochemical reactions and cathodic and anodic behaviors. [7]

A technique, that is used for estimating corrosion rates, is the linear polarization method. The measured current for the potentials can be used to get corrosion rates. The current is measured for the potential that is applied on the specimen. It is often used to measure corrosion rates of structures for which it is not possible to measure weight losses. By putting the current density measurement in logarithmic scale a plot can be obtained from which the corrosion rate can be determined. Using the Tafel extrapolation method the corrosion rate and the corresponding corrosion potential can be obtained. The extrapolation is carried out by finding the meeting point of the extended linear parts of the anodic and cathodic plots. The point, where the lines cross, indicates the corrosion current and corrosion potential. In Figure 2.13 the method is visualized. [8]

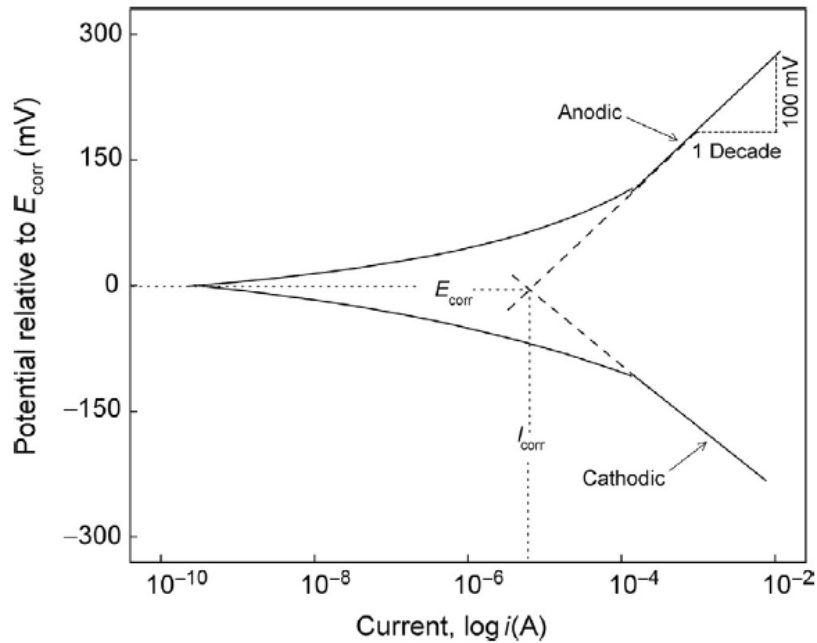


Figure 2.13: Corrosion rate determination by Tafel extrapolation [8]

The corrosion rate can be determined with the Faraday's law by using the obtained current density, atomic mass, number of electrons exchanged by the anodic reaction, the Faraday's constant and the density of the material [18]:

$$CR = 3.27 \times 10^{-7} \frac{i_{corr} \times a}{n \times \rho_{metal}} [mm/y] \quad (2.15)$$

where:

i_{corr} = current density $\mu A/cm^2$

a = atomic mass in g/mol

n = number of electrons consumed per single reaction (valency)

ρ_{metal} = density of the corroding species in g/cm³

This method, to determine the corrosion rate of a metal, is used in the experiments to check for differences in corrosion behavior of the steels S355ML and S355J2 that are used offshore. This is described in section 4.1.2.

2.4.3 Weight loss measurements

Weight losses can be obtained measuring the weight of a specimen before exposing to a corrosive environment and measuring the weight after cleaning the specimens from rust after the exposure period. The procedure requires high precision weight loss measurements and sufficient time of exposure to the corrosive environment, such that the weight loss is significant and measurable.[19]

The corrosion rate can be calculated from :

$$CR = (K \times W)/(A \times T \times D)[mm/y] \quad (2.16)$$

where:

K = a constant (8.76×10^4)

W = mass loss in grams

A = area in cm²

T = time of exposure in hours

D = density in g/cm³

2.5 Corrosion protection techniques in the offshore environment

Structures in the marine environment are most often equipped with corrosion protection. Conventionally the prevention techniques are used for prevention of general corrosion. Coating and passivation techniques are used to form a barrier between the metal and the corrosive environment. Another option that is often used in offshore wind farms is cathodic protection. DNVGL provides principles and recommendations for the corrosion protections systems for offshore wind turbines (DNVGL-RP-0416). [1]

Dependent on the location, relative to the sea level, different corrosion protection methods are recommended. There are four zones specified;

1. the atmospheric zone,
2. the splash zone,
3. the submerged zone,
4. the buried zone.

In Figure 2.14 these zones are schematically shown.

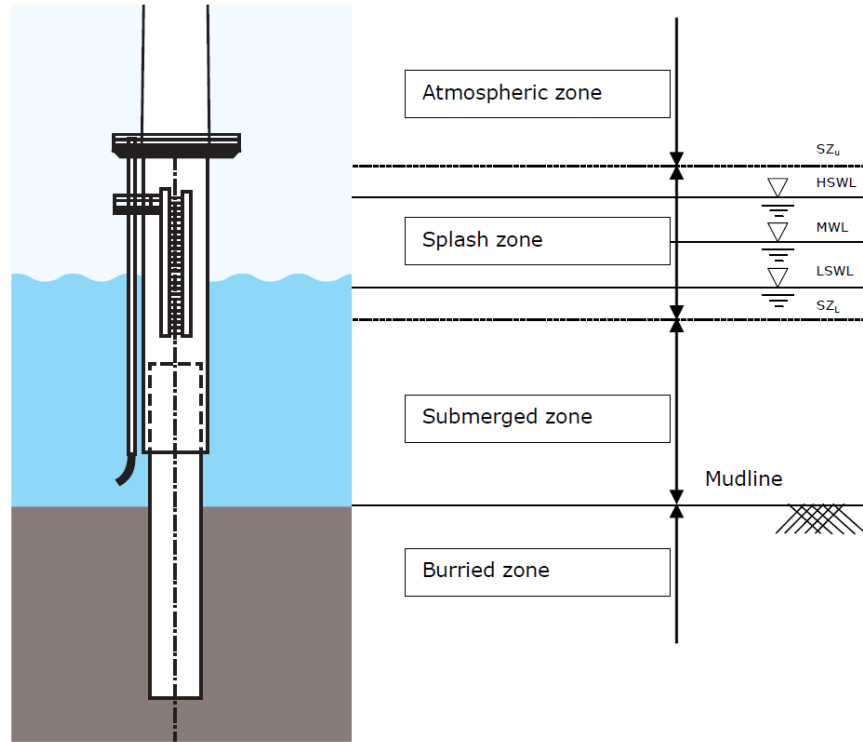


Figure 2.14: Levels and zones in the marine environment [1]

The slip joint will be located in the submerged zone. External steel surfaces in the submerged zone are recommended to have cathodic protection, but the use of coating is optional and is most often used to reduce the demanded capacity of the cathodic protection. DNVGL recommends that current drains by buried parts or sediments are taken into account for calculating the required current. However, DNVGL does not require that the internal surfaces of skirts and piles are included in the current drain calculations for the external cathodic protection system. The Slip Joint is considered to be a skirt for these calculations and therefore the surface of interface of the Slip Joint is not part of the current drain calculations for the external system.

A corrosion allowance or cathodic protection should be applied to the internal surfaces, again a combination with coating is allowed. If cathodic protection is used, the current drain calculation does have to take into account the internal surfaces of the skirts. In the submerged area, the corrosion allowance should be based on a corrosion rate of 0.10 millimeter per year according to DNVGL. Generally a wind turbine has a lifetime of 25 years and thus corrosion allowance requires an additional 2.5 millimeter steel on the primary structural parts. There is no additional requirement for the internal area of the interfaces between a skirt and monopile, such as the interface of the Slip Joint. [1]

Cathodic protection can be applied by either galvanic anode cathodic protection (GACP) or by active impressed current cathodic protection (ICCP). Both protect the structure by making the steel the cathode of the electrochemical cell. A GACP system uses a more active metal, which has a lower electrode potential than that of steel, which is placed near the steel structure and connected

to the steel structure. This active metal is called the sacrificial anode. The anodic reaction of iron is suppressed by applying an opposing current. The iron is polarized to the potential of the local cathodes, oppressing the corrosion. The steel will become cathodic due to supplied current from the sacrificial anodes.

In Figure 2.15 aluminum anodes are used. This will supply the current through the anodic reaction:



At the steel surface the electrons are consumed by the cathodic reaction:



The anodic reaction of steel i.e.:



is now suppressed.

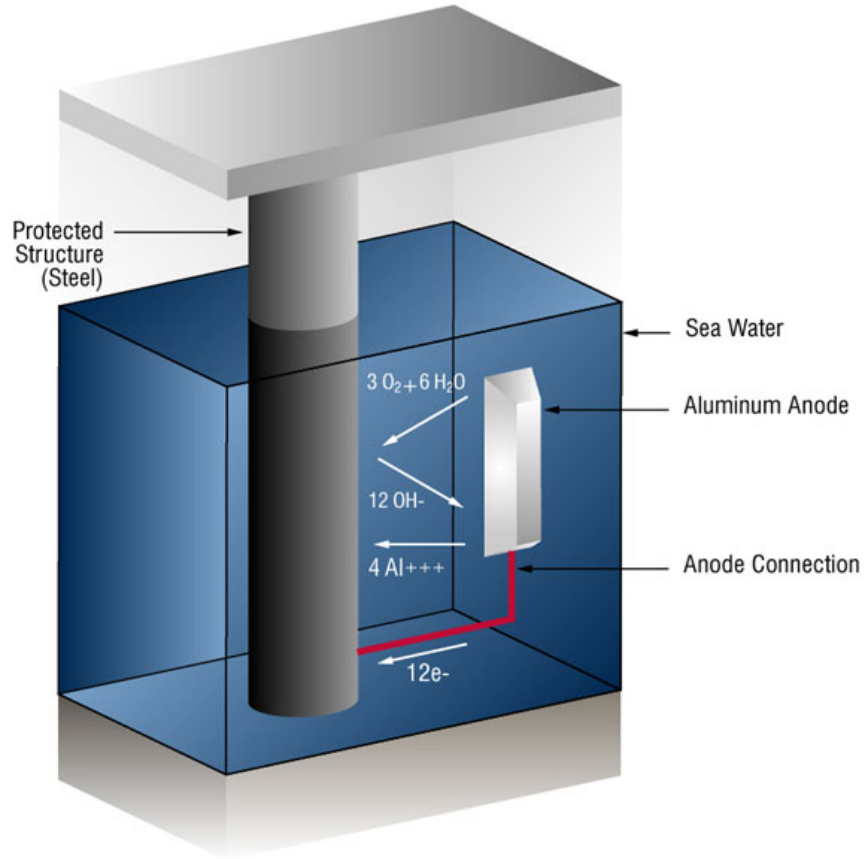


Figure 2.15: GACP system in seawater, with an aluminum anode. [20]

It is also possible to apply an electric current externally using a rectifier. The power supply applies a current such that the steel will shift its potential in the negative direction. In Figure 2.16 the system and the corresponding reactions are shown. A potential of at least -0.8 Volt, relative to a silver/silver chloride reference electrode, is sufficient to protect the steel. Most often the steel is

polarized to an even lower potential i.e. between -0.9 Volt and -1 .05 Volt. In this potential range, the current density demand of the cathodic protection is lowest. Over protection, for potentials more negative than -1.15 Volt, has the risk of a high production of hydrogen and hydrogen embrittlement of the steel. DNVGL describes the design for a cathodic protection system in RP-401 [21].

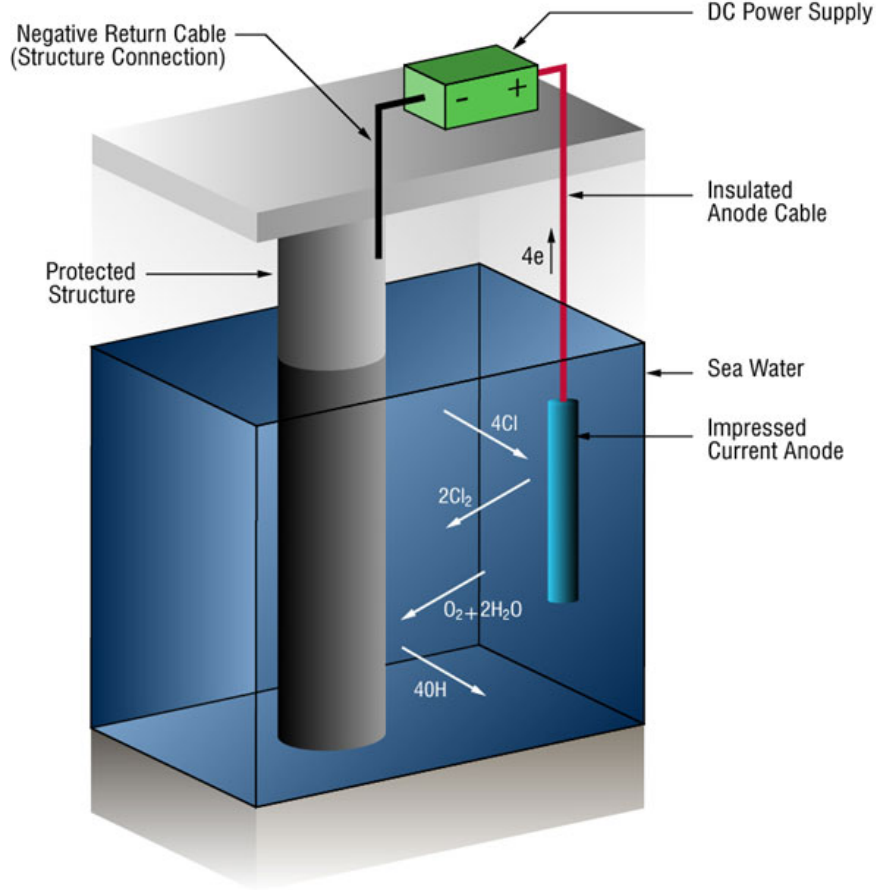


Figure 2.16: ICCP protection system [20]

Usually the anodes that are used for an ICCP system are much more noble than steel. The noble metal Titanium is often used in ICCP systems, it dissolves hardly. High currents in the marine environment cause an alternative anodic oxidizing reaction. Dissolved chloride ions form chlorine gas:



Chlorine will evaporate from the seawater. [22] A side-effect that could occur is the production of hydrogen. Hydrogen can be reduced at the cathode:



Adsorption of the hydrogen in the metal can lead to hydrogen embrittlement. DNVGL states that more negative potentials than -1.1V, relative to Ag/AgCl, in seawater have to be avoided to prevent hydrogen induced damage.

DNVGL describes in the recommended practice B401 the current density required to achieve cathodic protection. An initial and a final current demand has also been formulated. On a bare metal surface a current density is required, formulated by the initial current demand, to polarize the steel surface. The final current density is the density required when there is formation of a calcareous scale layer and marine growth. The current demand is calculated by equation (2.22). [21]

$$I_c = A_c \times i_c \times f_c \quad (2.22)$$

where:

A_c = The surface area that has to be protected

i_c = The relevant design current density (which are given for multiple environments and states)

f_c = The coating breakdown factor (depending on the type of coating, if used)

The required current density is in the order of 0.06 - 0.22 A/m² for seawater exposed bare metal surfaces. The coating breakdown factor is between 0 and 1. A value of 0 indicates that the coating is 100% insulating and thus protecting the steel fully from its environment. A coating breakdown factor of 1 indicates that there is no coating or a coating that does not insulate the steel surface. The coating breakdown factor can be calculated via the equation:

$$f_c = a + b \times t \quad (2.23)$$

where:

a = a constant depending on the coating properties and environment

b = also a constant depending on the coating properties and environment

t = time of exposure in years

DNVGL recommends values for the constant a and b , depending on the coating and water depth.

2.6 Conclusion

The most important subject discussed in this chapter is the corrosion process, its characteristics, the parameters that influence corrosion and the different types of corrosion. The priorities become clear, the corrosion phenomenon that is expected to occur in the Slip Joint is crevice corrosion. Nevertheless, in crevices with large gap sizes uniform corrosion will only occur if the diffusion of oxygen is sufficient. Uniform corrosion is in general less problematic while it is more predictable, crevice corrosion is less predictable. Furthermore, there are some electrochemical measurement techniques that can provide insight in corrosion behavior and corrosion rates. Finally, it is possible to prevent or reduce corrosion by using corrosion prevention techniques which are always used for offshore wind-turbines. There is, however, not much knowledge about the prevention of corrosion in the Slip Joint.

Crevice corrosion on structural steel, in large crevices as described in section 1.2, is still an area with no knowledge on its corrosion behavior. Crevice corrosion is likely to occur, but how and when can not be found in literature. There is a gap on knowledge in the literature for corrosion in these type of crevices. Research on crevice corrosion has mainly focused itself on very small crevices and mainly with other metals than structural steels. The next section discusses the research that has been carried out with relation to this topic and provides some more knowledge on crevice corrosion. There is a lot to gain in studying crevice corrosion for structural steels. The use of

structural steels in the marine environment is not new. The oil industry, for example, has used it for years. Structural steel will continuously be used in the marine environment. The offshore wind industry is just starting up and is growing. Crevices will occur in the offshore structures and thus knowledge about its behavior with relation to corrosion will be required to optimize designs and reduce costs of maintenance and over design. Due to the gap of knowledge in literature, a laboratory test is required to provide insight into crevice corrosion in the Slip Joint. The next section discusses previous tests. This information will be used to make the set-up as discussed in section 4.

3 Research to offshore corrosion in crevices

In this chapter relevant research to corrosion inside the Slip Joint is discussed to get knowledge on offshore crevice corrosion and test set-ups. The literature, that is discussed in this chapter, is used for designing the required test for this research.

3.1 Geometry effect

In an effort to predict the corrosion behavior in the environment of a crevice, Lee et al. and many others developed predictive models. These models take several reactions into account. Most models are based on transport in the solutions, like diffusion. According to the models, the crevice geometry is of dominant importance. A lot of research has been done into the scaling law. The scaling law is the ratio of two geometric measures, length and height, of a crevice that must be maintained as the scale of the crevice is altered. The scaling law describes the relation between the geometry of the crevice and the corrosion behavior. [23]

The scaling laws that are mostly applied or studied are L/h and L^2/h . Previous work has shown that L^2/h is applicable for crevices with low current at the mouth. L is the crevice length and h is the crevice gap, see Figure 3.1. [23] [24]

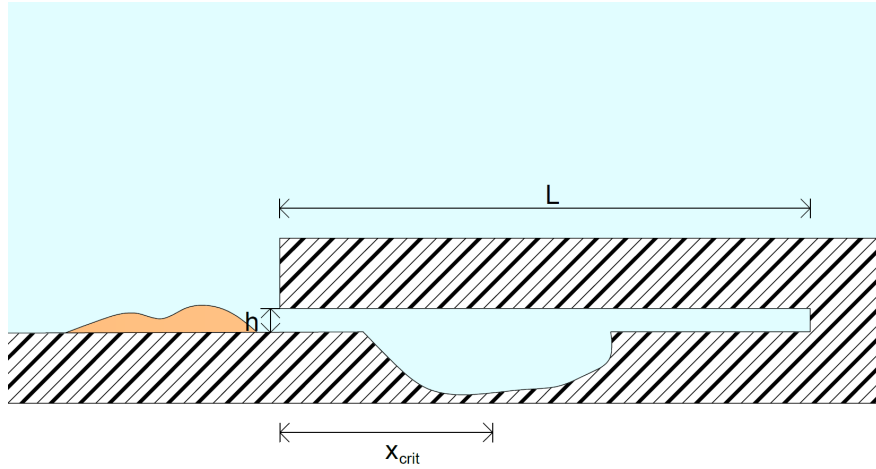


Figure 3.1: Scaling Law, L is the crevice length, h is the crevice height and x_{crit} is the critical crevice distance.

The most important conclusion of the studies by Watson and Gartland is that a critical crevice size exists. A study by Lee et al. [23] has shown that the gap height influences the value of x_{crit} , see Figure 3.1. x_{crit} is the distance from the crevice mouth to the location of attack inside the crevice, which will be larger for larger gap heights. This is due to the decrease of diffusion resistance in crevices with a bigger gap height, the concentration gradient of oxygen will be less steep as explained in section 2.3.3. A study of Abdulsalam and Pickering to the effect of the crevice opening dimension on the stability of crevice corrosion for nickel in sulfuric acid has resulted in:

$$x_{crit} = \frac{\kappa h w (E_{surf} - E_{crit})}{I} \quad (3.1)$$

where:

κ = the conductivity of the solution [$\frac{1}{\Omega m}$]

h = the crevice gap [m]

E_{surf} = the surface hold potential (V vs. SCE)

E_{crit} = the critical current density potential (V vs. SCE)

I = the measured total crevice current [A].

[23]

The critical potential is a potential for which a significant higher current (e.g. corrosion rate) is found. In the crevice the point the location of the attack marks the critical potential, E_{crit} . [7]

Xu and Pickering developed an analytical solution for determining the critical crevice distance. In their solution the crevice length was also one of the variables. The above given equation, equation 3.1, is a simplification of this model.

A study done by Pickering et al. showed that the corrosion attack will move towards the mouth of the gap when the crevice corrosion is stable. The area inside the crevice will increase due to the metal dissolution and formation of a pit. Due to the increased area, more current is produced. A shorter path length between the anode and cathode is then required for crevice corrosion. Pickering suggested that crevice corrosion does not occur in crevices that are higher than 0.4 millimeter. This conclusion was, however, based on a study towards crevice corrosion in stainless steel. [23]

As mentioned before, Lee et al studied the scaling law. This study was performed with controlled crevice geometries in nickel sheets. The crevices in this study had a length of 7mm and the height of the gaps ranged between 10 to 150 μ m. These specimens were immersed into a solution of 0.5M H_2SO_4 , to study the effect of the crevice gap and the critical distance for crevice corrosion over time. Via a micro-fabricated method with a semiconductor device these crevices were formed in the specimens. Furthermore, the results were compared to a computational model.

The results from this study showed that for larger gap heights, the critical distance where the anodic reaction occurs, x_{crit} , will move up into the crevice. Observed is that the time dependence is determined primarily by the evolution of the electrolyte composition. The increase in surface area of the active area due to the corrosion of the surface has less effect. Finally, as gaps became smaller, the attack became less uniform over the crevice. Larger gaps have much straighter bands of attack.

Additional studies were performed, for example a study by DeJong in 1999 [25] which used also a semiconductor device to fabricate crevices. Crevices were made in specimens of nickel and specimens of gold. The created crevices had a height of 1-100 μ m and a length of 7-8mm. The results were very promising, however difficulties in obtaining the deposition profiles from the experiments prohibited the possibility for a quantitative comparison. The results were the same as the results by the study of Xu and Pickering.

A study done by Neena Kaylisia Anak Brum in 2013 [26] has shown the differences between general corrosion and crevice corrosion and also the corrosion behavior inside crevices with different gap and depth dimensions. In this study crevices were formed in stainless steel specimens. Various crevice formers were created in the laboratory. The corrosion rate was analyzed, which was calculated via the observed weight loss. The results made clear that the amount of weight loss increased with increasing gap heights.

3.2 Corrosion of structural steel in seawater

In this research the material that is under investigation is the structural steel S355ML. This is part of the low carbon steels, sometimes called mild steels.

Steel in seawater does not corrode linearly over time. According to Melchers and Jeffrey in [27] the corrosion rate is behaving non-linear for the first five days. During this first period of corrosion, the steel is exposed fully to the oxygen of the bulk seawater. Then linear behavior is observed, see Figure 3.2, when the oxygen is consumed at the interface of the corroding surface it has to be replenished by transferring the oxygen through the iron-oxide layer on the surface. This will result in a constant corrosion rate. Corrosion products will be formed on the surface of the steel, causing the corrosion rate to drop and resulting in non-linear corrosion loss over time.

Biofouling will result in the following stages for some more non-linear corrosion behavior. On the long-term, the so-called anaerobic bacterial corrosion will create a constant environment which will make the corrosion rate constant again. Melchers and Jeffrey put specimens in seawater at three different locations at the Australian east coast to measure the corrosion rate during the first seven days. They took out one specimen-set every single day. One set was kept in the water for 29 days and checked for its mass loss after this period. They concluded from the data that the corrosion rate will become constant after five days of exposure.

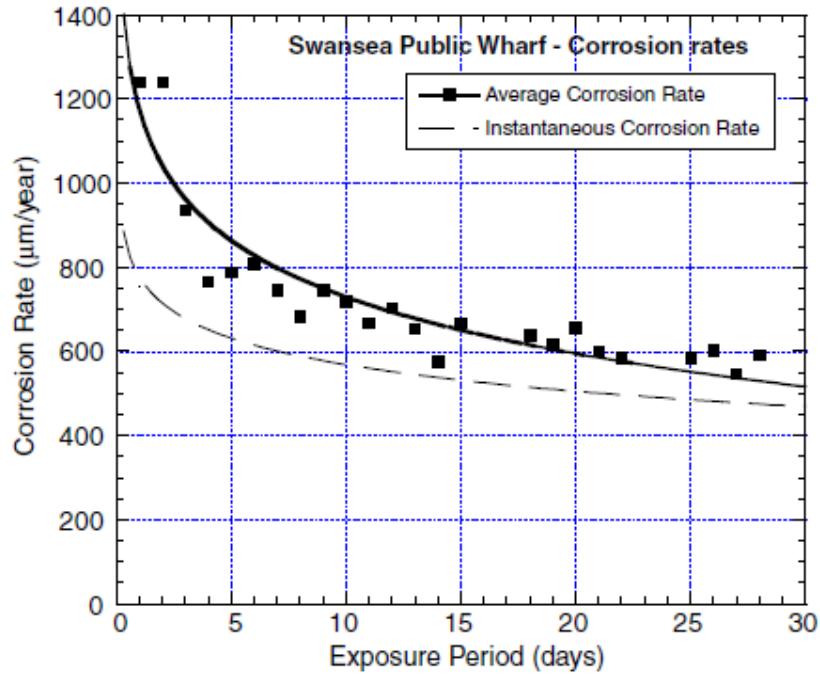


Figure 3.2: Corrosion rates observed by Melchers and Jeffrey for mild steel in seawater [27]

In 2011 Wan Nik et al. published their findings of corrosion behavior of mild steel at two different sites in seawater near the Kuala Terengganu coast [28]. Corrosion behavior due to the specific site conditions were compared. The specimens were weighed by an analytical balance before immersion at the sites. Specimens were taken out with 5 days of interval for 30 days. Corrosion products were

removed using sulphuric acid. Then the specimens were weighed again in order to obtain the mass loss. The corrosion rate was calculated, in assumption of uniform corrosion over the immersed surface, from weight loss methods. The results of this research showed that the percentage of weight loss increases with respect to time. Not only time is a parameter of corrosion, this study also showed that the difference in temperature and salinity influences the corrosion rate. This is also mentioned in chapter 2. The salinity and temperature both increased during the 30 days of immersion and the corrosion rate increased accordingly. In Figure 3.3 the data from this study is shown. After 15 days of immersion, the salinity at site 1 shows a sudden drop and the corrosion rate also drops although the temperature did not drop. The curve of the temperature of site 1 during the immersion period shows a clear resemblance with data of the weight loss, which evidently indicates the relation between the temperature and the corrosion rate.

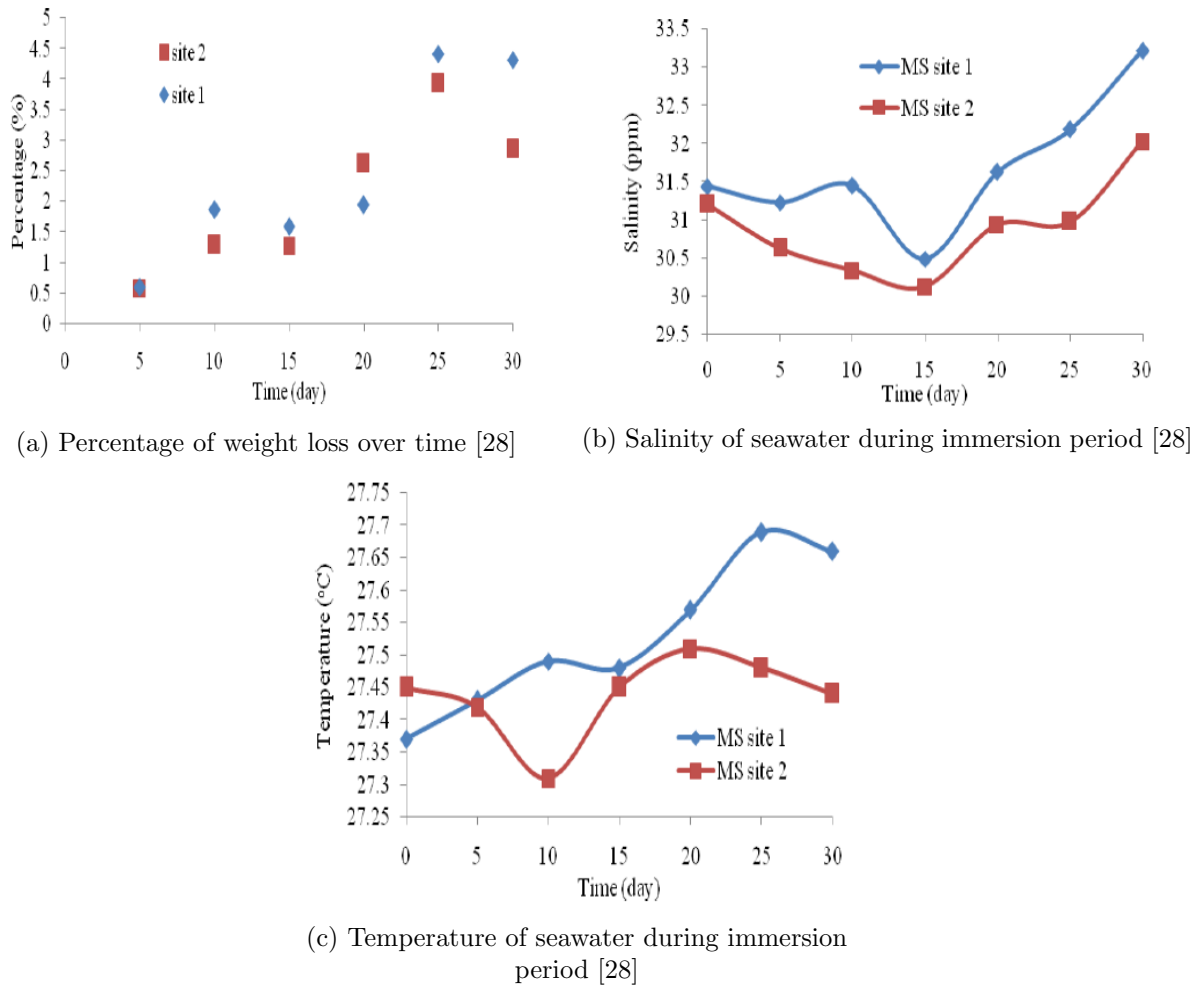


Figure 3.3: Data from the study of Wan Nik et al. showing the influence of time, salinity and temperature on the corrosion rate.

A research paper published in 2015 by Gassama et al. showed the results of exposing constructional steels to marine conditions [29] by using solutions of 0.5 M HCl, NaCl and NaOH. In this research two methods were used to study the corrosion behavior; 1). surface analysis for atmospheric tests and 2). electrochemical tests for immersed specimens. Part of the test program was to put the

rectangular specimens in a sodium chloride solution. The immersed experiments were conducted at a temperature of 25°C. Plots of the corrosion rate during the immersion period were made to assess the impact over time. The impact of salt in the solutions was studied, by measuring corrosion rates of identical specimens in distilled water. The added salt proved to increase the corrosion rate.

3.3 Methods for crevice corrosion experiments

To gain insight in the method of conducting these types of experiment, as discussed in the previous sections, the setup of the experiments will be discussed in this section. ASTM International, an American standardization organization, publishes guides for corrosion experiments. These guides will also be discussed in this section. The information of this section is used to set-up the experiment as discussed in section 4.

3.3.1 Specimen size, composition and preparation

In most corrosion experiments only small samples are used. In the study of Meclhers and Jeffrey the specimens had measurements of 100mm × 50mm × 3mm [27].

The specimens for the study to crevice corrosion life time of stainless steels by Matsushashi et al. were created by two steel sheets, one measuring 20mm × 50mm × 3mm and the other 20mm × 20mm × 3mm [30]. These specimens were wet ground in order to get the desired clean surface condition. In Figure 3.4 is shown how the crevice was created for this experiment.

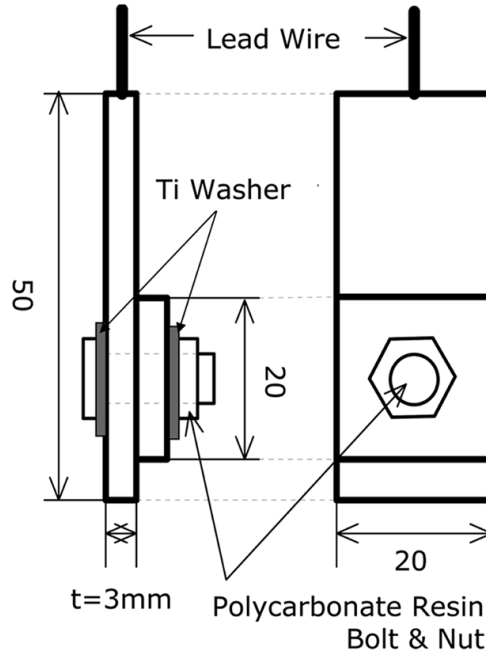


Figure 3.4: Schematic illustration of a specimen with a crevice [30]

The gap height is not regulated by the above discussed method. The plates are assembled by bolts without a washer or spacer between these two plates, such that a very small crevice occurs. This same method was used for a study conducted by Niu in 2018, which used steel plates of 40mm × 15mm × 2mm. These steel plates were abraded using sandpapers and were later degreased

with acetone. The bolts and washers were made of teflon, because teflon does not take part in electro chemical reactions. [31]

The above mentioned method of creating a crevice is not useful in determining corrosion rates and behavior for defined crevices and will therefore not be adopted in the experiment in section 4. In the experiments by Wan Nik steel specimens of $25\text{mm} \times 25\text{mm} \times 3\text{mm}$ were used [28]. The specimens were polished using emery paper and lubricated with distilled water. The polished specimens were then cleaned with acetone, washed using distilled water and dried in air. To store the specimens they were put in desiccators, which is a storage container capable of keeping or getting contents dry.

In the study of Lee et al, the specimens were squares of 1in^2 [23]. The crevices were formed using a semiconductor device to make very small crevices with gap heights of 7.3 to $86.5 \mu\text{m}$. Using this method it is possible to create crevices with accurate and relative small dimensions. The specimens were polished, cleaned, baked and cooled again. Furthermore, he samples were cleaned using ethanol, trichloroacetic acid and methanol. This method is used to study the influence of the crevice geometry on crevice corrosion.

The most frequently used method to form crevices is with the so called crevice washers, see Figure 3.5. The gap height is not controlled by this method. To get consistent results over multiple experiment specimens the bolting is carried out according to a prescribed procedure, for example, most often the bolts are prescribed to be fastened hand tight. The study by Bottoli et al. [32] used this method. In some other studies the torque has been measured.

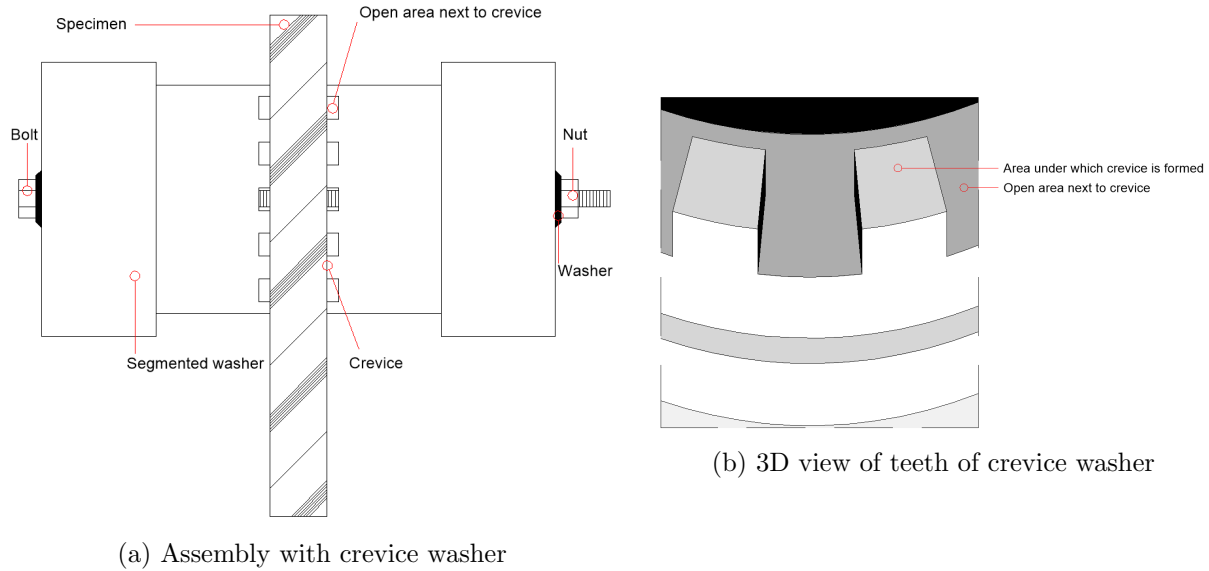


Figure 3.5: Washer as described by ASTM and used by Bottoli et al.

ASTM describes the method of using a washer to form crevices in G48. Additionally, ASTM suggests other crevice formers, for example blocks made out of teflon that are attached to the metal specimen with O-rings or rubber bands. These methods are not used to study the influence of the geometry, but to assess the relative crevice corrosion susceptibility. [33]

A crevice assembly used by Klassen et al. is made out of an embedded steel plate with a polymethyl methacrylate (PMMA), better known as perspex, cover to form the crevice. [34] A similar approach was used in the study by Chin and Sabde. They built a relative small crevice by bolting a PMMA plate to a steel plate to create a crevice of 0.8mm. The crevice was formed by a separating the steel plate from the PMMA plate with a gasket of polytetrafluoroethylene, better known as Teflon. [35]

In general at least two identical specimens are used for each variable that is tested in an experiment setup, to prove whether results are consistent or not. It then is possible to check for randomness and the reliability of the results. According to the Standard Practice for Laboratory Immersion Corrosion Testing of Metals (ASTM G31 [36]), the corrosion rates should deviate by $\pm 10\%$ maximum for identical tests. Exceptions that deviate more should be checked.

3.3.2 Test environment

Most corrosion experiments are carried out under laboratory conditions. The conditions in a laboratory are better controllable and thus should give more consistent results. Sometimes the specific behavior of seawater corrosion is mimicked by using an artificial equivalent solution. [30] Some other experiments use artificial seawater that is described by ASTM D1141 [37]. Using artificial solutions has the benefit of having the same chemical composition in the solution for every test and at the same time being able to control the solution in every test. From the literature it becomes clear that most crevice corrosion experiments use artificial solutions instead of using seawater.

As for experiments that study the corrosion behavior of steel in seawater without a crevice, the specimens are often placed in field. The experiments done by Melchers et al. and by Matsushashi the specimens were carried out on site. [38] [27] [30] Specimens on site are prone to biofouling, which influences the corrosion. This is beneficial to get results that are more applicable to realistic situations.

Depending on the research, the exposure time is variable. To obtain measurable results for weight loss observations, the specimens have to be corroded significantly. Mass losses due to corrosion after a relative short exposure time are not significant. For this reason ASTM standard G31 [36] suggests a minimum test duration in order to get measurable mass losses:

$$\text{Hours of exposure} = 50 / (\text{corrosion rate in mm/y}) \quad (3.2)$$

For the corrosion of 0.10 millimeter per year this would result in 500 hours e.g. 20 days.

3.3.3 Potentiostatic tests versus open circuit tests

Most studies related to crevice corrosion polarize the outer surface of the sample to a more noble value into the passive region, this method is based on the theory of IR drop in crevices as described in section 2.3.3. Due to the generated potential drop between the outside and inside of the crevice, crevice corrosion occurs directly with the polarization. In an open system, without an applied potential, the solution in the crevice and outside of the crevice has initially uniform concentrations of oxygen, there will initially be no separation of the anodic and cathodic reactions and thus there will be uniform corrosion at the metal surface in the crevice. After the depletion of oxygen in the crevice the separation of the anodic and cathodic reactions are initiated. This separation will then

cause the ohmic drop. In an open circuit system, an induction time is thus required. The open circuit system is therefore substantially different than the system with an applied potential via a potentiostat. [39]

3.3.4 Examination and measurements

There are multiple methods available to check crevice corrosion. ASTM G48 states that photographic reproduction of the specimen surface together with the specimen mass loss is sufficient to characterize crevice corrosion.[33] For pit sites however it is necessary, according to the standard, to examine it with a needle. This should expose possible subsurface attack.

Mass losses are measured by cleaning the specimens which removes the corrosion products. This can be done mechanically by brushing the specimens or by immersion in a specific acid. The specimens have to be weighed before put in the corrosive solution.

In some experiments, like done by Niu et al. [31], the open circuit potential of the the specimens is measured over time. This gives an indication of the corrosion processes occurring over time, see section 2.4.1.

3.4 Conclusion

In the Slip Joint the most risk comes from crevice corrosion. Crevice corrosion has been studied a lot, but not for similar geometries as the crevice of the Slip Joint. One of the most important aspects that is discussed in this chapter is the influence of the geometry on crevice corrosion. It is the main component that influences whether crevice corrosion will occur.

There are multiple methods used to prepare specimens with a crevice, for example washers made from teflon or PMMA plates bolted to the metal specimen. These samples are most often immersed in an artificial seawater equivalent solution. Most studies use a potentiostat to start crevice corrosion and speed up the process, otherwise a relative long immersion period is required (for a corrosion rate of 0.10mm/y at least 20 days). However, using a potentiostat to start crevice corrosion is not representative for checking corrosion rates which occur in open systems. Examination of crevice corrosion should be done by means of mass loss measurements and visual inspections.

As already became clear in chapter 2, there is still little known about the corrosion in a crevice of structural steels and of sizes as large as the crevice of the Slip Joint. Therefore, it is inevitable to perform tests to get more knowledge on the corrosion behavior in the crevice of the Slip Joint. The test will require specimens with multiple crevice geometries that could occur in the Slip Joint, because the crevice geometry has a major influence on the corrosion behavior. The test should be carried out without an applied potential in order to obtain corrosion rates that can be related to the crevice corrosion in the Slip Joint. A minimum immersion period of 20 days will be required if a corrosion rate of 0.10mm/y is taken into account. The next chapter will introduce the experiment design. The test design is based on different techniques that have been used to research crevice corrosion, such as presented in this chapter and chapter 2.

4 Designed experiment to study corrosion in the Slip Joint

This chapter discusses the experiment set-up that has been designed to investigate the offshore corrosion behavior of crevices that can be found in Slip Joints. A maximum gap of 12mm is possible to occur in the Slip Joint, as discussed in section 1.2, which is much bigger than the crevices that have been studied in previous studies. The scaling law, discussed in section 3.1, has only been studied for smaller crevices and for other material than structural steels. Furthermore, corrosion rates for these crevices are not known and often not part of crevice corrosion studies.

The experiment is designed to get corrosion rates and to see the corrosion behavior for different crevice geometries that could occur in the Slip Joint. A total amount of 260 steel plates and 37 different crevice geometries have been immersed and are studied for their corrosion behavior. In order to obtain a reliable experiment method, trial tests have been carried out prior to the main experiment as also will be discussed in this chapter. Additionally is checked whether ICCP can be applied on Slip Joint crevices in order to protect the steel in the crevice. Previous chapters have shown that there are numerous techniques to investigate corrosion in crevices. The design of the experiment is based on ASTM standards and the discussed literature.

4.1 Specimen material, preparation and geometry

4.1.1 Specimen material

As mentioned in section 1.2.3, the preferred steel grade for the Slip Joint is S355ML. This steel grade is not commercially available in small plate thicknesses. While these plates are tested in a laboratory environment, the size and weight is limited. A high precision balance has only limited capacity and thus heavy steel plates cannot be weighed on these balances. The steel grade S355J2 is also used often for offshore structures and is available in plates of 5mm thickness and has similar properties as discussed in section 1.2.3. This steel grade is therefore used for the experiments. In appendix 9.1 of this thesis the composition of the steel is given. The specifications stated to the manufacturer of the steel plates can also be found in this appendix.

In order to determine the differences in corrosion behavior between S355ML and S355J2 a polarization test has been carried out. As discussed in section 2.4.2 it is possible to measure corrosion rates, for structures for which it is not possible to measure weight losses, by using simulated experimental curves and carrying out the Tafel Plot analysis, see Figure 2.13.

For the Tafel Plot test, samples of S355J2 were prepared by cutting rectangles of 25mm \times 50mm from the steel plates as shown in the appendix. Cylinders were cut from a 150mm S355ML plate and these were cut in smaller cylinders of 5mm height and 25mm diameter. Prior to using the samples, a surface treatment was performed. The samples have been mechanically abraded with abrasive papers of grit size 80, 180, 320 and finally 800. The surface was then rinsed with alcohol by an ultrasonic cleaner and subsequently dried using an air dryer. In Figure 4.1 a sample of S355ML is shown, after abrading with a grit size of 80.

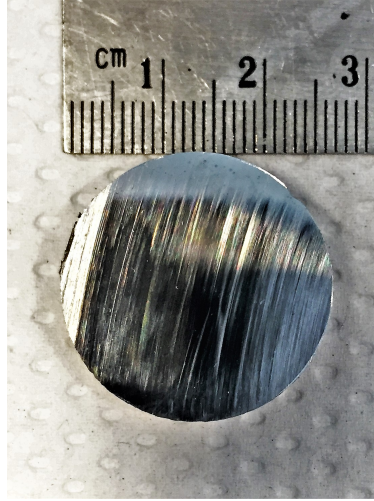


Figure 4.1: S355ML sample of 25mm diameter, after first abrading with grit size grade 80

The corrosion potential and corrosion current density was tested in a 3.5% NaCl solution at an ambient temperature in the laboratory. Electrochemical measurements were realized with the BioLogic VSP-300 potentiostat in a corrosion cell. An Ag/AgCl electrode was used as a reference electrode, a stainless steel counter electrode was used and a sample as working electrode. The working electrode was connected to the potentiostat by a copper strip and was exposed over an area of 2.54 cm^2 to the sodium chloride solution. In Figure 4.2 this set-up is shown.

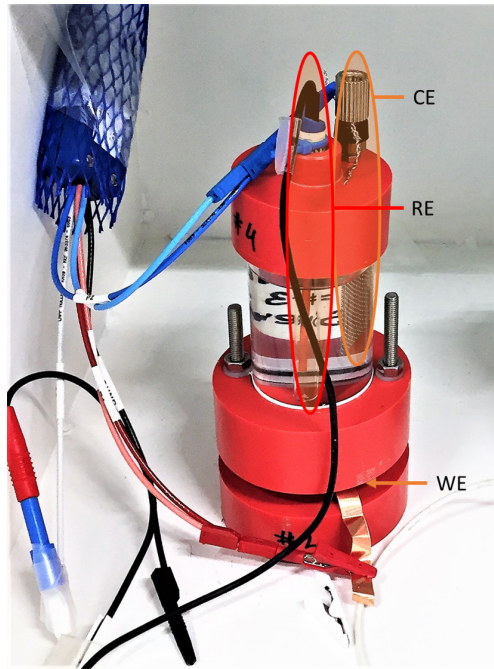


Figure 4.2: Corrosion cell with counter electrode, reference electrode and working electrode.

For the corrosion reaction a stabilization period of 30 minutes was applied. In Figure 4.3 the

measurements are shown of the test.

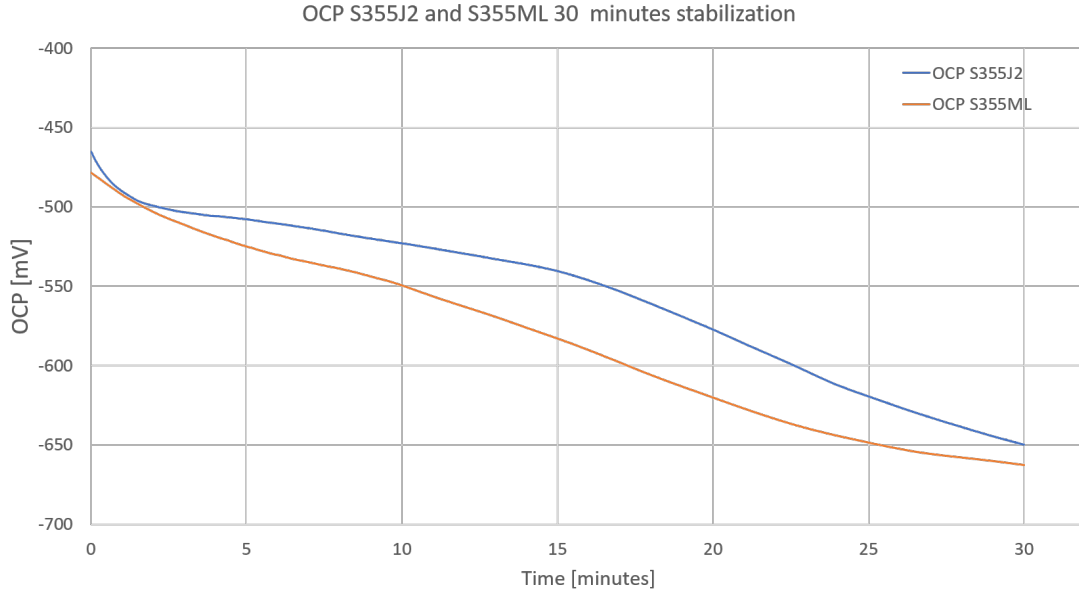


Figure 4.3: OCP during 30 minutes stabilization

After the 30 minutes the samples were polarized in the Tafel zone in a domain of $E_{corr} \pm 250$ mV and with steps of 0.167mV/s, as described by ASTM G59. [18] The resulting polarization curve is shown in Figure 4.4. The curves of the grades are similar and are closely to overlapping. This test shows a corrosion potential of -720 millivolt for S355J2 and a corrosion potential of -690 millivolt for S355ML. This is considered a small difference. Furthermore the difference is partly attributed by the difference in the reference electrodes, which was measured to be 10 millivolts.

With the help of the Tafel analysis the corrosion current and corrosion rate can be obtained. By linear intersecting the cathodic and anodic curves as indicated in Figure 2.13 the corrosion current, i_{corr} , can be found. In Figure 4.5 this is shown for a S355J2 sample. i_{corr} is estimated to be 0.015 milliamps. Using the obtained i_{corr} , the corrosion rate can be determined with equation 2.15. The same is done for S355ML which also gave an estimated corrosion current of 0.015 milliamps. The estimated corrosion rate for both steel grades, with an atomic mass of iron of 55.8, an exposed area of 2.54 cm² the numbers of electrons involved in iron is two as shown in equation 2.2, and the density of steel of 7.85 g/cm³ is:

$$CR = 3.27 * 10^{-3} \frac{0.015 * 1000 * 55.8 / 2.54}{2 * 7.85} = 0.07 mm/y \quad (4.1)$$

The test proves that the corrosion rates are in the same order of magnitude.

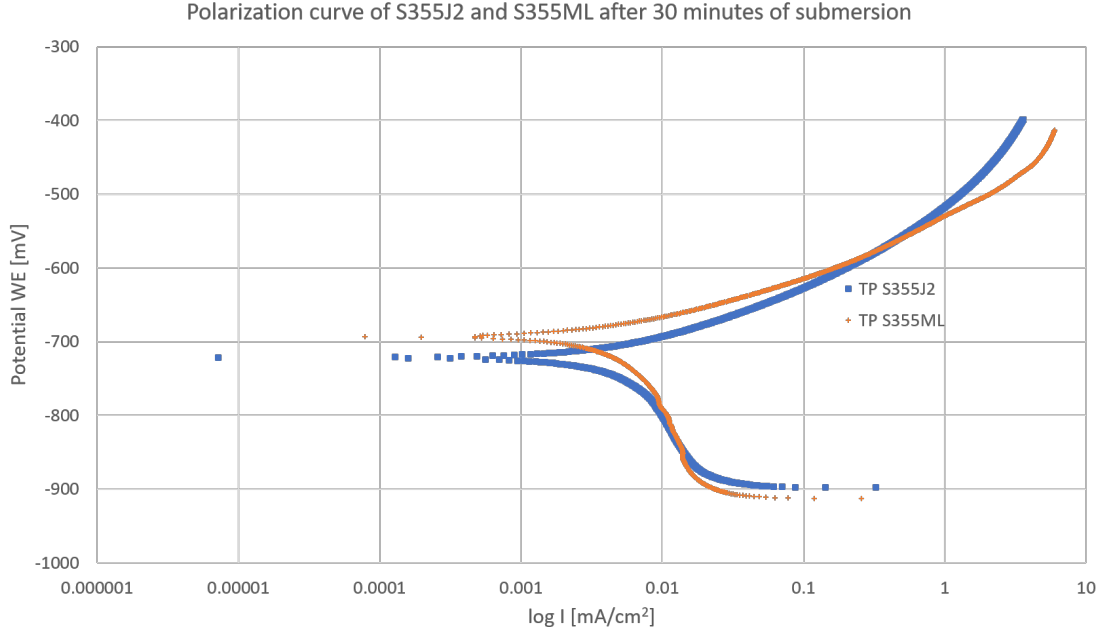


Figure 4.4: Polarization curve after 30 minutes of stabilization

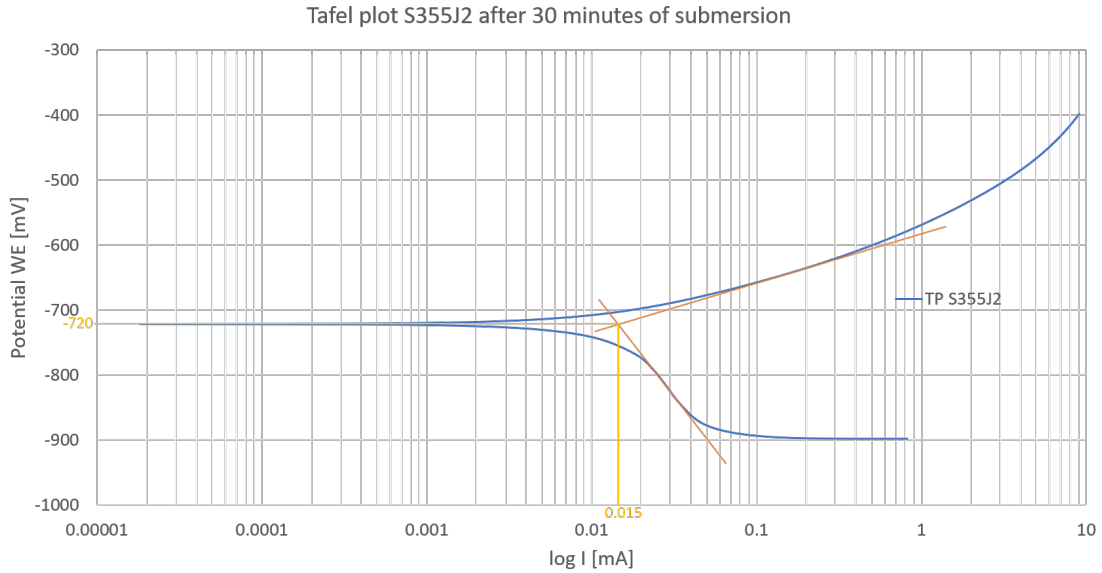


Figure 4.5: Tafel plot for S355J2 after 30 minutes of submersion

The EC-lab software is utilized which can create a Tafel fit that gives another estimated corrosion rate. This software directly calculates the corrosion rates after entering the input parameters equivalent weight, density of the corroded material and the exposed area. The resulting plot and estimated corrosion rate for S355J2 is shown in Figure 4.6. In Appendix 9.2 the tafel plots of S355ML are shown.

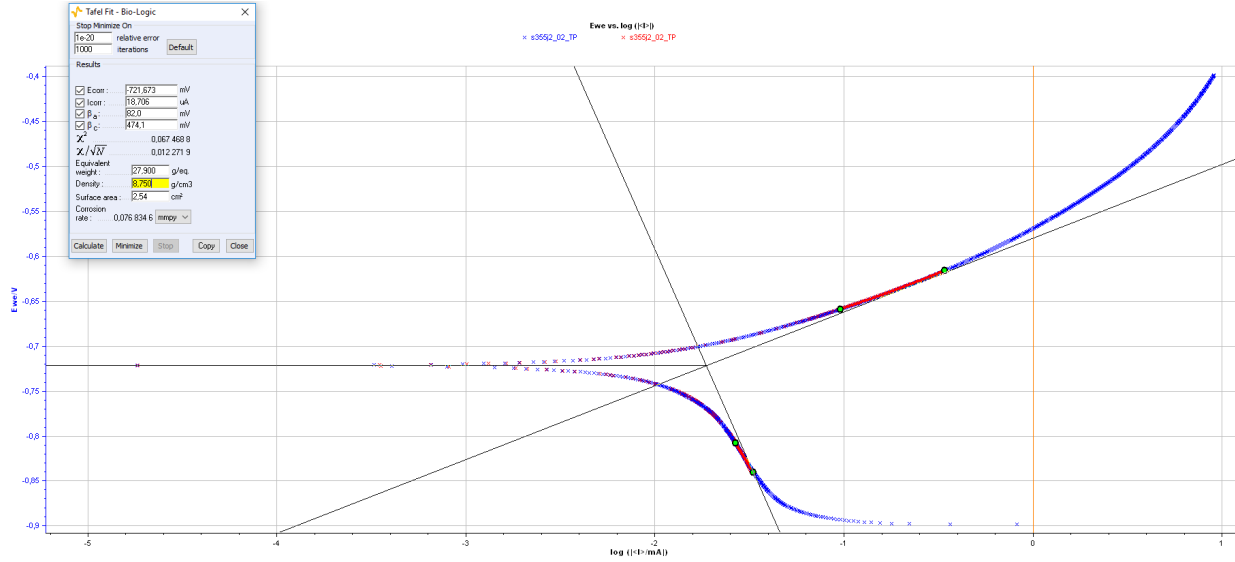


Figure 4.6: Tafel plot generated with EC-lab for S355J2 after 30 minutes of submersion

The EC-lab software estimates the corrosion rate of S355J2 to be a little higher than the corrosion rate of S355ML, see Table 4.1. As can be seen in Figure 4.6, the extrapolated linear part of the cathodic plot has a higher gradient than the gradient of the measurements in this area. By doing so, the software estimated a higher corrosion current and thus a higher corrosion rate. The difference is however not substantial, a small change in the fit of the Tafel plot will estimate the corrosion rate differently due to the log scale that is used for Tafel plots. The software too estimates the corrosion rate in the same order of magnitude, proving again that the corrosion rates of S355J2 and S355ML are similar. On top of that, Figure 4.4 clearly shows that both steel grades are very similar in terms of corrosion rate and corrosion behaviour.

Grade	Manual I_{corr} [mm/y]	EC-lab I_{corr} [mm/y]	Manual E_{corr} [mV]	EC-lab E_{corr} [mV]
S355J2	0.07	0.076	-720	-722
S355ML	0.07	0.063	-695	-694

Table 4.1: S355J2 compared to S355ML with Tafel plots

An additional measurements has been carried out for which the stabilization period was extended to 24 hours. In Figure 4.7 the results are plotted. The measurements show a 'shoulder' in the anodic branch of the curves, which might be related to corrosion products on the steel surface that have a passivating effect. It might also be related to oxygen depletion in the solution, caused by the 24 hours of free corrosion. A study by Flitt et al. mentions that such 'shoulder' suggests localized corrosion.[40] It is possible that local corrosion was initiated between the sample and the corrosion cell of Figure 4.2. Due to the shoulder in the anodic portion of the curve, Tafel extrapolation is not possible. A corrosion rate can thus not be obtained according to the Tafel method. Without the Tafel extrapolation is still visible that the corrosion current is again in the same order of magnitude, although, here again it appears that S355J2 shows higher corrosion currents. Using test results of S355J2 would thus be conservative.

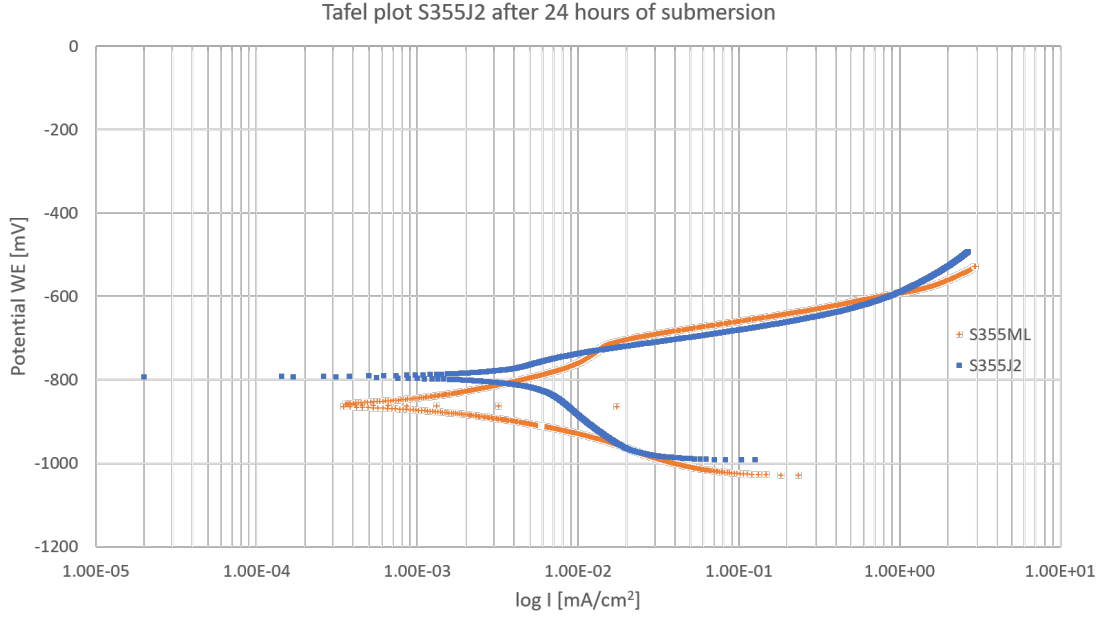


Figure 4.7: Polarization curve after 24hours of stabilization

4.1.2 Specimen preparation

In order to be able to distinguish the steel plates during the experiment, they are labeled with low stress stamps. Codes are given to each specimen, these can be found in Appendix 9.3. Prior to assembly, the steel plates were cleaned with ethanol to remove greases and dirt from the surface in order to prevent contamination during the test. After the cleaning procedure, measurements were carried out. The dimensions of the steel plates and spacers were measured and also the weight of the steel plates were measured. This procedure is suggested by ASTM G1, which is the Standard Practice for preparing, cleaning, and evaluating corrosion test specimens.[19]

The specimens are assemblies of two connected steel sheets with a spacer in between to form the predetermined crevice geometries. The crevice at the interface of the Slip Joint will also consist between two steel sheets, therefore is chosen to use this method. In crevice experiments that were discussed in chapter 3, the crevice is created by the assembly of one metal plate to a non metal material that does not influence the electrochemical reactions. For this reason the spacer is made of high density polyethylene (HDPE) that is non corrosive and an insulator. HDPE is stiff enough to avoid significant compression during assembly, and therefore does not have any significant influence on the required crevice size. A total of 35 different sizes of spacers have been made to form the 35 different crevice geometries that have been tested. In section 4.1.3 this will be discussed in more detail. The specifications that were submitted to the manufacturer of the spacers can be found in appendix 9.1. Each spacer is also cleaned with ethanol, to prevent it from polluting the steel plates. The specimens are assembled using stainless steel bolts. In Figure 4.8 and Figure 4.9 the assembly can be found.

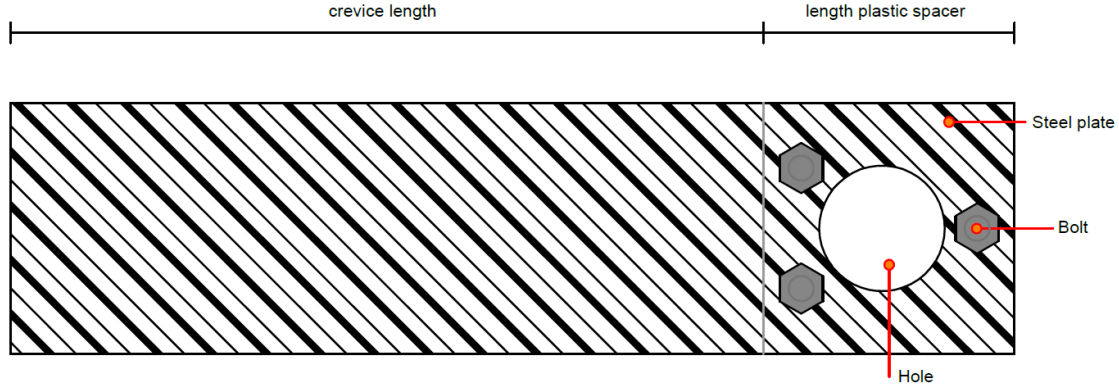


Figure 4.8: Specimen front view

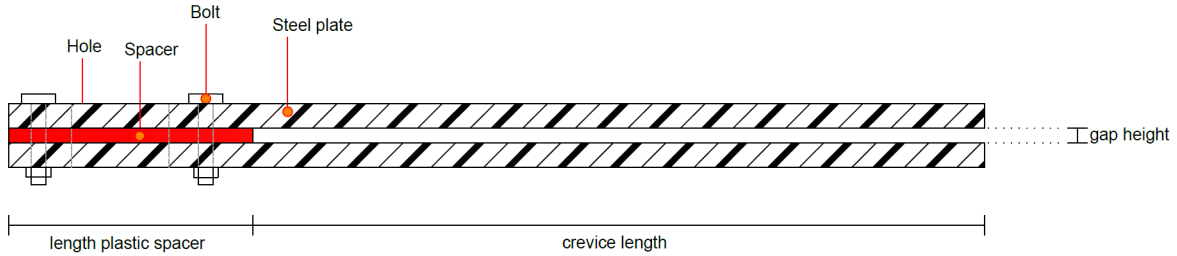


Figure 4.9: Specimen side view

A test has been carried out to find out how to assemble the spacer and the steel watertight. Without any preventative measures the assembly would not be watertight. First is tested whether double sided tape would make the assembly water tight. The specimen was made and immersed in water for a short period. After immersion and disassembling the specimen it became clear that the specimen was not watertight. Using the silicone tape between the steel and the spacer and compressing it by bolting the assembly tight was the second tested method. Again it was proved to be not watertight. Finally a test was performed in which silicone sealant was applied between the steel plates and the spacer, see Figure 4.10a. This proved to be working and therefore this method is used in the experiments.

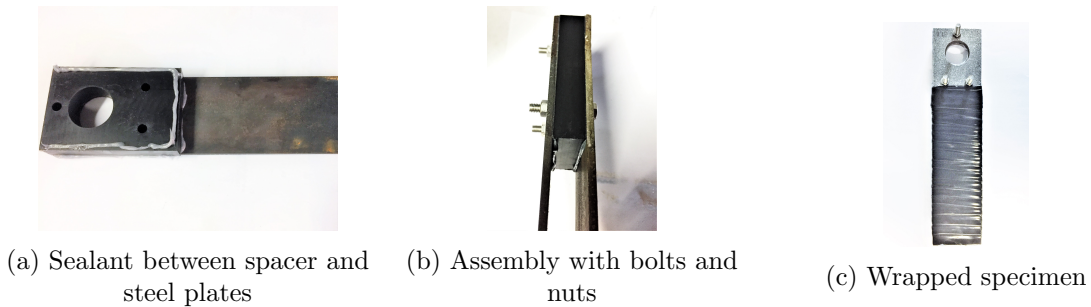


Figure 4.10: Assembly of specimen

To close the sides of the specimens two options were considered. The first was to check whether it was possible to only close the edges of the specimens. The second option was to check whether

it would be better to fully wrap the outer surface and only leaving the mouth opened. In Figure 4.11a the first option is shown and in Figure 4.11b the second option is shown.



(a) Option one, closing only the edges of the specimen



(b) Option two, fully wrapped specimen

Figure 4.11: Options for closing the crevice

By wrapping, the outer surface of the steel plates are covered as well. Covering the outer surface will help to measure only the corrosion activity inside the crevice. The corrosion of the outer surface is prevented and thus will not influence the mass loss of the steel plate or potential measurements. The corrosion loss of the outer surface of option one was a too big part of the total corrosion loss, it made the weight loss measurements in the crevice less precise. In conclusion, option two is chosen to use in the experiments.

To assure that the required crevice height was achieved after assembly, the height of the gap at the mouth of the crevice of the specimen was measured using a caliper.

A step-by-step approach to prepare the test can be found in the method state in appendix 9.1.

4.1.3 Specimen geometry

As described in Chapter 3 for corrosion in crevices a certain critical geometry will result in crevice corrosion as described in Chapter 2. In other words, different crevice geometries will result in different corrosion rates and corrosion behavior. Because of the fact that there is no database available with corrosion rates for structural steel in seawater this experiment is designed to get insight into corrosion rates for different crevice geometries that are possible to occur in the Slip Joint. The corrosion of crevices with different gap heights is therefore checked. Additionally the influence of the depth of the crevice will be checked. The assumption is that for certain gap heights and lengths the crevice corrosion is more critical than for others. This assumption is based on the scaling law and the influence of the potential drop as described in the previous chapters, chapter 3 and 2 respectively.

As already mentioned, the crevices will be formed with two steel plates. The steel plates are 225mm long, 50mm wide and 5mm thick. Multiple crevice sizes are made by using multiple spacer geometries, ranging between 75mm to 175mm in length and 2mm to 14mm in thickness. Resulting in crevices of 50mm to 150mm deep and with gap heights of 2mm to 14mm. The width of all crevices is

50mm. Figure 4.12 shows the definition of the width, length and height of the crevice. In literature the crevices that are tested have often a gap height over crevice length ratio of approximately 1/10. This is taken into account by taking the ranges for length and gap height. Crevice corrosion is therefore likely to occur for multiple specimens. The table below, Table 4.2, shows the crevice geometries that are tested per batch. In appendix 9.3 the codes of the specimens are given and in the appendix is also shown in which batch each specimen has been tested.

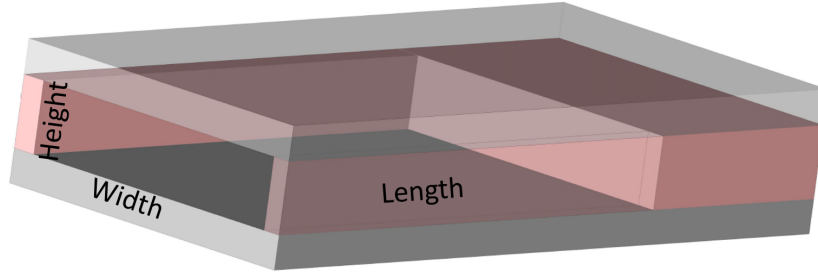


Figure 4.12: Specimen definitions of width, length and height

Test batch no.	w [mm]	l [mm]	h [mm]
Batch 1	50	50	2, 4, 6, 8, 10, 12 & 14
Batch 2	50	75	2, 4, 6, 8, 10, 12 & 14
Batch 3	50	100	2, 4, 6, 8, 10, 12 & 14
Batch 4	50	125	2, 4, 6, 8, 10, 12 & 14
Batch 5	50	150	2, 4, 6, 8, 10, 12 & 14

Table 4.2: Tested crevice geometries (width \times length \times height)

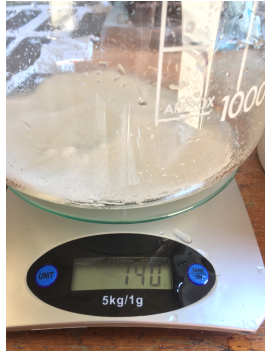
ASTM prescribes to use at least duplicate test specimens. In laboratory tests, corrosion rates of uniform corroding duplicate specimens should usually be within a $\pm 10\%$ margin of each other. [36] For crevice corrosion such percentage is not available. Thus, to provide a better statistical basis for the results, three specimens were made for each crevice geometry.

4.2 Test environment

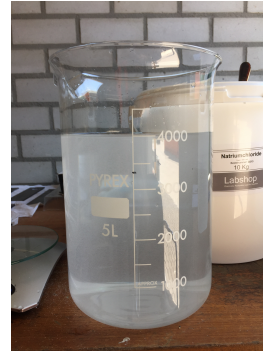
4.2.1 Salt water solution

Seawater contains approximately 3.5% (35 g/L) salt. In literature it is found that most experiments related to crevice corrosion use an artificial solution. An artificial solution is beneficial for the reproducibility of the test which is the basis for using a 'simple' solution. Seawater will be different from location to location and will change over time. ASTM D1141 prescribes an artificial seawater solution in which various predetermined salts are dissolved. Literature, however, shows that a solution with 3.5% sodium chloride can also be used to mimic seawater corrosion. Gassama et al. for example used a NaCl solution to mimic the marine environment. [29] Sodium chloride solutions are often used in crevice corrosion studies, like Kelly et al. used it to study a paradox between two theories of crevice corrosion. [41]

Because a 3.5% sodium chloride solution is used often, is controllable, and is very reproducible for multiple batches this has been used in the tests. The NaCl concentration can be monitored relatively easy, this will be discussed in more detail in 4.2.3. In order to be able to check possible differences in corrosion rates due to the environment, every test batch will contain reference steel plates to check the uniform corrosion rates. Uniform corrosion rates in seawater is known for multiple sites and in multiple other solutions.



(a) 140g salt in the beaker



(b) Batch of 4L

Figure 4.13: Salt water solution preparation

ASTM G31 suggests to use a minimum ratio of water of 0.20 mL per mm^2 of exposed area in an immersion test. [36] This is taken into account and the tubs have been filled with 85L of the sodium chloride solution, for which a maximum total exposed area of 381.400 mm^2 is immersed. (The total exposed area is the cumulative area of the exposed area of all specimens going into one tub.) Resulting in a ratio of 0.22 mL/mm^2 , which gives a margin of 10% to the suggested minimum ratio.

4.2.2 Temperature

In section 2.2.4 became clear that the temperature influences the corrosion rate. Therefore the temperature must remain constant in order to be able to compare the results of each batch and to make the test reproducible. The temperature is controlled by doing the test in a temperature controlled shipping container. The seawater temperature for the North Sea varies between 1°C and 18°C . [42] The temperature used during the test is based on a laboratory temperature, the temperature is set at 21°C ($\pm 0.1^\circ\text{C}$). Although this does not represent the seawater temperature, it will only make a small difference to the corrosion rates. The corrosion process speeds up slightly. The reference steel plates will make sure that the results can be related to actual seawater situations.

4.2.3 Controlling the environment

Section 2.2.2 showed that the salinity influences the corrosion rate and therefore it was controlled during the tests. Using a sound velocity probe the water density and salinity was checked. Furthermore the water level had to be maintained, such that the full crevice would be under water at all times. The batches, containing the test solution with the samples, were replenished with water regularly. Two times per week the water density has been checked and either distilled water or a sodium chloride solution was added to the batch, to maintain the correct water level and to maintain the salinity.

The temperature was kept level by the container and thus was constant during the test.

4.3 Immersion of the samples

4.3.1 Immersing of specimens in the tub

The specimens were immersed by hanging them from a wooden frame. Multiple batches were used to be able to immerse all specimens. Each tub was equipped with reference steel plates, which were exposed to uniform corrosion. The final set-up is shown in Figure 4.14, 4.15 and 4.16.

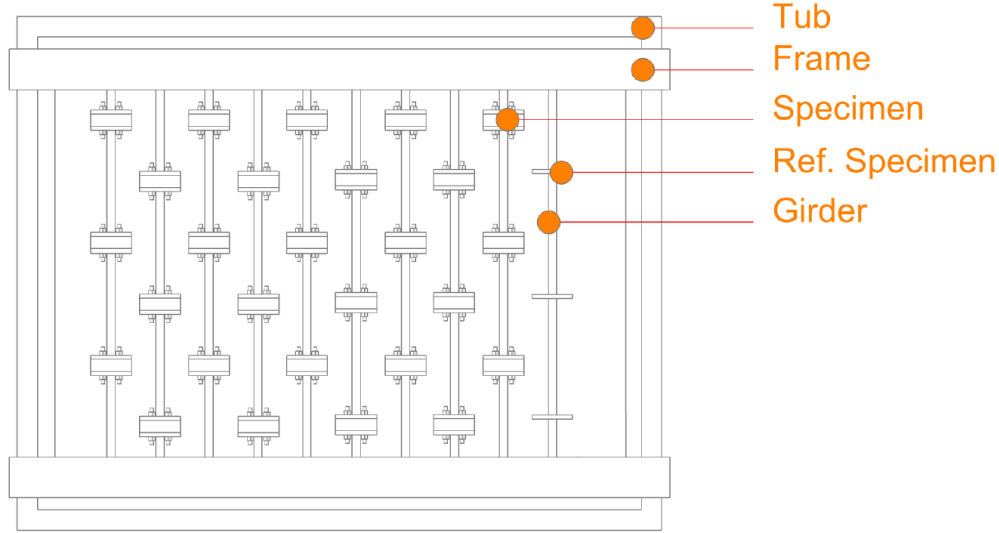


Figure 4.14: Top view of set-up

The specimens were immersed for 160mm deep, sufficiently to have the full crevice immersed. A side view of this configuration is shown in Figure 4.15.

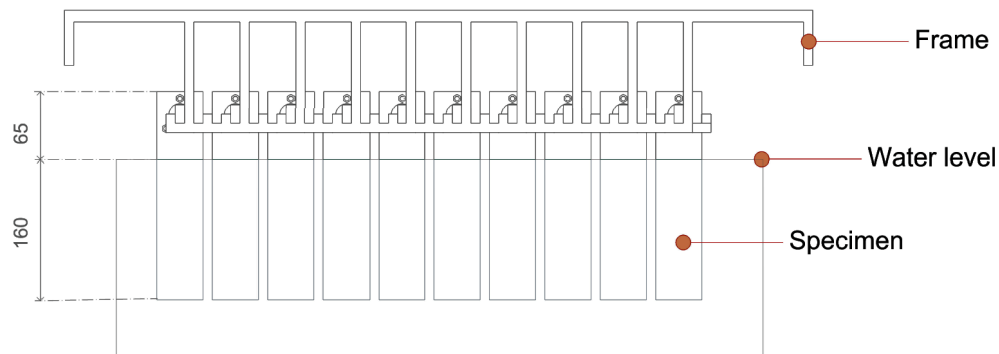


Figure 4.15: Configuration of immersed specimens

The sets are based on crevice length. Each specimen with a crevice length of 50mm was put in Tub 1, with a crevice length of 75mm was put in Tub 2 and so on. In Figure 4.16 the result is shown. The specimens were first immersed upside down, to let all air out of the crevice and prevent for trapped air in the crevice. Directly they were put back upward and assembled on the girders.



Figure 4.16: Result of specimens in the tub

4.3.2 Activities during immersion

During the immersion period, water evaporates and the tub was therefore topped up twice per week, as already discussed in section 4.2.3. The potential of the specimens have also been monitored during the experiment. At least twice times per week the potential of the specimen has been measured using an Ag/AgCl reference electrode and a digital multimeter. A few specimens have been measured continuously during a certain period, in order to be able to track possible short term changes. These measurements also used Ag/AgCl reference electrodes. In Figure 4.17 the set-up with the potential loggers is shown.

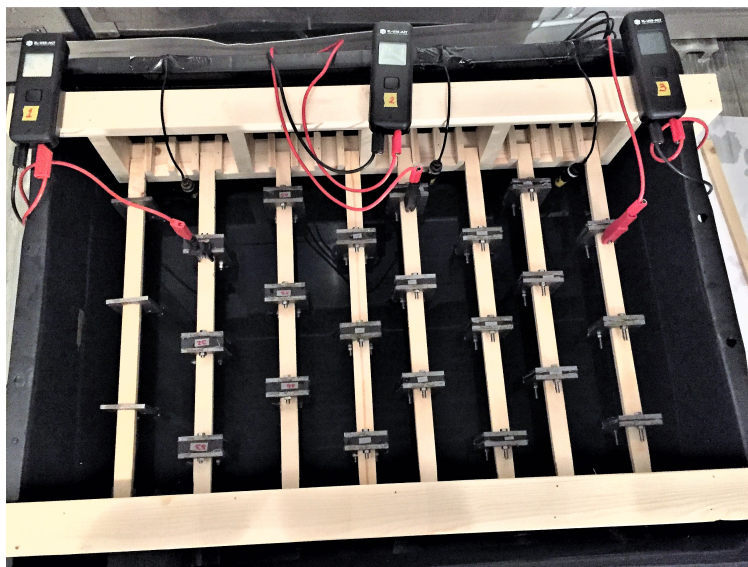


Figure 4.17: Tub with potential loggers connected with specimens

As mentioned, ASTM G31 advises the duration of an immersion test. Corrosion of structural steel

in the permanent immersion zone exhibits low corrosion rates in the order of 0.035 millimeter per year. [6]. This results for structural steels in:

$$\text{Duration of test in h} = 50/0.035 = 1429 \text{hours} \quad (4.2)$$

This time is sufficiently long for a differential in aeration to develop. A sufficient amount of mass is lost during this period such that it can be measured by a high precision balance. To be on the safe side, the specimens were kept in the tub for at least 60 days (or 1450 hours).

4.4 Pull out of specimen and cleaning

The specimens were taken out of the tub after the required 60 days of immersion. Each specimen was dried using a blow dryer. Next the specimens were disassembled, photographed, rinsed with ethanol and the steel plates were dried again.

Loose, bulky corrosion products were removed from the steel plates. To further clean the steel plates an acid solution that is prescribed by the ASTM standard practice G1 (Standard Practice for Preparing, Cleaning and Evaluating Corrosion Test Specimens) is used. ASTM proposes multiple acid solutions for removing corrosion of multiple metals. A solution containing hydrochloric acid and hexamethylene tetramine has been used in this case, this can be found in the ASTM standard practice. [19] During immersion in this solution, the corrosion products are dissolved from the steel plates.

After the cleaning procedure, the specimens were weighed. The loss of mass and corrosion rate has been calculated. Using the the total exposed surface area of the specimen and the mass lost during the test, the average corrosion rate can be obtained via the formula [19]:

$$CR = (K \times W)/(A \times T \times D)[mm/y] \quad (4.3)$$

where:

K = a constant (8.76×10^4)

W = mass loss in grams

A = area in cm^2

T = time of exposure in hours

D = density in g/cm^3

4.4.1 Potentials

Potential measurements are carried out throughout the test. The potential of the system is an interesting parameter in monitoring the electrochemical reactions. The expected potentials are between -0.6 [V] and -0.8 [V] for the uniform corroding reference specimens. [43] A change indicates that the reactions at the surface of the specimen are changing. The expectation is that the potential will decrease gradually when the corrosion reactions are starting up. As time passes it is expected that the steel passivates and the potential will increase, due to formation of a rust layer. Measured potentials will be plotted over time. To check the influence of the geometry of the gap the data will be checked for correlation.

4.5 Trial test to check test parameters

A trial test has been carried out prior to the main test, to validate the time of immersion, to validate the design of the frame, to validate the procedure of controlling the solution over time, and to validate the potentials over time. In this trial test 30 bare steel plates were immersed, so no samples with a crevice. Four different distances between the steel plates were used, to check whether it would influence the corrosion behavior. A distance of 15 centimeter, which is assumed to be free hanging and thus uniform corrosion should occur. Furthermore smaller distances of 2 centimeter and 1 centimeter were applied. And finally five specimens were immersed against each other. The potentials were measured three times per week and the solution was replenished two times per week.



Figure 4.18: Immersed steel plates for trial test, with varying distance

There are a few notable observations from the trial test. First of all, the distance of the wooden frame to the water level was too close. The wooden frame was getting wet and this caused fungi growth on the wooden frame. This resulted in the conclusion that the distance between the water level and the frame should be bigger than two centimeter. This was accomplished by increasing the level of the frame relative to the water level and making the specimens sufficiently long such that the full crevice in the main test would remain submerged.

The open circuit potential of the specimens during the trial test showed an average of -0.610 Volts. The potential was expected to be more negative. After cleaning the specimens after the immersion period, according to the procedure as described in section 4.4, it became clear that the steel plates contained a layer of mill scale. The layer of mill scale influenced the corrosion behavior significantly, see Figure 4.19a. Without a layer of mill scale this specimen would have corroded uniform over the full surface. Weight loss measurement could not be obtained due to the mill scale. The process of cleaning the specimens from rust dissolves the mill scale, see Figure 4.19b, and thus weight loss measurements due to the rust could not be obtained. The specimens of the main test were therefore sandblasted to get the required surface condition.



(a) Trial specimen with mill scale after immersion (b) Trial specimen after removal of the mill scale by the cleaning procedure

Figure 4.19: Trial specimen after immersion and after cleaning

Although relevant corrosion data could not be obtained due to the mill scale on the specimens, the trial test gave the opportunity to improve the experiment set-up.

4.6 Immersion of crevices ending in a void

The crevice geometries in the Slip Joint will not be constant in height, length or width. A crevice in the Slip Joint can start with a big gap height at the mouth and end in a small gap height at the back, and the other way around.

For crevices with a constant height, an increase in height will cause the required aeration drop and potential drop for crevice corrosion to shift deeper into the crevice. A crevice which has a higher crevice near the mouth and becomes smaller near the end will show the same result. For a bigger crevice height near the mouth, location of the required aeration drop and potential drop will move deeper into the crevice.

More interesting is to test what happens if the crevice ends with a big crevice height or with a void. The narrow crevice in front of the void will increase the resistance for oxygen transport to the void and will cause a potential drop. While it is not known what the influence of the narrow crevice is on the corrosion in the void, this has been tested.

Specimens with cubical voids are used because the cubical shape is easily to reproduce and easily to control. In Figure 4.20 an example of a tested specimen is shown. (During the test the shown side was closed by wrapping as shown in Figure 4.10c. This specimen has a 100 millimeter long crevice from the mouth of two millimeter height and ends in a 50mm long by 14mm high void. Furthermore a specimen with a crevice height of four millimeter has been tested, the void size was left unchanged. Again, to provide a good statistical basis for the results, three specimens were made for each specimen geometry.

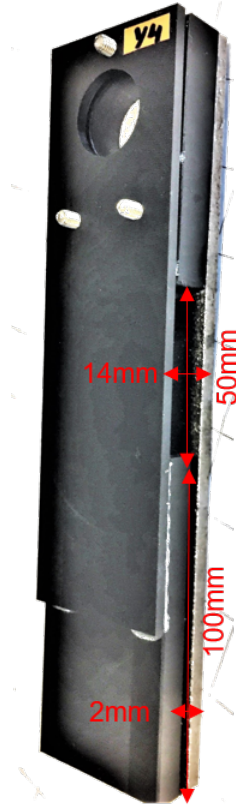


Figure 4.20: Specimen with a crevice ending in a void, side view.

The specimens were prepared, immersed and cleaned according to the same method as described in section 4.1, section 4.2, section 4.3, and section 4.4.

4.7 ICCP test

The monopile can be protected from corrosion by using an ICCP system. ICCP on the monopile will influence the potential and corrosion behavior in the Slip Joint as well. However, currents from the ICCP system will not easily penetrate the small crevices. [44] Non the less, studies indicate that crevice corrosion can be prevented by cathodic protection. Bates studied whether a cathodic protection system could prevent crevice corrosion of stainless steels. This study showed that the crevice corrosion could be stopped by polarizing the specimens to the protection value. [45] To check whether ICCP can be used to prevent corrosion in a S355J2 crevice and the influence of ICCP on Slip Joint crevices, a test has been carried out.

Specimens were made according to the method as described in section 4.1, with only one adjustment. To keep the two steel plates electrical isolated from each other, instead of using stainless steel bolts and nuts, Teflon bolts and nuts were used for assembly of the specimens. This isolation was used to test whether ICCP applied on one of the steel plates would influence the potential of the other steel plate. The crevice size of the first tested specimen was 2mm high, 50mm wide and 50mm long. A longer crevice of 150mm was tested secondly. A crevice height of two millimeter was chosen because this is the narrowest crevice that has been tested in the previous test and narrow crevices have more resistance to polarization. If these narrow crevices can be polarized, it is assumed that it is possible to polarize wider specimens as well. A PalmSens 4 potentiostat is used to polarize the

specimen to the required protection potential of -0.9 Volts, as discussed in section 2.5. Potential loggers were used to measure the potential of the specimens over time. Two Ag/AgCl reference electrodes have been used and a titanium wire has been used as counter electrode. In Figure 4.21 this set-up is shown.

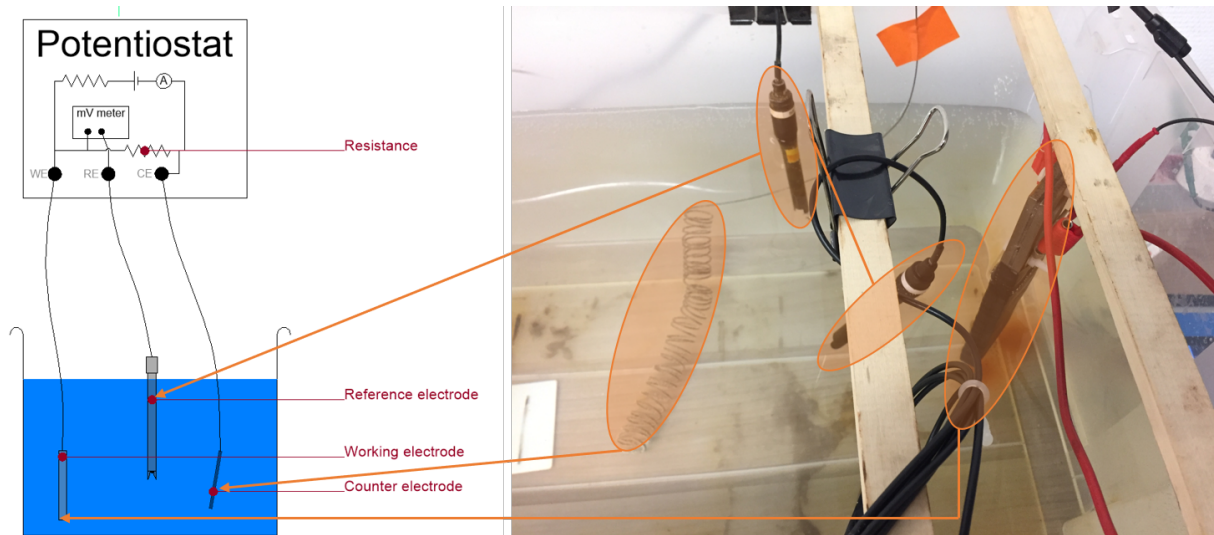


Figure 4.21: ICCP set-up

A trial test was carried out to validate the system. ICCP was applied on a piece of S355J2 steel by immersing this steel plate only for one centimeter, exposing 49.2 cm^2 . In this way it was possible to check whether the PalmSens 4 was able to polarize this surface area for a period of a week. During the test a 3.5% NaCl solution, as described in 4.2, was used.

The potential data of the trial test is shown in Figure 4.22. The protection potential was obtained during the first 3 days. After three days the ICCP circuit was broken due to a loose clamp. After restoring the circuit, the PalmSens was not able to polarize the system to the protection potential. After six days the test was aborted.

The applied current during the trial test is shown in Figure 4.23. This data also shows the break of the circuit after three days, furthermore it shows a spike in the applied current after the first day. This spike is caused by an unintended disruption of the solution due to movement. The potential data shows that this did not influence the protection potential to a great extent. The applied current is on average 4.4 milliamps on the surface of 49.2 cm^2 . This results in a current of 0.9 A/m^2 which is much higher than the normally required current density between $0.06\text{--}0.22 \text{ A/m}^2$ as discussed in section 2.5. This was caused by a high resistance of the counter electrode, the submerged surface of the counter electrode was not sufficiently large.

The trial test resulted in the conclusion that the surface of the counter electrode should be increased to reduce its resistance and thus to reduce the required current output of the PalmSens 4. Once the ICCP system proved to work, specimens with a crevice were tested. The results of these tests are discussed in chapter 5.

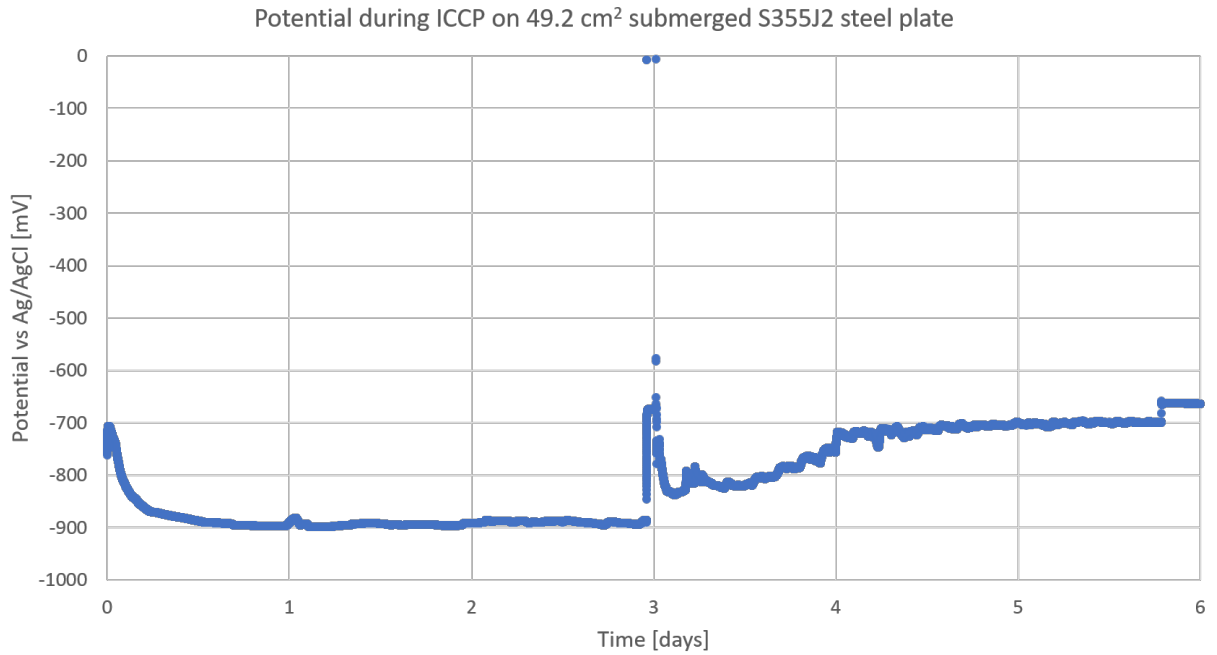


Figure 4.22: Measured potential during trial test

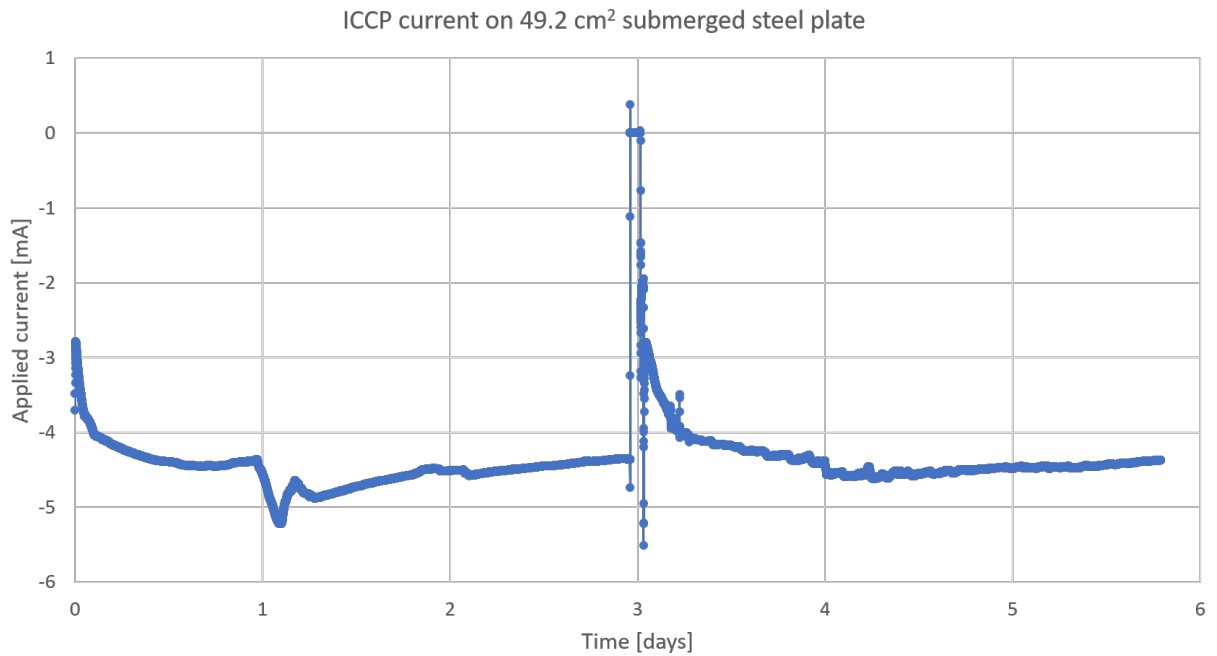


Figure 4.23: Applied current during trial test

5 Results of the experiments

5.1 Open circuit potential measurements and visual inspection

5.1.1 Open circuit potential measurements and analysis

Because each specimen has been tested in threefold, the average is taken of the measurements of the three identical specimens and the standard deviation has been calculated to check the scatter of the results.

Potential measurements on reference specimens

The potentials were measured at least two times a week. The change of the potentials did not require more frequent measurements. The potentials were measured using the multimeter and an Ag/AgCl reference electrode. The open circuit potential for uniform corrosion, in the 3.5% salt water solution at 21°C, is on average -669 millivolts with a standard deviation of 3.3 millivolts. In Figure 5.1 the average potential of the reference specimens from batch 1 to 5 are shown. (In table 4.2 can be found which specimens are tested in each batch.) In the begin stages of the immersion, the potential moves down toward more negative potentials in the range of -660 to -690 millivolts. This indicates the initiation of the corrosion reactions as given in section 2.1. Once a layer of rust is formed the potential stabilizes, indicating that the corrosion reactions are coming to a steady state.

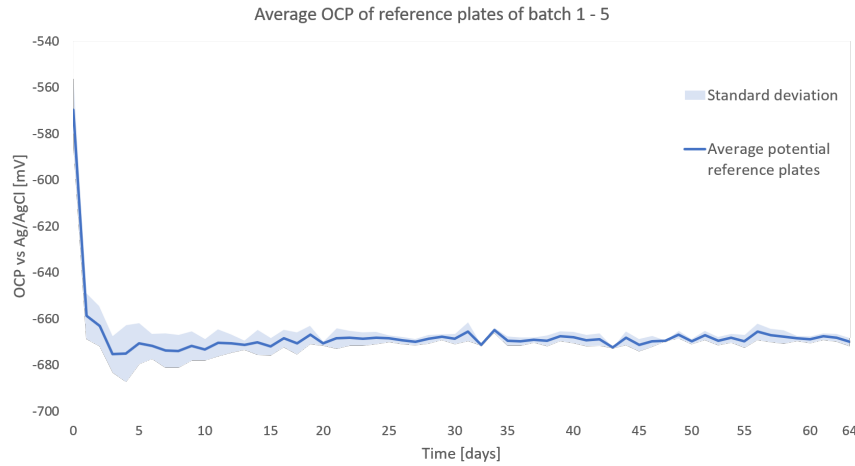


Figure 5.1: Average OCP of the reference plates of batch 1 to 5

During the initiation phase the measurements are slightly more disperse, in later stages, the data is very identical. This can be related to the required time for stabilization of the system. From the results it can be concluded that the test has been consistent over each batch. The standard deviations, also plotted in Figure 5.1, do also indicate consistency. An example of a rusted reference specimen is presented in Figure 5.2. The rust formation and visual inspection showed that the reference plates corroded uniformly.



Figure 5.2: Corroded reference plate showing uniform corrosion

Potential measurements on specimens with a crevice

The potential data of the specimens with a crevice length of 50 millimeter show a different trend compared to the potentials of the reference plates, as can be seen in Figure 5.3. The average potential of the reference plates is plotted by the red dotted line. The average potential of the specimens with a crevice height of 14mm of this batch start, like all specimens, at a more positive value of about -560 millivolts. It drops directly to a lower value of about -640 millivolts and then gradually evolves, in about 35 days, more towards the uniform corrosion potential of -670 millivolts. The decreasing potential indicates that the corrosion behavior is still unstable during this period. It stabilized in the final 20 days of the immersion period, at a potential that is even more negative than the uniform corroding reference plates. The geometry clearly influences the corrosion behavior. A possible explanation for the slower decreasing potential is that the corrosion is limited by the diffusion of cations into the crevice and it takes longer to initiate stable corrosion. Probably the differential in aeration is not sufficient to separate the cathode and anode reactions which results in uniform corrosion. That the potential is slightly more negative can be related to the difference in corrosion products on the steel surface. The stable red rust on the uniform corroded reference plates has a slightly passivating and nobelizing effect, that was not found on the regarded specimen.

Another possible explanation, for the trend towards more negative potentials, is that oxygen depletes in the total electrolyte such that the differential in aeration drops over time and becomes insufficient to support the differential aeration cell. The measurements suggest that during the final 30 days, uniform corrosion reactions are dominant.

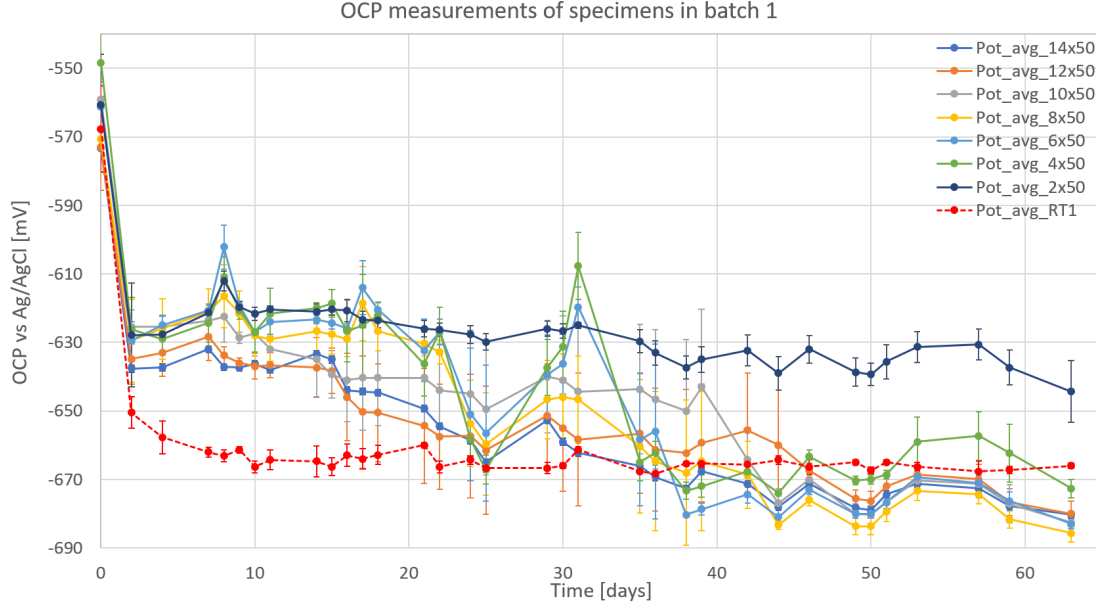
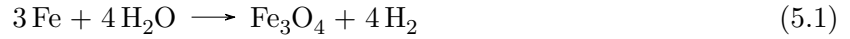


Figure 5.3: OCP measurements of the specimens in batch 1

Visual inspection of these specimens suggest that the specimens, which end up in the potential range of uniform corrosion, indeed corroded over the full exposed surface. In Figure 5.4 a picture of one of the steel plates, from the specimens with a crevice of 14mm height and 50mm length, is shown. The red area is the commonly known rust $\text{Fe}(\text{OH})_3$. The black area can be either $\text{Fe}(\text{OH})_2$ or $\text{Fe}_3\text{O}_4 \cdot \text{H}_2\text{O}$. $\text{Fe}(\text{OH})_2$ can be greenish black because of incipient oxidation by air, which normally would form $\text{Fe}(\text{OH})_3$ at the outer surface of the oxide film if it has access to dissolved oxygen. [7] The rust $\text{Fe}_3\text{O}_4 \cdot \text{H}_2\text{O}$ can be formed in areas with limited oxygen by the reaction with water:



The other specimens show similar results for both the potential data and the visual inspection. Looking at the data more closely it can be concluded that for crevices with a smaller height the potential data is more positive. Diffusion is more limited in smaller crevices and therefore could explain the spread. There are some small peaks and there is one bigger peak in the potential data around the immersion period of 30 days. A possible explanation is that the formation of the rust layer over time, will make the potential shift to more positive/noble values (for example starting after 25 days for specimens with a crevice height of 6mm and 4mm. Accumulation of rust in the crevice decrease the diffusion of oxygen and cations into the crevice. This even could induce the differential aeration cell and local crevice corrosion. When the rust drops out of the crevice, the diffusion is possibly restored and uniform corrosion can take over again. In smaller crevices it is likely that rust will accumulate easier and will not drop out easily, which could explain the steady potential of the 2 millimeter high crevice.

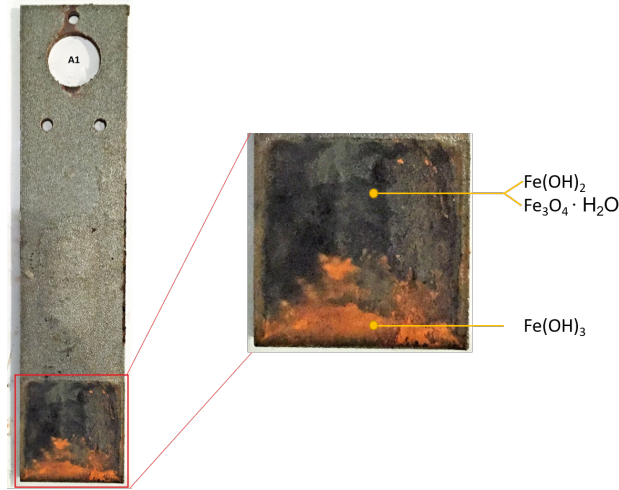


Figure 5.4: Corroded steel plate A1 of specimen S1 with a crevice of 14mm height and 50mm long. (The exposed area is indicated by the red box.)

The specimens with a crevice of 2mm height separates itself from the rest by being more or less stable at a potential of about -630 millivolts. This indicates that the corrosion behavior have come to a stable form that is possibly different than the uniform corrosion of the reference plate. By visual inspection of the specimens it also looks different from the other specimens, like in Figure 5.4. In Figure 5.5 the steel plates of one of the specimens with a crevice height of 2mm and 50mm long is shown after the immersion period. There is a distinct border visual. The top part seems unaffected and the bottom part near the mouth shows rust formation, thereby indicating local attack.



Figure 5.5: Corroded steel plate A20 and B20 of specimen S20 with a crevice of 2mm height and 50mm long. (The exposed area is indicated by the red box.)

The measurements present higher potentials for samples with crevice corrosion. The change in corrosion potential reflects a change in one or both of the anodic and cathodic reactions. As an example, if the corrosion potential becomes more positive this can be attributed to a decrease of the anodic reaction because of the growth of a rust film that has a passivating effect. It can also be related to an increase in the cathodic reactions. [46] For corrosion the anodic reaction and cathodic reaction are respectively:



The total reaction:



The corresponding potential is formed out of both half-reactions occurring in the salt water. Crevice corrosion will draw chloride ions to the crevice, see section 2.3.3, changing the environment and causing hydrolysis in the crevice. The environment in the crevice is thus different than the environment around a uniform corroding steel plate. Because the corrosion potential is dependent on the environment, this will change the corrosion potential of a specimen with a crevice. Furthermore, the corrosion potential is an indication of the facility to corrode. Thus, the change in corrosion potential can also be caused by increased resistance that is caused by the narrow crevice and accumulating rust in the crevice.

Batch 2, 3, 4 and 5 relatively containing crevices of 75mm, 100mm, 125mm and 150mm length and varying crevice heights, show similar results. Generally, the narrower crevices measure less negative potentials. The potentials are shown in Figure 5.6, 5.7, 5.8 and 5.9.

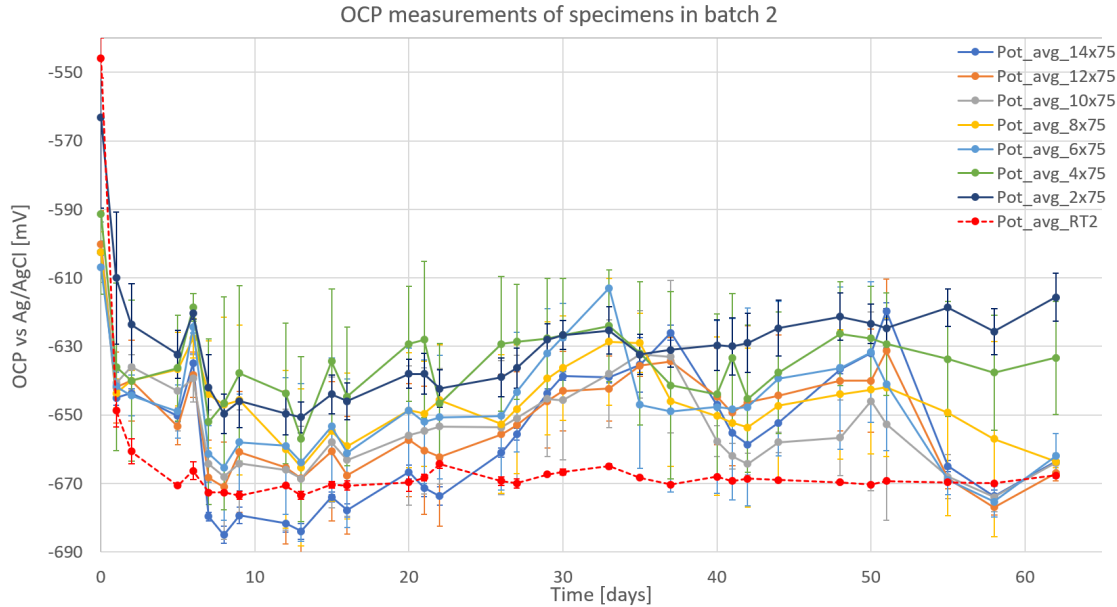


Figure 5.6: OCP measurements of batch 2

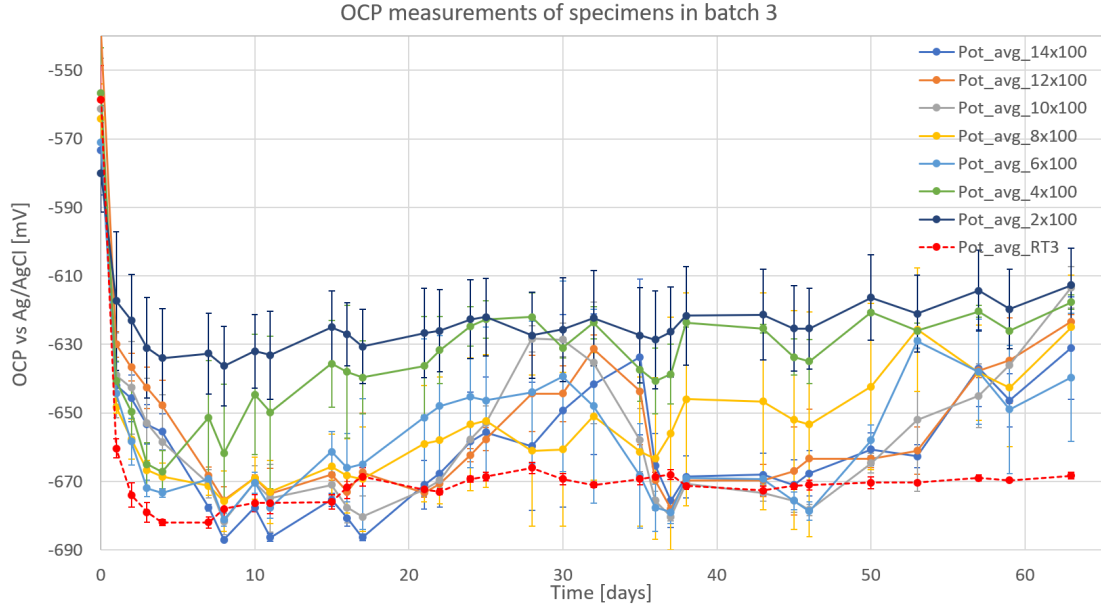


Figure 5.7: OCP measurements of batch 3

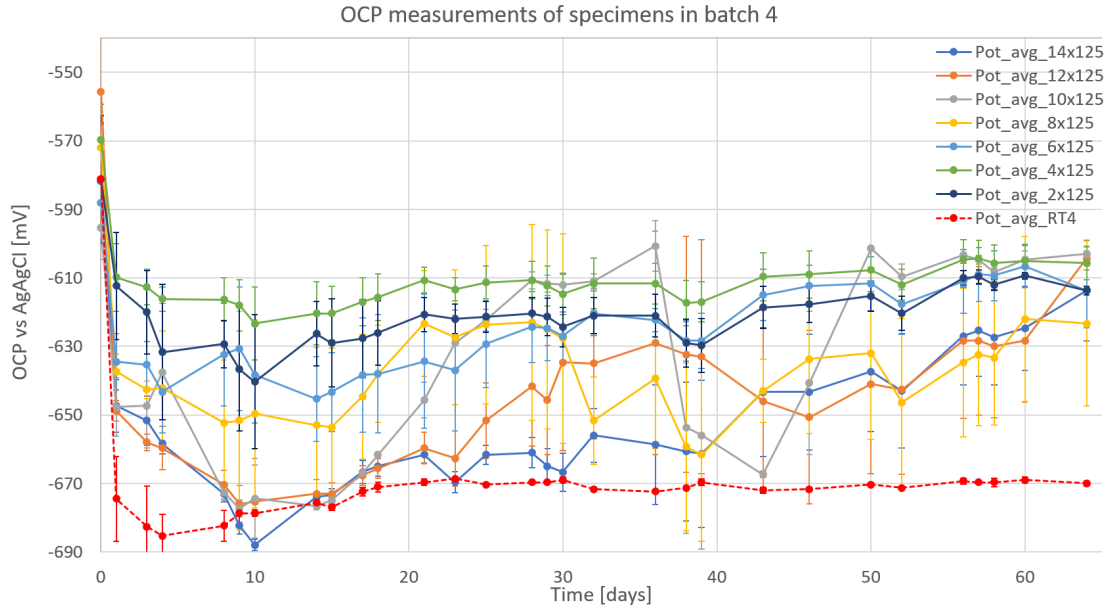


Figure 5.8: OCP measurements of batch 4

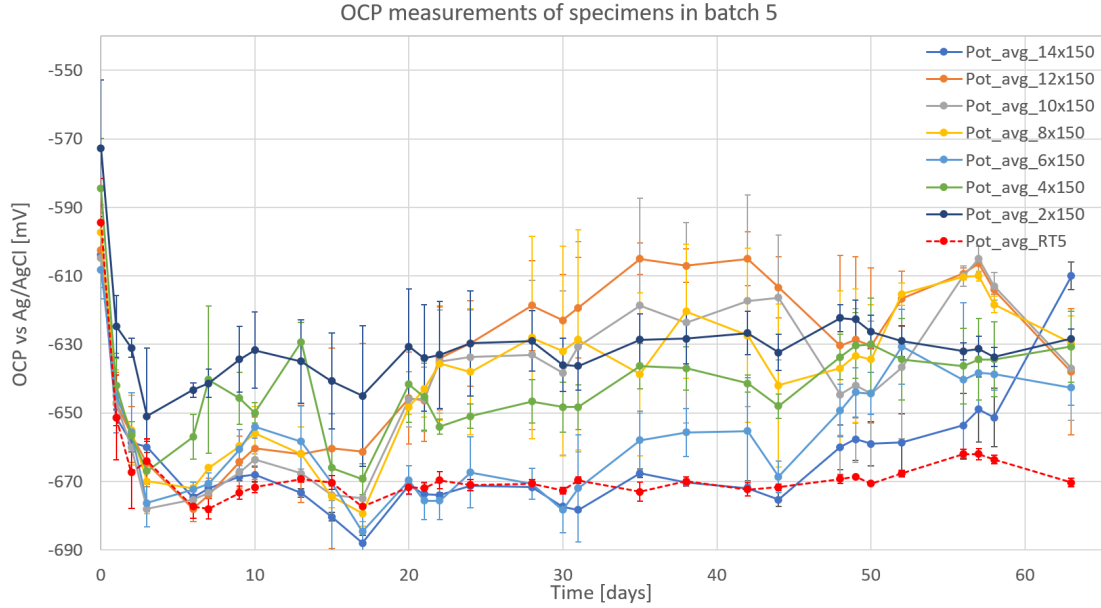


Figure 5.9: OCP measurements of batch 5

It seems that there is a relation between the crevice height and potential measurements. The data indicate that there are two boundaries, the boundary of the uniform corroding reference plate at -670 millivolts and the boundary around -630 millivolts. The potentials of the samples with the crevices are between these two boundaries and seem to go to the upper boundary if the crevice is narrow and long enough.

When looking at the trend of the potential over time, it seems that there are three distinguishable trends. First of all in batch 1 the potentials of the specimens seem to become more negative over time as has already been discussed. Secondly, some potential measurements showed a more sinusoidal effect such as of batch 2 and 3, see Figure 5.6 and Figure 5.7. This suggest that local corrosion was occurring but was not stable. Thirdly, the potential measurements of batch 4 and 5 show a gradual trend towards the potentials around -630 millivolts, suggesting the establishment of local corrosion in these specimens that was stable in the end. Especially the more narrow crevices show this tendency, in all cases the narrow specimens with a crevice of two millimeter high are directly at corrosion potentials around -630 millivolts, see Figure 5.13.

The sudden drops of the unstable potentials are not easy to explain and are probably caused by sudden changes in the environment or by movements during replenishment of the electrolyte. The measurements indicate more stable corrosion for longer crevices, which can be explained that the deeper crevices are less influenced by changes in the environment outside of the crevice. Local corrosion behavior will therefore establish more easily in longer crevices. This can also be seen in Figure 5.10, the longer crevices show more positive potentials that indicates local corrosion attack. This will also be caused by the increase of resistance with the reference electrode due to the increase of the crevice length.

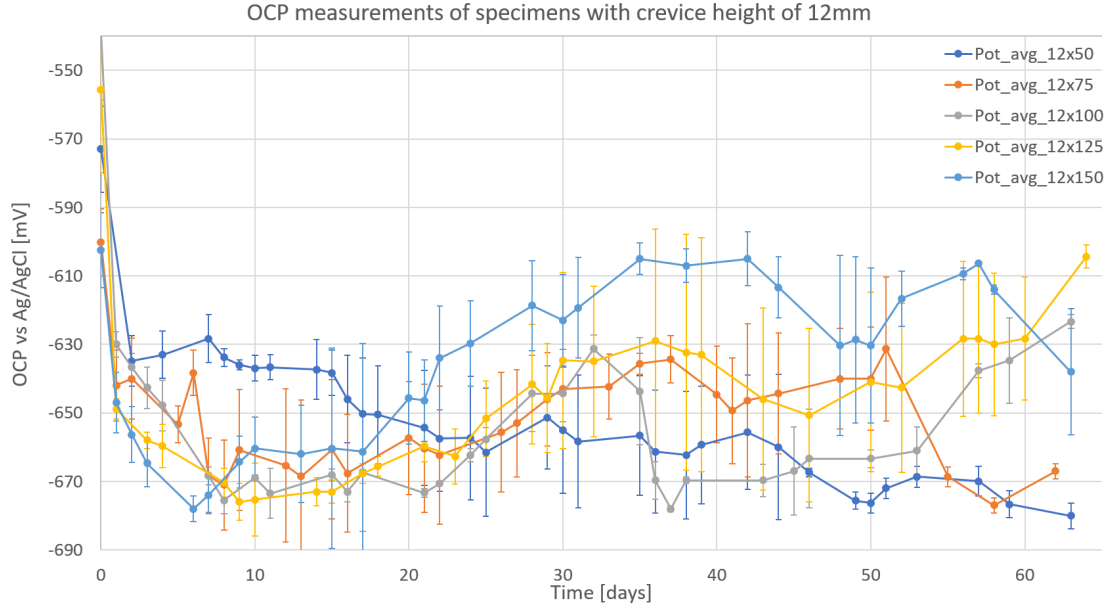


Figure 5.10: OCP measurements of crevices with a gap height of 12mm and crevice lengths of 50mm, 75mm, 100mm, 125mm and 150mm.

As another example, a similar plot is shown for crevices with a gap height of 8 millimeter in Figure 5.11. Again the short crevice of 50 millimeter is steadily dropping and then staying at a potential of about -670 millivolts. The specimens with a three times longer crevice of 150 millimeter goes to a potential of about -630 millivolts and stays around this value during the immersion period. The measurements of the crevices with lengths of 125 and 100 millimeter do show that they go up to that also go up to this more positive value. The crevice with a length of 75 millimeters is now more positive than it was for a crevice height of 12 millimeter, indicating the influence of the crevice gap height. At the end of the immersion period its potential ends more negative however, around -660 millivolts.

The results show that for narrower crevices, more positive potential values are reached sooner and do not show sudden drops to more negative values. However, if the crevice becomes longer/deeper, this more positive values are obtained as well and also become more stable. From the potential data it does seem that both the crevice length and height have influence on the corrosion behavior. To further support this statement, in Figure 5.12 and 5.13 the plots of the potentials for crevices with a gap of relatively 4 millimeter and 2 millimeter are shown. It becomes clear that for smaller crevices the potentials tend to be more positive. The potentials of the specimens with a crevice of 2 millimeter are all in the more positive region around -630 millivolts, the shortest crevice length of 50 millimeter is still sufficient to support the tendency to more positive potentials for crevices.

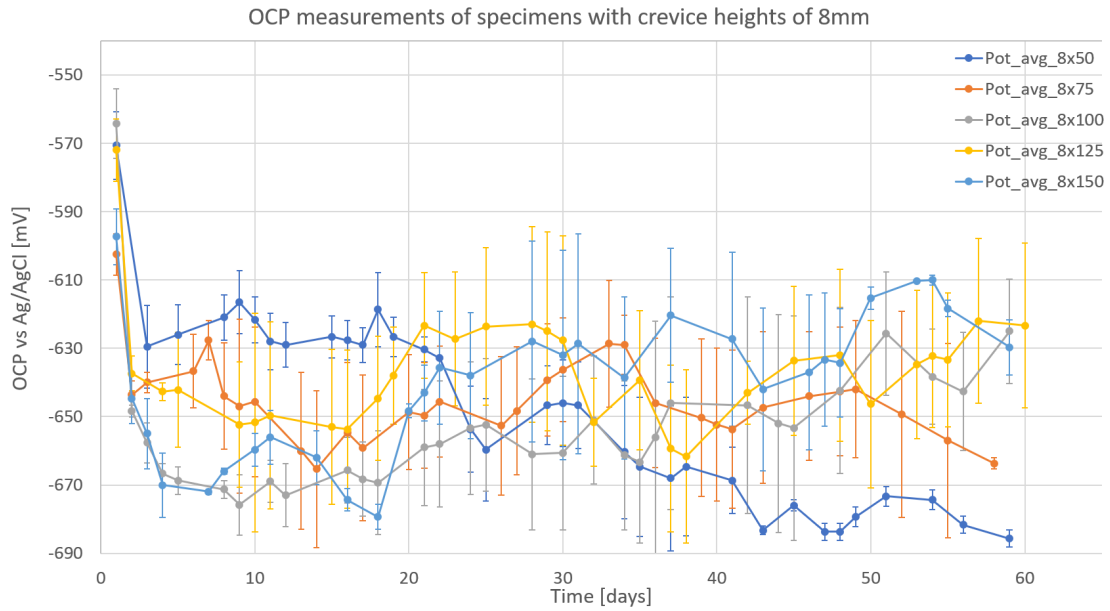


Figure 5.11: OCP measurements of crevices with a gap height of 8mm and crevice lengths of 50mm, 75mm, 100mm, 125mm and 150mm.

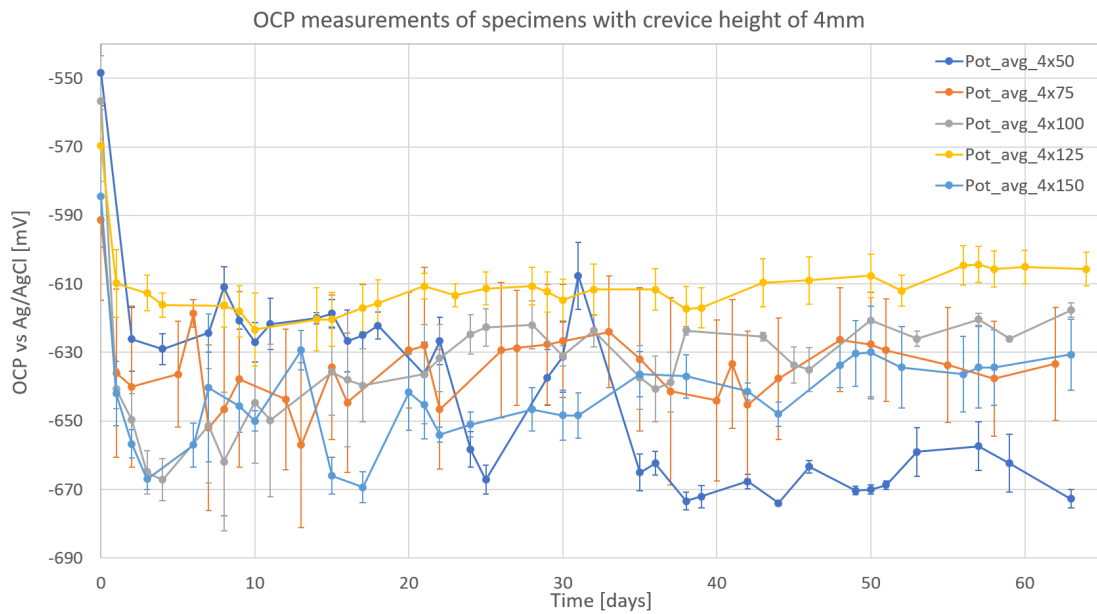


Figure 5.12: OCP measurements of crevices with a gap height of 4mm and crevice lengths of 50mm, 75mm, 100mm, 125mm and 150mm.

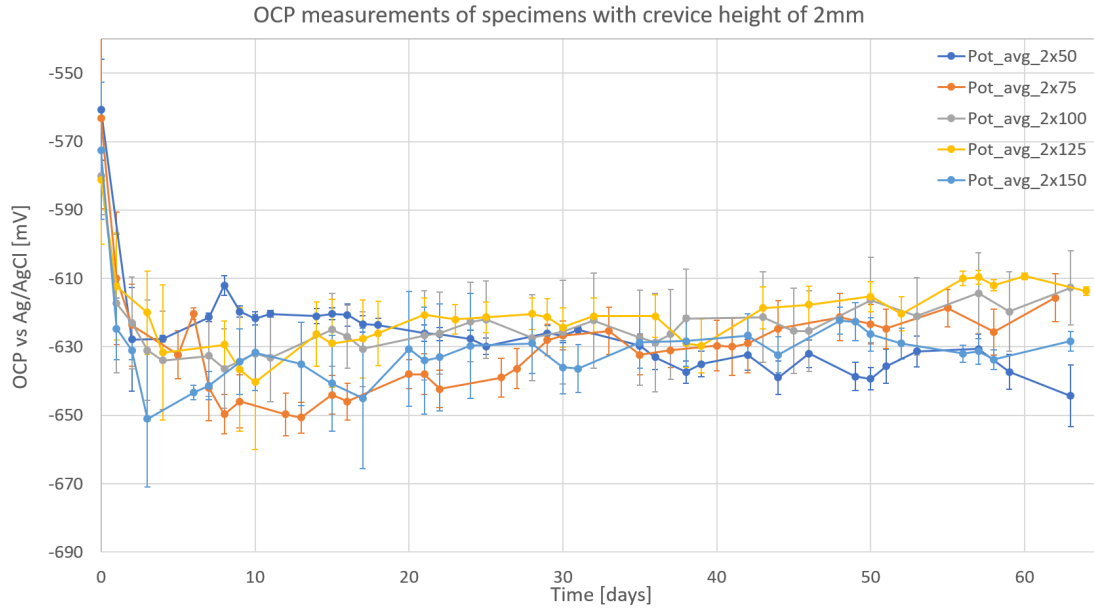


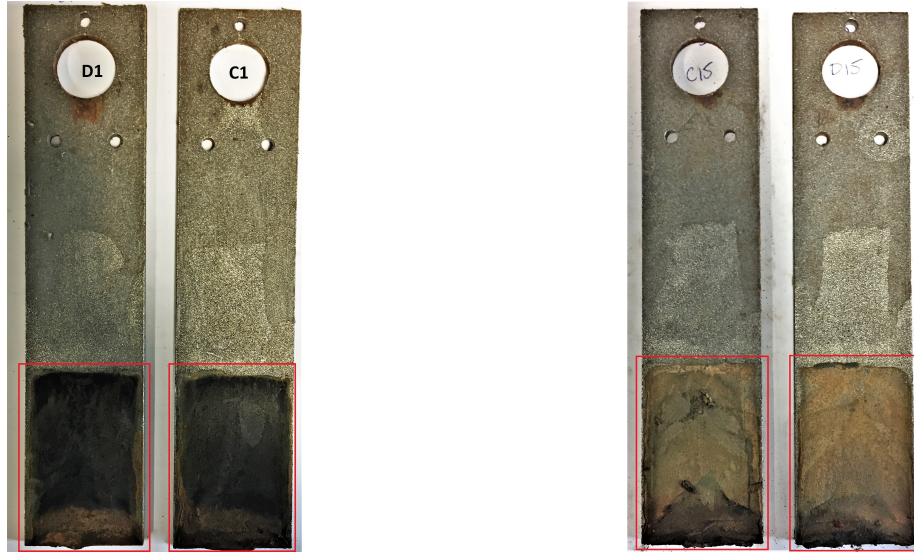
Figure 5.13: OCP measurements of crevices with a gap height of 2mm and crevice lengths of 50mm, 75mm, 100mm, 125mm and 150mm.

In order to check whether the measurements indicate changed corrosion behavior due to the crevice and even the phenomenon crevice corrosion as described in section 2.3.3, the specimens are visually inspected. Such as already done in this section for the specimens immersed in batch 1, with the help of the images in Figure 5.4 and 5.5.

5.1.2 Visual inspection analysis on potentials

After visual inspection of the specimens of batch 2 (batch 1 is already discussed in section 5.1.1), with crevices of 75 millimeter length and crevice gap heights of 14, 12, 10, 8, 6, 4 and 2 millimeter it seems that the potentials do indicate local attack. The specimens which ended up with more positive potentials, specimens with a crevice height of 4 and 2 millimeter see Figure 5.6, also show something different from the other specimens. The attack looks more local and is less uniform. The other specimens with a crevice height between 14 and 6 millimeter show a more uniform attack. In Figure 5.14 examples are shown of these samples that show corrosion attack over the full exposed area.

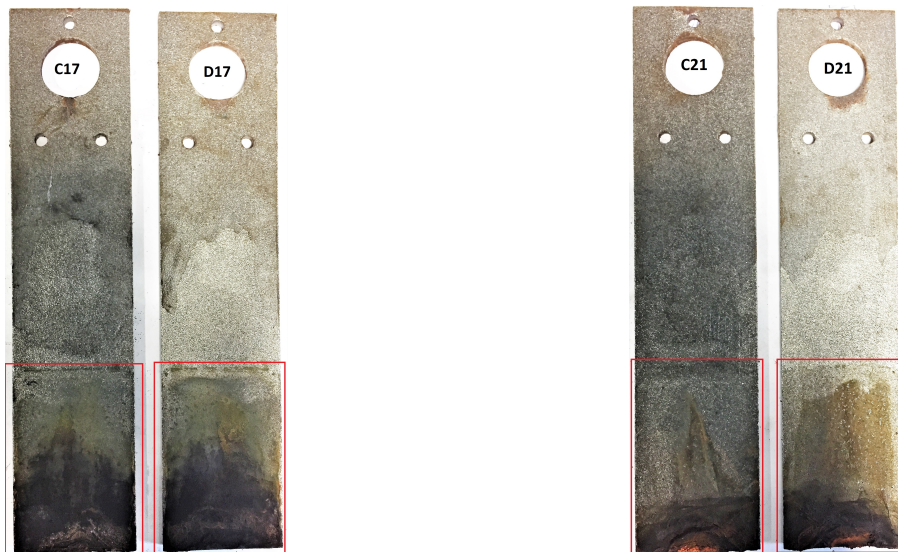
The specimens with crevice heights of 4 and 2 millimeter, which had more positive potentials over the full period of immersion, do show more local attack. In Figure 5.15 an image of the steel plates from a specimen with a gap height of 4 millimeter and with a gap height of 2 millimeter is shown. The local attack is more clear for the crevice with a gap height of only 2 millimeters.



(a) Corroded steel plate C1 and D1 of specimen with a crevice of 14mm height and 75mm long. (The exposed area is indicated by the red box.)

(b) Corroded steel plate C15 and D15 of specimen with a crevice of 6mm height and 75mm long. (The exposed area is indicated by the red box.)

Figure 5.14: Corroded steel plates with crevice lengths of 75mm with potentials in the area of -670 mV



(a) Corroded steel plate C17 and D17 of specimen with a crevice of 4mm height and 75mm long. (The exposed area is indicated by the red box.)

(b) Corroded steel plate C21 and D21 of specimen with a crevice of 2mm height and 75mm long. (The exposed area is indicated by the red box.)

Figure 5.15: Corroded steel plates with crevice lengths of 75mm with potentials in the area of -630 mV

When taking a look at the potentials of the specimens with a crevice length of 100 millimeter, see Figure 5.7, it seems that again only the specimens with a gap height of 2 and 4 millimeter were constantly in the more positive region of -630 millivolts. Looking at the corroded steel plates

this again seems to be the specimens which suffered from a more local attack. In Figure 5.16 an image of steel plates of two of these specimens are shown as an example of the set. It seems even that, especially for the specimen with a gap height of 2 millimeter in Figure 5.16b, there is an area that is totally left untouched by corrosion attack. An explanation could be that it has been the passive area during the time of immersion which is often explained in literature to be part of crevice corrosion, see section 2.3.3.

The specimens with a higher gap again show more uniform attack. As an example the images of the steel plates of two specimens are shown in Figure 5.17. Looking more closely to the steel plates of Figure 5.17b, it seems that there is some local corrosion build-up near the bottom of the plate. A possibility is that the specimen was suffering from crevice corrosion at some times during the immersion, but not over the full period of immersion, which could also explain the changes in the potential measurements.



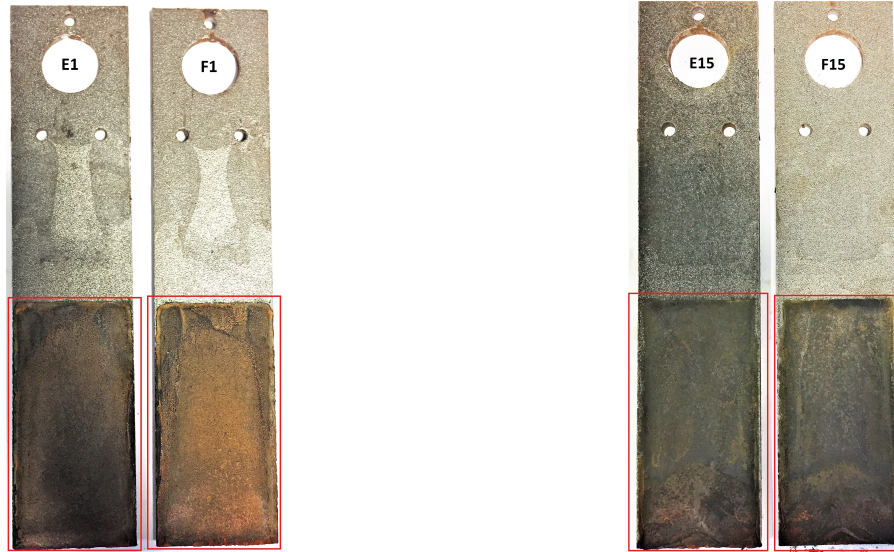
(a) Corroded steel plate E17 and F17 of specimen with a crevice of 4mm height and 100mm long. (The exposed area is indicated by the red box.)

(b) Corroded steel plate E21 and F21 of specimen with a crevice of 2mm height and 100mm long. (The exposed area is indicated by the red box.)

Figure 5.16: Corroded steel plates with crevice lengths of 100mm with potentials in the area of -630 mV

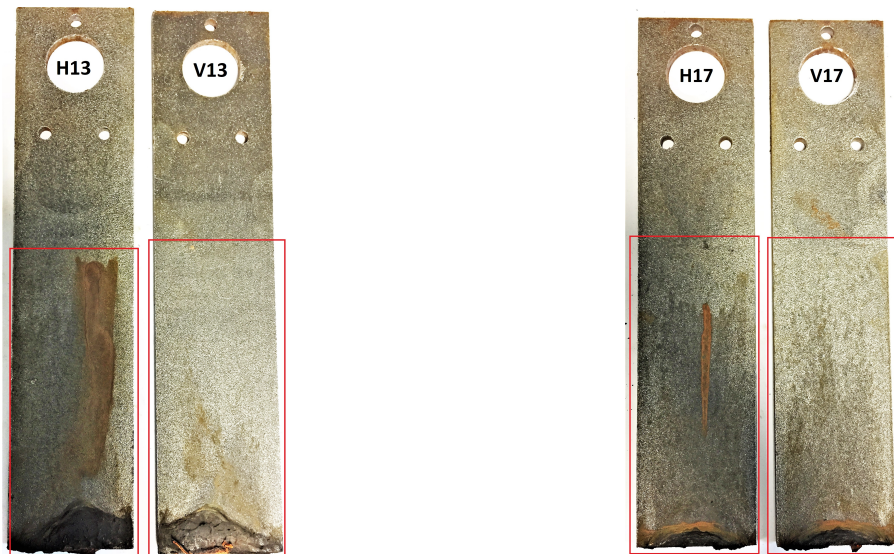
From the measurements that are shown in the plot of Figure 5.8 one would expect that the specimens with a crevice of 6, 4 and 2 millimeter again will show local corrosion behavior. The potentials of these specimens are more or less constant in the area of -630 millivolts. After visual inspection this proves to be correct, see Figure 5.18 in which two examples are shown of steel plates from crevices with a 6 and 4 millimeter gap height after immersion. It shows local corrosion especially near the bottom, however also deeper in the crevice there is some local attack visible.

The potential measurements of the other specimens are less stable and thus suggest that crevice corrosion was not stable or even not occurring during the immersion. This also proves to be correct, see Figure 5.19.



(a) Corroded steel plate E1 and F1 of specimen with a crevice of 14mm height and 100mm long. (The exposed area is indicated by the red box.) (b) Corroded steel plate E15 and F15 of specimen with a crevice of 12mm height and 100mm long. (The exposed area is indicated by the red box.)

Figure 5.17: Corroded steel plates with crevice lengths of 100mm with potentials in the area of -670 mV

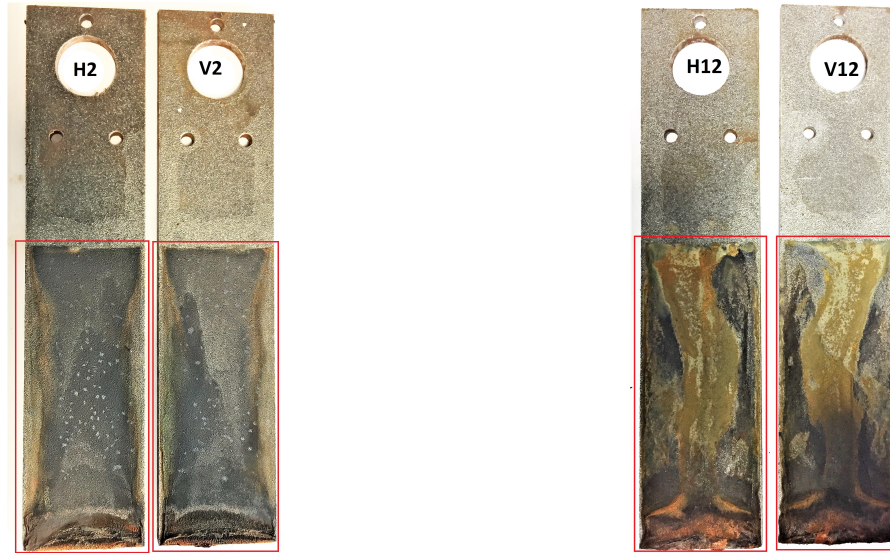


(a) Corroded steel plate H13 and V13 of specimen with a crevice of 6mm height and 125mm long. (The exposed area is indicated by the red box.) (b) Corroded steel plate H17 and V17 of specimen with a crevice of 4mm height and 125mm long. (The exposed area is indicated by the red box.)

Figure 5.18: Corroded steel plates with crevice lengths of 125mm with potentials in the area of -630 mV

The steel plates of the specimen with an 8 millimeter gap height, H12 and V12 as shown in Figure 5.19b, is not corroded uniformly but also did not corrode as local as the steel plates shown in Figure 5.18. The plates from a specimen with a crevice height of 14 millimeter also does not show a real

uniform corrosion pattern. Looking closely it even seems that small dotted areas were attacked, which might suggest pitting corrosion. Pitting is not likely to occur, because in general structural steels or mild steels generally do not suffer from pitting corrosion as indicated in section 2.3.2.

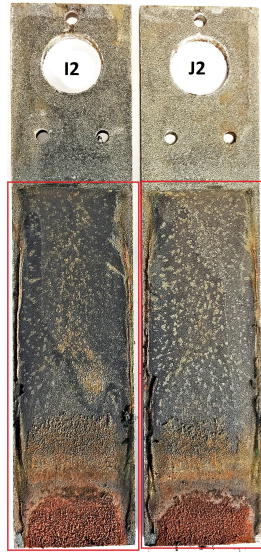


(a) Corroded steel plate H2 and V2 of specimen with a crevice of 14mm height and 125mm long. (The exposed area is indicated by the red box.)

(b) Corroded steel plate H12 and V12 of specimen with a crevice of 8mm height and 125mm long. (The exposed area is indicated by the red box.)

Figure 5.19: Corroded steel plates with crevice lengths of 125mm with unstable and/or more negative potentials

The longer crevices of 125 millimeter already showed more corrosion build-up near the mouth and less uniformly distributed corrosion over the crevice, see Figure 5.19. This is also expected for the longer crevices of 150 millimeter. The potential measurements, presented in Figure 5.9, show that again the smallest crevice has been corroding at a potential around -630 millivolts. After 20 days of immersion almost all specimens were measuring potentials around the value of -630 millivolts and some even more positive. However, two specimen sets were at this -630 millivolts boundary only during the final 10 to 15 days. Remarkable is that the crevice of 6 millimeter gap height has measured more negative values around -670 millivolts during the first 45 days of immersion. For the bigger gap of 14 millimeters it is not strange to show these behavior, while it also shows this in the other plots. The visual inspection of these specimens with a crevice gap of 6 millimeter, shows more similarities with the steel plates as shown in Figure 5.19. In Figure 5.20b these plates are shown. The shown steel plates in Figure 5.20a show more corrosion build up near the mouth and again some small dotted area can be identified. Moving from the mouth (the bottom) it seems that this specimen did not corrode very severe with this longer crevice. The surface is not really uniformly corroded. As it was for the other steel plates from specimens with a crevice, it does not show similar corrosion compared to the uniform corrosion of the reference plates, see Figure 5.2.



(a) Corroded steel plate I2 and J2 of specimen with a crevice of 14mm height and 150mm long. (The exposed area is indicated by the red box.)



(b) Corroded steel plate I13 and J13 of specimen with a crevice of 6mm height and 150mm long. (The exposed area is indicated by the red box.)

Figure 5.20: Corroded steel plates with crevice lengths of 150mm with unstable and/or more negative potentials



(a) Corroded steel plate I8 and J8 of specimen with a crevice of 10mm height and 150mm long. (The exposed area is indicated by the red box.)



(b) Corroded steel plate I21 and J21 of specimen with a crevice of 2mm height and 150mm long. (The exposed area is indicated by the red box.)

Figure 5.21: Corroded steel plates with crevice lengths of 150mm with potentials in the area of -630 mV

Again the specimens, which showed a constantly more positive potential around -630 millivolts, did corrode more local as the example shows in Figure 5.21b. The steel plates of Figure 5.21a measured a potential around -630 millivolts after 20 days of immersion and seem to be a combination of both

the specimens with more negative potentials and the specimens which were constantly more positive. A possibility is that during the first 20 days, the specimen corroded more or less uniformly and after this period started to build up local crevice corrosion.

In general it seems that the specimens with a narrow crevice proved to be very susceptible to local crevice corrosion. The build up of rust near the mouth of the crevice even partly blocked the crevice mouth for the narrow crevices, see Figure 5.22. This could be an explanation for the reason why the small crevices are more likely to show local corrosion attack.



Figure 5.22: Rust forming a blockade at the mouth of a small crevice

5.2 Weight losses and corrosion rates

5.2.1 Weight losses

After the immersion period, the specimens were cleaned from their rust as described in section 4.4. After the cleaning, the weight loss of each steel plate was measured. In Figure 5.23 the weight loss of the specimens is plotted with the corresponding standard deviation around the average. The weight loss of the uniform corroded reference plates in batch 1, is on average 4 grams. The weight loss of the specimen with a crevice gap of 14 millimeter height and 50 millimeter length is on average 1.13 grams. Looking at the specimens with more narrow crevices the weight loss reduces. An explanation for this reduction in weight loss could be that for more narrow crevices the resistance to diffusion of oxygen and other cations into the crevice is higher and thus the corrosion process is controlled by the diffusion. In the previous paragraph the pictures also showed that the specimens with more narrow crevices suffered from more local corrosion attack. It is very likely and possible that due to the local attack the average weight loss of these specimens drops.

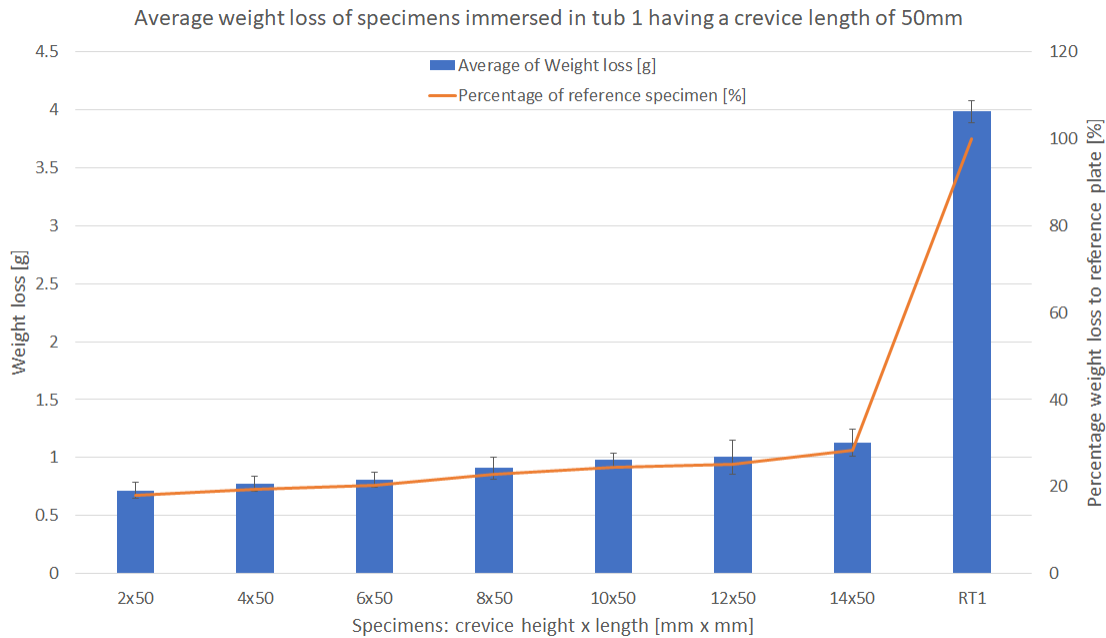
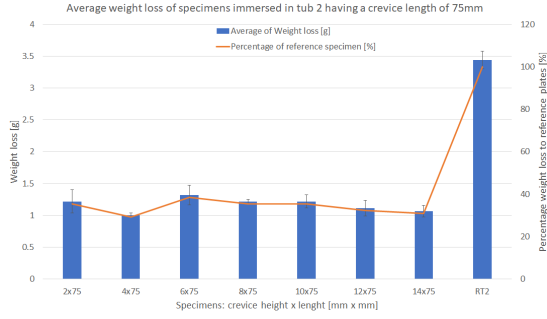


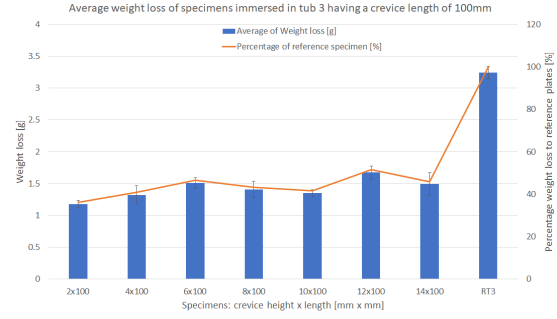
Figure 5.23: Weight loss of specimens in batch 1 having a crevice length of 50mm. The weight loss of the uniform corroding reference plate is included in the plot (RT1).

The weight loss of the specimens differs a lot from the weight loss of the steel reference plate, it is only $\pm 20\%$ (indicated by the orange line in Figure 5.23). The exposed area of both differ significantly. The exposed area for the specimens in batch 1 is only 5500 mm^2 . The exposed area for the reference plates is about 18000 mm^2 . The weight loss should be corrected for the exposed area, this is done in section 5.2.2.

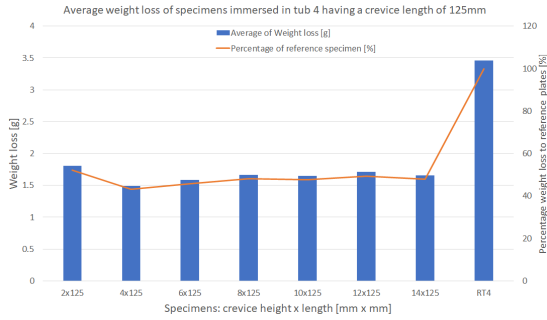
Looking at the weight losses from the other batches, this pattern of increasing weight loss for higher crevices seems to disappear. The influence of the changing gap seems not to have influence on the weight loss, however visual inspection showed that certain specimens were definitely corroding differently.



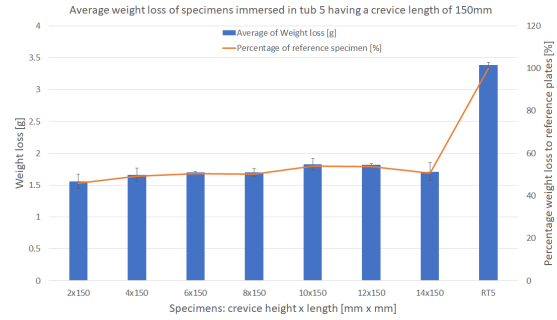
(a) Weight loss of specimens in batch 2 having a crevice length of 75mm. RT2 is the reference.



(b) Weight loss of specimens in batch 3 having a crevice length of 100mm. RT3 is the reference.



(c) Weight loss of specimens in batch 4 having a crevice length of 125mm. RT4 is the reference.



(d) Weight loss of specimens in batch 5 having a crevice length of 150mm. RT5 is the reference.

Figure 5.24: Weight losses of specimens with lengths 75, 100, 125 and 150mm

Instead of comparing weight losses, it is better to check the corrosion rates. These correct for the exposed area and the time of immersion.

5.2.2 Corrosion rates

Using the obtained weight losses, the corrosion rates have been calculated according to the following equation (taken from section 4.4) :

$$CR = (K \times W) / (A \times T \times D) [mm/y] \quad (5.5)$$

where:

K = a constant (8.76×10^4)

W = mass loss in grams

A = exposed area in cm^2

T = time of exposure in hours

D = density in g/cm^3

As with the other data, first the corrosion rates of the specimens with a crevice length of 50 millimeter are checked. The trend will look similar as for the weight loss, while the exposed surface and immersion period did not differ between those specimens. In Figure 5.25 this can be observed. Note that the percentages, relative to the corrosion rate of the uniform corroded reference plates, are much higher than it was for the weight losses. This is caused by correcting for the exposed area.

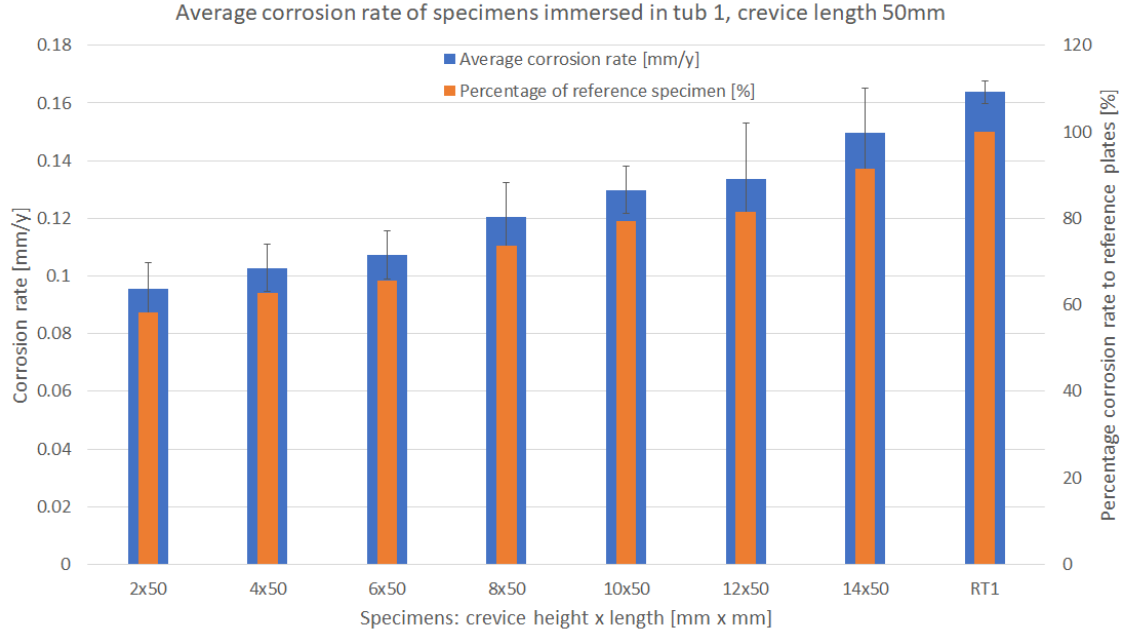
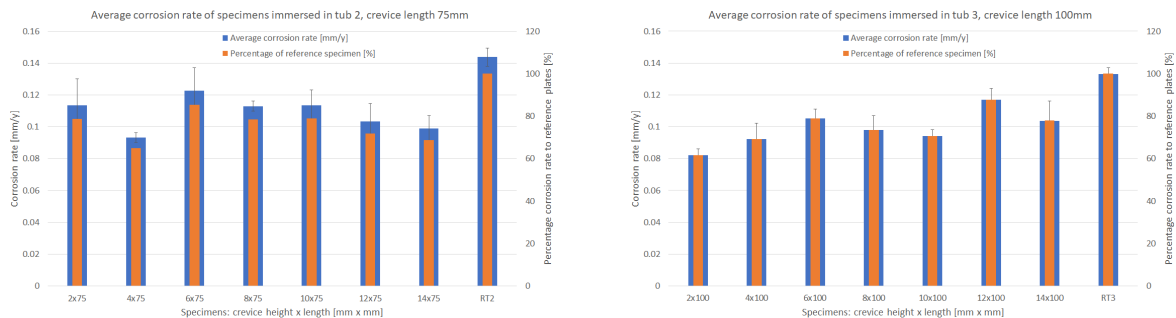


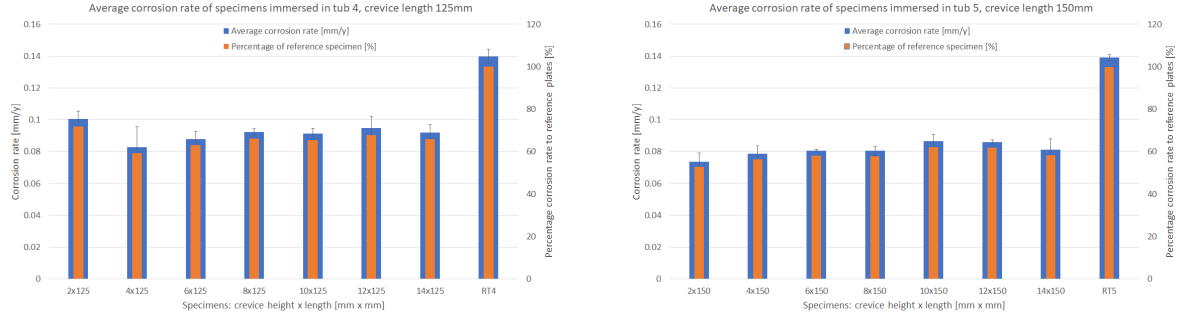
Figure 5.25: Corrosion rate of specimens in batch 1 having a crevice length of 50mm. The corrosion rate of the uniform corroding reference plate is included in the plot (RT1).

The corrosion rate of the specimen with a crevice height of 2 millimeter and 50 millimeter length is on average 0.096 millimeter per year. The corrosion rate of the wider gap, 14 millimeter, is much higher, it is on average 0.15 millimeter per year. Looking at the data for longer crevices as displayed in Figure 5.27 it does not directly provide new understanding of possible trends. The corrosion rate of the uniform plate is more than 0.16 millimeter per year. This is more than the 0.10 millimeter per year that should be taken into account according to DNVGL. The corrosion rate of the laboratory test is higher because of the higher temperatures in the laboratory environment. Furthermore was a salt solution used instead of seawater which makes that the two different corrosion rates can not directly be related.



(a) Corrosion rate of specimens in batch 2 having a crevice length of 75mm. RT2 is the reference. (b) Corrosion rate of specimens in batch 2 having a crevice length of 100mm. RT3 is the reference.

Figure 5.26: Weight losses of specimens with lengths 75 and 100mm



(a) Corrosion rate of specimens in batch 4 having a crevice length of 125mm. RT4 is the reference. (b) Corrosion rate of specimens in batch 5 having a crevice length of 150mm. RT5 is the reference.

Figure 5.27: Weight losses of specimens with lengths 125 and 150mm

In order to check the influence of the gap height of the crevice on the corrosion rate, all data off the specimens with the same crevice height have been combined. This will visualize what the influence of the geometric parameters is on the corrosion rate. In Figure 5.28 it is visible that changing the gap height is influencing the corrosion rate only little.

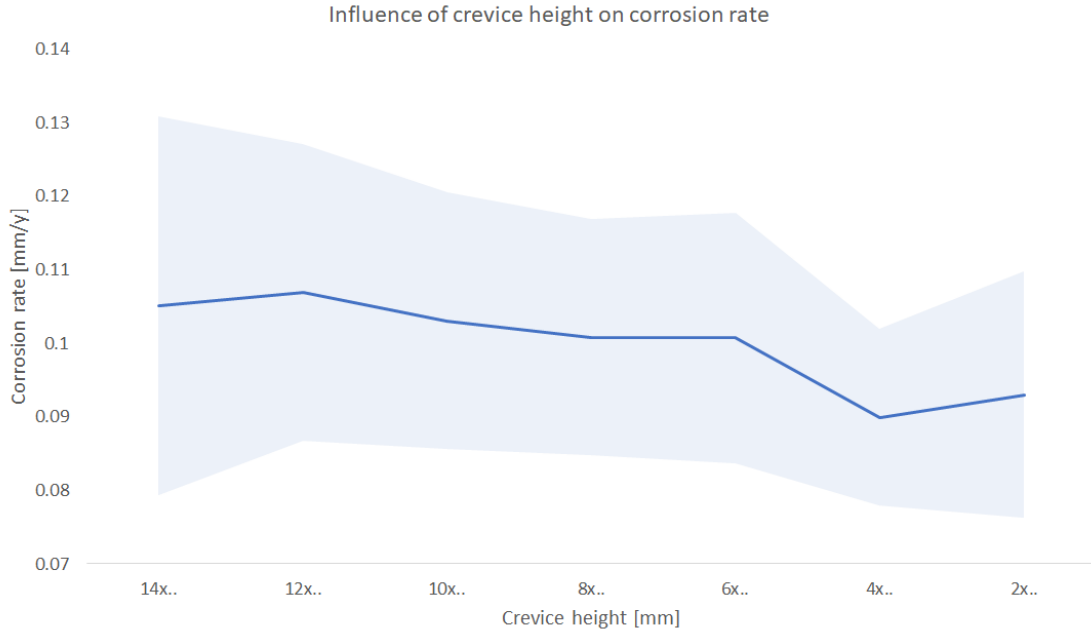


Figure 5.28: Influence of the crevice height on the corrosion rate. The light blue area is the standard deviation from the mean.

The more narrow crevices showed a little lower corrosion rates, especially the corrosion rate of the specimens with a 4mm crevice height showed lower corrosion rates. Using the student t-test is checked whether this is a significant difference:

$$t = \frac{\bar{x} - \bar{y}}{\sqrt{\frac{s_x^2}{n_x} + \frac{s_y^2}{n_y}}} \quad (5.6)$$

where:

t = the required t-value

\bar{x} = the mean of set 'x'

\bar{y} = the mean of set 'y'

s_x = standard deviation of set 'x'

s_y = standard deviation of set 'y'

n_x = number of data points of set 'x'

n_y = number of data points of set 'y'

The used level of significance is 5% and a 1 tailed test is used.

The results showed that there is a significant difference between the measured corrosion rate for a 4 millimeter gap and the wider gaps, see Figure 5.29. There is no significant difference between the 4 millimeter crevice height and the 2 millimeter crevice height. Furthermore there is a significant difference between the value measured of the 2 millimeter crevice height and the 12 millimeter crevice. Although most data is not significant different, this does suggest that the specimens with smaller crevices had a lower corrosion rate.

Crevice height [mm] ↓	2 →	4	6	8	10	12	14
2		0.29	0.12	0.11	0.07	0.03	0.08
4	0.29		0.03	0.03	0.01	0.01	0.03
6	0.12	0.03		0.49	0.36	0.19	0.30
8	0.11	0.03	0.49		0.36	0.19	0.30
10	0.07	0.01	0.36	0.36		0.30	0.40
12	0.03	0.01	0.19	0.19	0.30		0.42
14	0.08	0.03	0.30	0.30	0.40	0.42	

Figure 5.29: T-Test for corrosion rates with varying crevice heights

The same type of analysis can be carried out for the crevice length. There is a clear trend in the corrosion rate visible, for deeper/longer crevices the corrosion rates drop. An average corrosion rate of 0.12 millimeter per year was found for the specimens with a crevice length of 50 millimeter, the longest crevices of 150 millimeter measured a corrosion rate of 0.08 millimeter per year.

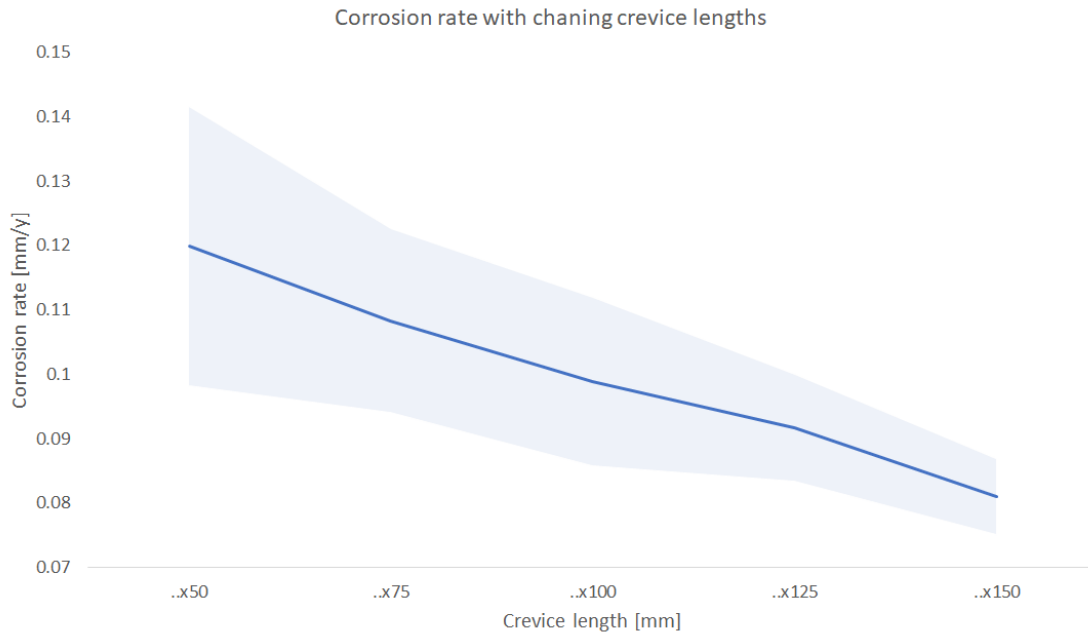


Figure 5.30: Influence of the crevice length on the corrosion rate. The light blue area is the standard deviation from the mean.

To be thorough, again the student t-test is used. All values from the t-test show that the data is significant different for each crevice length. The length of the crevice had a significant influence on the corrosion rate. Another trend can be observed. The standard deviation is getting smaller for longer crevices. An explanation could be that in longer crevices the main part will remain undisturbed by the environment outside of the crevice. In longer crevices there is a longer water column that is stagnant and will stay stagnant and thus is less influenced by certain actions during the test, such as replenishment of the electrolyte. The transport of oxygen towards the end of a longer crevice is less, due to the longer path the oxygen has to travel. This will also make that the overall corrosion rate can drop and that the length of the crevice seem to have more influence on the corrosion rate than the crevice height.

Crevice height [mm]	50	75	100	125	150
50		0.03	0.00	0.00	0.00
75	0.03		0.02	0.00	0.00
100	0.00	0.02		0.02	0.00
125	0.00	0.00	0.02		0.00
150	0.00	0.00	0.00	0.00	

Figure 5.31: T-Test for corrosion rates with varying crevice lengths

To further investigate the influence of the length and height of the crevice in Figure 5.32 a table of

the corrosion rates for each crevice geometry is shown. The color scaling in the table shows that the corrosion rate drops for increasing crevice lengths and for decreasing crevice heights.

Influence crevice length and height on corrosion rate [mm/y]

		Length →				
Height ↓		50	75	100	125	150
	2	0.10	0.11	0.08	0.10	0.07
	4	0.10	0.09	0.09	0.08	0.08
	6	0.11	0.12	0.11	0.09	0.08
	8	0.12	0.11	0.10	0.09	0.08
	10	0.13	0.11	0.09	0.09	0.09
	12	0.13	0.10	0.12	0.09	0.09
	14	0.15	0.10	0.10	0.09	0.08

Figure 5.32: Influence of the crevice height and length on the corrosion rate.

5.3 Results of crevices ending in a void

5.3.1 Open circuit potential measurements and visual inspection

In Figure 5.33 the OCP measurements of the reference plates for this test are shown by the red line. The other lines show the measurements of the reference plates of the previous test, batch 1 to 5. The potentials of the reference plates of this test show that the test is consistent with the other test. The environmental circumstances such as temperature and solution properties have been consistent for each batch, this test is considered as batch 6.

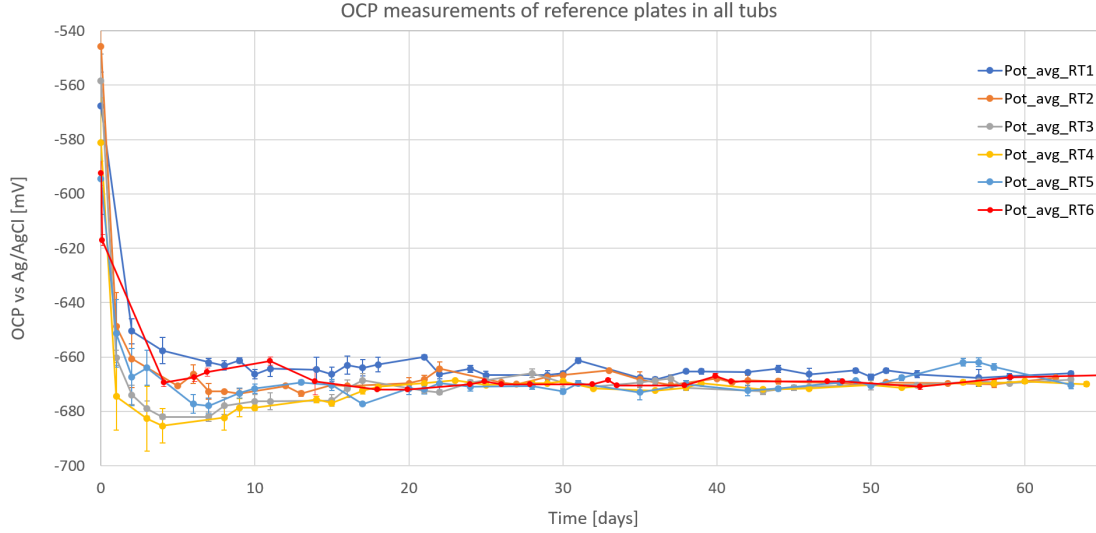


Figure 5.33: OCP measurements of all reference plates. Batch 1 to 5 are from the crevice corrosion test. Pot_avg_RT6 are the OCP measurements of the reference plates of the batch of the crevices with a void.

The standard deviations of the measurements of the reference plate of this test, as shown in Figure 5.33, were very low. This indicates that the specimen properties, such as surface roughness, were consistent over the specimens. The resulting corroded surface also was identical to the reference plates of the other batches, see Figure 5.2. It can be concluded that this test has been carried out in accordance to the other test.

The potential data of the specimens, see Figure 5.34, show consistent results with the previous test. The blue line shows the OCP measurements of the specimen with a crevice of 2mm height in front of the void. The orange line shows the OCP measurements of the specimen with a crevice of 4mm in front of the void. In red the OCP measurements of the reference plates. Again the potentials are more positive than the uniform corrosion potential. The potentials are similar to the potentials of specimens with a regular crevice of 2 or 4 millimeter high, such as shown in Figure 5.12 and Figure 5.13. This indicates that the corrosion behavior is also similar to the specimens with the regular crevices of two and four millimeter high. There are two drops of the average potential of the specimen with a four millimeter high crevice, after 30 days and after 60 days. These can not be explained easily. It can be errors in the measurements or caused by unstable corrosion caused by the void.

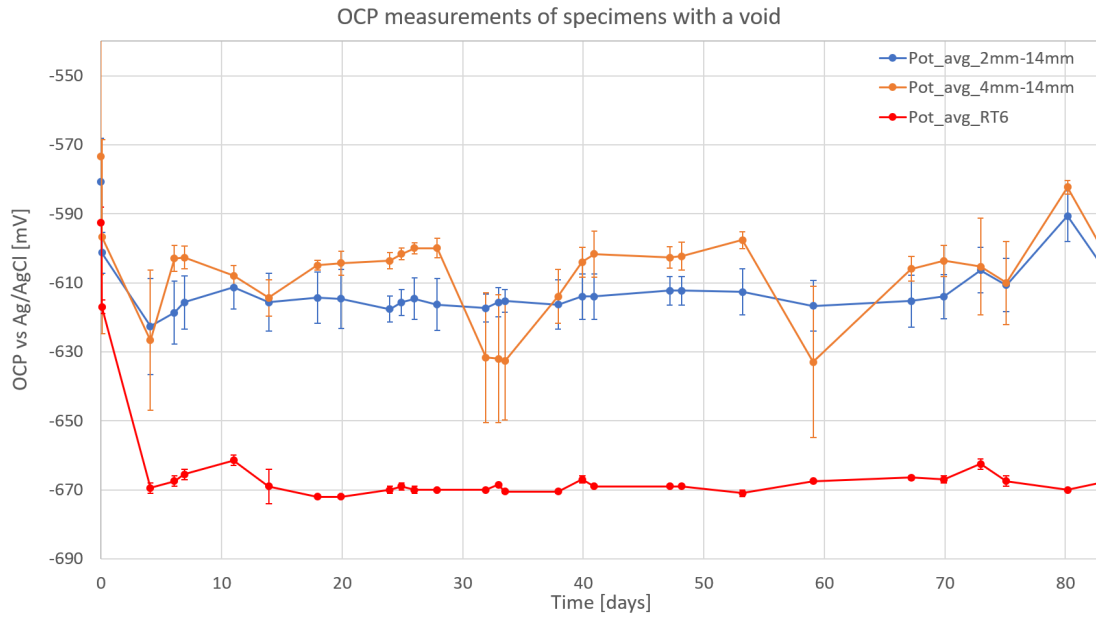


Figure 5.34: OCP measurements of specimens with a void.

Visual inspection of the corroded steel plates show that the corrosion attack is concentrated at the surface area of the crevice and not near the void. In Figure 5.35 an example is shown. The rust formation looks similar to the rust formation as shown for the two millimeter high crevices as shown in Figure 5.15 and in Figure 5.16.



Figure 5.35: Corroded steel plate Y1 of a specimen with a 2mm high crevice and a 14mm high void.

One of the specimens showed a distinct boundary of the rust formation at the transition to the void, see Figure 5.36. This was found on a specimen which had a crevice of 4 millimeter high in front

of the 14 millimeter high void. The boundary indicates that for this specimen the void influenced the corrosion. The influence was only little however, because the rust deposit is more located near the mouth of the specimen. The OCP data of this specific specimen is checked, but did not show a deviation to the other potential data, although the two drops could not be explained.



Figure 5.36: Corroded steel plate Y4 of a specimen with a 4mm high crevice and a 14mm high void.

5.3.2 Weight losses and corrosion rates

The weight loss of each steel plate was measured. In Figure 5.37 the weight loss of the specimens is plotted with the corresponding standard deviation around the average. The weight loss of the uniform corroded reference plates in this test is on average 5.2 grams. The weight loss of the specimens with a crevice height of 2 millimeter in front of the void is on average 1.3 grams and the weight loss of the specimens with a crevice height of 4 millimeter in front of the void is on average 1.2 grams. Comparing these weight loss measurements to the weight losses of the other test, as discussed in section 5.2.1, shows that the weight loss of the reference plates for this test is higher. This is caused by the longer immersion period during this test. In the other test the specimens were immersed for 60 days and in this test the specimens were immersed for 80 days. To be able to really compare the results with the other test, the corrosion rates have been calculated.



Figure 5.37: Weight loss of specimens in batch 6, having a void of 14mm high at the rear of a crevice. The weight loss of the uniform corroded reference plates is included in the plot (RT6).

To correct for the period of immersion and for the exposed area, the corrosion rates of the specimens have been calculated according to equation 5.5. Results are plotted in Figure 5.38. The corrosion rate of the uniform corroded reference plate is 0.16 millimeter per year, this is similar to the results from the previous test. The corrosion rates of the specimens with a void are lower than the uniform corrosion rate. This was also the case for the specimens with a regular crevice. The corrosion rates are compared to the corrosion rates of specimens with only a regular crevice, but with the same exposed area.

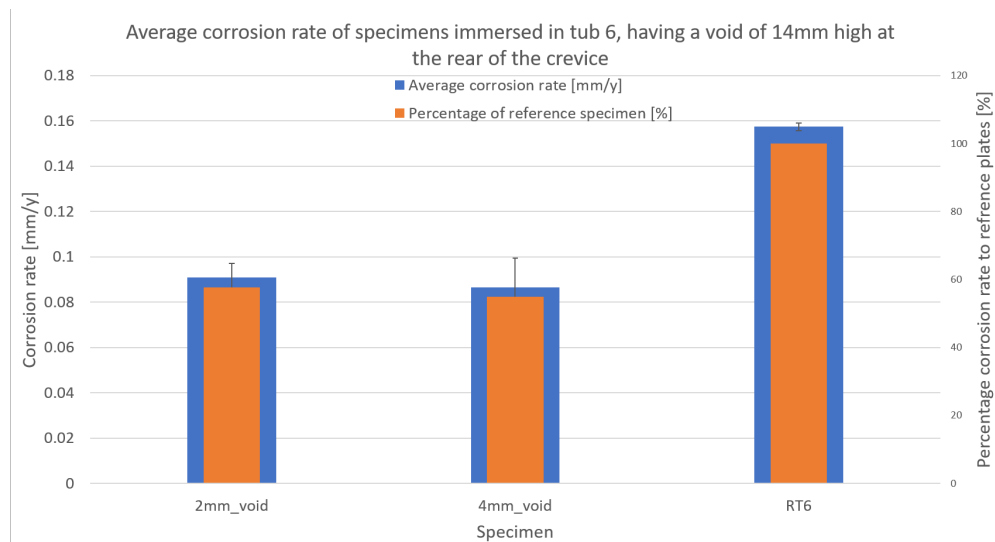


Figure 5.38: Corrosion rate of specimens in batch 6, having a void of 14mm high at the rear of the crevice. The corrosion rate of the uniform corroded reference plates is included in the plot (RT6).

In order to be able to check whether the void influenced the corrosion behavior the corrosion rates of have been compared to the corrosion rates of the regular crevices with the same exposed area. The specimens with a regular crevice of 2 and 4 millimeter high and a length of 150 millimeter, from batch 5, have the same exposed area as the specimens of this void test. The only difference between the two is that in this test a void of 14 millimeter high is created at the rear of the crevice. In Figure 5.39 the corrosion rates of the tests are plotted in one graph. The average corrosion rate of the crevices with a void are higher than the corrosion rates of the regular crevices. The percentage relative to the uniform corroded reference plates are however more similar.

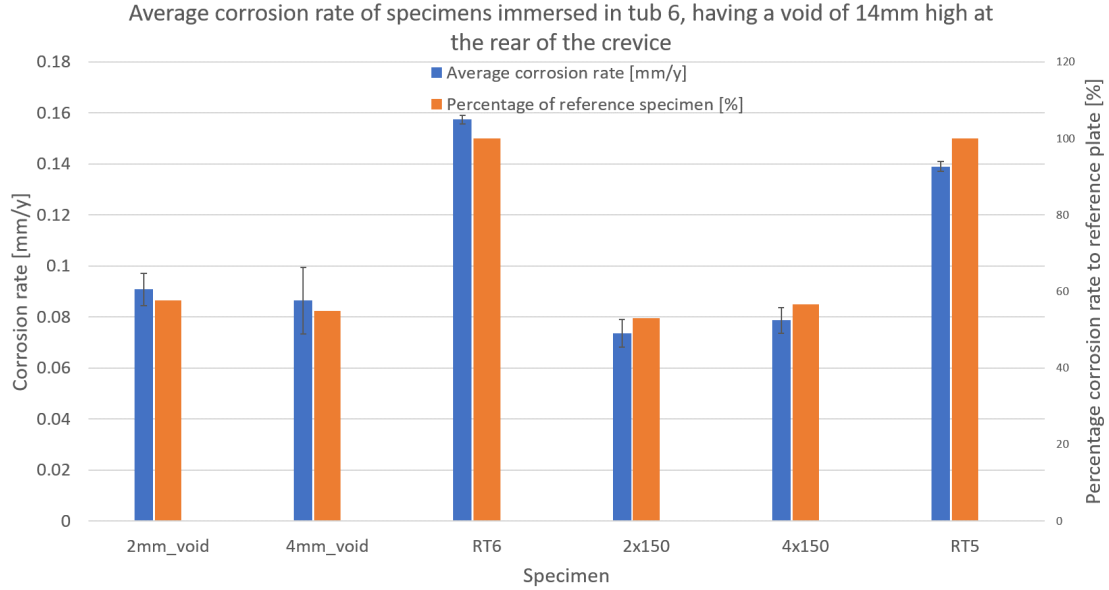


Figure 5.39: Corrosion rates of crevices with a void compared to regular crevices of similar geometries.

To check whether the differences are significant the Student T-test is used as given in equation 5.6. The used level of significance is still 5%, and an one tailed test is used to check whether the corrosion rate of the crevices with a void are significantly higher. The results, given in Figure 5.40, indicate that there is a significant different between the corrosion rate of the regular 2 millimeter crevice and the specimen with a crevice of 2 millimeter and a void. All the specimens are significant different to the uniform corroded reference plates.

	2mm_void	4mm_void	2x150	4x150	RT5	RT6
2mm_void		0.35	0.02	0.05	0.00	0.00
4mm_void	0.35		0.15	0.25	0.01	0.01
2x150	0.02	0.15		0.19	0.00	0.00
4x150	0.05	0.25	0.19		0.00	0.00
RT5	0.00	0.01	0.00	0.00		0.00
RT6	0.00	0.01	0.00	0.00	0.00	

Figure 5.40: T-Test for corrosion rates of crevices with and without a void

The uniform corroded reference plates are also significantly different to one another according to

the T-test. This suggests that the corrosion rate in batch 6 was higher in general. A possible scenario is that the environmental conditions during this test have been different, although the potential data indicates otherwise. To check whether this influences the T-test, the corrosion rates of batch 6 and batch 5 have been corrected by dividing the corrosion rates of the specimens by the corrosion rates of the reference plates. The T-test was carried out again for the corrected and normalized corrosion rates of the specimens, see Figure 5.41. After correcting, there are no significant differences according to the T-test.

	2mm_void	4mm_void	2x150	4x150
2mm_void		0.35	0.15	0.39
4mm_void	0.35		0.40	0.40
2x150	0.15	0.40		0.19
4x150	0.39	0.40	0.19	

Figure 5.41: T-Test for corrosion rates of crevices with and without a void corrected to the uniform corrosion rates of their batches

5.4 ICCP on crevices

The typical cathodically protected submerged offshore structures is recommended to be polarized to a protection potential between -900 and -1050 millivolts (versus Ag/AgCl). A ICCP system is considered to protect the structure if a potential value between -800 and -1150 millivolts is obtained. More positive values are considered as under protection and more negative values are considered as over protection. [47]

Figure 5.42 shows the potential data of the polarized steel plate from the specimen with a crevice of 2mm×50mm×50mm. The data shows that the steel plate is polarized in the zone of protection. The ICCP system was set to polarize the plate to -900 millivolts. The measured potential was -880 millivolts. The 20 millivolt difference in measured potential and applied potential is caused by the difference in resistance of the potential logger and the PalmSens 4 potentiostat. Two runs were conducted. After the first run finished, the potential directly becomes more positive and goes to the corrosion potential. After one day the ICCP system is turned on again. The potential directly goes back to the protection potential. During the test the potential is constant which indicates that the ICCP is stable. Unfortunately the ICCP current data was lost due to a malfunctioning device memory of the PalmSens 4.

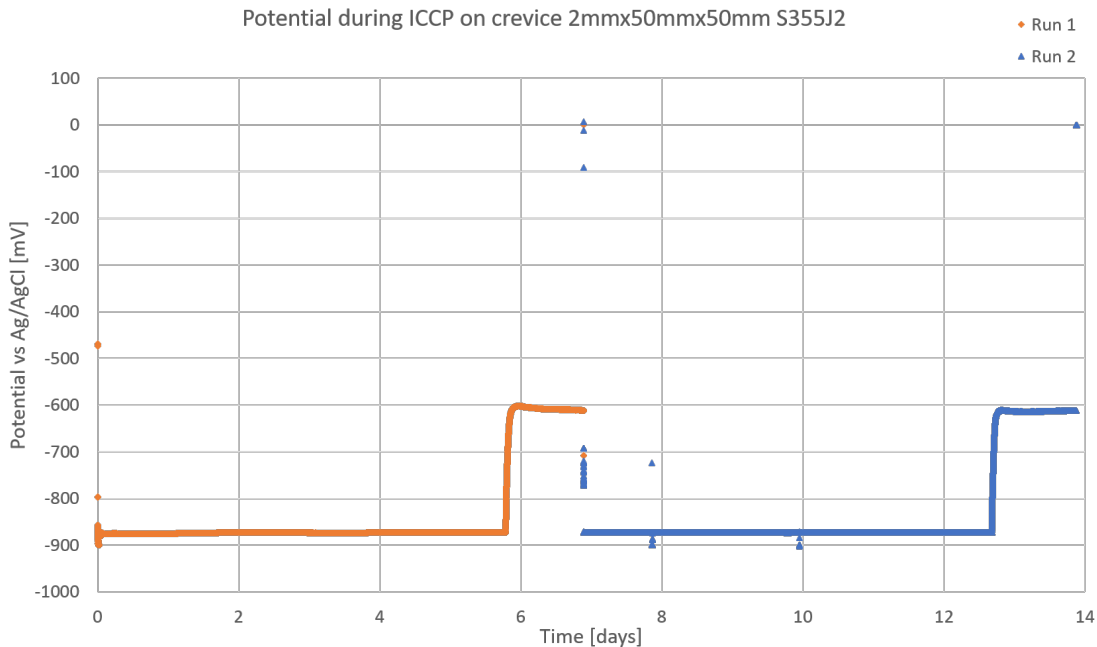


Figure 5.42: ICCP on a crevice of 2mm high, 50mm wide and 50 long.

During the test, potentials were measured of the isolated steel plate of the specimen that was not connected to the polarization cell. The data is shown in Figure 5.43. It becomes clear that, although the system is not directly connected to the ICCP cell, the isolated steel plate of the specimen is influenced by the applied current. During the test the potential is around -660 millivolts. This is a little more negative than the OCP measurements for these crevice geometries as shown in Figure 5.3. Once the ICCP system is off, after 6 days and after 13 days, the potential is climbing to a potential of -630 millivolts. This potential has also been measured in the OCP measurements of Figure 5.3 for an unpolarized specimen.

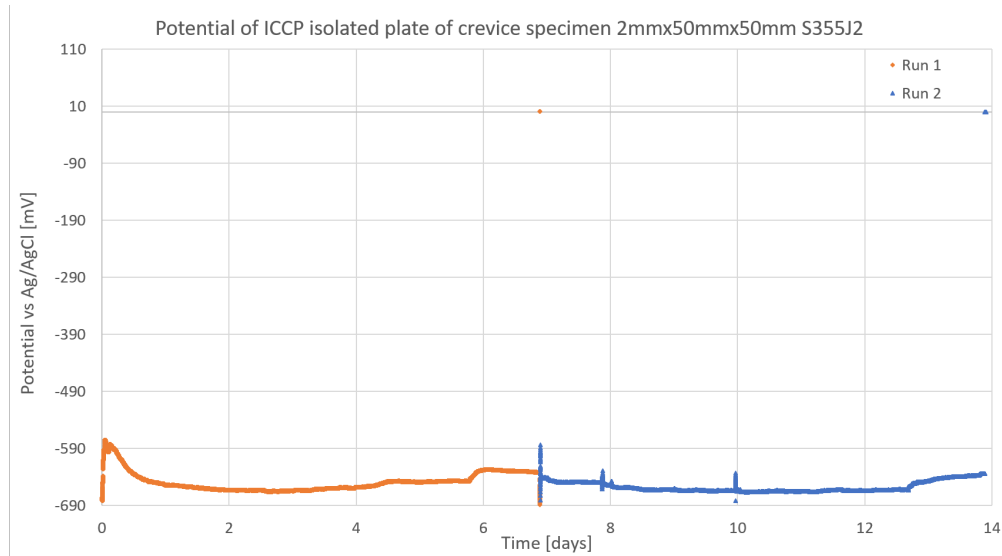


Figure 5.43: Potential of isolated steel plate during ICCP

Figure 5.44 shows the potential data obtained by testing ICCP on a crevice of 2 millimeter high, 50 millimeter wide and 150 millimeter long. Again the steel plate is perfectly polarized to the corrosion protection potential. During this test two consecutive tests were conducted. After three and a half day the first run was aborted, such that a second longer run could be started. During the short period that the ICCP was off, the corrosion potential directly climbs. This also occurs after 9 and half days, when the ICCP test is finished and the ICCP is off again. The potential goes directly to a corrosion potential of -630 millivolts which is in line with the data shown in Figure 5.9 for such specimens.

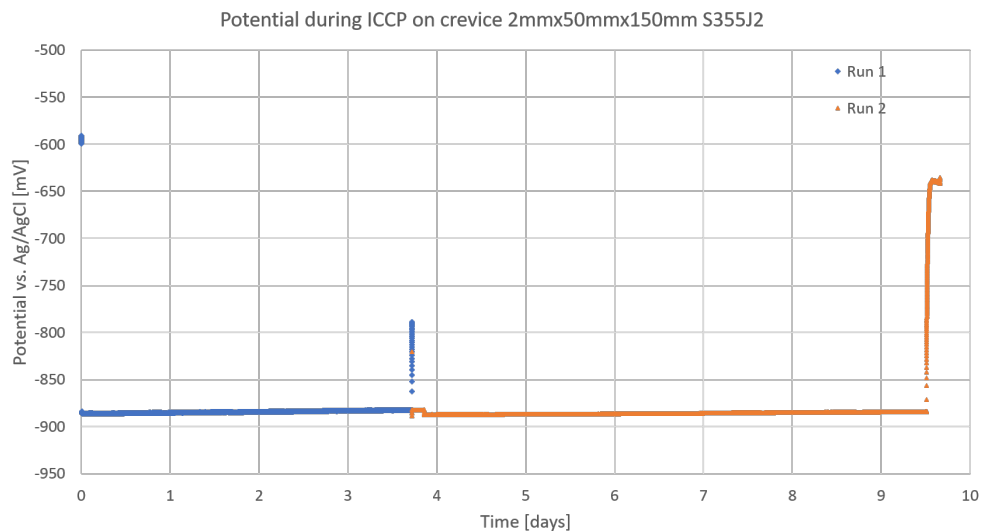


Figure 5.44: Potential on a crevice of 2mm high, 50mm wide and 150mm long.

The current that was applied by the ICCP system during the test is shown in Figure 5.45. It shows that in the first stage the PalmSens 4 applies a high current to polarize the specimen quickly and

then requires a current of 0.6 milliamps to keep the specimen polarized in the protection potential. During the second run this same average current is measured. The exposed surface was 77.5 cm^2 , this implies that a current of 0.08 A/m^2 was required to keep the specimen protected. This value is between $0.06\text{--}0.22 \text{ A/m}^2$, as is normally required for offshore submerged steel as is discussed in section 2.5.

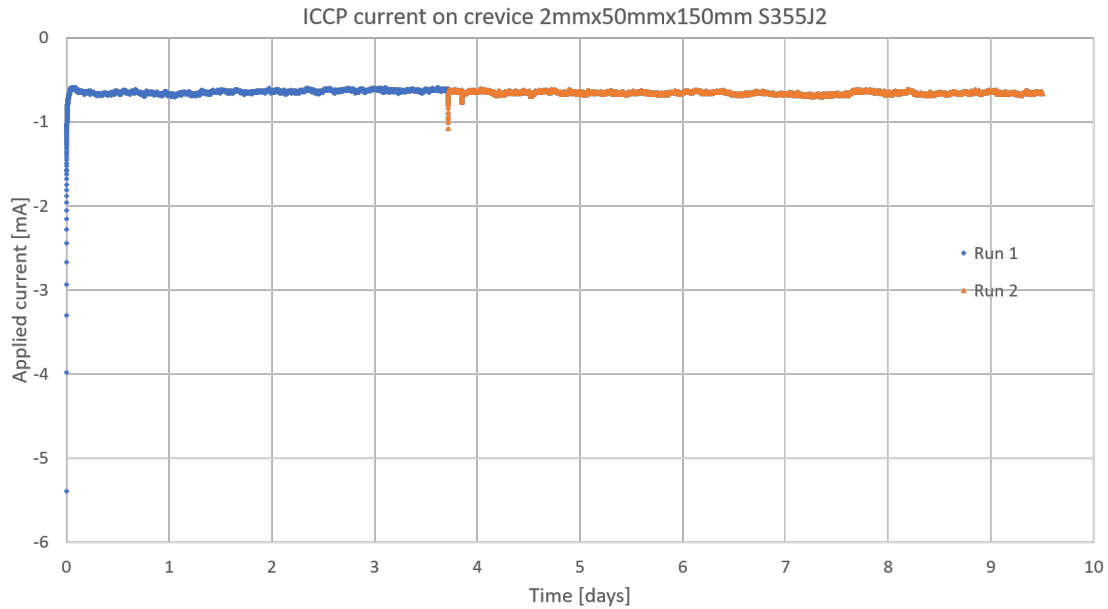


Figure 5.45: Applied current by ICCP on $2\text{mm} \times 50\text{mm} \times 150\text{mm}$ crevice

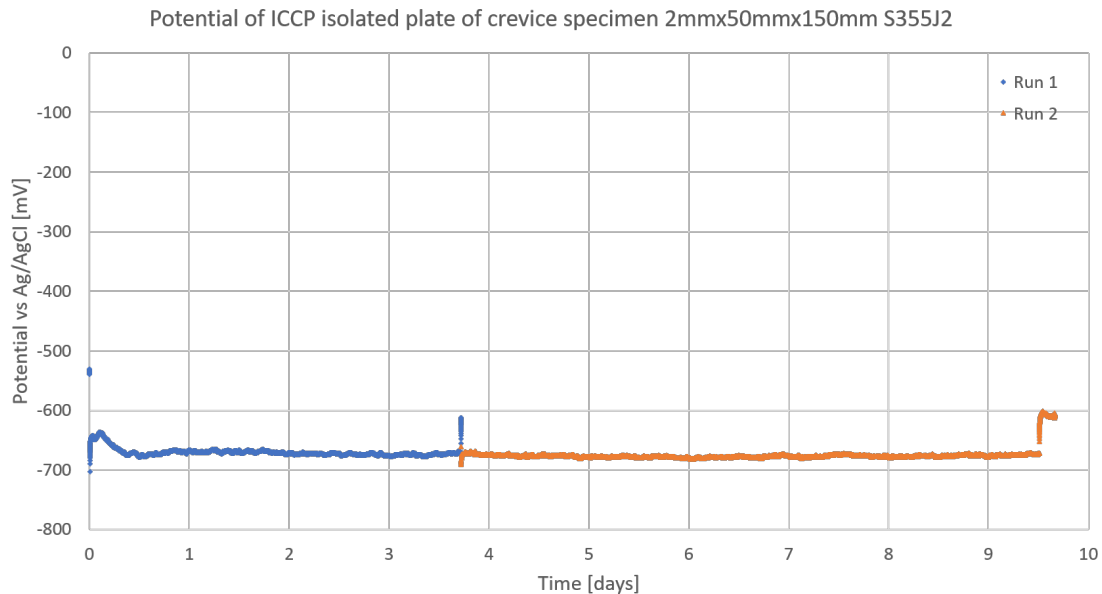


Figure 5.46: Potential of isolated steel plate during ICCP of $2\text{mm} \times 50\text{mm} \times 150\text{mm}$ crevice

The potential data of the isolated steel plate of the specimen is presented in Figure 5.46. The

potential of this steel plate is on average -680 millivolts during the period that ICCP is turned on. This is more negative than the corrosion potential that has been measured for similar crevices shown by the data in Figure 5.9. The data also shows that once ICCP is off, the potential becomes less negative such as of the data of Figure 5.9. The ICCP influences the potential and thus the corrosion behavior, although the steel plate is isolated from the ICCP system.

5.5 Conclusion

The data of the immersion test in which multiple crevice geometries have been immersed show that the test was carried out in a consistent manner and that the test is reproducible. The potential data from the reference plates show consistent results over each test batch. Therefore, it is possible to compare the results from each batch.

The potential data in combination with the visual inspection showed that more positive potentials, relative to the uniform corrosion potential, indicated crevice corrosion attack. The potential data suggest that the smaller crevices are more prone to crevice corrosion. This is logical, while depletion of oxygen in a small crevice is more likely to occur due to the smaller opening through which oxygen can be transported. The corrosion products in the crevice indicated that the oxygen content in the crevice was low, especially in the deeper parts. The red rust near the mouth of the crevice in combination with the black rust that follows indicates a differential in oxygen content in the crevice.

The corrosion rates of the specimens showed that especially the length influences the corrosion rate. It was observed that specimens which were attacked by crevice corrosion showed areas that were not attacked. This area grows for longer crevices, while the crevice corrosion remains to occur near the mouth of the crevice. The formula used for calculating corrosion rates requires to divide the weight loss by the total exposed area. Thus if the local corrosion attack does not change with increasing crevice lengths, the calculated corrosion rate will go down because of dividing the same weight loss over a bigger exposed area.

The test of crevices with a void showed similar results to the crevice corrosion test. The results indicate that the void did not influence the potentials or the corrosion rates. Non the less, for other geometries of the crevice and void this might be different.

Finally the results of the ICCP test suggest that ICCP can succesfully be applied to crevices. During period that ICCP was applied on the crevices the protection potential was obtained. The required current to obtain the protection potential was in the range of what is normally expected for offshore submerged steel. The results also showed that a plate that is isolated from the ICCP system still is influenced by the applied ICCP.

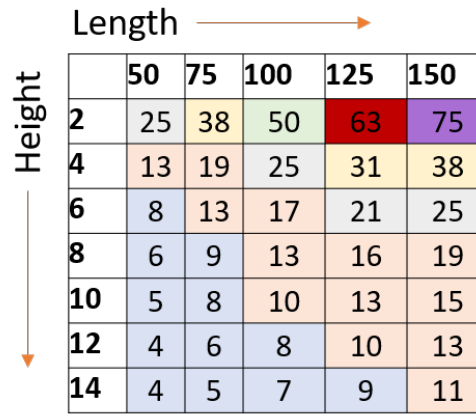
6 Discussion of the test and the results

6.1 Interpretation of the results

6.1.1 Corrosion behavior and geometry effect

As discussed in section 1.3 the focus of this research is to study corrosion behavior in the offshore submerged Slip Joint crevices. The literature study indicated that crevice corrosion is very likely to occur in such crevices and that the geometry of the crevice influences the corrosion behavior. For crevices, as found in the the Slip Joint, there is insufficient knowledge in terms of corrosion rates or corrosion behavior, therefore tests were necessary.

The conducted tests show that crevice corrosion will occur in crevices such as those present in the Slip Joint. Oxygen will deplete in the crevice causing a difference in oxygen content between the crevice and the outer environment, starting the crevice corrosion. Crevice corrosion is proven to be dependent on the crevice geometry. The relation between the corrosion behavior can be described by the scaling law, as was mentioned in section 3.1. According to the theory, L/h is assumed to be the proper scaling factor for metals with high corrosion currents such as steel in seawater. In order to check whether the scaling law theory can be applied to the results of this test, the L/h scaling factors have been calculated and distributed into five different colored groups as can be seen in Figure 6.1. The distribution is composed of groups of scaling factors between 0-10, 10-20, 20-30 and 30-40 and because the scaling factors 50, 63 and 75 did not fit into a group, these were individually used. According to the theory, these groups should show similar corrosion behavior.



	50	75	100	125	150
2	25	38	50	63	75
4	13	19	25	31	38
6	8	13	17	21	25
8	6	9	13	16	19
10	5	8	10	13	15
12	4	6	8	10	13
14	4	5	7	9	11

Figure 6.1: Scaling factor L/h and distributed groups

The average OCP measurements of crevices with the same geometry has been calculated to check whether the above individual groups show similar corrosion potentials. In Figure 6.2 the obtained values are shown including a color scale which enables to see a trend that is similar to the distribution of the scaling factor groups. The lower scaling factors show more negative corrosion potentials that are closer to the uniform corrosion potential. Specimens with a higher scaling factor show less negative corrosion potentials, which indicated local corrosion behavior.

	Length →				
Height ↓	50	75	100	125	150
2	-627	-630	-624	-621	-631
4	-642	-634	-633	-611	-642
6	-645	-647	-657	-625	-658
8	-648	-645	-653	-637	-640
10	-646	-653	-656	-634	-642
12	-652	-651	-653	-645	-635
14	-655	-655	-659	-652	-663

Figure 6.2: Average OCP of each crevice geometry, color graded

To check whether a trend of the potentials can be observed that is related to the scaling law, the average potential per group has been calculated. In Table 6.1 these averages are shown for each group as defined in Figure 6.1. The obtained values show that for higher scaling factors, less negative potentials are observed. This clearly indicates a trend for the potential measurements, the potential becomes less negative for higher scaling factors. In the previous chapter it was already observed by visual inspection that these potentials can be related to the corrosion behavior in the crevice. The less negative potentials showed more localized corrosion behavior and more negative potentials show more uniform corrosion. This was related to the length and height of the specimens. Especially the narrow crevices showed local attack, but with increasing crevice lengths the local attack was observed in less narrow crevices as well, see Figure 5.21a.

Group (see Fig. 6.1)	Range L/h	Average OCP [mV]
Blue	0-10	-651
Orange	10-20	-645
Grey	20-30	-636
Yellow	30-40	-628
Green	50	-624
Red	63	-621
Purple	75	-631

Table 6.1: Average OCP for scaling law ranges

The trend becomes visible in the plot of potential versus the scaling law, see Figure 6.3. A linear and a logarithmic trend line are fitted to the data, the corresponding formulas are shown in the figure. The linear trendline will not be suitable for higher scaling factors. For high scaling factors the OCP can become positive according to the linear scaling factor, which will not be observed for corroding steel in seawater. For low scaling factors the OCP will go to the uniform corrosion potential which were on average -670 millivolts during the test. The linear trendline however would give a potential of -652 millivolts when the scaling factor goes to zero. The logarithmic trendline does a better job for extrapolated calculations to higher or lower scaling factors. Scaling factors below 1 however can not be applied to this trendline while the natural logarithm becomes negative for these values. But if the scaling factors goes to 1, the OCP would be estimated to be -675 millivolts which is close

to the uniform corrosion potential and that is expected for these low scaling factors. If the scaling factor increases, the potential becomes more positive as well.

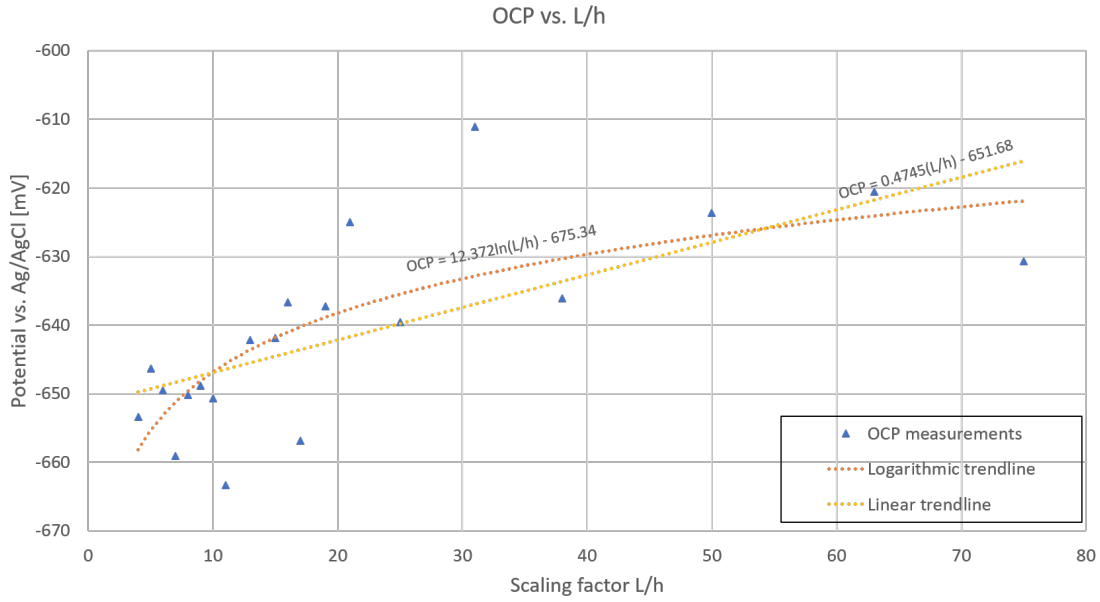


Figure 6.3: OCP versus scaling factor

6.1.2 Corrosion rates and geometry effect

In section 5.2.2 it is stated that both the crevice height and crevice length influence the corrosion rate. Narrower crevices show lower corrosion rates. This can be related to the observation that for narrower crevices the corrosion was more local as was explained in section 5.2.2. The measured corrosion rates in crevices are thus a function of, at least, length and height of the crevice. To check this trend for the scaling law, the average corrosion rate per group has been calculated. In Table 6.2 these averages are shown for each group such as defined in Figure 6.1. Scaling factors between 0 and 10 show higher corrosion rates than the rest. The other groups are showing lower corrosion rates.

Group (see Fig. 6.1)	Range L/h	Average CR [mm/y]
Blue	0-10	0.115
Orange	10-20	0.094
Grey	20-30	0.089
Yellow	30-40	0.092
Green	50	0.082
Red	63	0.100
Purple	75	0.074

Table 6.2: Average CR for scaling law ranges

To check the trend, the corrosion rate is plotted versus the scaling factor L/h , see Figure 6.4. For scaling factors in the range of 0 to 10, the corrosion rate drops rapidly for increasing values of the scaling factor. Corrosion rates of specimens with low scaling factors are close to the uniform corrosion rate. Visual inspection also showed that a lot of the specimens with a wide crevice, and thus a high scaling factor, corroded uniformly. The measured corrosion rates, for scaling factors of 10 and higher, show that the corrosion rate is drops less rapidly when the scaling factor becomes higher.

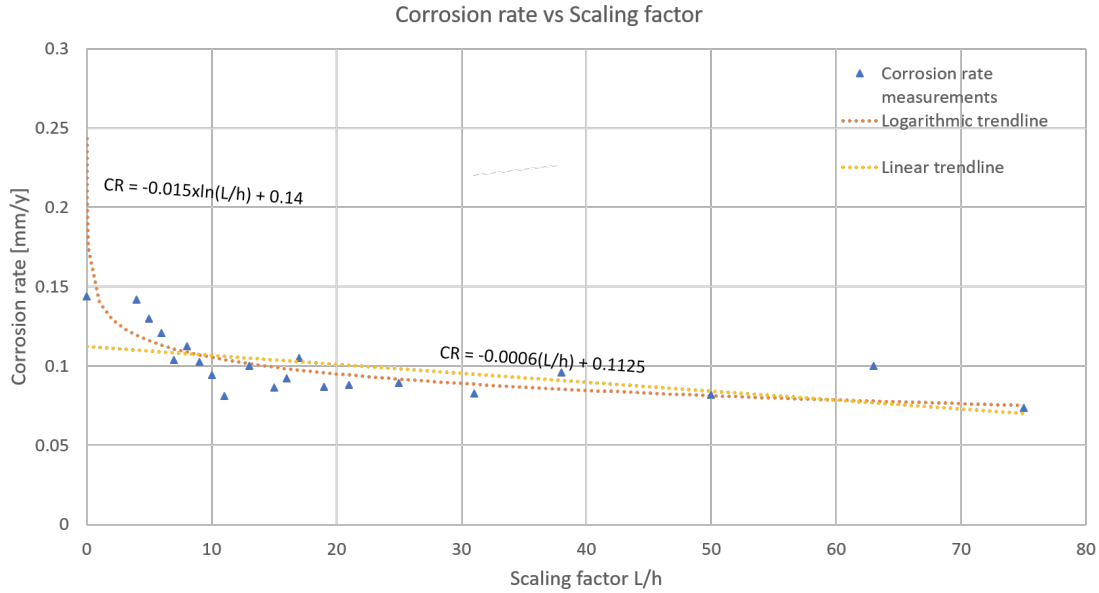


Figure 6.4: Corrosion rate versus scaling factor

A linear trendline and a logarithmic trendline are fitted to the data. The linear trendline suggests that the corrosion rate for uniform corrosion is 0.11 mm/y. This is significantly lower than the average measured uniform corrosion rate during the test, which was 0.14 mm/y. The logarithmic trendline fits better to the low scaling factors but for scaling factors going to zero the scaling law goes to infinity. In Figure 6.5 a new trendline is proposed. The trendline is fitted to data related to scaling factors above 10, in order to represent corrosion rates that are related to crevice corrosion only, and not uniform corrosion. With the corresponding formula the corrosion rate for each crevice geometry can be predicted.

In section 5.2.2 it is stated that the corrosion rates increase for increasing gap heights. The trendline of Figure 6.5 confirms the statement. In section 3.1 has been mentioned that Neena Kaylisia Anak Brum had the same conclusion after studying the geometric effect to crevice corrosion in stainless steel. The result is thus in line with previous studies.

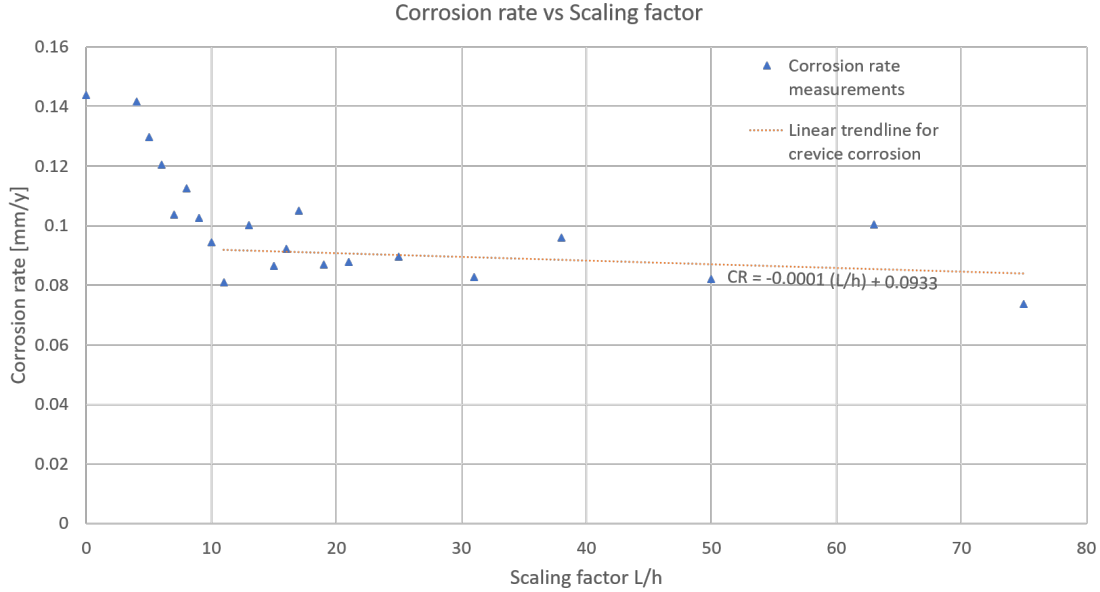


Figure 6.5: Corrosion rate versus scaling factor with a trendline for crevice corrosion

6.1.3 The influence of a void to crevice corrosion

An additional test has been carried out in which is checked what the influence is of a crevice that does not have a constant crevice height. A crevice in the Slip Joint will not have a constant crevice height. The potential measurements, that are shown in section 5.3 Figure 5.34, indicate no influence of the void. The potential measurement are similar to the potential measurements of the regular crevices. The observed corrosion rates also were not significantly different, if corrected by the uniform corrosion rates. The visual inspection showed a clear boundary in the rust formation, see Figure 5.36. Non the less a clear difference between crevices with a void and regular crevices was not found.

It can not be concluded that there is no differences for crevices with a void in general. The test was only carried out for crevices of two and four millimeters high and both with a length of 100 millimeter in front of the 50 millimeter long void. The tested crevices were sufficiently small and long that the oxygen drop inside the crevice was sufficient to have local corrosion in the front of the crevice and thus the void indeed did not influence the corrosion behavior. Based on the observation in Figure 5.36 it is likely that when a crevice is higher or shorter, the void will influence the corrosion behavior inside the crevice. The tested regular specimens, with a crevice of two and four millimeter, endorse the assumption that the corrosion only occurs in the front part of the crevice. This can be seen in Figures 5.18 and 5.21.

6.1.4 The influence of ICCP on crevice corrosion

The test in which ICCP was applied on the crevice showed that it was possible to polarize the specimen to the protection potentials. The system was able to polarize the specimen quickly and it could keep it stable in the protection potential. Furthermore the applied current was also stable

over time and was in the range of expected currents for ICCP on steel in seawater conditions. The data from the test suggest that ICCP can successfully be applied to crevices.

The potential data of the isolated steel plates shows that ICCP influences the potential of these plates, although that these plates were not directly polarized. The measured potential was more negative due to the ICCP. In the main test, the free corroding crevices showed mirrored rust patterns which is a sign of coupled corrosion behavior of both steel plates in the crevice. In Figure 6.6 an example is given. The steel plates both show a line of rust that is identical to one another. It seems that the corrosion currents in the crevice will flow in similar paths. The electric field of both plates seem to be connected in the small crevices. The electric field is the gradient of the solution potential. The solution in a small crevice will be similar to both steel plates, the solution properties will not change significantly over the short distance between both steel plates. In small crevices it is therefore possible that the electrical field is similar to both steel plates.

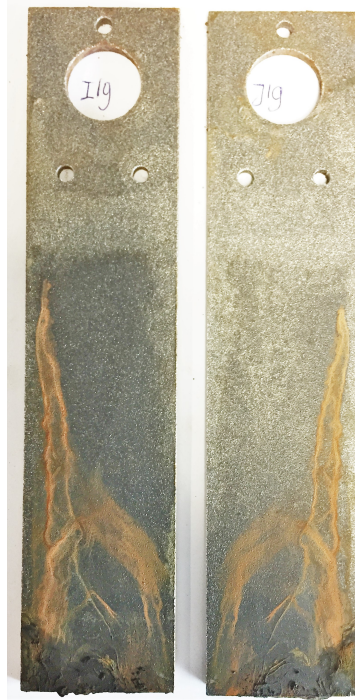


Figure 6.6: Corroded steel plate with a crevice of $2\text{mm} \times 50\text{mm} \times 150\text{mm}$ showing mirrored rust formation. Note, no ICCP was applied on these plates.

6.2 Practical appliance of results

6.2.1 Laboratory corrosion versus offshore corrosion

The obtained results can be used to optimize the Slip Joint design in relation to corrosion. However, there are some limitations to the use of these results.

First of all, the test was done in a laboratory environment which is different from the offshore environment. As mentioned in section 4.2.2 seawater temperature for the North Sea vary between 1°C and 18°C . [42] The temperature during the test was 21°C , resulting in higher corrosion rates as

discussed in section 2.2.4. The measured corrosion rates can be considered conservative relative to corrosion rates in lower temperatures.

Another difference to the corrosion in an offshore Slip Joint is the electrolyte. The sodium chloride solution that has been used in the test made the test reproducible and controllable, such that the test results can be compared to one another. The seawater environment contains biological activity that was not present in the test. As mentioned in section 2.2.5 biological activity influences corrosion behavior. For example, in crevices where oxygen is depleted the anaerobic environment can attract sulfate-reducing bacteria that actively reduce SO_4 forming a cathodic reaction that makes the oxidation of iron possible. Although that a 3.5% sodium chloride solution represent similar electrical solution resistant as seawater and will show similar corrosion behavior, the chemical compounds in seawater influences the corrosion behavior. For example, the chemical composition of seawater changes over time due to changes in temperature, exposure to sunlight and so on.

The solution in the batches were stagnant. Around an offshore applied Slip Joint the seawater will flow. Flowing seawater will increase the transport of oxygen towards a corroding steel surface. The increase in oxygen transport will change the corrosion behavior. Corrosion rates will increase due to the flowing water, especially in the first period of the corrosion process, because rust formation will block the flowing water after a while. The depletion of oxygen, that is required for crevice corrosion to occur, will also be influenced. There are two possible scenarios:

1. Seawater flows around the Slip Joint, which increases the oxygen transport near the mouth of the crevice. This results in a shift of the location of the crevice corrosion attack deeper into the crevice, because the required oxygen drop will occur deeper into the crevice. (Compared to the test observations);
2. Seawater flows trough the crevice of the Slip Joint, which will make that crevice corrosion becomes unlikely to occur. Because oxygen is replenished in the crevice by the flowing water, the required oxygen drop will not occur and uniform corrosion will occur.

On top of the transport of oxygen by flowing seawater it will transport the corrosion products from the crevice. The passivizing effect of the corrosion products will reduce if seawater is flowing trough the crevice. Corrosion rates in the crevice will therefore increase. Furthermore, loads on the foundation will cause the matching conical sections of the Slip Joint to move relatively to one another. The movements will break up the rust in the crevice and thus the accumulation of rust inside the crevice will be less compared to the tested crevices.

A surface treatment of the steel specimens was necessary to ensure that each specimen had the same surface conditions, which is required for obtaining reproducible and comparable results. Offshore applied Slip Joints are not exposed to such surface treatments.

6.2.2 Empirical model to estimate offshore crevice corrosion rates

The test clearly shows that crevices in the Slip Joint can develop local corrosion attack. This means that during the design process it should not be left disregarded. Local corrosion attack will influence the fatigue lifetime of the Slip Joint. It is however not advised to use the trendline given in Figure 6.5 for design purposes, because the given trendline is fitted to the average crevice corrosion rate. For design purposes, the standard deviation of the corrosion rates should be taken

into account. In section 4.1.3 was mentioned that corrosion rates of uniform corroded duplicate test specimens should be in a $\pm 10\%$ margin for uniform corrosion. As shown in Table 6.3, the uniform corroded reference plates meet this 10% margin. The corrosion rates of the specimens with a crevice showed bigger differences between the duplicate test specimens. For corrosion rates of the same crevice geometries differences up to 40% have been measured. Using the results of the test for design purposes requires thus to use a safety margin to the measured corrosion rates.

Batch	Compared specimens	Difference Corrosion rate [%]
Batch 1	R1 vs R2	-4.0
	R2 vs R3	-1.8
	R1 vs R3	6.0
Batch 2	R4 vs R5	-8.0
	R5 vs R6	-0.3
	R4 vs R6	9.0
Batch 3	R7 vs R8	2.2
	R8 vs R9	5.3
	R7 vs R9	-7.0
Batch 4	R10 vs R11	2.2
	R11 vs R12	5.9
	R10 vs R12	-7.6
Batch 5	R13 vs R14	-3.1
	R14 vs R15	2.6
	R13 vs R15	0.5

Table 6.3: Corrosion rate differences in percentages

Based on the results, a linear model is formulated which serves to predict crevice corrosion rates with the help of the scaling factor. The process is illustrated by Figure 6.7. Assumed that the corrosion rates are normal distributed around the mean, the standard deviation is used to calculate the upper bound of the corrosion rates in a 98% confidence interval. This was done by adding two times the standard deviation to the measured average corrosion rate. The result is shown by the orange dots in the Figure. This means that in practice corrosion rates will be lower in 98%. The corresponding trendline is used to check the trend of the adapted data. The trendline is then shifted such that the highest obtained value in the confidence interval is in the trendline. This gives a conservative estimation for the corrosion rate with:

$$CR_{crevice}(L/h) = -0.0002 \times \frac{L}{h} + 0.1387 \quad (6.1)$$

in which $\frac{L}{h}$ is the scaling factor. The model is conservative with regard to the measured corrosion rates. The model estimates the corrosion rates on average 57% higher than the average measured corrosion rates.

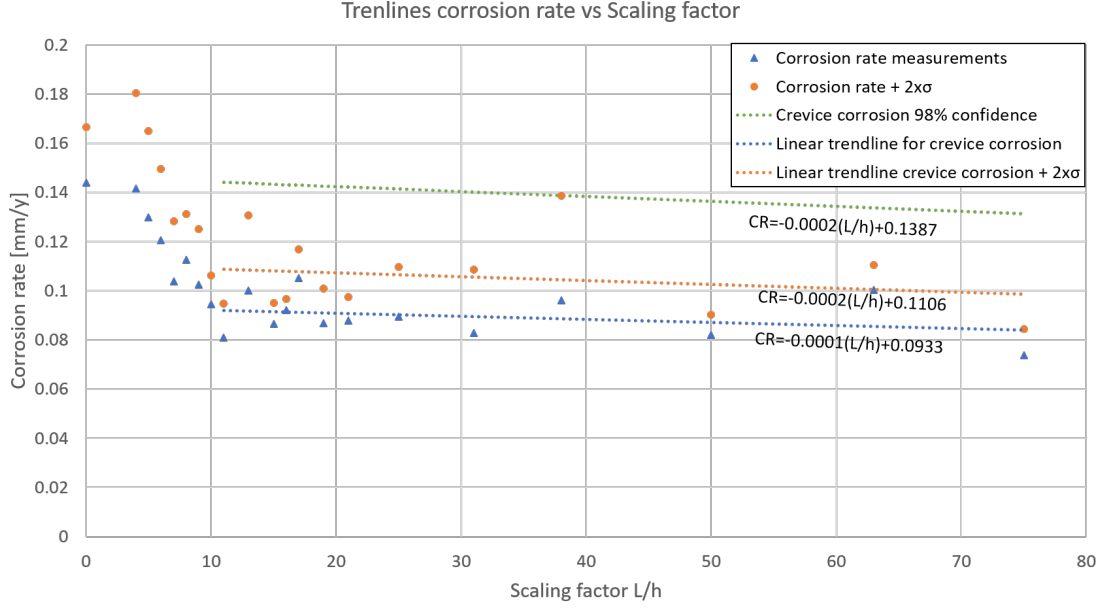


Figure 6.7: Corrosion rate estimation advised for design purposes based on trendlines

A similar approach can be used for calculating the expected uniform corrosion rate for S355J2 steel plates. With an average of 0.14 millimeter per year and a standard deviation of 0.011 millimeter per year, the upperbound of the 98% confidence interval would give a corrosion rate of 0.17 millimeter per year. This result is in line with the corrosion rates that Reinhart calculated for first year steel corrosion as is discussed in section 2.3.1. DNVGL states that a corrosion rate of 0.10 millimeter per year should be used in designing for corrosion allowance. Using a value of 0.17 millimeter per year thus seems to be over conservative. The differences are due to the fact that the measured corrosion rates are related to early corrosion of steel, these are much higher than the corrosion rates that are observed on specimens that are immersed for a longer period as was shown in Figure 2.8. Furthermore, as discussed in section 6.2.1, the corrosion rates of the laboratory test will be different to the corrosion rates that will be observed in offshore Slip Joints due to differences in the conditions.

The model of equation 6.1 has to be adjusted to account for different environmental conditions by using uniform corrosion rates. The corrosion rate of the uniform corroded reference plates was on average 44% higher than the crevice corrosion rate. Assuming that this will be the case in other environments as well, the model can be improved by using the uniform corrosion rates that are used in design calculations, such as recommended by DNVGL-RP-0416 for example.[1] The improved model is then given by:

$$CR_{crevice}\left(\frac{L}{h}\right) = -0.0002 \times \frac{L}{h} + CR_{uniform} + 0.0024 \quad (6.2)$$

in which $CR_{uniform}$ is the design uniform corrosion rate. When the uniform corrosion rate in an environment is known, the corrosion rate of a crevice with known geometry can be estimated with this model. For example, for a measured uniform corrosion rate of 0.10 millimeter per year, the corrosion rate in a crevice with a length of 90 millimeter and height of 3 millimeter is estimated to be: $-0.0002 \times \frac{90}{3} + 0.1 + 0.0024 = 0.0964 \text{ mm/y}$ While uniform corrosion was observed for specimens

with a scaling factor lower than 10, the uniform corrosion rate will apply for these crevices and the model should thus be used only for scaling factors higher then 10. In Figure 6.8 an example of estimations is given for uniform corrosion rates of 0.14 millimeter per year and 0.10 millimeter per year is given.

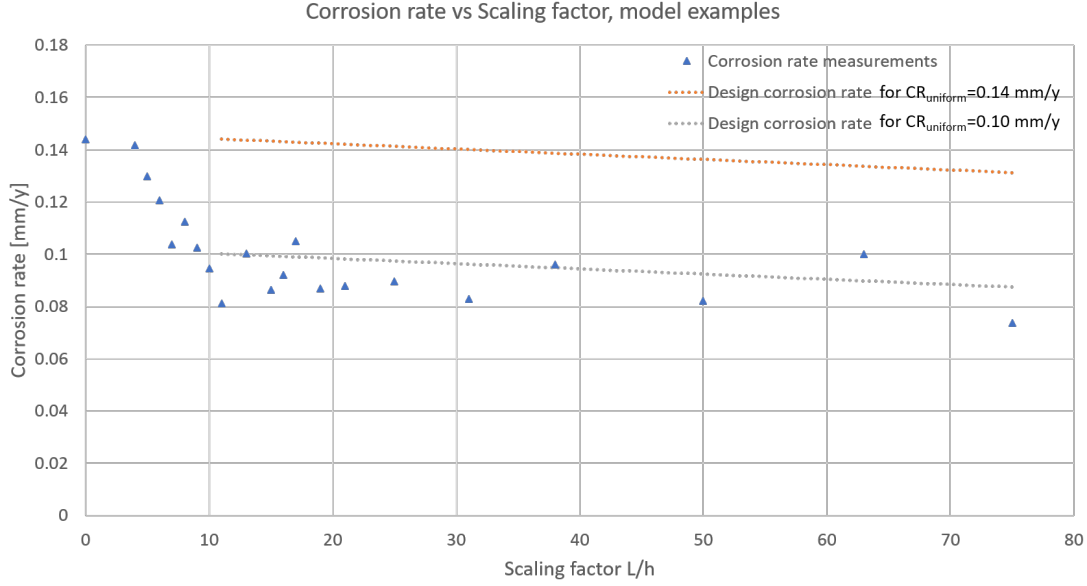


Figure 6.8: Example of resulting corrosion rates estimations from the empirical model for uniform corrosion rates of 0.14mm/y and 0.10mm/y

As was done for the crevices with a void the corrosion rates can be normalized by dividing the corrosion rates by the uniform corrosion rates of the reference specimens from each batch. In Figure 6.9 the influence of the normalized corrosion rates are shown. The color grading shows a similar result as was presented by Figure 5.32.

Influence crevice length and height on normalized corrosion rates

		Length →				
Height ↓		50	75	100	125	150
	2	0.58	0.79	0.62	0.72	0.53
	4	0.63	0.65	0.69	0.59	0.57
	6	0.65	0.85	0.79	0.63	0.58
	8	0.74	0.79	0.74	0.66	0.58
	10	0.79	0.79	0.71	0.65	0.62
	12	0.82	0.72	0.88	0.68	0.62
	14	0.91	0.69	0.78	0.66	0.58

Figure 6.9: Influence crevice height and length on normalized corrosion rates

To see whether this influences the empirical model, the same approach is used to formulate an adapted model. A trendline is fitted to the average data, then this line is shifted 57% higher to obtain the same safety as was done for the unnormalized data, see Figure 6.10

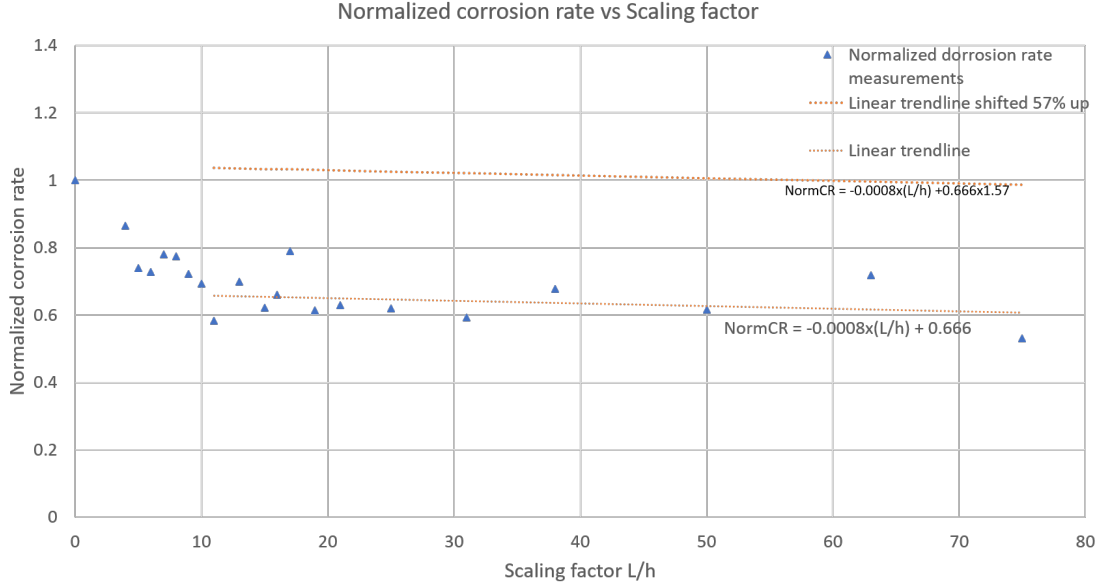


Figure 6.10: Normalized corrosion rate versus scaling factor with trendlines

The obtained trendline does not have to be adjusted for different uniform corrosion rates, because it is already normalized. The empirical model thus becomes:

$$CR_{crevice}\left(\frac{L}{h}\right) = -0.0008 \times \frac{L}{h} \times CR_{uniform} + 1.05 \times CR_{uniform} \quad (6.3)$$

The model has been compared to the model of equation 6.2. The corrosion rate drops less rapidly for increasing scaling factors if the normalized data is used. In Figure 6.11 estimations with both models are given for uniform corrosion rates of 0.14 millimeter per year and 0.10 millimeter per year.

As can be seen in Figure 6.10, the normalized model is more conservative. Normalization by dividing through the uniform corrosion rates is risky, because the obtained uniform corrosion rates also show scatter. This scatter can be caused by multiple aspects that are unrelated to the corrosion in the crevice. Furthermore, the randomness of the specimens with a crevice is already taken into account. Therefore, it is advised to use the model given by equation 6.2.

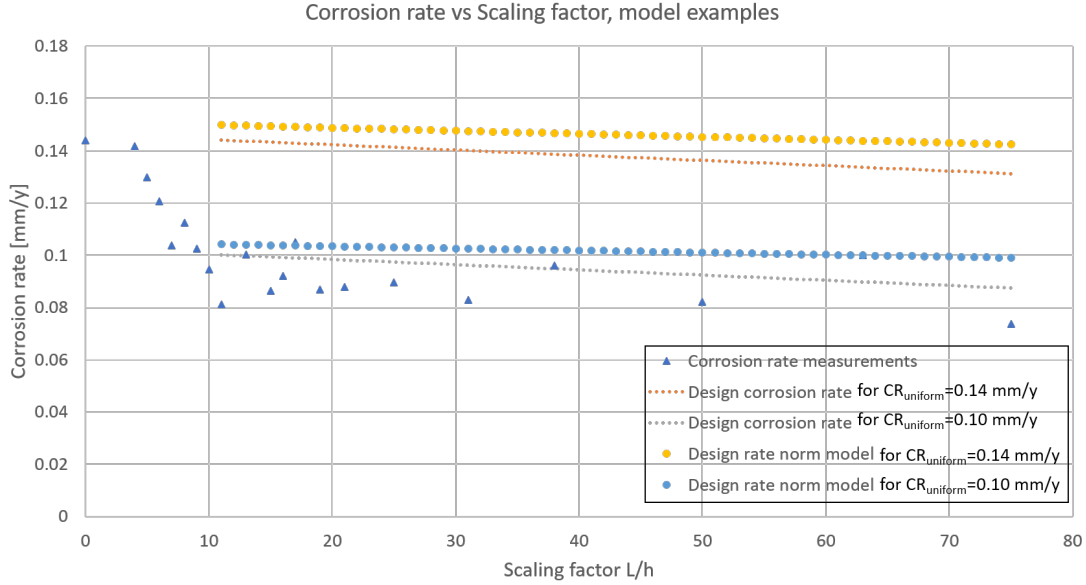


Figure 6.11: Example of resulting corrosion rates estimations from the empirical models for uniform corrosion rates of 0.14mm/y and 0.10mm/y

6.2.3 Implications of the results to the Slip Joint design

Because local corrosion is observed in the test it is necessary to take this into account in the design of the Slip Joint. The measured corrosion rates are lower compared to uniform corrosion rates, but the attack is local. Local loss of thickness will have an effect on the fatigue life time of the Slip Joint. As the fatigue life time is reduced by corrosion, it is crucial to fully understand its influence to be able to design the Slip Joint connection.

Also, it should not be forgotten that the calculated corrosion rates are an average over the exposed areas during the tests. Local corrosion rates can be higher and thus cause a local loss of thickness that is higher than the uniform loss of thickness. For the calculations of the corrosion rate, the weight loss has been divided by the full exposed area. However, in the crevices there are areas that become passive, for example in Figure 5.18. (This is also described by Lee et al. [23].) Especially the narrow crevices showed only a small area with rust formation, indicating local attack. For the narrow crevices, the crevice corrosion occurs only in the first one to two centimeter of the crevice. Because the area of attack is much smaller than the exposed area, the corrosion rate will be higher on the locally attacked areas. The attacked area is changing over time, as described in section 3.1. The location of attack will move, over time, towards the mouth. It is therefore, difficult to estimate the corrosion rates that occur on the local attacked areas. These corrosion rates will be higher than the measured corrosion rates. In order to give an idea of a possible local corrosion rate, an estimation is given for the specimen in Figure 5.18b. The roughly estimated area of attack for this given specimen (one plate) is 10 cm². The weight loss of this plate was 1.041 grams. This results in an estimated corrosion rate of:

$$CorrosionRate = (8.76 * 10^4 \times 1.041) / (10 \times 1536 \times 7.85) = 0.76[mm/y] \quad (6.4)$$

Compared to the uniform corrosion rate this is a high corrosion rate, it is five times higher. It is approximately eight times higher compared to the calculated corrosion rate of 0.09 millimeter per year for this specimen.

It is advised to take mitigating measures to prevent such corrosion in the Slip Joint. The carried out ICCP test showed promising results, but also other mitigating measures can be applied. For example, closing the edges of the Slip Joint will lock up the local environment from the external environment. The electrical circuit with the external environment, required for crevice corrosion, is then broken. The proposed model can be used to calculate the loss of thickness if mitigating measures are failing.

6.3 Improvements and further research

To optimize the design, there are a number of opportunities. These can be broadly divided into additional tests required for relating the obtained data to offshore corrosion in crevices, and improvements of the carried out test to get more detailed information the corrosion behavior in steel crevices with large scaling factors.

6.3.1 Additional tests

The Tafel plots of S355J2, in section 4.1.1, indicated slightly higher corrosion rates compared to S355ML. In order to optimize designs of structures of S355ML, corrosion rates of S355ML should be examined to a greater extend. Corrosion rates from weight loss measurements, from a immersion period of 60 days in NaCl, of uniform and crevice corrosion of S355ML specimens can be used to check whether the proposed model in section 6.2.2 is applicable to S355ML.

As already has been mentioned flowing water will influence crevice corrosion. To check the influence of flowing water, this could be tested by submerging the specimens in a flowing solution. Crevice corrosion should be tested at multiple flow velocities and flow directions relative to the crevice. Additionally the influence of a flow of water through the crevice should be checked, this will increase transport of oxygen into the crevice. Resupplied oxygen in the crevice will change the corrosion behavior in the crevice.

As mentioned in 6.2.1, the movement of the conical sections of the Slip Joint will cause rust layers to break and thus will influence the corrosion behavior in the Slip Joint. The influence of the break down of the rust layer should be tested. Because a rust layer has a passivizing effect, the break down of the layer will cause the corrosion rates to increase.

The results of the ICCP test suggest that ICCP was successfully applied to protect the crevice against corrosion. The test showed a stable protection potential can be applied to the crevice. Due to the relatively short period of the test corrosion, reliable corrosion rate measurements could not be carried out, see section 4.3.2. Corrosion rates of a specimen with ICCP protection will show the influence of ICCP and its level of protection. By applying ICCP for a longer period, for example 60 days such as the immersion test, it is possible to do weight loss measurements that are reliable. A comparison of the corrosion rates of crevices with and without ICCP can be carried out in order to check the influence of ICCP on the corrosion rates of a crevice. Furthermore, ICCP was tested on only two different specimens and two different crevices. ICCP should also be tested for other crevice sizes and the sample size should be bigger to get reliable data.

6.3.2 Improvements on the test set-up

The immersion tests showed that local corrosion can occur in crevices of the Slip Joint and corrosion rates in these crevices were obtained. As discussed in section 5.2.2 the fully exposed area of the crevice was used to calculate corrosion rates. The obtained value could therefore be considered as an average of the full exposed area. Locally the corrosion rates have been higher. As discussed in section 6.2.3, correcting for this effect is difficult. Unfortunately there is no literature available in which a method for such correction is formulated.

A possibility would be to use a specimen assembly such as proposed in Figure 6.12. By embedding smaller steel samples into a plastic it is possible to check the corrosion rate of multiple sections in the crevice. In the case of the example in the figure, six different corrosion rates can be obtained. The six embedded specimens will have to be electrically connected, such that a current flow is still possible. This is required for crevice corrosion, because in a crevice there is a net current from the inside of the crevice towards the mouth of the crevice. The plate can again be assembled such as described in section 4.1.2. By doing weight measurements of each of the embedded steel samples the corrosion rate of each sample can be calculated. Still local corrosion rates on these individual samples can be different from the average of each sample, but the estimation will be improved.

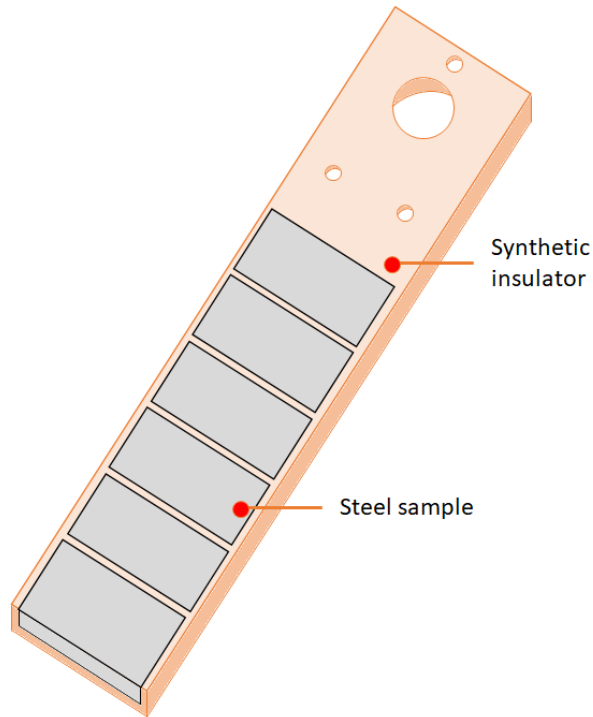


Figure 6.12: Specimen with multiple sections of steel

During the immersion test OCP measurements were carried out in order to track the corrosion behavior over time of each specimen. In order to monitor crevice corrosion in the Slip Joint there are other measurement methods available that are more feasible to use in offshore Slip Joints. As an example, one could use pH measurements to check the acidity of the crevice or use an oxygen meter to check oxygen concentrations in crevices. By checking the pH and oxygen content during the immersion test of crevices it is possible to measure the critical pH and oxygen content for which

crevice corrosion is occurring. Furthermore, the data can be used to monitor the crevices in a Slip Joint.

As a result of the geometries that have been tested, the test of the specimens with a void showed no significant differences. Different crevice and void geometries will likely show that a void will influence the corrosion behavior. Testing wider crevices or less long crevices relative to the void will make the difference, because the location of attack of crevice corrosion will move deeper into the crevice. The required crevice environment will then be influenced by the void.

7 Research conclusion and recommendations

This research has searched for an answer to the question: 'What corrosion behavior can be expected in offshore submerged Slip Joint crevices?' To be able to answer this question, a test was designed and was carried out. The obtained results have been analyzed and presented.

7.1 Conclusion of the test design

In literature was found that there is only little known about crevice corrosion behavior in steel crevices that are relatively large. Test methods to study corrosion in these crevices were not readily available. Therefore, an experiment was designed that would test the corrosion behavior in crevices in relevant gap heights and lengths. Multiple trial tests have been carried out in order to optimize the test method. The result was an experiment that proved to be able to qualitatively and quantitatively determine the corrosion behavior of the tested crevices with large scaling factors such as found in the Slip Joint.

The designed test method is preferred over alternative methods, as mass loss measurements from immersion tests provides valuable corrosion rate estimations. The quality and reliability was proved by the reproducibility between each batch. The potential data and the corrosion rates, especially of the uniform corrosion rates, showed a relatively small standard deviation between each single test batch. Thereby showing that the test method proves to generate reliable results such that trends can be observed.

The method is flexible for testing other parameters, such as testing ICCP on the specimens. Only a few adaptations were necessary to test specimens with ICCP. As a result it is possible to compare test results of the different tests. Another possibility is to change the test environment but still use the method of assembling crevice specimens. These tests can provide insight in the influence of environments.

Stable test conditions are required to get accurate and reproducible results. These required conditions have been established in the design process of the test. For example the immersion period, the method for controlling the test solution and the temperature are formulated. On the other hand, the laboratory conditions such as the controlled temperature and the controlled sodium chloride solution will limit the applicability of the results. To a certain extend it is possible to relate the results of the laboratory test to the offshore Slip Joint environment.

7.2 Conclusion of the results

In total 260 steel plates have been tested by an immersion test in order to research the corrosion behavior in 37 different crevice geometries. Additionally an ICCP test is carried out on specimens with a crevice. During the immersion test, potentials of the specimens have been measured and after the immersion period weight losses have been measured, furthermore the test specimens have been visually inspected on their corrosive behavior. The results show that local corrosion attack in the crevices will occur and that the geometry of the crevice will influence the corrosion behavior.

The potential data in combination with the visual inspection of the tested specimens indicated that local corrosion attack will give more positive corrosion potentials relative to uniform corrosion potentials. Furthermore, the potential data indicates that crevice corrosion occurs, and is stable,

in the smaller crevices. This observation was confirmed by the visual inspection of the corroded specimens. The black corrosion products on the tested specimens also indicated less oxygen content in the deeper parts of the crevice. Red rust, that is being formed at areas that have access to oxygen, was found more near the mouth of the crevices. These observations show that a difference in oxygen concentration was developed.

From the measured weight losses, corrosion rates were calculated. A trend of decreasing corrosion rates for increasing crevice lengths and decreasing crevice heights was observed. This trend has been further investigated with the help of the scaling law which describes the relation between the geometry of the crevice and the corrosion behavior. Although the scaling law has been investigated for other metals and for smaller crevice geometries in other studies, the results show that the scaling law is also applicable for the crevices in a steel structure with relatively large geometries.

In order to check the influence of crevices which are not continuous and have a certain void, a test has been carried out with specimens that contained a void at the back of the crevice. The results showed no significant difference to regular crevices. The tested specimens, however, had relatively long and narrow crevices such that the corrosion only took place in the front of the crevice and so the corrosion process did not seem to get influenced by the void. It is expected that for shorter and less narrow crevices the corrosion will get influenced by the void.

A model has been created, discussed in section 6.2.2, which can be used to estimate corrosion rates in crevices for design purposes. The developed model takes into account that an environment and the steel properties will influence the corrosion rate by requiring the uniform corrosion rate of the metal in the environment as input. If the uniform corrosion rate of a metal in an environment is known and the crevice geometry is known, the corrosion rate in the crevice can be estimated. Although that the empirical model has these properties, there are still some limitations. The crevice of the offshore Slip Joint will be exposed to environmental conditions that were not tested. The limitations are identified in section 6.2 and require some additional tests that also have been identified.

Finally, a test has been carried out to check the influence of ICCP on crevice. The results are very promising, since the ICCP system was able to maintain the protection potential during the full test period. Furthermore, the current was in a range that can be expected for offshore corroding steel. Therefore, it is advised that ICCP should be applied on a test specimens for a longer period, such as 60 days, in order to check for the influence on the weight loss. Only two crevice geometries were tested. Thus, in order to be sure that ICCP works for all possible geometries in the Slip Joint, multiple crevice geometries have to be tested.

In short, the test results show that the corrosion behavior that can be expected in the Slip Joint is either uniform corrosion or local crevice corrosion which is dependent on the geometry. The corresponding corrosion rates are dependent on the geometry and can be estimated with a model. By creating a test method to research these crevices and by obtaining a data-set this research contributed to the study of crevice corrosion in steel crevices. In order to further explore the corrosion behavior in crevices between steel plates, there is still some research required.

7.3 Crevice corrosion research recommendations

The conducted tests showed that localized corrosion can be observed in large crevices. The test however could not be used to identify the specific local corrosion rates, because the corrosion rate

is by definition an average of the exposed area. To further understand to which extend crevice corrosion affects the integrity of a structure, it is recommended to investigate the local corrosion rates. Thereby, the edge of the steel plates can influence the corrosion behavior through the so called edge effect. With the help of local mass losses, the edge effect can be analyzed as well.

It is also recommended to investigate the influence of certain environmental aspects on the corrosion in the crevice, such as the influence of a flowing solution. Flowing water will increase the transport of oxygen and can thus influence the corrosion behavior in the crevice. Additionally biological activity in the crevice should be researched. Biological activity can influence the corrosion behavior by, for example, anaerobic bacteria that can take part in corrosion reactions.

To get more insight in the development of crevice corrosion in large crevices, the changes of the solution in the crevice over time should be investigated. By investigating the pH or oxygen content and correlating the obtained data with the observed corrosion behavior, it becomes possible to detect crevice corrosion from such measurements. Once it is possible to correlate crevice corrosion with the crevice solution characteristics, it becomes possible to use these measurement techniques to monitor offshore Slip Joint crevices, or other crevices, on crevice corrosion. Besides the opportunities for inspection, such tests can also be used to investigate the incubation time of corrosion in these crevices.

7.4 Slip Joint design recommendations

The local corrosion occurrences that are expected to occur in the Slip Joint should be taken into account during the design process of the Slip Joint, because local loss of thickness will influence the structural integrity. Especially in the fatigue limit state design this local effect will cause problems. An estimation of the thickness loss over the lifetime of the structure can be done with the help of the proposed model. Because it is observed that in crevices the corrosion attack was sometimes concentrated on local areas in the crevice, the influence of the estimated loss of thickness at such local area on a structure should be investigated.

In order to improve the prediction of corrosion behavior in the Slip Joint it is advised to further investigate the structural behavior of the Slip Joint. First of all, movements of the Slip Joint cones relatively to one another will influence the corrosion by a possible pumping effect and it will disrupt growing rust layers. When such behavior is known, it is easier to predict the corrosion behavior in the Slip Joint and tests can be designed to investigate the corrosion under these conditions.

Finally, ICCP systems are commonly used to protect monopiles against corrosion and the test of ICCP on specimens with a crevice showed promising results. Therefore, it is advised to further investigate whether the ICCP system that is used to protect the monopiles can be extended to protect the Slip Joint as well. The crevices in the Slip Joint can be longer than the tested crevices and thus the ICCP might only be effective at the outskirts of the Slip Joint. Non the less, this could prove to be effective, while the corrosion attack was especially observed at these locations. Possible other mitigating measures should focus on either protecting the steel in the crevice from the environmental directly, by a coating for example, or lock up the crevice environment from the external environment. If ICCP is not effective, it is thus still advised to search for possible mitigating measures, because local corrosion attack is very likely to occur in the crevices of the Slip Joint.

8 Bibliography

References

- [1] DNV GL, “Recommended Practice - Corrosion Protection for wind turbines,” p. 31, 2016. [Online]. Available: <http://www.dnvgl.com>
- [2] L. R. Hilbert, A. R. Black, F. Andersen, and T. Mathiesen, “Inspection and monitoring of corrosion inside monopile foundations for offshore wind turbines,” in *European Corrosion Congress 2011*, Stockholm, 2011, pp. 2187–2201.
- [3] J. Van Der Tempel and B. Lutje Schipholt, “The Slip Joint connection - Alternative connection between pile and tower,” DOWEC, Tech. Rep., 2003.
- [4] R. Singh, *Corrosion Control for Offshore Structures*, 1st ed. Oxford: Elsevier, 2014.
- [5] DNV GL, “Fabrication and testing of offshore structures,” 2017.
- [6] B. Davison and G. W. Owens, *Steel Designers’ Manual: The Steel Construction Institute: Sixth Edition*, 2008.
- [7] R. W. Revie and H. H. Uhlig, *Corrosion and Corrosion Control*. JOHN WILEY & SONS, INC., 2008.
- [8] B. N. Popov, *CORROSION ENGINEERING Principles and Solved Problems*, 1st ed. Columbia: Elsevier, 2015.
- [9] P. Gellings, *Inleiding tot Corrosie en Corrosiebestrijding*, 2nd ed. PPI Enschede, 2006.
- [10] D. A. Jones, *Principles and Protection of Corrosion*, 2nd ed. Prentice hall, 1996.
- [11] S. Paul, “Modeling to Study the Effect of Environmental Parameters on Corrosion of Mild Steel in Seawater Using Neural Network,” *ISRN Metallurgy*, vol. 2012, pp. 1–6, 1 2012.
- [12] T. Vance, “Oil and Gas Biofouling.” [Online]. Available: <http://biofoulingcorrosion.co.uk/Services-for/Oil-Gas>
- [13] P. R. Roberge, *Corrosion Engineering : Principles and Practice*. McGraw-Hill, 2008.
- [14] X. Zheng, “A novel model for crevice corrosion of lap joints,” *Corrosion*, vol. 57, no. 7, pp. 634–642, 2001.
- [15] J. H. Heiser, “Corrosion of Barrier Materials in Seawater Environments,” Environmental and Waste Technology Center Department of Advanced Technology, New York, Tech. Rep., 1995.
- [16] M. Raunio, “Basic approaches and goals for crevice corrosion modelling,” p. 50, 2015. [Online]. Available: <http://www.vtt.fi/inf/julkaisut/muut/2015/VTT-R-02078-15.pdf>
- [17] H. W. Pickering, “THE SIGNIFICANCE OF THE LOCAL ELECTRODE POTENTIAL WITHIN PITS, CREVICES AND CRACKS*,” Tech. Rep. 3, 1989.
- [18] ASTM International, “G59: Standard Test Method for Conducting Potentiodynamic Polarization Resistance Measurements 1,” p. 4, 2014. [Online]. Available: www.astm.org,

- [19] —, “G1: Standard Practice for Preparing, Cleaning, and Evaluating Corrosion Test Specimens,” p. 8, 1999.
- [20] R. Baxter and J. Britton, “Offshore Cathodic Protection 101: What it is and how it works,” *Deepwater Corrosion Services Inc.*, 2013.
- [21] DNVGL, “RP-B401 Cathodic protection design,” 2017. [Online]. Available: <http://www.dnvgl.com>,
- [22] M. Funahashi, “SELECTION GUIDELINES FOR USING CATHODIC PROTECTION SYSTEMS ON REINFORCED AND PRESTRESSED CONCRETE STRUCTURES,” Tech. Rep. [Online]. Available: www.mui-int.com
- [23] J. S. Lee, M. L. Reed, and R. G. Kelly, “Combining Rigorously Controlled Crevice Geometry and Computational Modeling for Study of Crevice Corrosion Scaling Factors,” *Journal of The Electrochemical Society*, vol. 151, no. 7, pp. 423–433, 2004.
- [24] P. Marcus, *Corrosion Mechanisms in Theory and Practice*, Philippe Marcus, Ed. CRC Press, 1995.
- [25] L. A. Dejong, *Investigations of Crevice Corrosion Scaling Laws Using Microfabrication Techniques and Modelingn (MSc Thesis)*. University of Virginia, 1999.
- [26] N. K. A. Brum, *Study of Geometric Effect to the Crevice Corrosion Behaviour in Stainless Steel (BSc Thesis)*. University Malaysia Pahang, 2013.
- [27] R. E. Melchers and R. Jeffrey, “Early corrosion of mild steel in seawater,” *Corrosion Science*, vol. 47, no. 7, pp. 1678–1693, 2005.
- [28] W. B. Wan Nik, F. Zulkifli, M. M. Rahman, and R. Rosliza, “Corrosion Behavior of Mild Steel in Seawater from Two Different Sites of Kuala Terengganu Coastal Area,” *International Journal of Basic & Applied Sciences IJBAS-IJENS*, vol. 11, no. 6, pp. 75–80, 2011.
- [29] D. Gassama, A. A. Diagne, I. Yade, M. Fall, and S. Faty, “Investigations on the corrosion of constructional steels in different aqueous and simulated atmospheric environments,” *Bulletin of the Chemical Society of Ethiopia*, vol. 29, no. 2, pp. 299–310, 2015.
- [30] R. Matsushashi, Y. Tadokoro, S. Tsuge, and T. Suzuki, “Estimation of Crevice Corrosion Life Time for Stainless Steels in Seawater Environments,” Nippon Steel, Tech. Rep. 99, 2010.
- [31] L. B. Niu, K. Okano, S. Izumi, K. Shiokawa, M. Yamashita, and Y. Sakai, “Effect of chloride and sulfate ions on crevice corrosion behavior of low-pressure steam turbine materials,” *Corrosion Science*, vol. 132, pp. 284–292, 2018.
- [32] F. Bottoli, M. S. Jellesen, T. L. Christiansen, G. Winther, and M. A. Somers, “High temperature solution-nitriding and low-temperature nitriding of AISI 316: Effect on pitting potential and crevice corrosion performance,” *Applied Surface Science*, vol. 431, pp. 24–31, 2018.
- [33] ASTM International, “G48-11: Standard Test Methods for Pitting and Crevice Corrosion Resistance of Stainless Steels and Related Alloys by Use of Ferric Chloride Solution,” p. 11, 2015.
- [34] R. Klassen, P. Roberge, and C. Hyatt, “A novel approach to characterizing localized corrosion within a crevice,” *Electrochimica Acta*, vol. 46, no. 24-25, pp. 3705–3713, 2001.

- [35] D. Chin and G. Sabde, "Current Distribution and Electrochemical Environment in a Cathodically Protected Crevice," *Corrosion*, vol. 55, no. 3, pp. 229–237, 1999.
- [36] ASTM International, "G31-72: Standard Practice for Laboratory Immersion Corrosion Testing of Metals," p. 8, 2004.
- [37] —, "D1141 Standard Practice for the Preparation of Substitute Ocean Water," p. 3, 2013.
- [38] R. E. Melchers and R. Jeffrey, "Influence of water velocity on marine immersion corrosion of mild steel," *Corrosion*, no. January, pp. 84–94, 2004.
- [39] M. K. Sawford, B. G. Ateya, A. M. Abdullah, and H. W. Pickering, "The Role of Oxygen on the Stability of Crevice Corrosion," *Journal of The Electrochemical Society*, vol. 149, no. 6, p. B198, 7 2002.
- [40] H. J. Flitt and D. P. Schweinsberg, "A guide to polarisation curve interpretation: Deconstruction of experimental curves typical of the Fe/H₂O/H⁺/O₂ corrosion system," *Corrosion Science*, vol. 47, no. 9, pp. 2125–2156, 9 2005.
- [41] R. G. Kelly and K. C. Stewart, "Combining the Ohmic Drop and Critical Crevice Solution Approaches to Rationalize Intermediate Attack in Crevice Corrosion," Tech. Rep.
- [42] "Global Sea Temperatures." [Online]. Available: <https://www.seatemperature.org>
- [43] K. Borko, B. Hadzima, and F. Pastorek, "The Corrosion Properties of S355J2 Steel Welded Joint in Chlorides Environment," *Periodica Polytechnica Transportation Engineering*, 6 2018.
- [44] U.S. Department of the Interior Bureau of Reclamation, "Corrosion and Cathodic Protection," Materials Engineering Research laboratory, Bureau of Reclamation, Denver, Colorado, Tech. Rep., 2013.
- [45] J. Bates, "Cathodic Protection to Prevent Crevice Corrosion of Stainless Steels in Halide Media," *Corrosion Journal*, vol. 29, no. 1, pp. 28–32, 1973.
- [46] S. Hiromoto, "Corrosion of metallic biomaterials," in *Metals for biomedical devices*, Mitsuo Niinomi, Ed. Woodhead, 2010, ch. 4, pp. 99–121.
- [47] Y. Yang, J. Scantlebury, and E. Koroleva, "A Study of Calcareous Deposits on Cathodically Protected Mild Steel in Artificial Seawater," *Metals*, vol. 5, no. 1, pp. 439–456, 3 2015.

9 Appendices

9.1 APPENDIX 1: Work Method Statement

In the first appendix, the Work Method Statement that has been made as a guide for the work conducted for the experiments is shown. This document is used to communicate the experimental work and to mitigate possible risks as much as possible.

Experiment

Work Method Statement

Corrosion Behavior Inside a Slip Joint

- Insight on Corrosion in Offshore Applied Alternative Transition Pieces for Wind Turbines -

Contents

1	Overview	1
2	Scope	2
2.1	Project description	2
2.2	Scope method statement	2
2.3	Objectives, targets and indicators	2
3	Resources	3
3.1	Permanent equipment	3
3.2	Consumable equipment	4
4	Experimental set-up	5
4.1	Preparations	5
4.1.1	Preparing the tubs	5
4.1.2	Preparing the steel plates	6
4.1.3	Measurements of the steel plates	7
4.1.4	Measurements on specimen elements	9
4.1.5	Assembly of steel plates with the spacer	10
4.1.6	Closing the sides of the specimens	12
4.1.7	Preparing the salt water solution	12
4.2	Immersion of the specimens	14
4.2.1	Immersing and assembly of specimens in the tub	14
4.2.2	Activities during immersion	17
4.3	Specimen cleaning	17
4.3.1	Withdrawal of specimens	17
4.3.2	Chemical cleaning	17
4.3.3	Weighing the plates	19
4.3.4	Storage of the plates	19
5	Health and Safety	20
5.1	Hazards	20
5.1.1	Dropping objects	20
5.1.2	Incorrect tool handling	20
5.1.3	Breaking glass	20
5.1.4	Ethanol fire/explosion	20
5.1.5	Exposure to chemicals	20
5.2	Preventative measures and first aid	21
5.2.1	Dropping objects	21
5.2.2	Incorrect tool handling	21
5.2.3	Breaking glass	21
5.2.4	Ethanol fire/explosion	22
5.2.5	Exposure to chemicals	22
5.3	Risk assessment	23

6	Appendices	24
6.1	Appendix A: Steel plates drawing	25
6.2	Appendix B: Wegusta steel certificate	26
6.3	Appendix C: HDPE spacers drawing	27

1 Overview

Name	Koen de Bruin
Mobile	+31642028191
Mail	Koen.deBruin@vanoord.com
Project	144461
Experiment address	Graanweg 28, Moerdijk
Start Date	June
Duration	4 Months

Table 1: Project information details

	Name	Title
Author and Contact	Koen de Bruin	Graduate student
Authorised by	Sander Suur	Supervisor (Sr. Structural Engineer)
Authorised by	Nils Verkleij	Supervisor (Materials Engineer)
Authorised by	Yaiza Gonzalez Garcia	Supervisor (Corrosion and Electrochemistry scientist)

Table 2: Authorities

In Emergency			
Name	Gert Valk	Name	Bert van Maaren
Title	Yard Manager	Title	Yard Superintendent
Tel	+31 651001708	Tel	+31 653546741

Table 3: Emergency Contact Details

2 Scope

This chapter provides a general project description and the scope of work covered under this method statement.

2.1 Project description

Currently corrosion behavior in the Slip Joint is unknown. Van Oord has created a Master Thesis project covering the research towards corrosion inside the slip joint. To investigate corrosion behavior in the slip joint, experiments are performed. The main goal for the experiments is to determine the corrosion rates in the slip joint.

2.2 Scope method statement

The activities during the experiment and the activities needed for evaluation are described in this method statement. In order to set up the experiment, the ASTM guidelines are closely followed where applicable. Manufacturing of specimen elements by third parties, is not part of this document. Acquisition of supplies play a major role on the outcome and reliability. All materials used will therefore be described in this document.

The following work method statement has been developed to provide a reproducible and repeatable test. This document will also provide a safe work system and ensure a quality standard in the tests. Any significant deviation from this procedure must first be documented and authorized. The contact person for questions is Koen de Bruin (contact details are given in section 1).

First the required resources are summarized in section 3. In section 4 the preparations, testing period, cleaning and evaluation during the testing period will be discussed. Finally, in section 5, a review of the involved hazards and precautions is given. All the work is carried out at the Van Oord yard located in Moerdijk.

2.3 Objectives, targets and indicators

The objective is to obtain corrosion rates which can be directly related to the corrosion in the slip joint via an empirical model. This will be obtained by getting accurate and reliable data.

3 Resources

This chapter lists the required resources and tools for this project.

3.1 Permanent equipment

The following equipment is used for the experiment and will be reusable for other projects.

Object	Used to/for	Specifications
Balance	weigh solution	5kg capacity. 1g readout.
Precision Balance	measure specimen weight	750g cap. 1mg readout.
Tubs	submersion of specimens in salt water	$80 \times 63 \times 38$ [cm]
Press stamps	label specimens	Hardened steel symbols.
Caliper	measure specimen geometry	300mm capacity. 0.01mm readout.
Multimeters	measure potential of specimens	Voltcraft VC130-1
Reference electrodes	measure potential of specimens	Ag/AgCl to saturated KCl
Lab coat	personal protection against chemicals	-
Hammer	label specimens with press stamps	-
Utility knife	multiple purposes	snap-off
Wrenches	specimen assembly	-
Caulk gun	sealing specimens	-
Laboratory glassware	chemical solutions	-
Glass stir	stir salt solution	-
Cotton towel	clean equipment	-
Cotton cloth	clean specimens with ethanol	-
Nylon brush	clean the specimens	-
Spray bottles	handle chemicals/water	250mL. Plastic.
Blowdryer	dry specimens	-
USB voltage data loggers	log potentials over time	Easy Log EL-USB-ACT
Thermostat container	store at $21^{\circ}\text{C} \pm 0.1^{\circ}\text{C}$	Artic Storage 6×2.5 [m]

Table 4: Permanent equipment

3.2 Consumable equipment

The following equipment is used during the experiment and are for single use only.

Object	Use to/for	Specifications
Steel plates	create specimen for immersion	S355J2 bare steel
HDPE plates	create the crevice for the specimens	-
Bolts and nuts	assemble specimens	M5 - 30mm - RVS
Timber frames	specimen immersion	-
Salt (NaCl)	prepare test solution	In buckets of 5kg and 10kg
Distilled water	prepare test solution	5L jerrycans
Ethanol	clean specimens from greases	Denatured
Hydrochloric acid	create cleaning agent to dissolve corrosion product	36%
Hexamethyleentetramine	create cleaning agent to dissolve corrosion product	-
Safety gloves	personal protection against chemicals	Nitrile and Latex
Paper towel	housekeeping purpose	-
Silicone sealant	seal crevice between specimen sheets	Den Braven SILICONE-NO
Silicone tape	close sides of specimens	0.5mm \times 25mm \times 3m

Table 5: Consumable equipment

The steel plates that are mention in Table 5 are manufactured by Wegusta Holland according to prescribed tolerances as shown in appendix 6.1. In appendix 6.2 the material properties are given by the certificate from Wegusta Holland.

The HDPE plates are manufactured by Vink Techniek according to the prescribed drawing which can be found in appendix 6.3.

4 Experimental set-up

4.1 Preparations

The experiments can only be carried out after the necessary preparations. The main focus of the preparation is the required work on the specimens. Once the specimens are immersed, the corrosion process will start directly and this is irreversible. The specimens are not reusable and therefore the specimens should be prepared very carefully .

4.1.1 Preparing the tubs

Before the tubs are taken into use, they will be cleaned. The tubs are cleaned by rinsing with regular tap water. A bucket will be filled with tap water, this water will be poured over the sides of the tub. The inside of the tub is then cleaned with a brush. The contaminated water is poured out of the tub into a drain. To rinse out the tub properly, another bucket of water will be poured over the insides of the tub. The water is poured out of the tub again and the tub will be dried with a cotton towel. The clean tub will be placed at its dedicated location in the temperature controlled container (21°C \pm 0.1°C), see Figure 1.



Figure 1: Accurate temperature controlled container

All tubs will be marked with a number on the outside. The tubs are numbered from one to ten, see Figure 2. Although the container is leveled, the tubs will be checked on their level with a spirit level. Non-level tubs will be slimmed to reach straight level.

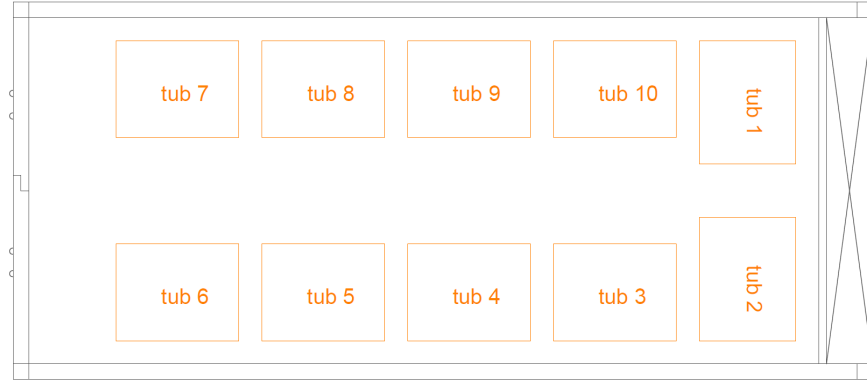


Figure 2: Floor plan container

The tub will be filled with salt water, containing a total of 3.5% sodium chloride. In section 4.1.7 the preparation of the salt water solution is described.

4.1.2 Preparing the steel plates

The specimens consist of two steel plates and a plastic spacer. These are mounted by a bolted connection. Both, the steel plates and plastic spacers, are manufactured to the required dimensions and with four required holes. The hole with a diameter of 25mm is required to slip the specimen on the frame, the other three holes of 5.5mm are used for assembling the specimens with bolts, as can be seen in Figure 3.

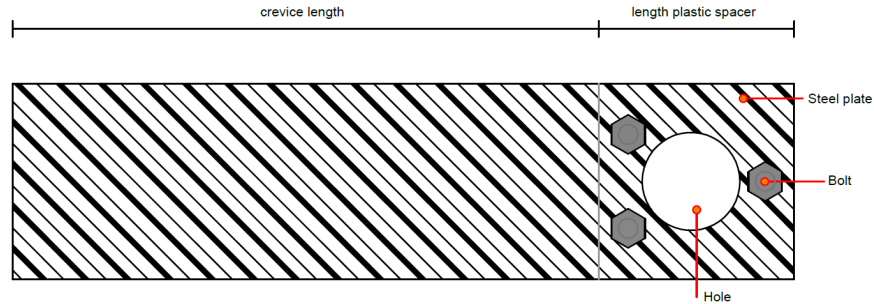


Figure 3: Specimen front view

The steel plates will be labeled using low stress stamps and a hammer. The plates are put on a concrete floor covered with clean A4 paper sheets. The required stamp is taken out of its box and put at the left top of the plate. The stamp will get at least one firm blow with the hammer. In Figure 4 the result is shown for an example steel plate. Each steel plate will be assigned a unique number, which is used for the log file. Every steel plate will get a stamp at the front only. In the first tub, 21 specimens with a crevice will be immersed together with 3 steel plates for reference. Therefore 45 steel plates will have to be labeled. These will get labels from A1 to A21, B1 to B21 and R1 to R3. For the following tub again 45 steel plates will be labeled. These will get labels from C1 to C21, D1 to D21 and R4 to R6. In the same manner the steel plates for the other tubs will be labeled.



Figure 4: Specimen labeled A3 (test specimen)

Prior to the assembly of the specimens, the steel plates are cleaned with ethanol to remove greases and dirt from the surface. Clean latex gloves will be used to prevent greases and dirt to transfer through contact. A clean spray bottle is opened and a funnel is placed on the spray bottle. A 5L jerry can of ethanol is taken from the storage rack and opened. Approximately 250mL of ethanol is poured from the jerry can into the spray bottle through the funnel. The jerry can is closed and directly stored back on the storage rack. Then the spray bottle will be closed. A cloth of cotton is soaked with ethanol sprayed from the spray bottle. Using the soaked cloth, the steel plates are wiped clean one by one. The cleaned specimens will be put on a clean sheet of paper. The used cloths are disposed into a dedicated bin. After the cleaning procedure, the steel plates are only allowed to be touched when wearing sterile gloves, to prevent contaminating the steel plates.

4.1.3 Measurements of the steel plates

Once the specimens are clean, all measurements will be carried out. The dimensions will be measured and the weight will be measured. The dimensions are measured with a caliper which has an accuracy of 0.01mm, see Figure 5.

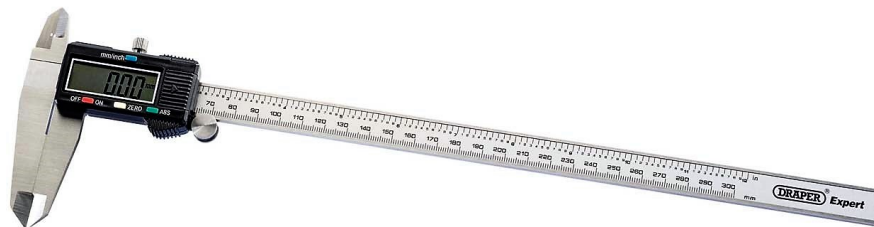


Figure 5: 300mm caliper with 0.01mm accuracy

Firstly a small working area will be created by covering the table top with clean paper. Latex gloves

will be used. Then, the caliper is taken from the shell and out of its box. The first dimension that is going to be measured is the length of the steel plate. All dimensions that are going to be measured are listed in Figure 6.

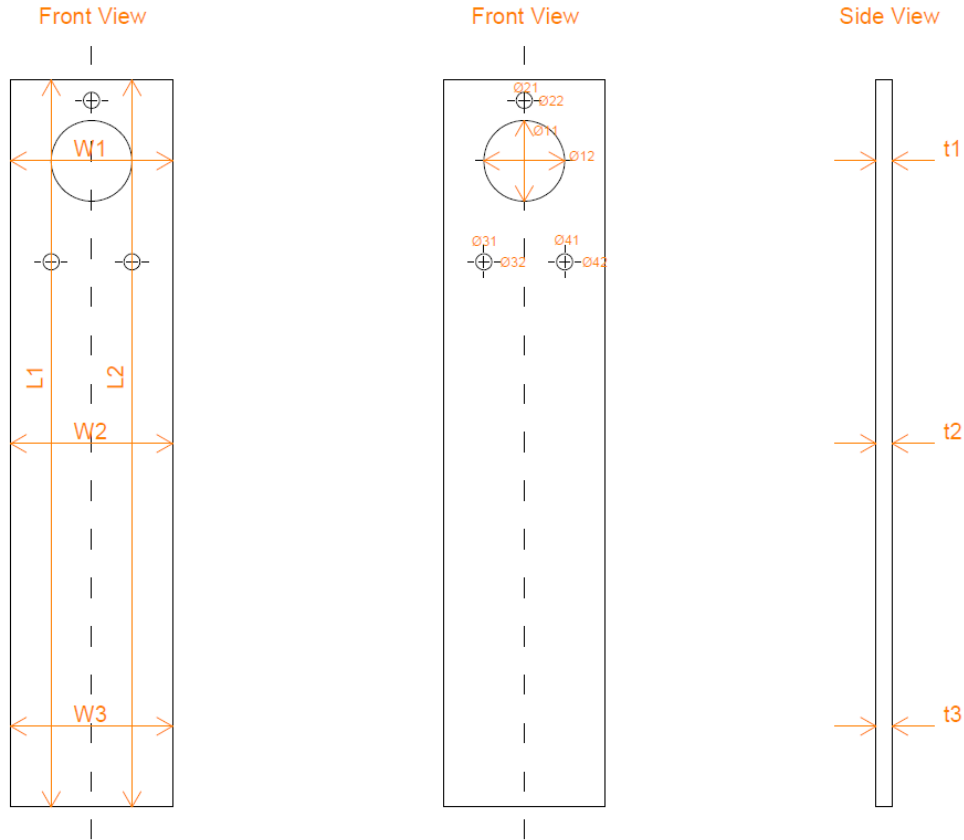


Figure 6: Steel plate measurement locations

In total 16 measurements will be carried out for every single steel plate. All the measurements are logged in an Excel file.

After measuring the dimensions of the steel plates, the plates will be weighed on the high precision balance, KERN PLJ 700-3CM, reading in milligrams. This balance is shown in Figure 7. The glass cover of the balance will be removed (otherwise the specimen does not fit). Air movements, due to wind or breathing, can influence the balance measurements. Air movements are blocked by placing a cardboard box over the balance.



Figure 7: KERN PLJ precision balance

Firstly the balance is checked to be level, if necessary the legs of the balance will be adapted. Again latex gloves will be used. The balance is turned on. The steel plate is placed on the balance as shown in Figure 8. The weight is read from the display and noted in the Excel file.

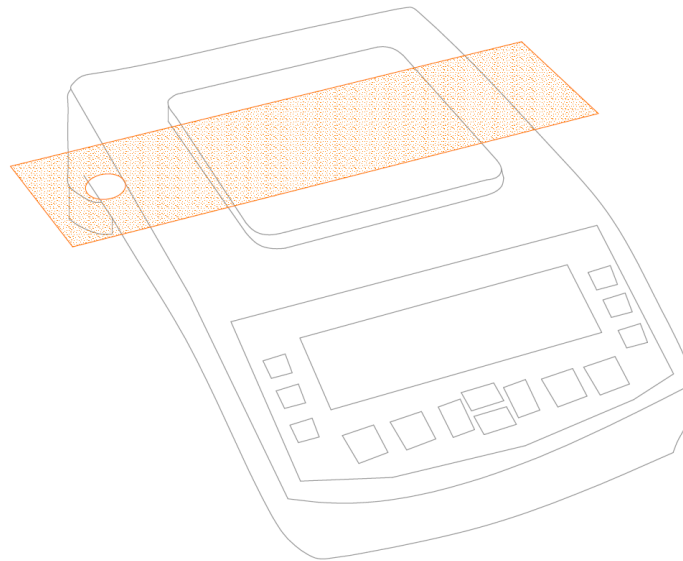


Figure 8: Position of steel plate on the balance

4.1.4 Measurements on specimen elements

In order to assess the weight loss properly, all specimen elements are measured in advance of immersion. Knowing the weight of every element makes sure that the weight of the used silicone sealant, which will be applied in a later stage, can be calculated.

The weight of the steel plates will be measured as discussed in the previous paragraph. Prior to weighing the spacers, they are cleaned with ethanol. Then they are labeled with a specimen number using tape. Each spacer for the corresponding specimen is weighed on the precision balance (1mg read-out), furthermore the bolts and nuts and the tape that will be used in that combination are going to be weighed with the precision balance. The resulting measurements will be logged in the Excel file and the combination of steel plates with spacer, bolt and nuts are stored together and will later be assembled together.

There are two more weight measurements going to be carried out, as discussed in the next two paragraphs. All weight measurements that are necessary prior to the test are summarized in the table below.

Order	Measurement	Scale
1	Steel plates	0.001g precision balance
2	Spacers	0.001g precision balance
3	Bolts	0.001g precision balance
4	Assembly of steel plates with spacer and sealant	1g precision balance
5	Total assembly with wrapping	1g precision balance

Table 6: Weight measurements

4.1.5 Assembly of steel plates with the spacer

In order to make the assembly between the spacer and steel plates watertight, silicone sealant is used. Firstly, the plastic spacer will be cleaned with ethanol to remove dirt and greases. A clean paper sheet is spread over the working bench and ethanol is sprayed from a spray bottle on a paper cloth. The paper cloth is used to wipe the spacer clean. The cleaned spacer will be put down on the clean sheet.

The bottle of silicone sealant is put into a caulk gun and then the bottle will be cut open with a utility knife. A small line of sealant is applied on the spacer, see Figure 9a, after which it is attached to a steel plate. This is done for both steel plates, as can be seen in Figure 9c. The steel plates that are used for the specimens will be with corresponding labels. For example in the first tub, the first specimen will get steel plates A1 and B1.

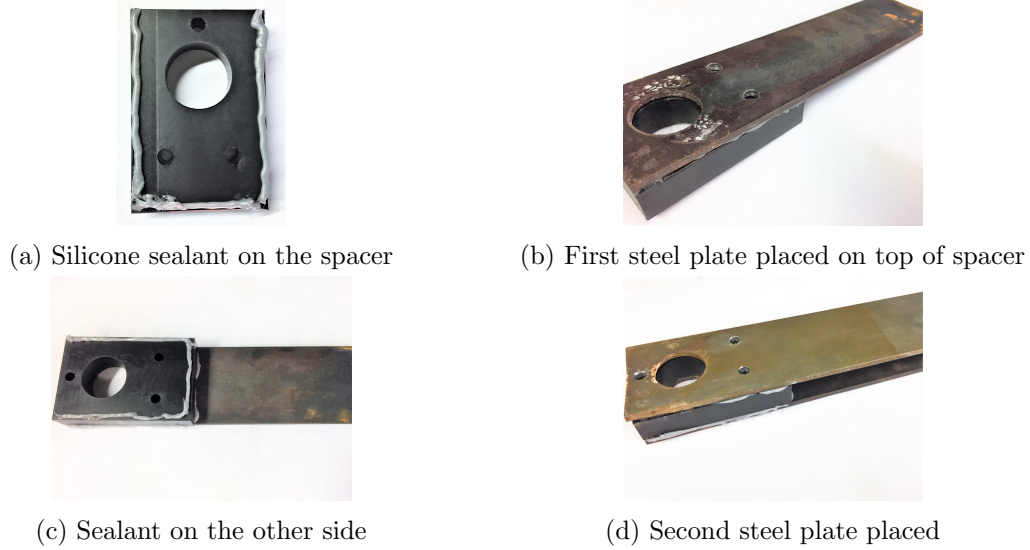


Figure 9: Applying silicone sealant between the specimen parts

The specimens are assembled using stainless steel M5 hex bolts with a length of 30mm. The three required bolts are put through the dedicated holes in the specimen. The specimen is turned over carefully, because the sealing is not cured at this moment. The bolts are put through further such that the nuts can be assembled on the bolts. The bolts will be tightened using a wrench. By tightening the bolts, the sealant will partly be squeezed out of the connected elements. This excessive sealant is removed carefully with a blade after at least 12 hours of curing.



Figure 10: Assembly of the bolts

An cross sectional overview of all elements required for this assembly is shown in Figure 11.

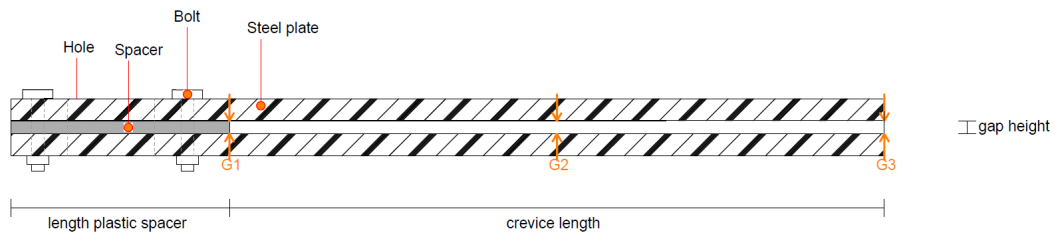


Figure 11: Specimen gap measurement locations

Before closing the sides of the specimen. The gap height of the gap will be measured at both ends of the crevice and in the middle of the crevice with the caliper. In Figure 11 the locations for the

measurements are indicated by the orange arrows. The measured gap heights are logged in the Excel file.

To be able to calculate the amount of silicone sealant used for this step the assembly will be weighed on a balance with a 1g read-out. The resulting weight is logged in the Excel file.

4.1.6 Closing the sides of the specimens

The side as shown in Figure 11, of the specimen will be closed using silicon tape. Firstly the specimen is put on its side and silicon sealing is applied to the edges of the steel plates and on the edges of the spacer, see Figure 12a. A 225mm long piece of tape is cut from the roll with a utility knife. This piece will be put on the side of the specimen by lightly pressing it on the sealant. After closing the first side, the specimen is turned over. The other side is now closed in the same manner, resulting in a crevice with only an opening at the bottom.



(a) Silicon sealant



(b) Result with silicon tape

Figure 12: Closing the sides of the crevice

Before immersing the specimens, they will be weighed on the balance with a 1 gram read out. The measured weighed will be logged in the Excel file.

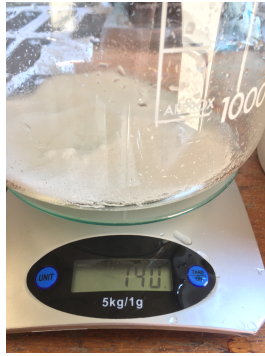
4.1.7 Preparing the salt water solution

Seawater contains approximately 3.5% (35 g/L) salt, therefore a 3.5% sodium chloride solution will be prepared. Distilled water is used to prepare the salt water. The prepared batch volume is four liters. The amount of salt required for this batch is:

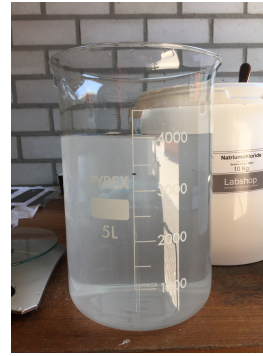
$$\frac{\text{weight}}{\text{volume}} \% = \frac{\text{weight of solute}}{\text{volume of solution}} \times 100 \quad (4.1)$$

$$3.5\% \times \frac{4}{100} = 0.14 \text{ [kg]}$$

Firstly a 5L jerrycan with distilled water will be opened. Secondly a glass beaker is put on the balance with 1g read-out. The balance is turned on and then the beaker will be filled with 140g of sodium chloride by putting in scoops of salt from a bucket, see Figure 13a. This beaker is topped up with distilled water directly from the jerrycan, until the beaker contains four liters of the solution, see Figure 13b.



(a) 140g salt in the beaker



(b) Batch of 4L

Figure 13: Salt water solution preparation

The beaker is emptied into the tub and the next four liter batch will be made according to the same procedure. The tub is filled with 17 batches, i.e. 68L. At this point, the wooden frame will be mounted on the tub. In Figure 14 the frame is shown. The specimens corresponding to the specific tub are mounted on the frame and will be divided over the frame, such that there is at least 5cm of space between the specimens.

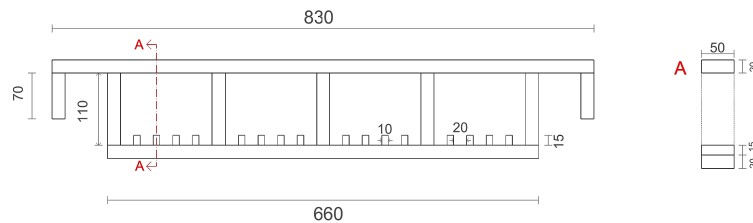


Figure 14: Drawing of frame

An additional sample is used to mark the required water level with PVC tape. The location of the tape is measured with a caliper and marks a 65mm distance from the top. The specimens are 225mm long and 160mm of this length will be submerged, leaving 65mm from the top dry. In Figure 15 the situation is shown. Using a pencil the 65mm distance will be indicated. The tape is then put on the specimen such that the lower edge marks the 65mm line. This specimen is put temporarily on the frame to mark the correct water level in the tub.

Subsequently the tub is filled further with batches of salt water, until a water level is reached at which 160mm of the specimen is submerged, indicated by the marked specimen. The marked specimen is taken from the frame, the water level will now be marked by sticking tape on the walls of the tub at the water level. The total used water and used salt will be logged in the lab-journal. In Figure 15 a cross sectional side view of the volume of the solution with the partly submerged specimens is shown.

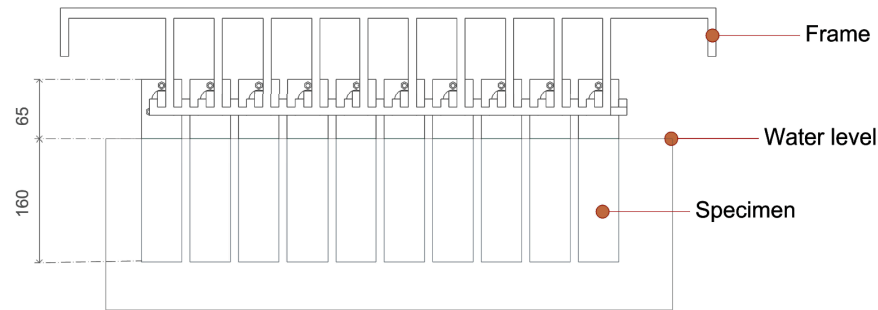


Figure 15: Submerged specimens

The salinity of the water is checked using a Valeport SWiFT SVP, see Figure 16. This is a sound velocity profiler which is able to measure the salinity and the density of the salt water. The probe will be connected to the laptop via Bluetooth and will be put into the water. The probe will be configured using the software on the laptop. After the configuration the probe will be started to do measurements for 30 seconds. The data is downloaded from the probe and the values of the water temperature, salinity and density will be noted in the lab-journal.



Figure 16: Sound Velocity Probe

If the measurements show that the salinity is either lower or higher than the required 3.5%, either salt or distilled water will be added to the tub respectively.

4.2 Immersion of the specimens

4.2.1 Immersing and assembly of specimens in the tub

Each frame will hold up 24 specimens. A single girder in the frame holds 3 specimens, 8 girders are used (see Figure 15 and Figure 17). An assembled specimen weighs approximately 950g. Girders are labeled by a number using a waterproof marker, each girder will have its own unique number. Tub 1 will contain girders 1.1 to 1.8, Tub 2 will contain girders 2.1 to 2.8 and so on.

To start, sterile latex gloves have to be used. A specimen is taken and will be submerged upside down in order to fill the crevice with the solution and let the air escape from the crevice. Still submerged, the specimen will be turned upright and is then taken partly out of the water, keeping the opening below water, such that the girder can be slid through the dedicated hole of the specimen. The girder is put down in the frame and the next specimen will be submerged upside down. The

specimen will be turned upright again and the girder is taken from the frame and is slid through the hole of this specimen. Once the girder contains three specimens it will be put on the frame for the immersion period. The three specimens will be spread out over the girder such that the specimens keep a minimum distance of 10cm from each other. The combination, of each girder with its specimens, is noted in the Excel file such that each specimen is traceable to its location in the tub. In Figure 17 the lay-out of the specimens in the tub is visualized.

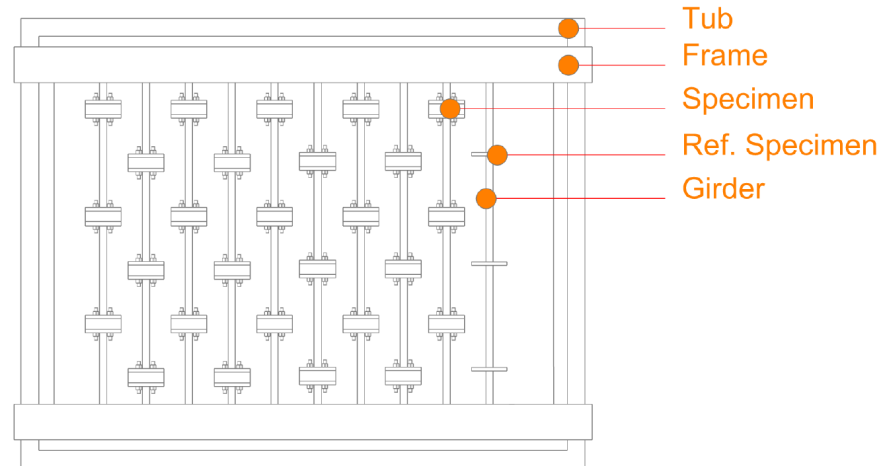


Figure 17: Top view of set-up

The final set-up is shown in Figure 18. This tub shows a full tub of only specimen with spacers. However, three steel plates will be put in the tub as reference between the tubs and as a reference for uniform corrosion. The uniform corrosion behavior of mild steels in sea water is known very well. A comparison with the corrosion in the crevice is therefore a good reference. Furthermore it is possible to compare differences between the tubs by comparing the data of the reference plates.

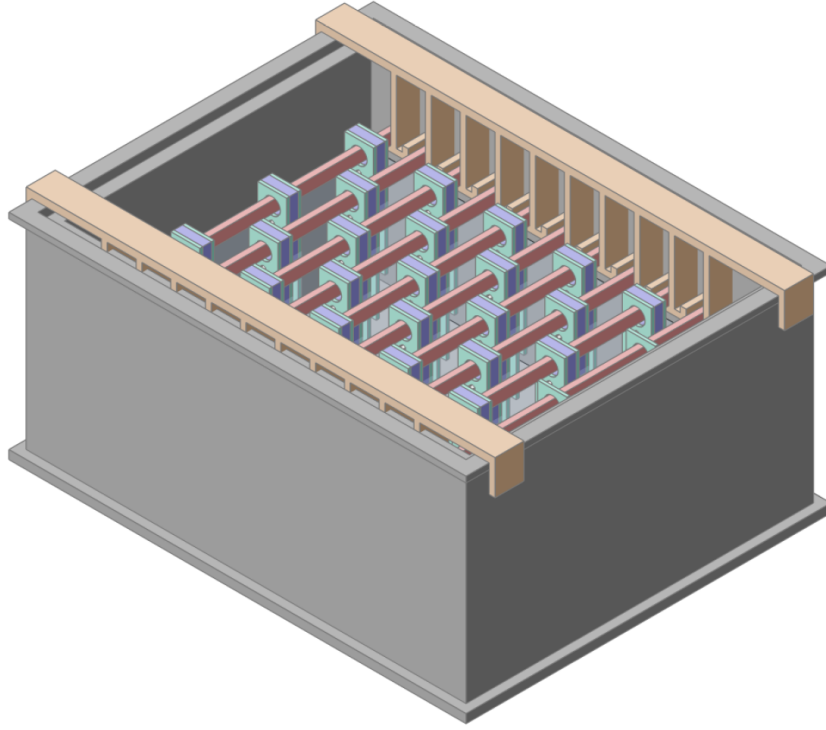


Figure 18: Final set-up

Different sets are immersed per tub, the variables are the dimensions of the spacers. In Table 7 the different spacers per tub are shown. Each specific dimension is immersed three times. For example, there are three specimens in tub 1 with a spacer of $50 \times 175 \times 2$ mm. Furthermore this tub will contain the three steel plates for reference.

Tub	$w \times l$ [mm]	t [mm]	t [mm]	t [mm]	t [mm]	t [mm]	t [mm]	t [mm]
1	(50 × 175)	2	4	6	8	10	12	14
2	(50 × 150)	2	4	6	8	10	12	14
3	(50 × 125)	2	4	6	8	10	12	14
4	(50 × 100)	2	4	6	8	10	12	14
5	(50 × 75)	2	4	6	8	10	12	14

Table 7: Spacer sizes per tub (width × length × thickness[mm])

The potential of each specimen is measured using a digital multimeter which will be connected to an reference electrode (Ag/AgCl versus KCl) , directly after submersion. The tip of the reference electrode is put into the tub, 10-25cm apart from the measured specimen and connected to the COM socket of the multimeter. A clamp will be put on the top of one of the steel plates and is connected with a banana plug to the millivolt socket of the multimeter. The multimeter will be switched on and the potential will be measured. The measurements will be logged in the Excel file. After 60 till 90 minutes the potential is measured again.

4.2.2 Activities during immersion

During the period that the specimens are immersed, water will evaporate from the solution. Therefore, the tub is topped up at least twice a week. Depending on the rate of evaporation this frequency is subject to change.

The potential of the specimens are be monitored during the experiment. At least twice a week the potential of both steel plates of the specimen will be measured using the reference electrode as used for the measurements at the start. Again, the clamp will be mounted on the top of the steel plate. The measurements are logged in the lab-journal.

Per tub three specimens are measured continuously during the first week. These specimens will be connected with a potential logging device. Again the reference electrodes are used. The potential logging device stores the measurements. Data will be processed using a laptop, to plot the potential data over time.

4.3 Specimen cleaning

The specimens will be taken out of the tub after a minimum of 60 days and up to a maximum of 65 days of submersion. The specimens will be cleaned and weighed afterwards. The cleaning process is described in this section.

4.3.1 Withdrawal of specimens

During this procedure sterile gloves have to be worn. It will reduce the possibility of contaminating the specimens. To prevent the specimens from corroding any further, this procedure is required. Specimens are taken out per single girder, each containing three specimens.

In order to hang the specimens free in air, the girder is clamped with a vise. Each specimen will be photographed on both sides before drying. While they are still on the girder, all sides of the specimens will be dried using a blow dryer. The fully dried specimen will be disassembled. Pictures are taken of the corroded side of the steel plates. The steel plates are then rinsed with ethanol using a spray bottle. Using the blow dryer again, the specimens will be dried from the ethanol.

The specimens are taken from the girder and put back on the table covered with clean paper. Pictures are taken from both sides of the rinsed steel plates. Remaining silicone sealant is carefully removed with the blade of a utility knife. Each dry steel plate will be weighed using the high precision balance with 1mg read-out. After testing the plates will be stored in a dry carton box. The removed silicone sealant is weighed with the high precision balance, also the bolts, nuts and wrapping will be weighed.

The next girder is then pulled out of the tub. The same procedure is applied to these specimens and is repeated until all specimens are out of the tub, dried and weighed.

4.3.2 Chemical cleaning

First, loose, bulky corrosion products will be removed from the dried steel plates by lightly brushing with a nylon brush. An acid solution will be prepared according to the proposed method by the ASTM standard practice G1 (Standard Practice for Preparing, Cleaning and Evaluating Corrosion

Test Specimens). This acid solution will remove the corrosion product from the plates. Nitrile safety gloves are going to be worn to protect the hands from the acid during the entire procedure. Furthermore a lab coat and safety goggles will be worn.

A fume hood will be used to draw toxic vapors from the local environment. A tall beaker and a wide beaker will be placed into the fume hood. Three ingredients are required to prepare the solution: hydrochloric acid together with hexamethylenetetramine dissolved in distilled water.

First 1500mL of the hydrochloric acid will be poured into the wide beaker for convenience. The hydrochloric acid is poured over to the tall beaker. 1500mL of the distilled water will be poured, from a jerry can, into the emptied wide beaker. Bit by bit the 1500mL of hydrochloric acid is added to the water by pouring the acid over the wall of the beaker. Between pouring, the solution is stirred using a glass stick. Stirring has to be done carefully, to prevent spills and accidents.

Using the precision balance (1mg precision), 10.5g of hexamethylene tetramine is dosed on a petri dish. The hexamethylene tetramine is put into the tall beaker. To be able to mix the hexamethylene tetramine easily, a small portion, approximately 200mL, of the solution is added to the tall beaker. The solution in the tall beaker is stirred until all solid parts are dissolved. Finally the rest of the solution in the wide beaker is added to the solution in the tall beaker. The final solution will be stirred with a glass stick.

A maximum of four steel plates will be placed slowly into the solution such that the corroded part is dissolved, see Figure 19. The plates are kept in the solution for a minimum of 10 minutes and to a maximum of 20 minutes. In the case of a tough corrosion layer which does not dissolve from the steel plates, the steel plate will be removed intermittent from the cleaning solution for light brushing in distilled water with a nylon brush. To complete the cleaning procedure, the plates will be rinsed with ethanol and are dried using paper towel. Once dried, photos of the steel plates are taken of both sides.



Figure 19: Steel plates in the cleaning solution

The used acid solution is stored in a dedicated waste container. These containers are picked up regularly by a chemistry waste service.

4.3.3 Weighing the plates

Following the cleaning procedure, the specimens will be weighed with the high precision balance (1mg precision) outside the fume cupboard. The glass cover of the balance will be removed. To block air movements, a carton box will be placed over the balance. Every single specimen will be weighed. Gloves will be worn to protect the specimens from any contamination. The measurements are noted on paper and later processed in an Excel file.

4.3.4 Storage of the plates

At the end of the total procedure, the steel plates will be stored in a carton box. To improve the quality of storage, the plates will be separated in the box by paper sheets. The box will be stored in the laboratory in an ambient atmosphere.

5 Health and Safety

This chapter describes all health and safety aspects including hazard identification and applicable Personal Protective Equipment related to the specific scope of work covered under this method statement. The work related hazards and risks are discussed in section 5.1. The required preventative measures will be discussed in section 5.2.

5.1 Hazards

The hazards related to injuries and damages to equipment are described in this section.

5.1.1 Dropping objects

Dropping objects can cause injuries and damage. The used distilled water comes in jerry-cans of 25 liter, the salt comes in 10 kilogram buckets.

5.1.2 Incorrect tool handling

During the preparation, the specimens are labeled using low stress stamps. For this task a hammer is used. A hammer can cause serious injuries.

A blow dryer can cause burns. The blow dryer also invokes an electrical hazard. If the hairdryer comes in contact with water there is a possibility of causing a shock or electrocution.

5.1.3 Breaking glass

Glass containers are used to prepare solutions. These glass objects can break due to misuse. Shattered glass can cause injuries. Damaged or broken glass can cause cuts. Heated glass can cause burns.

5.1.4 Ethanol fire/explosion

Ethanol is used as a cleaning agent. Ethanol is highly flammable. The vapors mix well with air, explosive mixtures can be formed.

5.1.5 Exposure to chemicals

Ethanol used during preparation can be hazardous. Inhalation can cause headaches, coughing, fatigue and drowsiness. Skin contact can cause dry skin. Eye contact can cause redness, pain and a burning feeling. Ingestion can cause a burning sensation, headache, confusion, dizziness and ultimately unconsciousness.

Hydrochloric acid, used for cleaning the specimens, can be harmful to humans and the environment. Hydrochloric acid itself is corrosive. Acidic mists can be formed. These mists are hazardous.

Hydrochloric acid has potential acute health effects. Contact can be painful. It is very hazardous in case of skin contact (corrosive, irritant, permeator) and of eye contact (irritant, corrosive). If the acid or mist comes into contact with the skin, eyes or internal organs, the damage can be irreversible or even fatal in severe cases. In case of inhalation it is slightly hazardous as a lung sensitizer, but

is non-corrosive for lungs. Inhalation can cause a burning sensation, coughing, laboured breathing, shortness of breath and a sore throat.

Liquid or spray mist may produce tissue damage, particularly on mucous membranes of eyes, mouth and respiratory tract. Skin contact can produce burns. Inhalation of the spray mist may produce severe irritation of respiratory tract, characterized by coughing, choking, or shortness of breath. Severe over-exposure can result in death. Inflammation of the eye is characterized by redness, watering, and itching. Eye contact can be corrosive and cause blurred vision. Skin inflammation is characterized by itching, scaling, reddening, or, occasionally, blistering. There is a potential chronic health effect. In case of skin contact it can act as a sensitizer. It can be toxic to kidneys, liver, mucous membranes, upper respiratory tract, skin, eyes, Circulatory System and teeth.

Repeated or prolonged exposure to the acid can produce damage to target organs. Repeated or prolonged exposure to spray mist may produce chronic eye irritation and severe skin irritation. It can even produce irritation to the respiratory tract, leading to frequent attacks or bronchial infection. Repeated exposure to highly toxic material may produce general deterioration of health by an accumulation in one or many human organs.

5.2 Preventative measures and first aid

On forehand one of the yard managers will be informed on the work that will be carried out.

5.2.1 Dropping objects

All heavy objects will be placed on the floor or flat table surface. This reduces the possibility of heavy objects to drop. No heavier objects than 25 kilograms will be lifted. This weight is still manageable to carry for an individual.

5.2.2 Incorrect tool handling

Damaged tools will not be used. Before using the hammer, it will be inspected. The hammer head has to be firmly attached to the handle. A hammer with a loose, cracked or splintered handle will not be used. A hammer with mushroomed or chipped face or with cracks in the claw or eye section will be discarded. Before swinging the hammer, enough clearance is taken from other objects or fellow workers. To prevent strains, awkward positions should be avoided. The side or cheek of the hammer will not be used for striking. During the use of a hammer, safety shoes and safety goggles will be worn at all times.

The blow dryer, including the electrical cable, will be inspected on damages. If damages are visible, the blow dryer will be replaced. If unused, the dryer will be unplugged. It will not be left where it can be pulled into a basin or tub. If the dryer falls into water or liquid it will not be reached for. First it will be unplugged and then it will be removed. A dryer that has been exposed to water or liquid will not be used again. To prevent overheating, the dryer will never be placed such that the openings are blocked.

5.2.3 Breaking glass

Before use, all glassware will be checked to ensure that it is free from cracks, flaws or scratches that may cause it to fail. Glass will be transported carefully and never in pockets. Glassware will not be stored on the floor. Hot glass will be treated with care and placed where no one can accidentally

come into contact with it before it has cooled. Damaged glassware will be disposed in the glass bin. A brush and dustpan will be used to clear up broken glass.

5.2.4 Ethanol fire/explosion

During the use of ethanol, no open flames or sparks are allowed. Smoking and contact with strong oxidants is not allowed. Only little amounts of ethanol will be used at once. Maximum 250mL will be poured out of a jerry-can. This jerry-can will then be closed directly and stored again. In case of spills, the ethanol will be rinsed with water and the room will be ventilated. The ethanol will be stored separately from strong oxidants.

5.2.5 Exposure to chemicals

Protective gloves and safety goggles will be worn while working with ethanol. During work, no eating, drinking or smoking is allowed. This reduces the risks of ingesting chemicals. In the case of inhalation, the involved person needs to get fresh air and rest. In the case of skin or eye contact, contaminated clothes have to be removed first. Secondly the skin should be rinsed with plenty of water and soap. Eyes should be rinsed with plenty of water for several minutes (contact lenses should be removed if possible). In case of severe eye contact, a doctor should be consulted. If ingested, the mouth should be rinsed and medical attention is required.

All fysical contact with hydrochloric acid will be avoided. A fume hood will be used to ventilate the working area and prevent inhalation. Nitrile gloves are going to be used in order to prevent skin contact. Furthermore a lab coat and safety goggles are used. In the lab, an eye shower and sink with faucet is available.

Pouring of the acid solution will be done with a funnel to prevent spills. To prevent overheating of the beaker, in which the solution will be formed, the hydrochloric acid has to be added to water and not the other way around. It is not allowed to add water to hydrochloric acid, during this experiment.

In case of inhalation, fresh air and resting in a half-upright position is required. Artificial respiration may be needed. Medical attention is required. In the case of skin contact, first the contact area should be rinsed for at least 15 minutes. Then the contaminated clothes have to be removed and again the skin area of interest should be further rinsed. The skin will be washed with disinfectant soap and the contaminated skin will be covered with anti-bacterial cream. Cold water can be used. Clothing have to be washed before reuse. Shoes has to be cleaned thoroughly before reuse. A doctor will be consulted. In the case of eye contact, first a check for contact lenses and then removing of the lenses will be done. Rinsing with water will be done using a dedicated eye shower. A doctor will be consulted immediately.

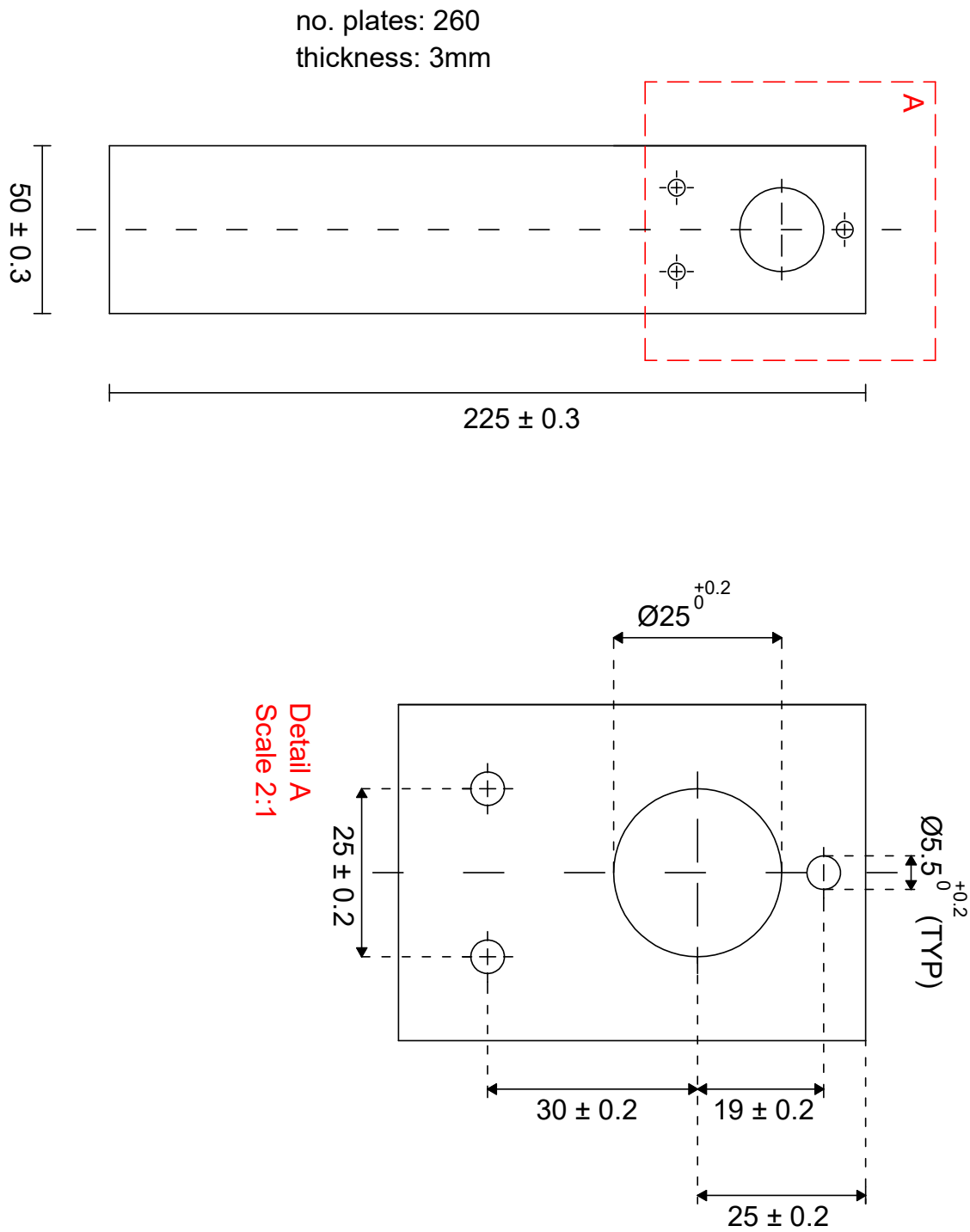
In case of a small spill, the acid will be diluted with water and mopped or absorbed with an inert dry material. The waste has to be placed in an appropriate waste disposal container. In case of a large spill, the leak will be stopped only if without risk. The spill will be absorbed with dry earth, sand or other non-combustible material. The spilled material must not be touched. Water spray has to be used to divert vapor drift and reduce vapors. Entry to sewers, basements or confined areas has to be avoided.

5.3 Risk assessment

Risk Assessment Worksheet														
Project Client Contractor Subcontractor	Corrosion Experiments			Prep Checked Authorised	RA Doc. No. Revision date Revision									
	RA date	Client	08-08-2018											
	Project number													
			0											
Attendees														
Name		Position	Company	Name		Position	Company							
Koen de Bruin		Graduate Student	Van Oord											
Hazard evaluation														
Item No.	Process step / Activity	Hazard	Consequence	Initial Risk			Van Oord Existing Safeguards	Additional safeguards Vessel / Project	By who	By when	Completion reference	Residual Risk		
				S	L	R						S	L	R
1	Use of tools	tools not used correctly	Injury	1	C	LOW	Replace damaged tools. Inspect tools, before use. Use tools like supposed to. Keep electrical tools from water or liquid and unplug when not used					1	B	LOW
2	Use of glass	breaking of glass	injury	1	C	LOW	Check for flaws. Transport carefully and not in pockets. Do not store on the floor. Dispose broken glass in bin and clean up with a brush and dustpan. Tread hot glass with care, place where accidental touching is not possible.					1	B	LOW
3	Working with Ethanol	fire	Serious Injury + damages	3	C	MEDIUM	Use small amounts. Open flames and smoking forbidden in workspace. Spills will be rinsed with plenty of water.					3	A	LOW
4	Working with chemicals	contact with skin	injury or illness + pollution	3	D	MEDIUM	Use correct and suitable gloves. Use labcoat and safety goggles. Use funnelhood. In case of spills, clean according to prescribed procedure. Dispose chemicals into dedicated bins. Drinking is not allowed when working with chemicals.					3	C	MEDIUM
5	Heavy objects	Dropping objects	Injury	2	C	LOW	Store heavy objects on the floor or level counters. Wear safety shoes. Very heavy object should be moved using dedicated lifting machinery.					2	B	LOW
6	Sharp objects	Cuts	Injury	2	C	LOW	Use safety gloves and safety shoes. Store sharp objects correctly.					2	B	LOW

6 Appendices

6.1 Appendix A: Steel plates drawing



6.2 Appendix B: Wegusta steel certificate



Page 1 of 1

26-FEB-18 11:05:43

MCB NEDERLAND B.V.

JF KENNEDYLAAN 59
5555 XC VALKENSWAARD
PAYS-BAS

CERTIFICATE 522917 **Date** 26-FEB-18 **Delivery** CH 538465 **Order** 89100
note No

Item	Customer referen	Product type	Grade (Standard norm)	Tvpe
4	4500411965 2300-0830-8001500	hot rolled coil	S355J2+N EN 10025-2:2004	3.1
3	4500411965 2300-0830-5001500	hot rolled coil	S355J2+N EN 10025-2:2004	3.1

Item	Product	Cast	Thickness	width	Weight	Sample	Re N/mm ²	Rm N/mm ²	A %	1	2	3	T (C)
	4G188160	N32690	500	1500	24249	Q	446	533	27				
4	4G129650	N35285	800	1500	23840	Q	495	596	26	58	52	50	-20

Cast		C	Mn	S	P	Si	Al	Cu	Ni	Cr	Mo	Nb	N2	V	Ti
N32690	LD	164	1251	12	9	15	35	31	18	17	2	29	47	1	18
N35285	LD	170	1482	12	12	16	59	40	22	27	4	35	39	3	23

Analysis of cast, unit : (X 0,001%) except N2, B, Ca : (X 0,0001%)

U BESTÄTIGUNG ÜBEREINSTIMMUNGSNACHWEIS UHP
nach Bauregelliste A Teil 1, Ausgabe 96/1

Certification type according to EN 10204-2004

Tensile test according to ISO 6892-1:2009

Impact test according to EN 10045-1:2004

Hardness test according to EN 6508-1:1999

Marking, aspect and dimension controls satisfactory. We certify that the products here-above fulfill the order requirements

Marking and dimensions control according to EN 10051 (according to SEL014E for Tear drop checker): without objections.

CE1148 - CPD - 20070424 Structural steel product hot-rolled. End uses: construction of buildings or civil engineering
Elongation, Tensile strength, Yield point, Toughness and Welding characteristics according to EN 10025-2 Durability:
No given performance
Tolerances on dimensions (Class D) and shape (Class N) according to EN 10029

LA LOUVIERE, 26-FEB-18

Quality control manager

Siege social : NLMK La Louvière s.a. - 2, rue des Rivaux - B 7100 La Louvière Belgique

Tel. : +32 (0)64 27.27.11 - Telefax : +32 (0)64 27.27.48 - email : info@eu.nlmk.com

Banca Monte Paschi Belgio s.a. 643-0021687-36 - IBAN BE 46 643002168736 RPM Mons - TVA BE - 0417.374.172



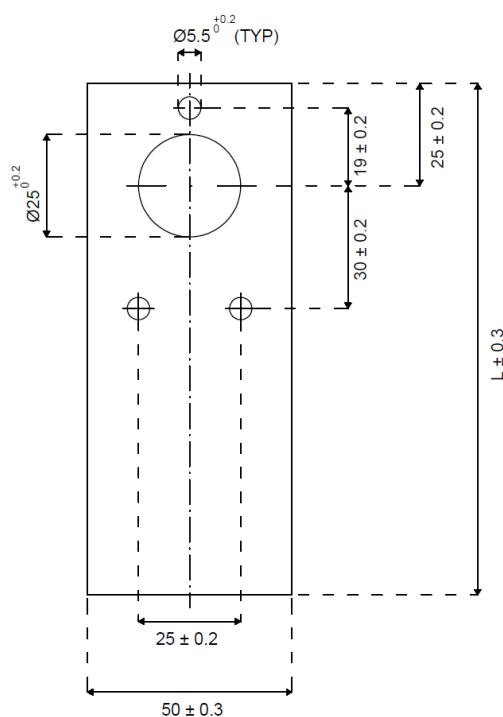
6.3 Appendix C: HDPE spacers drawing

PLASTIC 260PLAATJES AFMETINGEN EN HOEVEELHEDEN

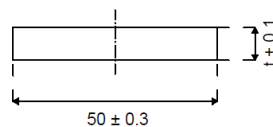
Gevraagd zijn 203 **HDPE** plaatjes van verschillende dikte en formaat. In de plaatjes moeten vier gaten worden gemaakt. Een gat met een diameter van 25 [mm] en drie kleinere gaten van 5.5 [mm]. Een tekening met detaillering is hieronder weergegeven.

De plastic plaatjes worden gebruikt als spacers voor een test opstelling en moeten daarom worden gemaakt volgens aangegeven tolerantie. De maximale tolerantie, gerelateerd aan de lengte en breedte van het proefstuk, is ± 0.3 [mm]. De maximale tolerantie, gerelateerd aan de gaten, is ± 0.2 [mm].

Front view



Bottom view



In de tabel hieronder staan de aantallen per plaatje, met de bijbehorende lengte en dikte.

	Thickness "t"						
	2	4	6	8	10	12	14
Length "L"	75	4	4	4	4	4	4
	100	4	4	4	4	4	4
	125	4	4	4	4	4	4
	150	4	4	4	4	4	4
	175	13	13	13	13	13	13

Tabel 1: Aantal plaatjes per lengte/dikte



Figure 9.2: Tafel plot comparison S355J2 and S355ML after 30 minutes of stabilization second test

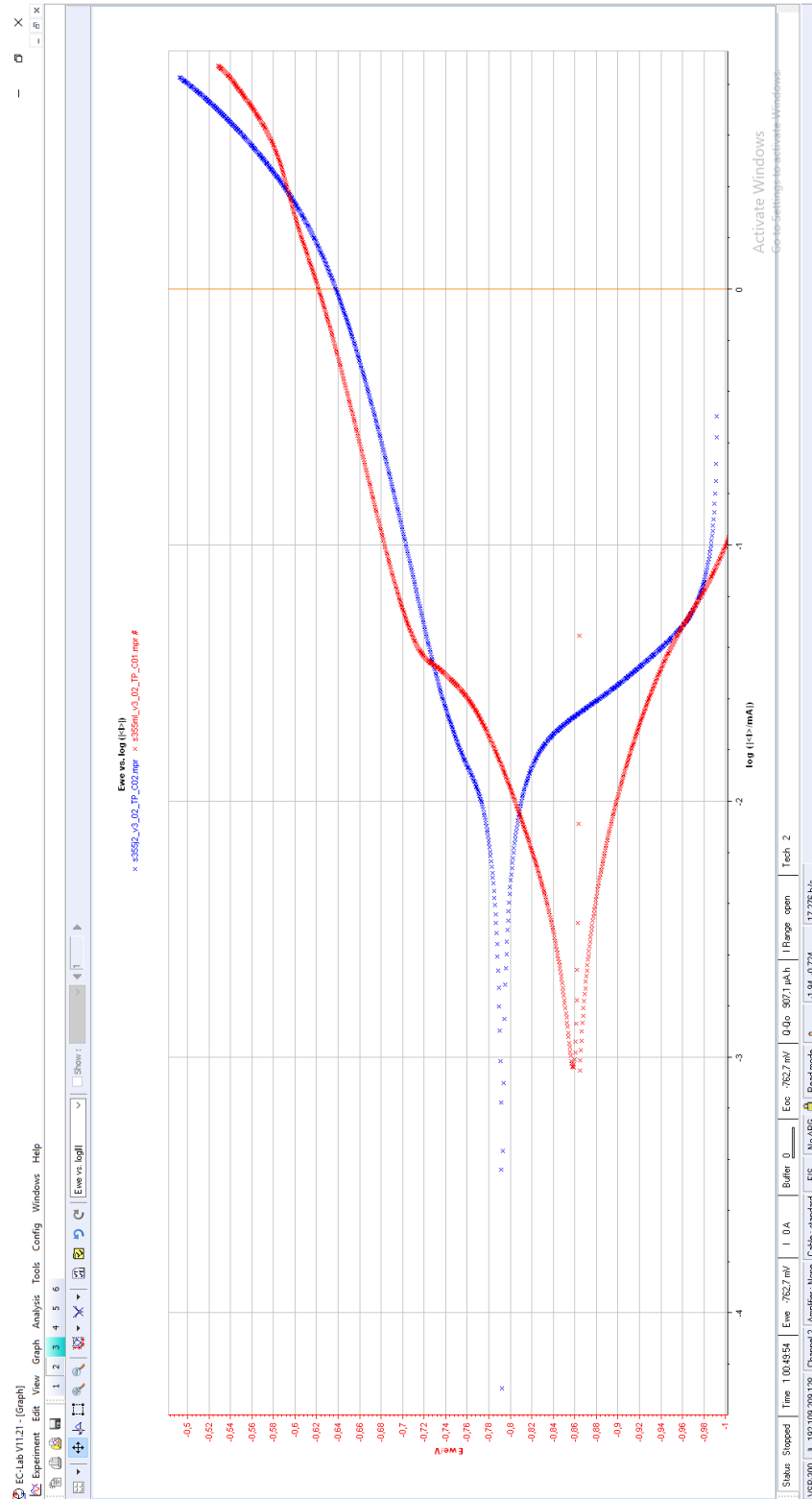


Figure 9.3: Tafel plot comparison S355J2 and S355ML after 24 hours of stabilization

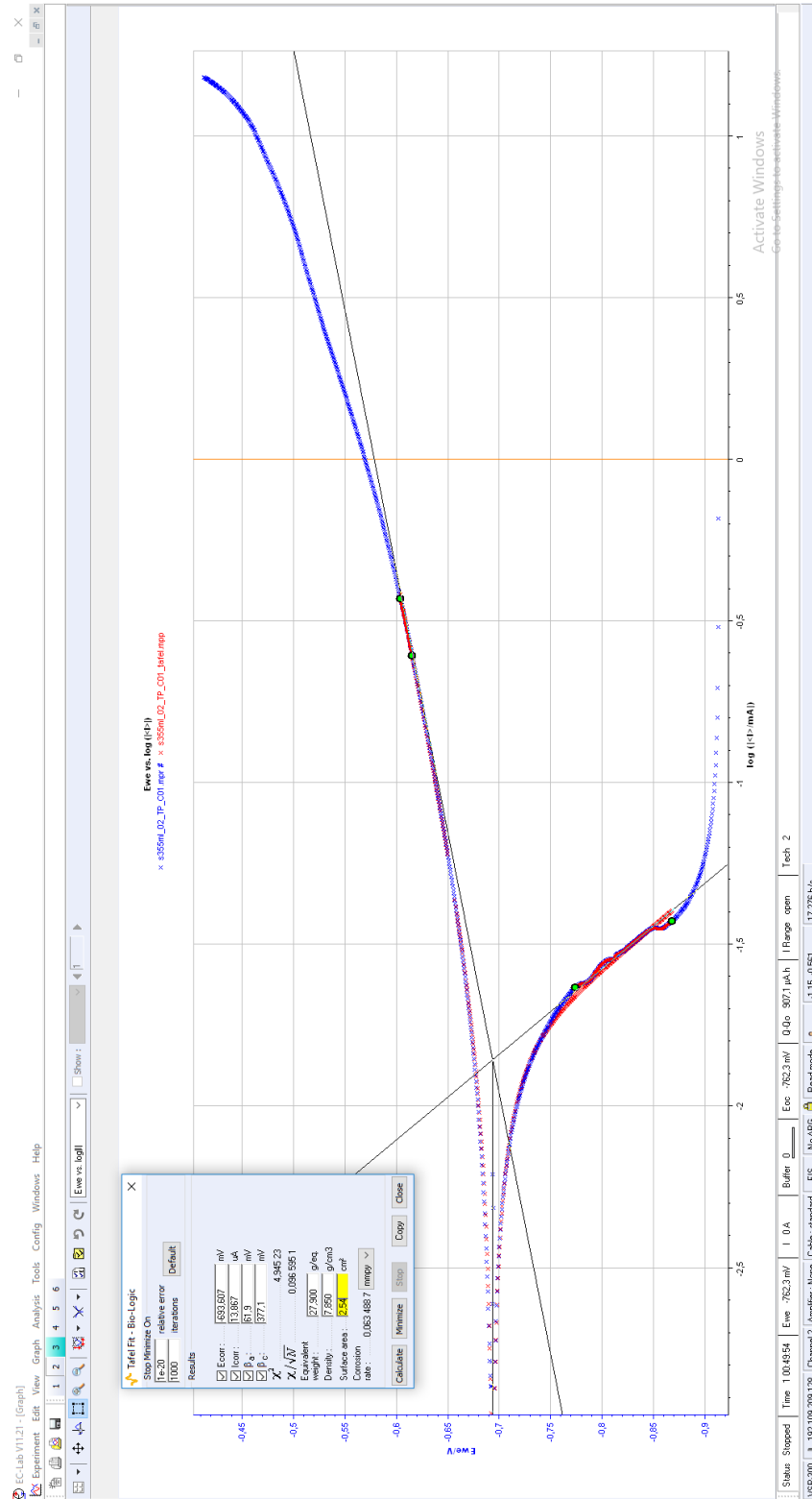


Figure 9.4: Tafel plot generated with EC-lab for S355ML after 30 minutes of submersion

9.3 APPENDIX 3: Specimen codes and set codes

Specimen	Description	Crevice [h×l×w]	Steel plates codes
S1	Specimen of batch 1	14×50×50	A1 & B1
S2	Specimen of batch 1	14×50×50	A2 & B2
S3	Specimen of batch 1	14×50×50	A3 & B3
S4	Specimen of batch 1	12×50×50	A4 & B4
S5	Specimen of batch 1	12×50×50	A5 & B5
S6	Specimen of batch 1	12×50×50	A6 & B6
S7	Specimen of batch 1	10×50×50	A7 & B7
S8	Specimen of batch 1	10×50×50	A8 & B8
S9	Specimen of batch 1	10×50×50	A9 & B9
S10	Specimen of batch 1	8×50×50	A10 & B10
S11	Specimen of batch 1	8×50×50	A11 & B11
S12	Specimen of batch 1	8×50×50	A12 & B12
S13	Specimen of batch 1	6×50×50	A13 & B13
S14	Specimen of batch 1	6×50×50	A14 & B14
S15	Specimen of batch 1	6×50×50	A15 & B15
S16	Specimen of batch 1	4×50×50	A16 & B16
S17	Specimen of batch 1	4×50×50	A17 & B17
S18	Specimen of batch 1	4×50×50	A18 & B18
S19	Specimen of batch 1	2×50×50	A19 & B19
S20	Specimen of batch 1	2×50×50	A20 & B20
S21	Specimen of batch 1	2×50×50	A21 & B21
R1	Reference specimen of batch 1	-	R1
R2	Reference specimen of batch 1	-	R2
R3	Reference specimen of batch 1	-	R3
T1	Specimen of batch 2	14×50×75	C1 & D1
T2	Specimen of batch 2	14×50×75	C2 & D2
T3	Specimen of batch 2	14×50×75	C3 & D3
T4	Specimen of batch 2	12×50×75	C4 & D4
T5	Specimen of batch 2	12×50×75	C5 & D5
T6	Specimen of batch 2	12×50×75	C6 & D6
T7	Specimen of batch 2	10×50×75	C7 & D7
T8	Specimen of batch 2	10×50×75	C8 & D8
T9	Specimen of batch 2	10×50×75	C9 & D9
T10	Specimen of batch 2	8×50×75	C10 & D10
T11	Specimen of batch 2	8×50×75	C11 & D11
T12	Specimen of batch 2	8×50×75	C12 & D12
T13	Specimen of batch 2	6×50×75	C13 & D13
T14	Specimen of batch 2	6×50×75	C14 & D14
T15	Specimen of batch 2	6×50×75	C15 & D15
T16	Specimen of batch 2	4×50×75	C16 & D16
T17	Specimen of batch 2	4×50×75	C17 & D17
T18	Specimen of batch 2	4×50×75	C18 & D18
T19	Specimen of batch 2	2×50×75	C19 & D19

T20	Specimen of batch 2	2×50×75	C20 & D20
T21	Specimen of batch 2	2×50×75	C21 & D21
R4	Reference specimen of batch 2	-	R4
R5	Reference specimen of batch 2	-	R5
R6	Reference specimen of batch 2	-	R6
U1	Specimen of batch 3	14×50×100	E1 & F1
U2	Specimen of batch 3	14×50×100	E2 & F2
U3	Specimen of batch 3	14×50×100	E3 & F3
U4	Specimen of batch 3	12×50×100	E4 & F4
U5	Specimen of batch 3	12×50×100	E5 & F5
U6	Specimen of batch 3	12×50×100	E6 & F6
U7	Specimen of batch 3	10×50×100	E7 & F7
U8	Specimen of batch 3	10×50×100	E8 & F8
U9	Specimen of batch 3	10×50×100	E9 & F9
U10	Specimen of batch 3	8×50×100	E10 & F10
U11	Specimen of batch 3	8×50×100	E11 & F11
U12	Specimen of batch 3	8×50×100	E12 & F12
U13	Specimen of batch 3	6×50×100	E13 & F13
U14	Specimen of batch 3	6×50×100	E14 & F14
U15	Specimen of batch 3	6×50×100	E15 & F15
U16	Specimen of batch 3	4×50×100	E16 & F16
U17	Specimen of batch 3	4×50×100	E17 & F17
U18	Specimen of batch 3	4×50×100	E18 & F18
U19	Specimen of batch 3	2×50×100	E19 & F19
U20	Specimen of batch 3	2×50×100	E20 & F20
U21	Specimen of batch 3	2×50×100	E21 & F21
R7	Reference specimen of batch 3	-	R7
R8	Reference specimen of batch 3	-	R8
R9	Reference specimen of batch 3	-	R9
V1	Specimen of batch 4	14×50×125	V1 & H1
V2	Specimen of batch 4	14×50×125	V2 & H2
V3	Specimen of batch 4	14×50×125	V3 & H3
V4	Specimen of batch 4	12×50×125	V4 & H4
V5	Specimen of batch 4	12×50×125	V5 & H5
V6	Specimen of batch 4	12×50×125	V6 & H6
V7	Specimen of batch 4	10×50×125	V7 & H7
V8	Specimen of batch 4	10×50×125	V8 & H8
V9	Specimen of batch 4	10×50×125	V9 & H9
V10	Specimen of batch 4	8×50×125	V10 & H10
V11	Specimen of batch 4	8×50×125	V11 & H11
V12	Specimen of batch 4	8×50×125	V12 & H12
V13	Specimen of batch 4	6×50×125	V13 & H13
V14	Specimen of batch 4	6×50×125	V14 & H14
V15	Specimen of batch 4	6×50×125	V15 & H15
V16	Specimen of batch 4	4×50×125	V16 & H16

V17	Specimen of batch 4	4×50×125	V17 & H17
V18	Specimen of batch 4	4×50×125	V18 & H18
V19	Specimen of batch 4	2×50×125	V19 & H19
V20	Specimen of batch 4	2×50×125	V20 & H20
V21	Specimen of batch 4	2×50×125	V21 & H21
R10	Reference specimen of batch 4	-	R10
R11	Reference specimen of batch 4	-	R11
R12	Reference specimen of batch 4	-	R12
W1	Specimen of batch 5	14×50×150	I1 & J1
W2	Specimen of batch 5	14×50×150	I2 & J2
W3	Specimen of batch 5	14×50×150	I3 & J3
W4	Specimen of batch 5	12×50×150	I4 & J4
W5	Specimen of batch 5	12×50×150	I5 & J5
W6	Specimen of batch 5	12×50×150	I6 & J6
W7	Specimen of batch 5	10×50×150	I7 & J7
W8	Specimen of batch 5	10×50×150	I8 & J8
W9	Specimen of batch 5	10×50×150	I9 & J9
W10	Specimen of batch 5	8×50×150	I10 & J10
W11	Specimen of batch 5	8×50×150	I11 & J11
W12	Specimen of batch 5	8×50×150	I12 & J12
W13	Specimen of batch 5	6×50×150	I13 & J13
W14	Specimen of batch 5	6×50×150	I14 & J14
W15	Specimen of batch 5	6×50×150	I15 & J15
W16	Specimen of batch 5	4×50×150	I16 & J16
W17	Specimen of batch 5	4×50×150	I17 & J17
W18	Specimen of batch 5	4×50×150	I18 & J18
W19	Specimen of batch 5	2×50×150	I19 & J19
W20	Specimen of batch 5	2×50×150	I20 & J20
W21	Specimen of batch 5	2×50×150	I21 & J21
R13	Reference specimen of batch 5	-	R13
R14	Reference specimen of batch 5	-	R14
R15	Reference specimen of batch 5	-	R15
Y1	Specimen batch 6 with void 14×50×50	2×50×100	K1
Y2	Specimen batch 6 with void 14×50×50	2×50×100	K2
Y3	Specimen batch 6 with void 14×50×50	2×50×100	K3
Y4	Specimen batch 6 with void 14×50×50	4×50×100	K4
Y5	Specimen batch 6 with void 14×50×50	4×50×100	K5
Y6	Specimen batch 6 with void 14×50×50	4×50×100	K6
R16	Reference specimen of batch 6	-	R16
R17	Reference specimen of batch 6	-	R17

Table 9.1: Specimen codes, description and geometry

Set	Batch	Crevice [h×l×w]	Specimens in set
14×50	1	14×50×50	S1, S2, S3
12×50	1	12×50×50	S4, S5, S6
10×50	1	10×50×50	S7, S8, S9
8×50	1	8×50×50	S10, S11, S12
6×50	1	6×50×50	S13, S14, S15
4×50	1	4×50×50	S16, S17, S18
2×50	1	2×50×50	S19, S20, S21
RT1	1	-	R1, R2, R3
14×75	2	14×50×75	T1, T2, T3
12×75	2	12×50×75	T4, T5, T6
10×75	2	10×50×75	T7, T8, T9
8×75	2	8×50×75	T10, T11, T12
6×75	2	6×50×75	T13, T14, T15
4×75	2	4×50×75	T16, T17, T18
2×75	2	2×50×75	T19, T20, T21
RT2	2	-	R4, R5, R6
14×100	3	14×50×100	U1, U2, U3
12×100	3	12×50×100	U4, U5, U6
10×100	3	10×50×100	U7, U8, U9
8×100	3	8×50×100	U10, U11, U12
6×100	3	6×50×100	U13, U14, U15
4×100	3	4×50×100	U16, U17, U18
2×100	3	2×50×100	U19, U20, U21
RT3	3	-	R7, R8, R9
14×125	4	14×50×125	V1, V2, V3
12×125	4	12×50×125	V4, V5, V6
10×125	4	10×50×125	V7, V8, V9
8×125	4	8×50×125	V10, V11, V12
6×125	4	6×50×125	V13, V14, V15
4×125	4	4×50×125	V16, V17, V18
2×125	4	2×50×125	V19, V20, V21
RT4	4	-	R10, R11, R12
14×150	5	14×50×150	W1, W2, W3
12×150	5	12×50×150	W4, W5, W6
10×150	5	10×50×150	W7, W8, W9
8×150	5	8×50×150	W10, W11, W12
6×150	5	6×50×150	W13, W14, W15
4×150	5	4×50×150	W16, W17, W18
2×150	5	2×50×150	W19, W20, W21
RT5	5	-	R13, R14, R15
2mm_void	6	crevice 2mm high, void 14mm high	Y1, Y2, Y3
4mm_void	6	crevice 4mm high, void 14mm high	Y4, Y5, Y6
RT6	6	-	R16, R17

Table 9.2: Specimen sets

List of Figures

Fig. 1.1	Components of an offshore wind turbine	1
Fig. 1.2	Slip Joint overview	2
Fig. 1.3	Installation procedure	4
Fig. 1.4	Local environment in the Slip Joint	5
Fig. 1.5	Dimensions monopile and transition piece	6
Fig. 1.6	Combined local out of roundness for the transition piece and the monopile	7
Fig. 1.7	Cone angle tolerances for the transition piece and monopile.	8
Fig. 1.8	Gap between the transition piece (in red) and monopile (in black) for the maximum deviation of the cone angle.	9
Fig. 1.9	Combined tolerances	10
Fig. 1.10	Maximum gap in slip joint for cone angle tolerance	12
Fig. 2.1	Uniform corrosion reactions	16
Fig. 2.2	Corrosion rate as function of pH for low alloy steel in aerated aqueous solution [9]	16
Fig. 2.3	Corrosion rate of iron as function of sodium chloride concentration [7]	17
Fig. 2.4	Seawater resistivity as a function of temperature [4]	18
Fig. 2.5	Temperature effect the corrosion rate of steel in water [7]	19
Fig. 2.6	Example of biofouling in marine environment [12]	19
Fig. 2.7	Uniform corrosion on a monopile at the Aeolus	21
Fig. 2.8	Development of corrosion rate over time of low-alloy steels [15]	22
Fig. 2.9	Schematic drawing of reactions occurring with pitting corrosion	23
Fig. 2.10	Schematic drawing of reactions with crevice corrosion	25
Fig. 2.11	Galvanic Series of metals in seawater versus a saturated Ag/AgCl reference electrode [8]	26
Fig. 2.12	Standard polarization cell	27
Fig. 2.13	Corrosion rate determination by Tafel extrapolation [8]	28
Fig. 2.14	Levels and zones in the marine environment [1]	30
Fig. 2.15	GACP system in seawater, with an aluminum anode. [20]	31
Fig. 2.16	ICCP protection system [20]	32
Fig. 3.1	Scaling Law, L is the crevice length, h is the crevice height and x_{crit} is the critical crevice distance.	35
Fig. 3.2	Corrosion rates observed by Melchers and Jeffrey for mild steel in seawater [27]	37
Fig. 3.3	Data from the study of Wan Nik et al. showing the influence of time, salinity and temperature on the corrosion rate.	38
Fig. 3.4	Schematic illustration of a specimen with a crevice [30]	39
Fig. 3.5	Washer as described by ASTM and used by Bottoli et al.	40
Fig. 4.1	S355ML sample of 25mm diameter, after first abrading with grit size grade 80	44
Fig. 4.2	Corrosion cell with counter electrode, reference electrode and working electrode.	44
Fig. 4.3	OCP during 30 minutes stabilization	45
Fig. 4.4	Polarization curve after 30 minutes of stabilization	46
Fig. 4.5	Tafel plot for S355J2 after 30 minutes of submersion	46
Fig. 4.6	Tafel plot generated with EC-lab for S355J2 after 30 minutes of submersion	47
Fig. 4.7	Polarization curve after 24hours of stabilization	48
Fig. 4.8	Specimen front view	49
Fig. 4.9	Specimen side view	49
Fig. 4.10	Assembly of specimen	49
Fig. 4.11	Options for closing the crevice	50

Fig. 4.12	Specimen definitions of width, length and height	51
Fig. 4.13	Salt water solution preparation	52
Fig. 4.14	Top view of set-up	53
Fig. 4.15	Configuration of immersed specimens	53
Fig. 4.16	Result of specimens in the tub	54
Fig. 4.17	Tub with potential loggers connected with specimens	54
Fig. 4.18	Immersed steel plates for trial test, with varying distance	56
Fig. 4.19	Trial specimen after immersion and after cleaning	57
Fig. 4.20	Specimen with a crevice ending in a void, side view.	58
Fig. 4.21	ICCP set-up	59
Fig. 4.22	Measured potential during trial test	60
Fig. 4.23	Applied current during trial test	60
Fig. 5.1	Average OCP of the reference plates of batch 1 to 5	61
Fig. 5.2	Corroded reference plate showing uniform corrosion	62
Fig. 5.3	OCP measurements of the specimens in batch 1	63
Fig. 5.4	Corroded steel plate A1 of specimen S1 with a crevice of 14mm height and 50mm long. (The exposed area is indicated by the red box.)	64
Fig. 5.5	Corroded steel plate A20 and B20 of specimen S20 with a crevice of 2mm height and 50mm long. (The exposed area is indicated by the red box.)	64
Fig. 5.6	OCP measurements of batch 2	65
Fig. 5.7	OCP measurements of batch 3	66
Fig. 5.8	OCP measurements of batch 4	66
Fig. 5.9	OCP measurements of batch 5	67
Fig. 5.10	OCP measurements of crevices with a gap height of 12mm and crevice lengths of 50mm, 75mm, 100mm, 125mm and 150mm.	68
Fig. 5.11	OCP measurements of crevices with a gap height of 8mm and crevice lengths of 50mm, 75mm, 100mm, 125mm and 150mm.	69
Fig. 5.12	OCP measurements of crevices with a gap height of 4mm and crevice lengths of 50mm, 75mm, 100mm, 125mm and 150mm.	69
Fig. 5.13	OCP measurements of crevices with a gap height of 2mm and crevice lengths of 50mm, 75mm, 100mm, 125mm and 150mm.	70
Fig. 5.14	Corroded steel plates with crevice lengths of 75mm with potentials in the area of -670 mV	71
Fig. 5.15	Corroded steel plates with crevice lengths of 75mm with potentials in the area of -630 mV	71
Fig. 5.16	Corroded steel plates with crevice lengths of 100mm with potentials in the area of -630 mV	72
Fig. 5.17	Corroded steel plates with crevice lengths of 100mm with potentials in the area of -670 mV	73
Fig. 5.18	Corroded steel plates with crevice lengths of 125mm with potentials in the area of -630 mV	73
Fig. 5.19	Corroded steel plates with crevice lengths of 125mm with unstable and/or more negative potentials	74
Fig. 5.20	Corroded steel plates with crevice lengths of 150mm with unstable and/or more negative potentials	75
Fig. 5.21	Corroded steel plates with crevice lengths of 150mm with potentials in the area of -630 mV	75
Fig. 5.22	Rust forming a blockade at the mouth of a small crevice	76

Fig. 5.23	Weight loss of specimens in batch 1 having a crevice length of 50mm. The weight loss of the uniform corroding reference plate is included in the plot (RT1).	77
Fig. 5.24	Weight losses of specimens with lengths 75, 100, 125 and 150mm	78
Fig. 5.25	Corrosion rate of specimens in batch 1 having a crevice length of 50mm. The corrosion rate of the uniform corroding reference plate is included in the plot (RT1).	79
Fig. 5.26	Weight losses of specimens with lengths 75 and 100mm	79
Fig. 5.27	Weight losses of specimens with lengths 125 and 150mm	80
Fig. 5.28	Influence of the crevice height on the corrosion rate. The light blue area is the standard deviation from the mean.	80
Fig. 5.29	T-Test for corrosion rates with varying crevice heights	81
Fig. 5.30	Influence of the crevice length on the corrosion rate. The light blue area is the standard deviation from the mean.	82
Fig. 5.31	T-Test for corrosion rates with varying crevice lengths	82
Fig. 5.32	Influence of the crevice height and length on the corrosion rate.	83
Fig. 5.33	OCP measurements of all reference plates. Batch 1 to 5 are from the crevice corrosion test. Pot_avg_RT6 are the OCP measurements of the reference plates of the batch of the crevices with a void.	84
Fig. 5.34	OCP measurements of specimens with a void.	85
Fig. 5.35	Corroded steel plate Y1 of a specimen with a 2mm high crevice and a 14mm high void.	85
Fig. 5.36	Corroded steel plate Y4 of a specimen with a 4mm high crevice and a 14mm high void.	86
Fig. 5.37	Weight loss of specimens in batch 6, having a void of 14mm high at the rear of a crevice. The weight loss of the uniform corroded reference plates is included in the plot (RT6).	87
Fig. 5.38	Corrosion rate of specimens in batch 6, having a void of 14mm high at the rear of the crevice. The corrosion rate of the uniform corroded reference plates is included in the plot (RT6).	87
Fig. 5.39	Corrosion rates of crevices with a void compared to regular crevices of similar geometries.	88
Fig. 5.40	T-Test for corrosion rates of crevices with and without a void	88
Fig. 5.41	T-Test for corrosion rates of crevices with and without a void corrected to the uniform corrosion rates of their batches	89
Fig. 5.42	ICCP on a crevice of 2mm high, 50mm wide and 50 long.	90
Fig. 5.43	Potential of isolated steel plate during ICCP	91
Fig. 5.44	Potential on a crevice of 2mm high, 50mm wide and 150mm long.	91
Fig. 5.45	Applied current by ICCP on 2mm×50mm×150mm crevice	92
Fig. 5.46	Potential of isolated steel plate during ICCP of 2mm×50mm×150mm crevice	92
Fig. 6.1	Scaling factor L/h and distributed groups	94
Fig. 6.2	Average OCP of each crevice geometry, color graded	95
Fig. 6.3	OCP versus scaling factor	96
Fig. 6.4	Corrosion rate versus scaling factor	97
Fig. 6.5	Corrosion rate versus scaling factor with a trendline for crevice corrosion	98
Fig. 6.6	Corroded steel plate with a crevice of 2mm×50mm×150mm showing mirrored rust formation. Note, no ICCP was applied on these plates.	99
Fig. 6.7	Corrosion rate estimation advised for design purposes based on trendlines	102
Fig. 6.8	Example of resulting corrosion rates estimations from the empirical model for uniform corrosion rates of 0.14mm/y and 0.10mm/y	103

Fig. 6.9	Influence crevice height and length on normalized corrosion rates	103
Fig. 6.10	Normalized corrosion rate versus scaling factor with trendlines	104
Fig. 6.11	Example of resulting corrosion rates estimations from the empirical models for uniform corrosion rates of 0.14mm/y and 0.10mm/y	105
Fig. 6.12	Specimen with multiple sections of steel	107

List of Tables

Tab. 1.1	Tolerances of the transition piece and monopile radius	10
Tab. 1.2	Tolerance combination	11
Tab. 1.3	Parameters used in the FE-model	11
Tab. 4.1	S355J2 compared to S355ML with Tafel plots	47
Tab. 4.2	Tested crevice geometries (width \times length \times height)	51
Tab. 6.1	Average OCP for scaling law ranges	95
Tab. 6.2	Average CR for scaling law ranges	96
Tab. 6.3	Corrosion rate differences in percentages	101